

Sigrid Drotleff from Agnetheln

# **Polymers and Protein-Conjugates for Tissue Engineering**

---



**Doctoral Thesis to obtain the  
Degree of Doctor of Natural Sciences (Dr. rer. nat.)  
From the  
Faculty of Chemistry and Pharmacy  
University of Regensburg**

June 2006

This work was carried out from August 2001 until June 2006 at the Department of Pharmaceutical Technology of the University of Regensburg.

The thesis was prepared under supervision of Prof. Dr. Achim Göpferich.

Submission of the PhD. Application: 06.06.2006

Date of examination: 11.07.2006

Examination board:	Chairman:	Prof. Dr. A. Buschauer
	1. Expert:	Prof. Dr. A. Göpferich
	2. Expert:	Prof. Dr. J. Heilmann
	3. Examiner:	Prof. Dr. S. Elz

To my family



# Table of Contents

<b>Chapter 1</b>	Introduction - Biomimetic Polymers for Pharmaceutical and Biomedical Sciences	<b>7</b>
<b>Chapter 2</b>	Goal of the Thesis	<b>53</b>
<b>Chapter 3</b>	Materials and Methods	<b>57</b>
<b>Chapter 4</b>	Synthesis and Characterization of Poly(ethylene glycol)co-poly(lactic acid)	<b>89</b>
<b>Chapter 5</b>	Investigation of Protein Adsorption on MePEG <sub>x</sub> PLA <sub>y</sub>	<b>109</b>
<b>Chapter 6</b>	Determination of Reaction Sites of Insulin	<b>127</b>
<b>Chapter 7</b>	Synthesis and Characterization of Lipophilized Insulin	<b>149</b>
<b>Chapter 8</b>	Summary and Conclusion	<b>167</b>
<b>References</b>		<b>171</b>
<b>Appendices</b>	Abbreviations	<b>192</b>
	Curriculum Vitae	<b>196</b>
	Acknowledgments	<b>198</b>



# Chapter 1

## Introduction - Biomimetic Polymers for Pharmaceutical and Biomedical Sciences

S. Drotleff<sup>1</sup>, U. Lungwitz<sup>1</sup>, M. Breunig<sup>1</sup>, A. Dennis<sup>1,2</sup>, T Blunk<sup>1</sup>, J. Tessmar<sup>3</sup>, A Göpferich<sup>1</sup>

<sup>1</sup> Department of Pharmaceutical Technology, University of Regensburg, Universitätsstraße 31, D-93053, Regensburg, Germany

<sup>2</sup> Department of Biomedical Engineering, Georgia Institute of Technology, 313 Ferst Drive, Atlanta, GA 30332-0535, USA

<sup>3</sup> Department of Bioengineering, Rice University, MS-142 PO Box 1892, Houston, TX 77251-1892 USA

Published in: European Journal of Pharmaceutics and Biopharmaceutics, 85 (2004) 385 - 407

# 1 Introduction

Besides the well-known application of low-molecular weight substances, like drugs, the application of bigger non-drug materials - like polymers, ceramics or metals - to the human body is valuable to treat, enhance, or replace a damaged tissue, organ, or organ function. Originating from their application in the biological environment, these materials are called biomaterials, because of their ability to replace or restore biological functions and exhibit a pronounced compatibility with the biological environment [1,2].

Biomaterials in general have been used for numerous applications in which their contact to cells and tissues via their surface is of utmost importance. Apart from their original use as a tissue replacement, they have increasingly been applied as carriers for drugs [3] and cells [4,5,6,7,8] in recent years. The characterization of the material interaction with cells was, thereby, frequently concentrated on issues such as biocompatibility [9,10,11,12], initiation of tissue ingrowth into the material's void space or host tissue integration. Although these properties are of paramount significance for biomaterial development and application, cell/material interactions have primarily been considered on a generalized scale, as the underlying mechanisms remain widely elusive due to the complexity and multitude of parameters involved. While research along these traditional lines has resulted in a number of biomaterials with significantly improved properties, the question arose in recent years if one could not take better advantage of biology's potential to interact with its environment more specifically. Doing so would facilitate the development of biomaterials for applications that require the control of cell behavior with respect to individual processes such as cell proliferation [13,14], cell differentiation and cell motility [15,16,17,18]. In an ideal case, this would allow for the 'design' of a material to elicit cellular responses that help the material to better perform its intended task. Applications for such designer-materials range from tissue repair or replacement to the controlled cellular uptake for the delivery of therapeutic agents [19,20].

There are two major categories of cell-biomaterial interactions: specific and unspecific. Unspecific interactions are usually difficult to control, because they are based on properties common to multiple cell types. These common cell characteristics include, for example, cell surface properties, such as the negative charge of the cell membrane, as well as ubiquitous



lipophilic membrane proteins or lipophilic proteins of the extracellular matrix that mediate unspecific adhesion to polymer surfaces.

Specific interactions, in contrast, are much more controllable as they are primarily related to the interactions of defined chemical structures, such as ligands that interact with their corresponding cell surface receptors [21]. The expressions 'biomimetic' and 'bioactive' have been coined to describe materials that are capable of such defined interactions [22,23]. In particular, biomimetic materials are materials that mimic a biological environment to elicit a desired cellular response, facilitating the fulfillment of their task [24,25]. It is obvious that drugs do not fit into such a definition, as their task is the interaction with cells 'per se'. Biomaterials of a natural origin also do not unequivocally fit into this category, because they do not mimic a natural environment, but rather provide one. Despite these crisp definitions, a gray zone exists in which materials cannot explicitly be classified.

So what is the blueprint of a biomimetic material after all? It is obvious that, for example, receptor ligands integrated into the material play an important role with respect to cell-material interactions. One has to bear in mind that the main task of a biomimetic material is not necessarily the specific interaction with a cell or tissue, but rather the fulfillment of the intended purpose, e.g. the targeting of a certain cell type or providing a scaffold structure for tissue growth; this specific interaction is intended as a tool for the material to achieve these goals. One of the first types of biomimetic materials targeted the integrin receptor to enhance cell adhesion to material surfaces [26,27]. Such materials contained exposed RGD motifs on their surface [28,29]. Other materials had cytokines tethered to their surface to target cell surface receptors that impact cell proliferation or differentiation [13,14,18]. Some of these materials have been extraordinarily successful and it is expected that more and more biomaterials will be developed that mimic the properties of biological environments in order to influence cells and whole tissues.

It is the goal of this review to give an overview of the field of biomimetic materials, which is scattered among different disciplines, such as biomaterials science, biomedical engineering, the medical sciences and pharmaceuticals. It is obvious that the definitions given above include a variety of material design principles and a number of material classes. Mimicking a natural environment could, for example, also be a matter of shaping a material on the micrometer and nanometer scale, dimensions that cells can 'sense' and respond to in defined way [30,31,32].

As a treating of the whole field is beyond the scope of this single paper, we will focus exclusively on materials that interact with cells via receptors. In the first chapter, we will elucidate the mechanisms by which cells can interact with their environment, which provide the basis for a rational material design. In the following chapter we will review the chemistry by which cell surface receptor ligands can be attached to the materials. Next we will consider two limiting cases: the scenario in which the dimension of the biomimetic material vastly exceeds the dimensions of a cell and the reverse case in which the cell is much larger than the material, which is then essentially in the nanoscale. In both cases, we report on the particular aspects of material design and actual developments. Finally, we review potential applications of biomimetic materials in tissue engineering, polymer-associated drug targeting and non-viral gene transfer into mammalian cells.

## 2 Mechanisms by which cells can interact with their environment

Mechanisms of cellular interaction with the environment are of paramount significance for biomimetic material development. In vertebrate tissues, many mechanisms exist that enable cells to communicate with their environment, specifically by means of signaling molecules. The principle of this interaction is that a ligand binds to its corresponding receptor leading to various intra- and extracellular responses. In this chapter, we will elucidate the biological principles of three interactions that are of interest for biomimetic material design: cell adhesion, morphogenic stimuli signaling and endocytosis.

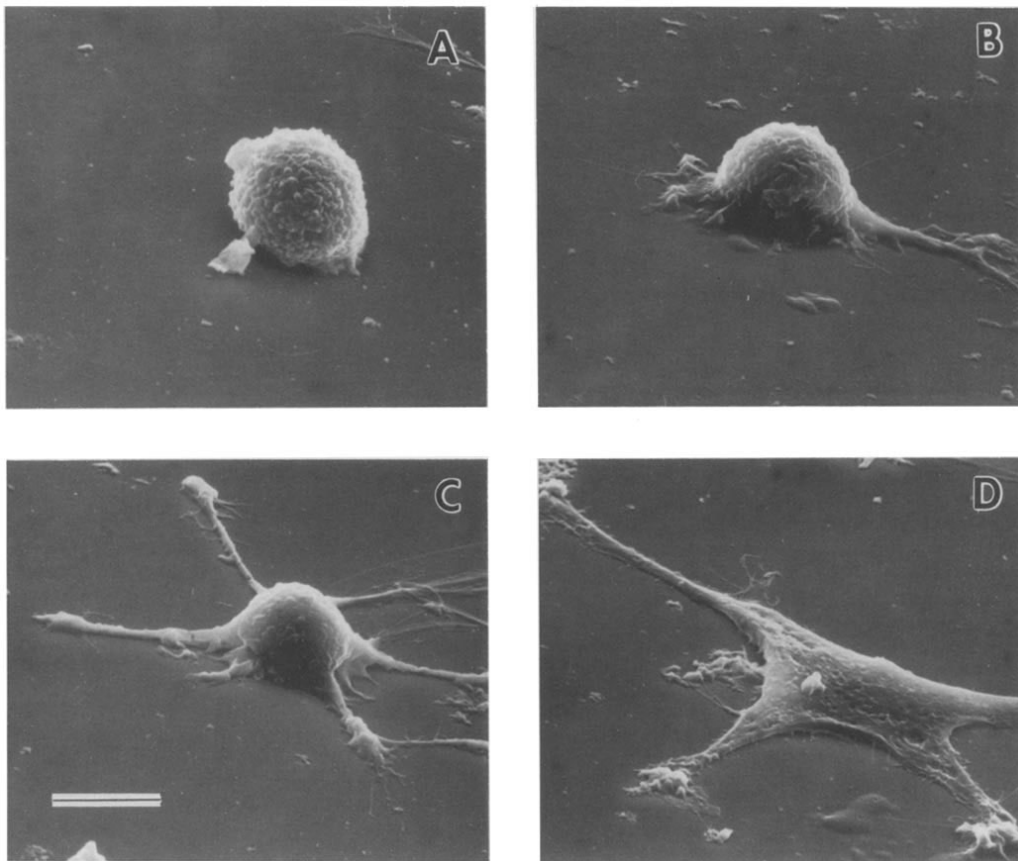


**Figure 1:** *Process of cell attachment to cell spreading. Scanning electron micrographs of adherent cells on substrates containing varying concentrations of covalently grafted peptide (GRGDY). (A) spheroid cells with no filapodial extensions; (B) spheroid cells with one to two filapodial extensions; (C) spheroid cells with greater than two filapodial extensions; (D) flattened morphology representative of well spread cells. Bar: 10  $\mu\text{m}$ . Reproduced from [38].*

## 2.1 Cell adhesion

Cell adhesion is a critical process in the field of biomaterials. In tissue engineering, for example, cell attachment is an obvious prerequisite for a number of important processes, such as cell proliferation or cell migration [33], but cell adhesion is an important component even for more established biomaterial applications such as orthopedic implants [34]. However, in many applications it may be crucial to ensure the adhesion of specific cell types. Therefore, a tremendous amount of research has been devoted to understand and, consequently, control cell adhesion.

### 2.1.1 Integrin-binding peptides

Cell-matrix adherens junctions enable cells to bind the extracellular matrix [ECM] by connecting the actin filaments of their cytoskeleton to the matrix. Members of a large family of cell-surface matrix receptors called *integrins* mediate this adhesion. Integrins are composed of two non-covalently associated transmembrane glycoprotein subunits ( $\alpha$  and  $\beta$ ). 18  $\alpha$ - and 8  $\beta$ - units have already been discovered, which form 24 known different heterodimers [35].

The tripeptide sequence Arg-Gly-Asp [RGD] has been identified as part of many natural integrin ligands and a motif on several ECM proteins [36]. The variety of receptors with different  $\alpha$  and  $\beta$  subunit combinations gives rise to differences in the receptor affinity of different RGD containing compounds. Many small adhesion peptides (RGD peptides) have been synthesized, for example RGD, YRGDS, CGRGDSY, as well as cyclic RGD peptides such as cyclo(RGDfK) [27]. About half of the 24 known integrin receptors bind to ECM molecules in a RGD dependent manner [37]. Due to the fact that integrins are distributed and used throughout the organism, the RGD sequence is an attractive compound to utilize in the stimulation of cell adhesion on synthetic surfaces.

Cell adhesion involves a sequence of four steps: cell attachment, cell spreading, organization of an actin cytoskeleton, and formation of focal adhesions (**Figure 1**) [28,38]. Following cell attachment, cells are sufficiently associated with the material to withstand gentle shear forces, whereas during the second phase the cell body becomes flat and its plasma membrane spreads over the substratum. Thereafter, actin organizes into microfilament bundles that form an actin cytoskeleton. A forth effect is the formation of focal adhesions that link the ECM to the actin

cytoskeleton. A great number of signaling events following the formation of focal adhesions are known [39].

### **2.1.2 Heparin-binding peptides and lectins**

Among the non-integrin surface receptors, proteoglycans, such as the syndecans [40], constitute a large family of molecules responsible for cell adhesion. They consist of a core protein to which the negatively charged glycosaminoglycan is covalently attached [28]. Therefore, the heparin-binding domains are rich in basic amino acids and numerous heparin binding sequences based on X-B-B-X-B-X or X-B-B-B-X-X-B-X structures have been identified [41], where B represents a basic amino acid and X a hydrophobic residue. KRSR, for example, was selectively used to promote osteoblast adhesion [42]. However, cell attachment using these sequences is usually less significant compared to integrin-binding RGD.

The carbohydrate-rich zone on the cell surface, known as the glycocalyx, can be characterized by its affinity for carbohydrate-binding proteins called lectins [43]. Wheat germ agglutinin [WGA], for example, recognizes these carbohydrates and can therefore be used for targeting cells [44].

## **2.2 Morphogenic and mitogenic factor signaling**

While the aforementioned mechanisms of communication were linked to the attachment of cells, morphogenic and mitogenic factors affect other processes such as cell mobility, cell differentiation cell proliferation. Growth factors are a class of bioactive molecules that hold great potential the development of biomimetic polymers. These polypeptides manage cellular activities through a complex network of intracellular signaling cascades. They engage in processes such as cellular proliferation, differentiation, migration, adhesion and gene expression. For each type of growth factor, there is a specific receptor or set of receptors, which some cells express on their surface and others do not.

The receptors for most growth and differentiation factors are a large family of transmembrane tyrosine protein kinases. They include receptors for vascular endothelial growth factor

[VEGF], fibroblast growth factors [FGFs], epidermal growth factor [EGF], insulin-like growth factor-I [IGF-I] and many others.

VEGF is, amongst other functions, the key regulator of normal and abnormal angiogenesis, a specific mitogen for vascular endothelial cells derived from arteries, veins, or lymphatics [45] and therefore used as a promising candidate for the stimulation of angiogenesis-dependent tissue regeneration.

FGFs are polypeptide growth factors that initiate mitogenic, chemotactic and angiogenic activity [46]. Some FGFs are potent angiogenic factors and most of them play important roles in embryonic development and wound healing. In contrast to VEGF, FGFs are pleiotropic, i.e. they control distinct and seemingly unrelated effects, because they stimulate endothelial cells, smooth muscle cells, fibroblasts and certain epithelial cells [47].

EGF exhibits mitogenic and motogenic activities [48,49] and is present in many cell types, including fibroblasts and epithelial cells. EGF, in addition to TGF- $\alpha$  (transforming growth factor- $\alpha$ ), is thought to be an important factor in inflammation and wound healing by stimulating neovascularization and chemotaxis of cells involved in wound healing [50].

IGF-I has successfully been shown to induce proliferation of chondrocytes and stimulate the synthesis of ECM components in an *in vitro* cartilage model [51]. Furthermore, it has been demonstrated that the IGF-I receptor is different from the insulin receptor, but there is communication between IGF-I and insulin and their receptors [52].

The TGF- $\beta$  superfamily comprises a large number of polypeptide growth factors [53] and, in contrast to the above mentioned factors, they activate receptors that are serine/threonine protein kinases [54]. TGF- $\beta$  has been shown to play a major role in wound healing and fibrosis, and has been recognized to be very important in tissue repair due to its ability to stimulate cells to deposit ECM [55]. TGF- $\beta$ 1, for example, is a key factor during bone development and regeneration [56,57].

A number of other extracellular signaling proteins are structurally related to the TGF- $\beta$ s and also belong to the TGF- $\beta$  superfamily. Among them, the bone morphogenic proteins [BMPs] play an important role in bone formation [54]. BMP-2 is reported to be a useful growth factor to increase osteoblastic differentiation of rat marrow stromal cells [rMSCs] [58,59].

## 2.3 Endocytosis

A third important biological principle is the particle uptake into cells via lipid bilayer vesicles formed from the plasma membrane, usually termed endocytosis. Being able to activate this mechanism using a biomimetic material would provide tremendous opportunities for delivering drugs and DNA more efficiently into the cell. Two main types of endocytosis are distinguished, generally classified as phagocytosis and pinocytosis. Phagocytosis involves the internalization of large particles ( $> 0.5 \mu\text{m}$ ), whereas pinocytosis describes the formation of smaller vesicles ( $< 0.2 \mu\text{m}$ ) [60]. These vesicles are initiated at specialized regions of the plasma membrane called clathrin-coated pits, which, in association with transmembrane receptors, can serve as a concentrating device for the internalization of specific extracellular macromolecules, a process called receptor-mediated endocytosis. The macromolecules bind to complementary cell-surface receptors, accumulate in clathrin-coated pits and enter the cell in clathrin-coated vesicles that end up in endosomes. Thereafter, the receptor proteins can be recycled, degraded in lysosomes or return a different plasma domain [61].

This process can be used for the uptake of molecules in hepatocytes, which express the asialoglycoprotein receptor [ASGPr], a receptor that selectively recognizes glycoproteins containing galactose residues [62]. The transport of macromolecules into the cell by receptor-mediated endocytosis with transferrin as a targeting moiety via the transferrin receptor can be utilized in rapidly dividing tissues [63]. Another possible uptake route to clathrin-mediated endocytosis is via caveolae [64].

### 3 Conjugation chemistry for biomimetic molecules

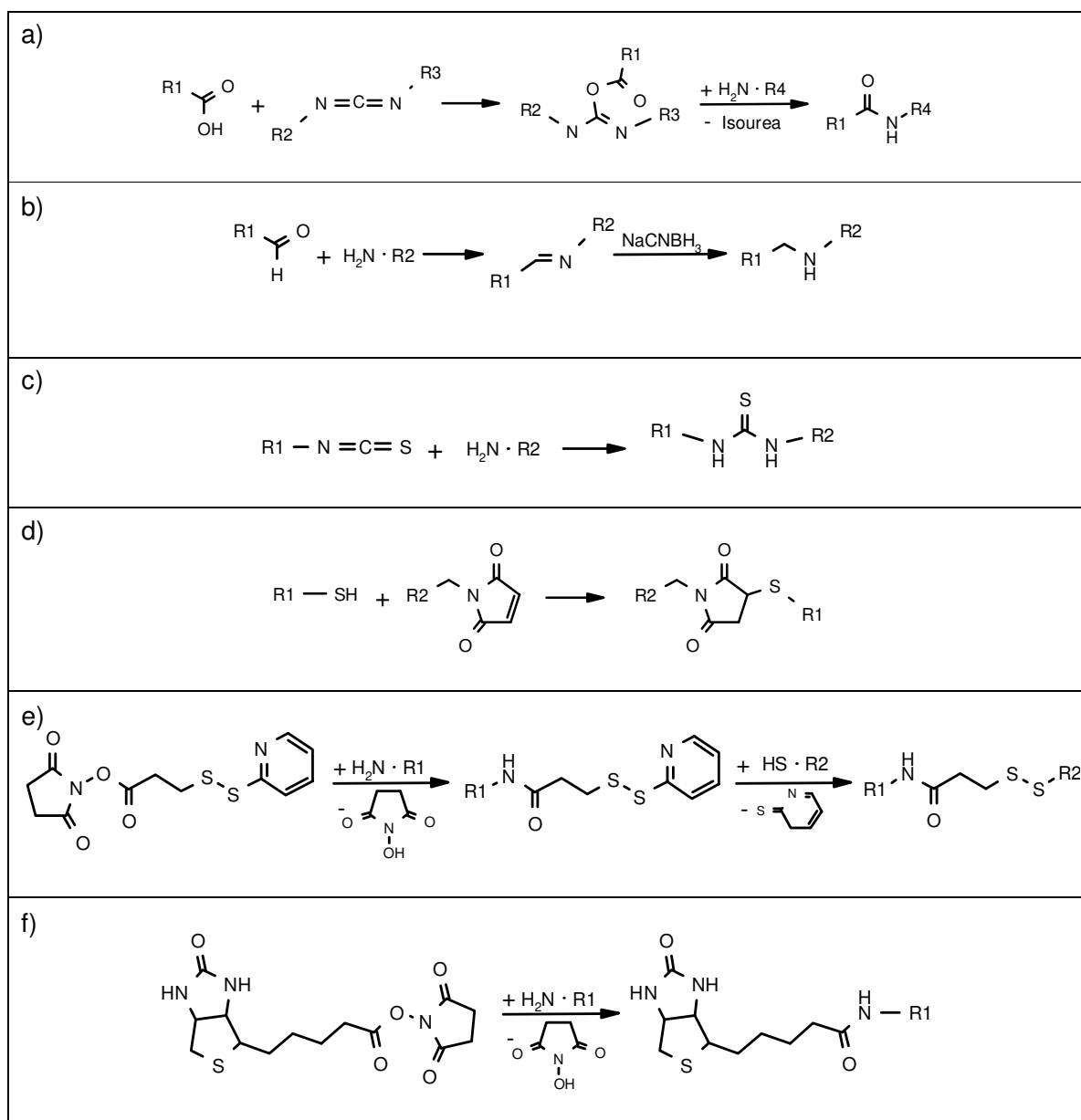
Biomimetic materials can be synthesized in numerous ways. One method includes a complete de novo synthesis of all components including the cell signaling entities. As this is different for each individual material, it is beyond the scope of this review to go into such details. An alternative is the design of the material that can be assembled from components. Molecules that are used for cell signaling are then considered one building block that is attached to the backbone of the material via functional groups on the polymer. This design strategy has the advantage that bioactive molecules can be bound to the material surface after processing the polymer into its final form. In this chapter we will review the most popular binding reactions that can be used for such an assembly.

#### 3.1 Carbodiimide-conjugation (Table 1 a)

Carbodiimides belong to the zero length cross-linking agents, forming bonds without the introduction of additional atoms or spacers. Their application is favorable in conjugation reactions, where such spacer might be detrimental for the intended use of the corresponding conjugates. Their applicability in both organic and aqueous solvents contributes to the wide spectrum of possible conjugation reactions.

Carbodiimides are widely used to activate carboxylate groups by the formation of highly reactive O-acylisourea intermediates [65]. This active species can then react with amine nucleophiles to form stable amide bonds. Water soluble carbodiimides, such as 1-ethyl-3-(3-dimethylaminopropyl)-carbodiimide hydrochloride [EDC], allow for an aqueous conjugation reaction of water soluble targeting molecules and polymers. To circumvent hydrolysis [66], organic soluble carbodiimides, like dicyclohexyl carbodiimide [DCC], have been used to form ester linkages or amides with the corresponding carboxylic acids at high efficacy in anhydrous solutions [67,68]. To avoid undesirable side reactions [69], N-hydroxysuccinimide [NHS] or N-hydroxysulfosuccinimide [Sulfo-NHS] can be added to form more stable NHS ester derivatives as reactive acylating agents. The corresponding NHS or Sulfo-NHS esters react readily with nucleophiles to form the acylated product, but only primary or secondary amines form stable amid or imide linkages, respectively [70].



**Table 1:** Conjugation mechanisms

a) Carbodiimide mediated reaction of amines with carboxylic acids.

b) Reductive amination.

c) Reaction of isothiocyanates with nucleophiles.

d) Reaction of maleimides with thiols.

e) SPDP mediated crosslinking of amines with thiols.

f) Biotinylation of amines.

Many examples of carbodiimide mediated conjugations are present in the literature: the T101-antibody has been directly conjugated to PLL taking advantage of the water solubility of EDC [71], folic acid was covalently bound to poly[aminopoly(ethylene glycol)cyanoacrylate-co-hexadecyl cyanoacrylate] using DCC/NHS mediated amide synthesis [72] and, in a different reference, folic acid was also linked to the terminal hydroxyl of the PEG block of poly(L-histidine)-co-poly(ethylene glycol) by DCC and 4-dimethylaminopyridine [DMAP] mediated acylation [73].

### 3.2 Reductive amination (Table 1 b)

Reductive amination results in a zero-length cross-linking between aldehyde and amine components, forming stable amine bonds without the introducing of additional, possibly unfavorable spacer.

Native carbohydrates contain aldehyde groups as reducing ends and can be directly coupled with amine-containing molecules, leading to the formation of a Schiff base intermediate. Unfortunately, the direct coupling of the reducing carbohydrates with amines suffers a rather low efficiency, due to the comparatively low concentration of the open structure in aqueous solution compared to the cyclic hemiacetal form. Alternatively, carbohydrates often also contain hydroxyl groups on adjacent carbon atoms, which can be oxidized to reactive aldehyde groups using sodium periodate [74,75].

After the reaction in an aqueous environment, Schiff bases are rapidly reversed to the corresponding aldehyde and amine by hydrolysis. The Schiff bases formed can be converted into stable secondary amine linkages by reductive amination using reducing agents, such as sodium cyanoborohydrid, which reduces Schiff bases efficiently while aldehydes do not react [76,77]. Carbohydrates like galactose have been directly coupled to polyethylenimine [PEI] by reductive amination [78], while transferrin, a glycoprotein, was oxidized using the periodate oxidation method before conjugation with the amine component PLL [79].

### 3.3 Isothiocyanate reaction with nucleophiles (Table 1 c)

Isothiocyanates are homobifunctional linkers, which react almost selectively with primary amines leading to the formation of stable thiourea compounds. Unfortunately, their use is afflicted with only poorly controllable reactions, the formation of rather random conjugates, as well as polymerization or intramolecular cross-linking giving byproducts with altered solubility.

The reaction has its pH optimum at an alkaline pH, where amines are deprotonated [80]. With the help of the isothiocyanate linker, galactose and lactose have been conjugated to PLL [81].

### 3.4 Reaction of maleimides with sulfhydryls (thiols) (Table 1 d)

Maleic acid imides (maleimides) are also an integral part of many heterobifunctional cross-linking agents, allowing for the covalent attachment of bioactive molecules to polymers in a two-step procedure. This minimizes the side reactions prevalent in the use of homobifunctional linkers. Over a pH range of 6.5-7.5, maleimides can be specifically alkylated at their double bond by a reaction with sulfhydryl (thiol) groups to form thioether bonds [82,83,84]. Although at a higher pH, some cross reactivity with amino groups can occur, as well as a ring-opening reaction caused by hydrolysis [85], the sulfhydryl specificity and stability of the maleimide group in aqueous solvents can be controlled by the pH of the reaction medium and the choice of maleimide derivative. The selective conjugation of sulfhydryls to maleimides has been applied by linking the thiolated OX26 monoclonal antibodies to hydroxy-polyethyleneglycol-maleimide [86] and in the attachment of cys-folate to poly(L-lysine) [PLL] [87].

### 3.5 Sulfhydryl (thiol)-reactive cross-linking agents (Table 1 e)

Another class of heterobifunctional cross-linking agents widely used in conjugation chemistry contain both an amine-reactive group, such as an NHS ester, and a sulfhydryl-reactive end, like the 2-pyridyldithio group in N-succinimidyl 3-(2-pyridyldithio)propionate [SPDP] [88,89]. Conjugation with these linkers follows a two-step or multi-step process, offering

more control over the route of reaction. The NHS esters are used to form stable amide linkages with primary amines resulting in sulfhydryl-reactive intermediates. In a second step, these intermediates are combined with the sulfhydryl-containing molecule to form a disulfide bond by a thiol-disulfide exchange [90]. These sulfhydryl-reactive intermediates can also be used to create a sulfhydryl group in the molecule to be attached by reducing the disulfide bond with reductive agents like DTT [91]; the resulting free thiol group allows for conjugation with various sulfhydryl-reactive groups, like maleimides or iodoacetal groups [92]. A sulfhydryl containing RGD-peptide [92] and thiolated transferrin [93] were covalently bound to PEI and PLL, respectively, using SPDP and DTT.

### 3.6 Biotin binding to avidin, streptavidin and neutravidin

Avidin and streptavidin consist of four subunits each carrying one biotin binding site in a pocket beneath the protein surface. The multivalent nature of these four binding sites enhances the sensitivity and selectivity for ligand interaction, favoring the use of avidin/streptavidin-biotin systems in immunoassay. Both proteins bind biotin by a non-covalent, biospecific interaction similar to receptor-ligand recognition with a dissociation constant of  $1.3 \times 10^{-15}$  M [94]. Biotin binds to avidin or streptavidin by its bicyclic ring, while the valeric acid side chain is not involved. Therefore biotinylation agents possess an acylating active group, such as an NHS ester, on the valeric side chain for binding of amine-containing molecules, creating a stable amide bond (**Table 1 f**). NHS-biotin, the simplest biotinylation agent, is insoluble in water, while the sulfo-NHS-biotin can be easily used under aqueous conditions. To enhance the accessibility of biotin to sterically hindered binding sites on streptavidin or avidin, long-chain derivatives, such as N-succinimidyl-6-(biotinamido)hexanoate [NHS-LC-biotin] and sulfo-NHS-LC-biotin, the water soluble derivative, have been developed [95]. To enable the recovery of targeting molecules from biotin binding, derivatives with cleavable long-chains, such as NHS-SS-biotin and sulfo-NHS-SS-biotin, have been introduced [96]. Replication-deficient adenovirus [97], EGF and PLL [98] and diamine polyethylene glycol [44] have been biotinylated using NHS-LC-biotin, NHS-SS-biotin and biotin, respectively, enabling non-covalent interaction with streptavidin, avidin or neutravidin.

## **4 Biomimetic polymers designed for manufacturing devices exceeding the dimensions of a single cell**

In many cases, biomimetic polymers are not designed to interact with individual cells, but rather with multiple cells or even whole tissues. This means that the materials are processed into devices with large surfaces compared to the dimensions of a single cell. Applications include the use as classical biomaterials to replace damaged or lost tissues or as cell carriers in tissue engineering applications. It is obvious that the boundary between these applications cannot be sharply drawn, however, as the signaling from the material surface to cells is an important feature in both cases. In recent years, the field of tissue engineering profited tremendously from the improvement of biomimetic materials as they allow to better control tissue development individual cells. In this approach, many biological aspects ranging from cell attachment to cell differentiation are involved and need to be understood and also controlled. In the following section, we illustrate how biomimetic polymers were designed based on already existing biomaterials.

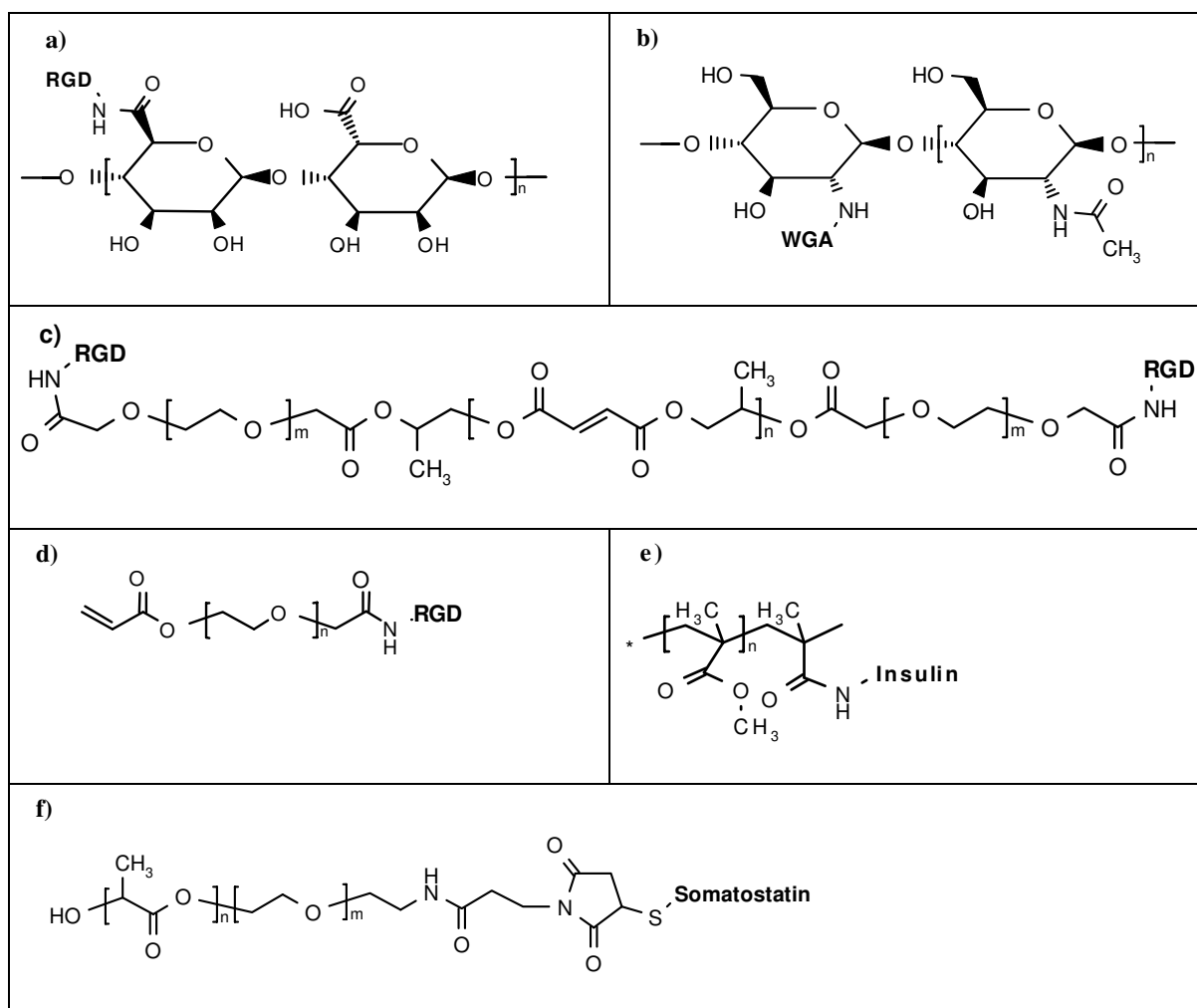
The polymers used for this approach can be divided in two major classes based on their physicochemical properties hydrogels, water swollen networks composed of hydrophilic polymers [99], from solid lipophilic materials that show little water uptake and at least initially maintain their mechanical properties when brought into an aqueous environment. Both classes exhibit certain advantages with regard to their applications. Hydrogels allow for high diffusion rates of nutrients, drugs and oxygen [100] and can often be injected with or without cells, allowing for a minimally invasive implantation [101]. Furthermore, they can easily adapt to the shape of the defect site by virtue of their flow properties and eventually harden by in situ gelation [101]. The main advantage of rigid polymers is their mechanical stability even after implantation, something that can be achieved for hydrogels only after cross-linking. Furthermore, these materials provide cells with a good environment for processes such as cell adhesion and migration [5].

## 4.1 Hydrogel materials

Hydrogel polymers for tissue engineering applications range from naturally derived to synthetic materials. Alginate, gelatin, agarose, fibrin, chitosan are examples of naturally derived polymers, whereas poly(ethylene glycol) [PEG], oligo(poly(ethylene glycol) fumarate) [OPF], poly(acrylic acid) [PAA] derivatives, and poly(vinyl alcohol) [PVA] represent synthetic materials. In the following sections, we will describe a selection of material classes that have been used extensively for the development of biomimetic polymers by the methods described above.

### 4.1.1 Alginates (Table 2 a)

Alginate, a linear polysaccharide copolymer of (1-4)-linked  $\beta$ -D-mannuronic acid and  $\alpha$ -L-guluronic acid, is widely used due to its low toxicity and ready availability [101]. Its main advantage is its easy modification with peptides due to the many free carboxylic acids on the polymer backbone and mild gelation conditions. Alginate gels can be cross-linked using divalent cations ( $\text{Ca}^{2+}$ ,  $\text{Ba}^{2+}$ , or  $\text{Sr}^{2+}$ ) or by covalent chemical cross-linking techniques [102,103]. A common approach to improve cell-alginate interactions is to covalently link the integrin binding peptide sequence RGD or its derivatives to the polymer backbone. The free carboxylic groups of the latter are activated using EDC/NHS and reacted with the terminal  $\text{NH}_2$ -group of the peptide [104,105,106]. Suzuki et al. tethered a BMP-2-derived oligopeptide to the alginate chains to enhance its suitability for bone tissue engineering [107].

**Table 2:** *Examples of biomimetic polymers*

*Materials derived from natural hydrogel type polymers: a) Alginate-RGD; b) Chitosan-WGA.*

*Materials derived from synthetic hydrogel type polymers: c) PPF-PEG-RGD; d) PEG-RGD.*

*Materials derived from lipophilic polymers: e) PMMA-Insulin; f) PEG-PLA-Somatostatin*

#### 4.1.2 Chitosans ( Table 2 b)

Chitosan is a linear polysaccharide of (1-4)-linked D-glucosamine and N-acetyl-D-glucosamine. It is quite suitable as a substrate for biomimetic polymers not only because of its structure, which is quite similar to the glycosaminoglycans found in native tissue [101], but also because the free amino groups in the polymer backbone are easily modified. Gelation occurs after increasing the pH of the chitosan solution [100,108] or extruding solutions into a nonsolvent [108]. The polymer is readily modified by the covalent attachment of molecules

with free carboxylic acids using carbodiimide chemistry. Wang et al. covalently bound wheat germ agglutinin, a lectin molecule, to chitosan to enhance cell-biomaterial interactions by first activating WGA using EDC and afterwards reacting these products with the amine groups of chitosan to form stable amide linkages [109].

### 4.1.3 **Fibrin**

Another naturally derived polymer is fibrin, a polypeptide. It is naturally formed during blood coagulation from fibrinogen, which is cleaved by thrombin and subsequently covalently cross-linked by factor XIIIa [110,111]. This natural substrate is a suitable candidate for implantation because it is degraded by enzymes. Schense et al. modified this polymer by incorporating the integrin binding adhesion peptides RGD and DGEA [111]. They designed bi-domain peptides, with a factor XIIIa substrate in one domain and a bioactive molecule in the other. During fibrin-cross-linking, the peptides were incorporated in the resulting hydrogel. Zisch et al. used the same method to bind VEGF derivatives to fibrin hydrogels [110].

### 4.1.4 **PEGs (Table 2 d)**

PEGs are very popular synthetic polymers frequently used in tissue engineering and drug delivery applications. Although PEG derivatives provide only endgroups for chemical modification, they are frequently used, because they are nontoxic and nonadhesive towards proteins, resulting in suitable model systems. In order to process PEG into a hydrogel, each end of the polymer chain must be modified with either acrylates or methacrylates, which are sensitive to photo-cross-linking [101,112]. As an example, PEG with two terminal hydroxyl groups can be converted to an acrylate with acryloyl chloride [112]. To enable sufficient cell-material interactions, like selective cell attachment, RGD-sequences have been grafted to this rather hydrophilic polymer [113,114,115]. Mann et al. reported reduced extracellular matrix production of cells cultured in these hydrogels [13]. They tried to overcome this shortcoming



by additionally binding TGF- $\beta$ 1 on a PEG-acrylate-spacer to the polymer via a radical reaction.

#### **4.1.5 Poly(propylene fumarate) derived copolymers with PEG [PEG-PPF] (Table 2 c)**

The amphiphilic triblock copolymer derived from a low molecular weight poly(propylene fumarate) [PPF] with two terminal PEG units represents another class of synthetic hydrogel forming materials and holds great promise for tissue engineering and drug delivery applications. Its aqueous solutions allows for a thermo reversible gelation with final cross-linking of the fumarate double bonds. This results in a system applicable in a minimally invasive manner. Moreover, these PPF-based hydrogels are biodegradable, because they contain several hydrolytically cleavable ester groups in the polymer backbone. Jo et al. synthesized a triblock copolymer consisting of two terminal carboxymethyl PEG units and one poly(propylene fumarate) block in the middle of the copolymer [116]. The terminal free carboxylic groups allow for conversion to succinimidyl esters using NHS/DCC chemistry resulting in polymers, which could be readily modified with RGD sequences. Numerous other derivatives of fumarate-derived polymers for hydrogel formation have been developed in recent years, such as oligo(poly(ethylene glycol) fumarate) [OPF] cross-linked with PEG-diacrylate [117,118].

#### **4.1.6 PAA derivatives**

Although acrylic acid derived polymers are known to degrade slowly, they are frequently used as tissue engineering scaffolds due to the easy structure modifications of the resulting hydrogels. In addition, some derivatives such as N-isopropylacrylamides show thermoreversible gelation. Stile et al. studied cell-material interactions on N-isopropylacrylamide based hydrogels modified with RGD-peptides and heparin-binding FHRRIKA-sequences [119]. Hydrogels were prepared by radical copolymerization of N-isopropylacrylamide, acrylic acid and N,N'-methylenebisacrylamide. The free acid groups stemming from acrylic acid were linked to diamino-PEG using EDC and N-hydroxysulfosuccinimide. With sulfosuccinimidyl 4-(maleimidomethyl)-cyclohexane-1-carboxylate, the free amine group of the immobilized PEG was converted to a double bond

sensitive to attack from free thiol groups of the peptides. Thus, the integrin-binding RGD-sequences and heparin-binding FHRRIKA-sequences were bound directly to the polymer backbone. A different acrylic acid derivative, N-(2-hydroxypropyl)methacrylamide) [HPMA], was altered by tethering RGD sequences or aminosugar residues, which interact with glycosyltransferases on cell surfaces, to the hydrogel [120]. Hydrogels were synthesized by radical copolymerization of HPMA with either RGD or glucosamine derivatives modified with methacryloyl residues.

## **4.2 Lipophilic and water insoluble polymers**

Lipophilic and water insoluble polymers have also been modified to form biomimetic polymers in recent years. Degradable materials are typically chosen for tissue engineering applications, because a gradual resorption of the material is necessary to achieve the ideal complete replacement of the defect with living, functional tissue. Non-degradable materials have, however, been investigated for research applications, to achieve increased biocompatibility or enhanced tissue integration of medical implants. Many non-degradable materials, such as polystyrene or polyacrylate, have furthermore been modified to yield biomimetic materials. The following chapter represents a selection of materials, more of which are described in the literature [121,122,123,124].

### **4.2.1 Polystyrene [PS]**

Although it is not biodegradable, polystyrene provides a good model system for lipophilic surfaces. To make use of the cell culture approved polymer, Park et al. synthesized a sugar-bearing PS derivative with RGD grafted to the polymer backbone using carbodiimide chemistry to investigate the changes in the behavior of hepatocytes on these modified polymer surfaces [125]. It also linked insulin to non-degradable poly(acrylic acid) chains and grafted them to standard polystyrene films [126].

#### **4.2.2 Poly(methylmethacrylate) [PMMA] (Table 2 e)**

PMMA can easily be modified following the hydrolysis of some methyl ester groups in a basic environment. Peptide sequences can be bound to PMMA surfaces through subsequent reaction of the obtained acid residues with amine groups of peptides using EDC chemistry [127]. An alternative constitutes the tethering of the bioactive molecule to an acrylate anchor and grafting this molecule to the PMMA backbone using UV-irradiation. Schaffner et al., for example, used this method to covalently link insulin to PMMA surfaces [128].

#### **4.2.3 Poly(lactic-co-glycolic acid) [PLGA] and poly(lactic acid) [PLA]**

The most frequently used materials for tissue engineering applications are PLGA [129] and PLA [130], because of their excellent biocompatibility, their FDA approval, and the established procedures to form rigid scaffolds for the cultivation of cells.

PLGA chains are terminated with a free carboxyl group, which can be used for modification of the polymer. In one example of PLGA modification, a galactose derivative was bound directly or via a PEG spacer to the acidic end of the molecule [129]. Using NHS/DCC chemistry, an amine containing galactose derivative or PEG diamine was tethered to the polymer. Lactobionic acid was then grafted to the remaining free amine group of PEG using carbodiimide chemistry. As the regular PLA chain contains few reactive centers and is also prone to hydrolysis, an alternating block copolymer of lactic acid and lysine was used to provide free reactive amine groups in the polymer backbone [131]. RGD peptides were then covalently attached to the resulting free amine groups using CDI as connecting molecule.

A new class of active PLA derivatives was designed by Tessmar et al. [25] (**Table 2 f**). To reduce uncontrolled protein adsorption to the lipophilic PLA, a diblock copolymer with hydrophilic PEG was synthesized, starting from PEG and D,L-lactide in the presence of stannous 2-ethylhexanoate [132,133]. The PEG chain terminates with an amine group presenting a possible modification site. To activate this polymer for protein attachment, the amine group was converted to a reactive carboxylic group using L-tartaric acid or succinic acid as a linker with standard carbodiimide chemistry. Alternatively, a thiolreactive group was introduced via  $\beta$ -alanin and maleic acid anhydride resulting in a thiol reactive maleinimide.

Insulin, as an aminecontaining protein, and somatostatin, a substance with a cleavable disulfide bridge, were shown to attach to these activated polymers. To process the active polymers, Hacker et al. developed a new anhydrous method for scaffold fabrication to maintain the binding activity, resulting in highly porous cell carriers, which can be easily modified with proteins for use in tissue engineering [24].

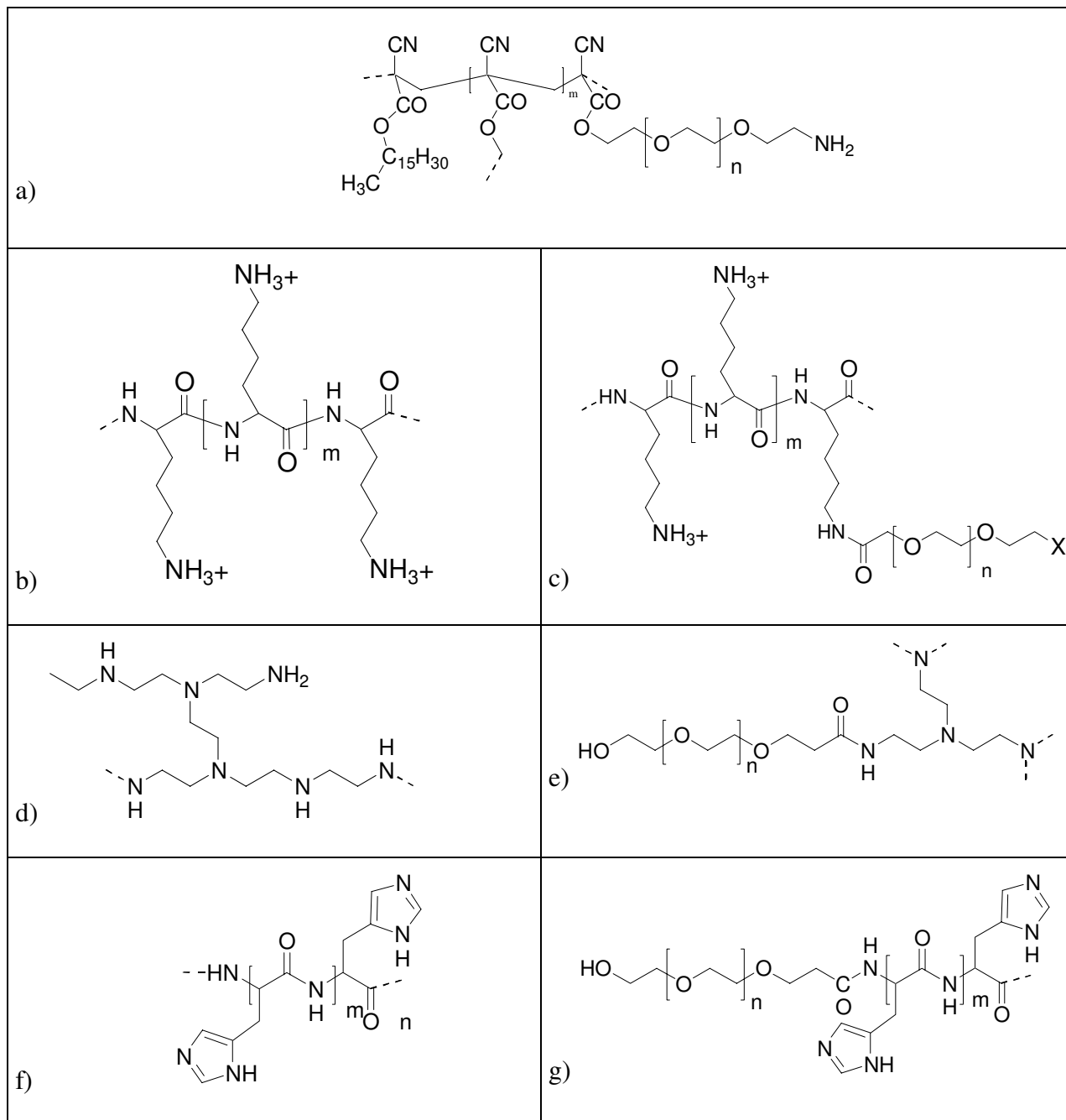
## **5 Biomimetic polymers designed for manufacturing devices with sizes below the dimensions of a single cell**

In this chapter, we will shed some light on biomimetic polymers developed especially for the manufacture of nanoparticulate delivery systems. Biomimetic nanoparticles hold great promise to facilitate the cellular uptake of drugs and DNA as well as for drug targeting applications. In contrast to many of the materials used for the interactions with tissues and multiple cells, a prominent design feature of the materials described here is that many of them are amphiphilic or have a block copolymer structure that facilitates the manufacture of colloidal aggregates.

Unfortunately, following intravenous administration, most particulates are rapidly removed from the bloodstream by the reticuloendothelial system [RES], typically due to phagocytosis by macrophages [134] in the liver and spleen, limiting the efficiency as drug delivery system. The formation of nanoparticles with an outer hydrophilic shield consisting of poly(ethylene glycol) [135], poloxamer [136], albumin [137], cyclodextrine [138,139] or transferrin [140] reduces unspecific cell adhesion, minimizing the rapid clearance by the RES, providing long circulating drug delivery systems [141,142].

EGF-antibodies, such as B4G7, growth factors like EGF or FGF, transferrin, or vitamins like folic acid or biotin were applied as targeting agents, because of the well-known over-expression of the corresponding cell surface receptors on tumor cells [143,144,145].

Again, a plethora of materials have been developed in recent years, which we cannot review exhaustively, but rather only on the basis of selected examples. We will thereby distinguish between materials that have primarily been designed for the delivery of drugs and those that have been designed for the delivery of DNA, which also have to condensate the DNA with the help of cationic building blocks.

**Table 3:** A few examples of polymers used for the preparation of nano-scaled materials

**a)** poly(H2NPEGCA-co-HDCA) synthesized by Stella et al. [72]; **b)** PLL; **c)** PLL-PEG, synthesized by Leamon et al. [79]; **d)** PEI; **e)** PEI-PEG, synthesized by Ogris et al. [136]; **f)** poly(HIS); **g)** poly(HIS-PEG), synthesized by Lee et al. [73]

## 5.1 Polymers for the preparation of nanoparticles for drug delivery

### 5.1.1 Polycrylate-blockcopolymers

Stella et al. synthesized a poly[aminopoly(ethylene glycol)cyanoacrylate-co-hexadecyl cyanoacrylate] [poly(H<sub>2</sub>NPEGCA-co-HDCA)] copolymer involving derivatization of the monomers followed by polymerization. The biodegradability of the copolymer was introduced by connecting the N-protected aminopoly(ethylene glycol) or n-hexadecanol to the cyanoacrylate backbone. The PEG-coated nanoparticles were prepared by subsequent precipitation. In contrast to other coupling strategies, which involve several reactive groups accessible for conjugation, the NHS ester of folic acid was selectively attached to the terminal amino group of the hydrophilic PEG block of the preformed poly(H<sub>2</sub>NPEGCA-coHDCA) nanoparticles [72] (**Table 3 a**). Li et al. encapsulated DNA into poly(H<sub>2</sub>NPEGCA-co-HDCA) nanoparticles using a water-oil-water solvent evaporation technique and coupled transferrin selectively to the terminal amino group of the PEG chains by reductive amination, establishing a potential delivery system of therapeutic genes to the target cells [146].

Pan et al. followed an elegant strategy leading to small shell cross-linked nanoparticles with an amphiphilic core-shell morphology, a rather unique design for a biocompatible long-circulating drug carrier system. The diblock [PAA-b-PI] was synthesized by nitroxide-mediated radical polymerization of tert-butyl acrylate and isoprene. Micelles were further stabilized by the intramicellar cross-linking of acrylic acid residues located within the shell domain of PAA-b-PI nanoparticles, using a homobifunctional diamino-cross-linking agent [147]. The remaining free carboxylate groups were activated with a water-soluble carbodiimide and coupled selectively with the terminal amino group of a folatetagged PEG-amine (**Figure 2**).

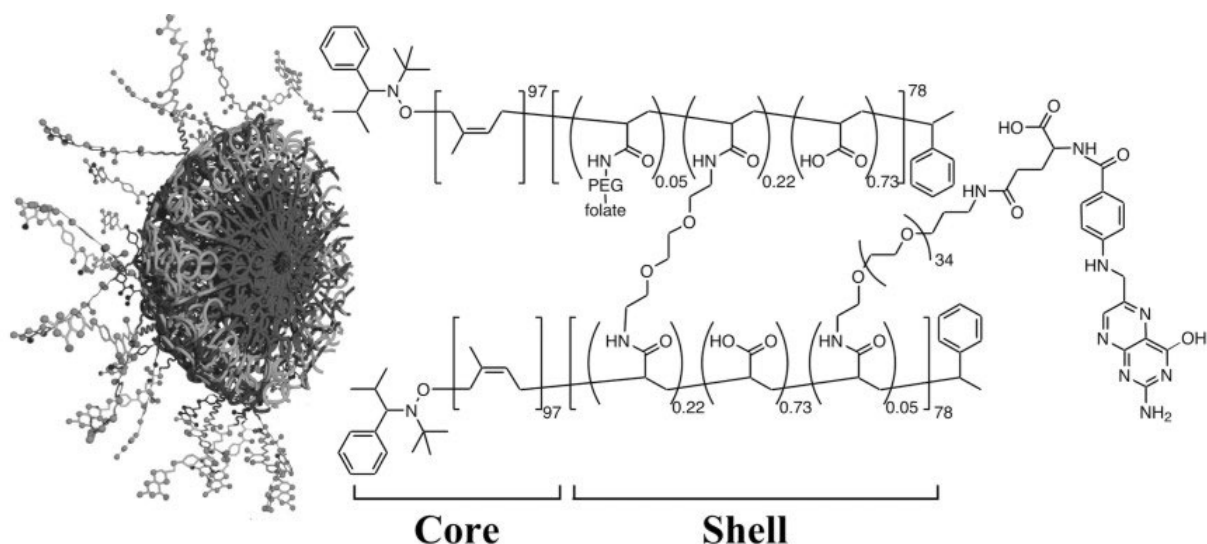


**Figure 2:** Intramicellar cross-linked [poly(acrylic acid)-b-polyisoprene]nanoparticles. A part of acrylic acid residues of PAA-b-PI micelles were activated followed by conjugation with a diamino linker to achieve intramicellar shell cross-linking. The remaining acrylic acid groups were coupled with the folate-PEG amine to prepare folic acid-conjugated shell cross-linked nanoparticles. Reproduced from Pan et al. [147].

### 5.1.2 Poly(ethylene glycol)-co-poly(caprolactone) [PEG-PCL]

Gref et al. prepared a unique model system for the study of cell-material interactions enabling tagging with any biotinylated ligand or even multiple ligand binding on the surface of engineered nanoparticles. For the synthesis of the amphiphilic PEG-PCL diblock copolymer, poly(ethylene glycol)-bis amine was conjugated to biotin by carbodiimidazole-mediated amide synthesis directed primarily to obtain the mono-biotinylated amino-PEG derivative [44]. The remaining amine group has been used as the initiator for the polymerization of  $\epsilon$ -caprolactone, catalyzed by stannous octanoate, to give the biotinylated PEG-PCL-copolymer. From this polymer, nanoparticles were formed by nanoprecipitation, in part using mixtures of biotin-PEG-PCL and PEG-PLA. The nanoparticle suspension can be incubated in avidin solutions and the final particles isolated by centrifugation. As a model substance, a biotinylated lectin, WGA, has been attached to the nanoparticle surface by adding it to the avidin-coated nanoparticle suspension. The potential use of these nanoparticles as drug



delivery systems for oral or even intravascular administration, as proposed by Gref et al., must still be investigated.

### **5.1.3 Poly(ethylene glycol)-co-poly(L-lactic acid)**

Olivier et al. described the so-called immunonanoparticles consisting of a mixture of methoxypoly(ethylene glycol)-co-poly(L-lactic acid) [MePEGPLLA] and maleimide-poly(ethylene glycol)-co-poly(L-lactic acid) [maleimide-PEGPLLA] tagged with monoclonal antibodies [MAb] to the rat transferrin receptor [86]. The MAbs undergo receptor-mediated transcytosis across the brain microvascular barrier via the endogenous blood-brain barrier transferrin transport system, enabling drug delivery targeted specifically at the brain. The copolymers were synthesized by ring-opening polymerization of L-lactide on the terminal hydroxyl group of the corresponding methoxy-poly(ethylene glycol) or maleimide-poly(ethylene glycol), catalyzed by stannous octanoate. The desired targeting peptide had been thiolated on the primary amino group using Traut's reagent. The nanoparticles were prepared using an emulsion/solvent evaporation technique using blends of MePEGPLLA and maleimide-PEGPLLA. The targeting peptide was then conjugated by the formation of a stable thioether to the PEG-shield of the prefabricated nanoparticles.

### **5.1.4 Poly(L-histidine)-co-poly(ethylene glycol) [Poly(His)-PEG]: Poly(ethylene glycol)-co-poly(L-lactic acid) –mixtures**

Poly(His)-PEG is a copolymer that forms nanoparticles containing a pH-sensitive [148] biodegradable and fusigenic [149] poly(L-histidine) [poly(His)] inner core, shielded by an outer PEG layer. Poly(His) has been synthesized by a base-initiated ring-opening polymerization of protected N-carboxy anhydride [NCA] of L-histidine and has been coupled to carboxylated PEG [73]. To achieve a selective internalization of the nanoparticles by tumor cells, DCC and DMAP-mediated ester formation has been used to covalently bind folic acid and aminated folic acid to the terminal hydroxyl group of the PEG blocks of the N-protected poly(His)-PEG-copolymer and PEG-PLA, respectively. The nanoparticles were prepared using blends of different weight ratios of PEG-PLA and poly(His)-PEG to control the pH-

sensitivity and stability of the micelles. The nanoparticles were loaded with the anti-tumor drug adriamycin [ADR], purified by dialysis and isolated by lyophilization (**Table 2 f**, **Table 3 f** and **Table 3 g**).

## 5.2 Polymers for non-viral gene delivery

Polycations spontaneously condense DNA due to the strong ionic interaction with the negatively charge phosphorous groups of the DNA backbone, leading to the formation of nanometer-sized particles, known as polyplexes [150].

The efficacy of the DNA complexation depends on the molecular weight and cationic charge density of the polymer and is important for the protection of DNA *in vitro* and *in vivo* and also for the stability of the resulting complexes [151]. Since most of these complexes enter the cells via unspecific endocytosis [152,153], the conjugation of a hydrophilic shield on the surface of the polyplexes reduces the competing unspecific cell adhesion in favor of the specific receptor-mediated uptake enabled by attached targeting molecules.

It has been shown that the ligand coupling using long PEG spacers improves the accessibility for receptor binding, leading to better cellular uptake and to reduced cytotoxic side effects [87,150].

Unfortunately, the direct PEGylation of the cationic polymers (pre-PEGylation) leads to derivatives with reduced DNA complexation efficacy. To overcome this problem, methods have been established to conjugate PEG to the pre-formed polyplexes (post-PEGylation) [154,155].

Below we will describe a few materials that have been used for DNA delivery that have been modified to achieve better efficiency with biomimetic principles. Many of them are derived from polycationic polymers, which were altered by the formation of block copolymers and/or the attachment of biologically active entities to allow for better cellular uptake and also extended bioactivity.

### 5.2.1 **Poly(L-lysine) [PLL] derivatives**

PLL itself has been widely used as non-viral vector for gene delivery, favored due to the biodegradability of the polypeptide and accessibility within a broad molecular weight range.

The  $\epsilon$ -amine groups in the side chain of the polyamide backbone exhibit multiple cationic charges in an aqueous environment at physiological pH. Several targeting molecules, such as growth factors, vitamins, transferrin and carbohydrates, have been tagged to PLL by conjugation to the primary  $\epsilon$ -amine groups. Unfortunately the majority of the delivered PLL-DNA polyplexes remains sequestered within the endosomal-lysosomal compartment, which dramatically reduces transfection efficiency [156,157].

Different research groups have supplemented polyplexes with endosomolytical substances, such as adenovirus [71,79,97,158,159], chloroquine [144,160], or endosome disruptive peptides [161,162], facilitating the release of the polyplexes from the endosome, yielding improved gene expression. Merwin et al. conjugated the T101 antibody, which specifically binds to the CD5 moiety exhibited on T lymphocytes, to poly(L-lysine) [PLL] using carbodiimide chemistry. The specificity and relative amount of interaction of the corresponding polyplexes with cells expressing the CD5 moiety was observed using the iodinated T101 derivative [71].

B4G7, a mouse monoclonal antibody, which is uniquely internalized by EGF receptor-mediated endocytosis, has been tagged to PLL through a stable disulfide bond by disulfide exchange with PLL-SH and B4G7-SS-pyridine using SPDP and DTT [163]. The extent of antibody-binding was evaluated by the binding assay using [<sup>125</sup>I]B4G7 and a competitive inhibition assay.

To achieve tumor cell targeting, the NHS ester of folic acid has been covalently bound to PLL by acylation of the primary amine functions of the polymer [157]. Transferrin, a carbohydrate residue containing protein, has been tagged to the polymer by sodium periodate oxidation and subsequently reductive amination [79,158] or also by disulfide linkage [93]. The corresponding polyplexes were formed after the conjugation of the targeting molecule.

Asialofetuin, a natural ligand of the hepatocyte-specific asialoglycoprotein receptor and the artificial ligand tetragalactose-peptide, have been coupled to PLL via disulfide linkages [164]. The tetragalactose has been linked to a synthetic peptide by reductive amination using sodium

cyanoborohydride and subsequent coupling to PLL. Both vectors were used in transfection experiments evaluating their targeting properties in direct comparison. A similar approach has been taken by Erbacher et al., who link galactose and lactose to PLL using isothiocyanate as a linker to prepare liver targeted non-viral vectors (**Table 3 b**) [81].

### 5.2.2 PLL-PEG-copolymers

To increase the mobility of the used targeting molecule, hydrophilic PEG can also be used as a spacer with the cationic poly(L-lysine). In another attempt to target the folate receptor, folate- $\gamma$ -cysteine was covalently bound to N-(hydroxysuccinimidyl-poly(ethylene glycol)-maleimide [NHS-PEG-maleimide] at the maleimide end of the polymer [87]. Then prefabricated PLL-DNA polyplexes were mixed with the folate-PEG-NHS and a folate-tagged PEG shield was **Table 3 c**).

### 5.2.3 Non-Covalent Conjugates of PLL

Another approach to actively targeting poly(L-lysine) takes advantage of the non-covalent attachment of targeting molecules using the ionic biotin-avidin/streptavidin-interaction. This conjugation strategy enables the attachment of any biotinylated or streptavidinylated targeting molecule to the corresponding match, creating a “universal” vector for a variety of different targeting sites. Here transfection experiments were performed to clarify the influence of complex structure on transfection efficiency *in vitro*, while the ability of *in vivo* applications still remains untested. Xu et al. attached epidermal growth factor [EGF] to PLL of varying chain lengths by biotinylating both EGF and PLL using NHS-SS-biotin [98]. The conjugation was then initiated by the addition of avidin, streptavidin or neutravidin followed by DNA complexation, using mediums with low and high ion concentration.

Wagner et al. conjugated replication-deficient adenovirus both covalently and non-covalently to PLL to assure the colocalization of the endosomolytically active adenovirus and the PLL-DNA polyplexes in the endosomal-lysosomal compartment. The covalent linkage was facilitated by a transglutaminase reaction [97]. To enable the non-covalent attachment,

streptavidin has been conjugated to mercaptopropionate-linked PLL by a stable disulfide bond using SPDP-modified streptavidin. Adenovirus has been biotinylated using NHS-LC-biotin, facilitating the optimal accessibility of biotin for the four binding sites of streptavidin. DNA was added to the corresponding adenovirus-PLL conjugates to form the so-called binary complexes, leading to a non-viral vector combining both DNA complexation and endosomolysis. To achieve active tumor targeting, transferrin-tagged PLL chains, formed via reductive amination, were added to the binary complexes, leading to the so-called ternary complexes.

#### 5.2.4 **Polyethylenimine (PEI) derivatives**

Because of the chemical structure of the trivalent amine, PEI exists in two forms, as either a linear or branched polyamine. By combining a high transfection efficiency and endosomolytical properties, enabling the accelerated release of PEI-DNA-polyplexes from the endosomal-lysosomal compartment, PEI prevails as a promising polymer for the design of non-viral vectors [152,165].

Several different targeting molecules have been tagged to polyamines to achieve active and specific transport of the DNA-polymer polyplexes into the cell interior. To achieve asialoglycoprotein receptor-mediated polyplex uptake, galactose-bearing PEI has been prepared by reductive amination and was then used for DNA complexation [78]. Similar to this approach, Bettinger et al. conjugated tetragalactose to PEI, confirming receptor selectivity by direct comparison to the tetraglucosylated PEI derivative [166].

Moreover, RGD peptides were also covalently bound to PEI to achieve specific cell adhesion, enhancing the cellular uptake [92]. Here, sulfhydryl-terminated RGD-peptides were used, facilitating the covalent attachment by disulfide bonds, formed by a SPDP-mediated disulfide exchange (**Table 3 d**).

### **5.2.5 Poly(ethylene glycol)-co-poly(ethyleneimine) [PEG-PEI]**

Using hydrophilic diblock copolymers, a transferrin-tagged PEG-PEI has been synthesized by coupling transferrin to PEI using sodium periodate oxidation and reductive amination with sodium cyanoborohydride [135,167]. The polyplexes were formed with plasmid DNA and PEGylated by adding the commercially available NHS ester of propionic acid poly(ethylene glycol) to the polyplex suspension (post-PEGylation). In both cases, improved transfection efficiency has been observed in *in vitro* and *in vivo* experiments, which has been attributed to the effective shielding properties of both PEG and transferrin as well enhanced cell uptake, due to the specific targeting by transferrin conjugation. (**Table 3 e**).

### **5.2.6 Non-Covalent Conjugates of PEI**

Similarly to PLL, epidermal growth factor was also non-covalently bound to PEI. The NHS ester of biotin-PEG was thereby linked to EGF via an amide bond leading to mono- and multi-PEGylated EGF derivatives. Afterwards, streptavidin was attached to the PEI-DNA polyplexes by ionic interaction and then mixed with the EGF-tagged biotin-PEG, leading to non-covalently bound complexes joined by the biotin-streptavidin interaction [168].

## 6 Examples for applications in tissue engineering

Biomimetic materials, in general, hold a great potential for specifically controlling cellular functions and behavior, which is of tremendous importance, where the creation of new tissues is concerned. Here we will illustrate that by giving a few examples from the field of tissue engineering.

To demonstrate the retained bioactivity of peptide sequences tethered to fibrin hydrogels, Schense et al. investigated the neurite outgrowth in hydrogels modified with the adhesion-mediating sequences RGD or DGEA, which exhibit different integrin specificity, or the non-adhesive sequence RDG [111]. Dorsal root ganglia from 8-day-old white chicken embryos were individually embedded in the different three-dimensional hydrogels. Additionally, soluble peptides were added to the hydrogel as a control, serving as competitive inhibitors. After 48 hours of culture, the incorporation of RGD resulted in reduced neurite outgrowth, whereas DGEA enhanced neurite outgrowth as expected. The use of RDG or supplemented soluble peptides led to the same level of neurite outgrowth as in unmodified fibrin (**Figure 3**).

Other hydrogels, like oligo(poly(ethylene glycol) fumarate) [OPF] derived hydrogels, were also modified with RGD sequences to promote the specific binding of marrow stromal cells [118]. Shin et al. investigated the influence of the polymer PEG chain length, cross-linking density, and the preincubation of marrow stromal cells [MSCs] with soluble RGD peptides on the extent of cell adhesion. Longer PEG chains, attached as peptide tethers, and previous blocking of the integrin receptors on the cell surfaces led to reduced cell adhesion, whereas the cross-linking density had no effect on the cell behavior. These results suggest that MSC attachment on the previously non-adhesive OPF gels can be achieved by means of peptide incorporation and an appropriate length of the peptide anchorage chain (**Figure 4**).

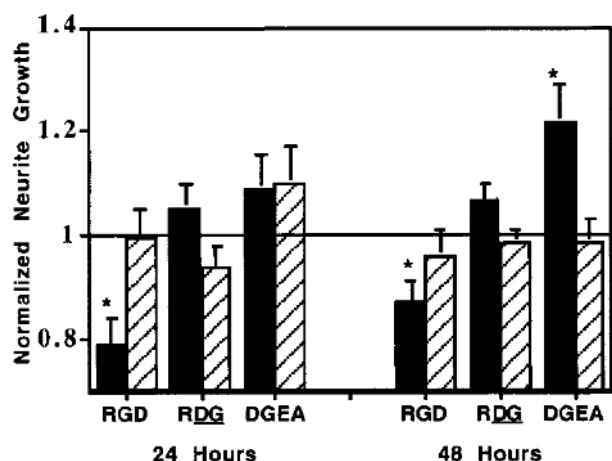


**Figure 3:** The effect of tethered peptide on neurite outgrowth in fibrin gels. All tested hydrogels were modified with covalently linked peptides. Cells were cultured with (hatched bars) or without (solid bars) soluble peptides additionally supplemented to the culture medium. (\*) means  $p < 0.05$  compared to the unmodified hydrogel. Error bars indicate standard deviation from the mean ( $n=3$ ). Reprinted with permission from Schense et al. [111].

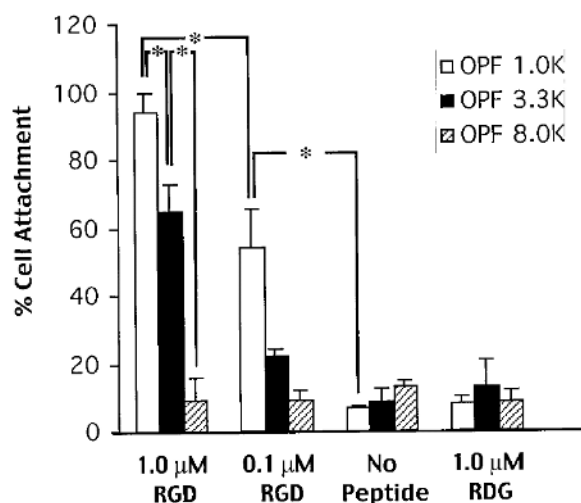


**Figure 4:** Percent cell attachment on different OPF hydrogels. Rat marrow stromal cells seeded on hydrogels fabricated by crosslinking OPF with PEG diacrylate. 1.0K, 3.3K, 8.0K represent the number average molecular weight of PEG prior to OPF synthesis. H 1X, H 3X, and H 5X, indicate a 1:1, 3:1, and 5:1 ratio of double bonds in PEG-diacrylate to those in OPF, respectively, correlating to cross-linking density of the resulting hydrogels. Error bars indicate standard deviation from the mean ( $n = 3$ ). Reproduced from Shin et al. [118].



The effect of various sugar-modified PLGA and PEG-PLGA diblock copolymers on hepatocyte cell attachment was examined by Yoon et al. [129]. Hepatocytes were isolated from 40-week-old male Sprague-Dawley rats and their attachment on different surfaces was investigated. The results indicate that galactose enhances cell attachment better than glucose, with only a maximum blend ratio of 1% of sugar-modified to unmodified polymer. Introduction of PEG spacers decreased the overall amount of attached cells; longer PEG chains resulted in even fewer adsorbed cells.

Besides the attachment of adhesion-mediating peptides, there are also applications where bigger proteins, like growth factors, are attached to the polymer surface, leading to extended bioactivity and distinct localization of the factor.

Suzuki et al. investigated the *in vivo* effect of BMP-2 derived oligopeptides on ectopic bone formation [107]. The peptides were either covalently linked or physically mixed into an alginate gel and 10 mg of the gel were injected in the calf muscle of Wistar rats. After 3 and 8 weeks, the implanted region was removed and stained with hematoxylin and eosin or van Kossa stain followed by microscopic observation. Implant groups with covalently linked oligopeptides showed osteoblast ingrowth and mineralization in the pores of alginate hydrogels after 3 weeks (**Figure 5 A**) and abundant trabecular bone formation was reported after 8 weeks of implantation. On the other hand, the control group with the non-covalently bound BMP-2 derivative showed no mineralization after 3 weeks (**Figure 5 B**) and after 8 weeks the hydrogel was completely bioabsorbed.

The effect of immobilized insulin on the culture of Chinese hamster ovary [CHO] cells was studied by Ito et al. [127]. Insulin grafted on poly(methylmethacrylate) films enhanced the proliferation of CHO not only compared to unmodified PMMA films, but also with regards to the addition of the same amount of free insulin. After harvesting the cells by EDTA treatment, new cells could be cultured on the films. Up to 4 utilizations were performed with only a slight decrease in insulin activity, possibly due to coverage of the films with proteins secreted from the growing cells.

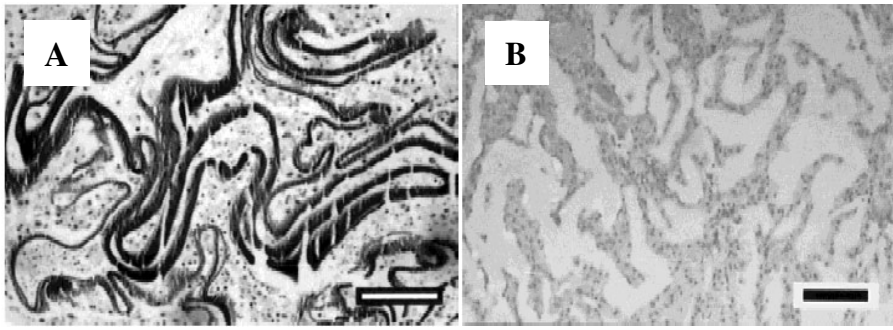


**Figure 5:** *Photomicrographs of alginate hydrogel implants modified with a BMP-2 derivative. Von Kossa staining after three weeks of implantation in calf muscle of rats. Scale bar 100  $\mu$ m. A) Implants with covalently linked peptide. Black stains indicate mineralization. B) Implants with mixed peptide show no mineralization. Reproduced with slight modifications from [107].*

## 7 Applications of nano-scaled materials

Under aqueous conditions, amphiphilic copolymers self-assemble into micelles containing a hydrophobic core surrounded by a shell composed of the hydrophilic blocks [169]. Different methods, such as diafiltration, dialysis, nanoprecipitation or emulsion techniques, have been used for the preparation of nanoparticles, which have been widely used as nanocontainers for drug and plasmid DNA delivery or in immuno assays [170].

A variety of biocompatible and biodegradable polymers have been used for the preparation of nanoparticles using folic acid as a tumor targeting unit, among them poly(H<sub>2</sub>NPEGCA-co-HDCA) and PEG-PLA or PEG-His-copolymers. Poly(H<sub>2</sub>NPEGCA-co-HDCA) nanoparticles were tagged with folic acid to an extent of 14-16% calculated on the total number of PEG chains (**Figure 6**) [72]. The recognition efficacy of the attached folic acid by the folate binding protein [FBP], the soluble form of the folate receptor, was demonstrated by surface plasmon resonance analysis, enabling the real-time analysis of the molecular association. FBP was immobilized on an activated dextran-coated gold film on the surface of a sensor and the folic acid-tagged nanoparticles were allowed to interact with the modified surface of the sensor, revealing even lower dissociation constants compared to free folic acid. Stella et al. attributes the greater binding affinity of the folate-conjugated nanoparticles to the stronger interaction with the FBP receptor clusters with the multivalent form of the ligand folic acid on the nanoparticle surface. The corresponding nanoparticles lacking the folic acid tag, did not associate with the immobilized FBP.

Lee et al. conjugated folic acid to the PEG shield of pH-sensitive poly(His-PEG) and PEG-PLA blended poly(His-PEG) nanoparticles, incorporating adriamycin [73]. The application of a mixture of polymers for the preparation of nanoparticles increased their stability against dissociation and facilitated the controlled pH-dependent release of the antitumor agent triggered by only slight changes in the pH, similar to those measured in the tumor interstitial fluid. The cytotoxic effect of ADR was evaluated using folic acid-tagged nanoparticles as well as non-targeted nanoparticles with human breast adenocarcinoma cells, confirming that the cytotoxicity of ADR-loaded nanoparticles was dependent on the pH of the environment. The conjugation with folic acid increased the cytotoxicity, indicating an enhanced uptake of nanoparticles by endocytosis. This effect could even be augmented by the fusigenic effect of

poly(His), facilitating the endosomal release of ADR after the particle uptake by human breast adenocarcinoma cells[MCF-7].

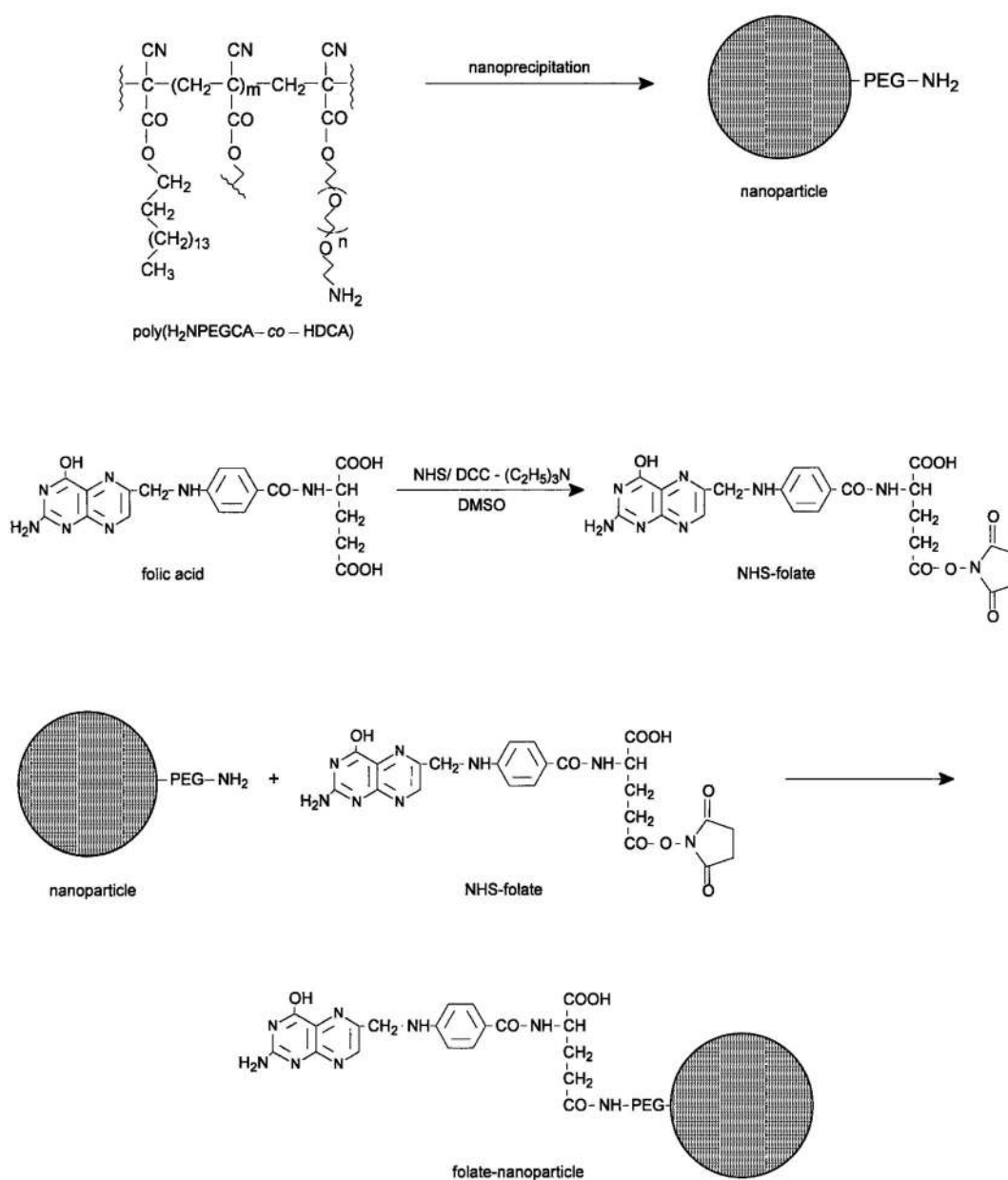


**Figure 6:** Preparation of poly( $H_2NPEGCA-co-HDCA$ ) nanoparticles and conjugation with folic acid. Nanoparticles with an outer amino-PEG layer were prepared by nanoprecipitation of poly( $H_2NPEGCA-co-HDCA$ ). In a second step folic acid was transformed to the succinimidyl ester, using DCC, NHS, and conjugated to the terminal amino group of the PEG block on the nanoparticle surface. Reproduced from [72].

Another approach of active targeting has been followed by Li et al.: the coupling of transferrin, an iron-transporting serum glycoprotein, onto the surface of PEG-coated biodegradable polycyanoacrylate nanoparticles to deliver incorporated plasmid DNA as a therapeutic device into tumor cells [146]. The DNA was microencapsulated utilizing a double emulsion technique with the addition of polyvinyl alcohol to prevent the relaxation of DNA into the linear form, which exhibits less efficient gene expression [171]. The cell association studies were performed with K562 cells, using tagged and untagged nanoparticles, revealing an improved target cell binding. The application of free transferrin decreased the extent of association of the transferrin-labeled nanoparticles with the cell surface, confirming the selectivity of the receptor interaction.

Gref et al. prepared nanoparticles from biotinylated PEG-PCL-copolymer enabling the attachment of any ligand, or even a multiple ligand coupling, by taking advantage of the biospecific interaction of biotin and avidin [44]. The PCL-block displays the hydrophobic core, which can be used for drug incorporation, while the flexible PEG blocks serve as spacer for the biotin coupling, enabling maximal accessibility for the biotin-binding site beneath the avidin surface. The nanoparticles were prepared using biotinylated PEG-PCL and PEG-PLA blends and were obtained in a size range of 90-100 nm, which only slightly increased after the binding of avidin. Biotinylated WGA, a model lectin, which specifically recognizes cell surface carbohydrates, such as N-acetyl-D-glucosamine and N-acetylneuraminic acid, was used to target anticancer drugs to colon carcinoma cells. Nanoparticles consisting of PLA, PEG-PLA, PEG-PCL and ligand-decorated PEG-PCL were used in cell association and cytotoxicity experiments performed on the human colon adenocarcinoma cell line Caco-2, measuring the cell-associated radioactivity by incorporating radioactively labeled PLA into the core of the nanoparticles. Only the WGA-tagged nanoparticles showed specific interaction with the cell surface, leading to a 12-fold increase in cell association. The biotin labeling enables the attachment of any biotinylated ligand by the addition of avidin, facilitating a broad use in the design of drug delivery systems (**Figure 7**).

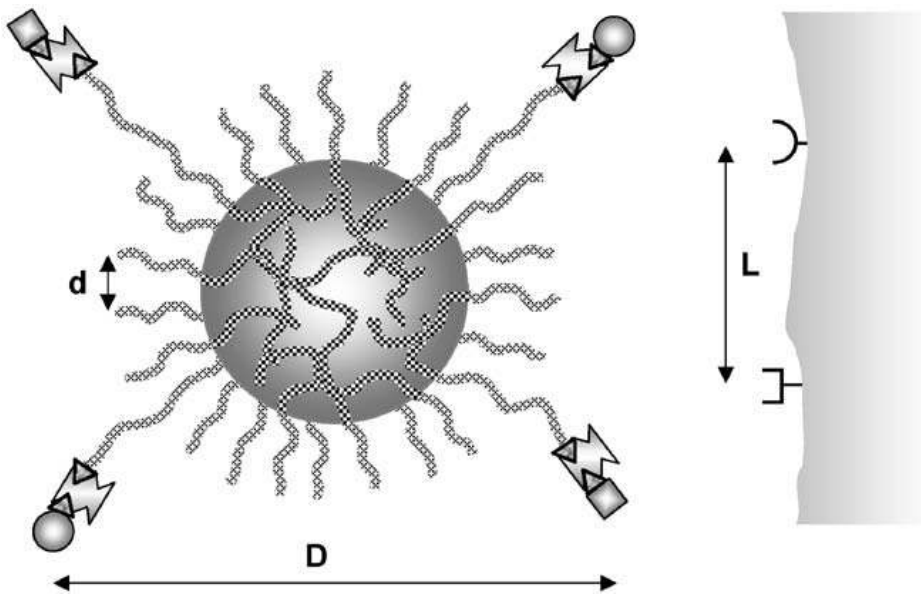


**Figure 7:** Schematic representation of a core-corona nanoparticle coated with a PEG ‘brush’ (distance  $d$  between two terminally attached PEG chains). Several PEG chains carry a covalently linked biotin molecule ( $\blacktriangle$ ), which binds one avidin molecule ( $\bowtie$ ). Three biotin binding sites remain available to enable the further attachment of different biotinylated ligands, separated by a distance  $D$ , through interaction with avidin. The functionalized nanoparticle (left) could further interact with a target cell (right) bearing two different surface receptors at a mean distance  $L$  from one another. Reproduced from Gref et al. [44].

## 8 Applications for non-viral gene delivery

Gene therapy could become a promising tool for the treatment of inheritable or acquired diseases by delivering DNA into living cells to correct genetic abnormalities [172].

Viral vectors provide high transfection efficiency and can deliver DNA into specific cell populations. The risk of immunogenic or toxic reactions triggered by the viral components of the vector, however, as well as viral recombination or undesired activation of potential oncogenic sequences, restricts their application in human gene therapy [173,174,175]. Despite a lower transfection efficiency and limited duration of the resulting gene expression, using non-viral vectors for this purpose may be a promising strategy to overcome such difficulties [176]. Unfortunately, most non-viral vectors provoke membranolysis or host cell complexation, leading to a tremendous loss of viable transfected cells. To enhance the transfection efficiency in specific cells and reduce cytotoxic effects on other tissues, targeting molecules have been attached.

To achieve better cell specificity, Merwin et al. conjugated T101 murine monoclonal antibodies, which bind to the CD5 moiety on the surface of T lymphocytes, covalently to PLL [71]. Jukat cells and T lymphocytes, as CD5 positive cells, were used in a radioactive competitive cell binding assay. To examine the specificity of receptor binding, the HUH-7 hepatocyte cell line without the CD5 moiety was used as a negative control. Sub-cellular fractionation allowed for the detection of the polyplexes in different cell compartments, revealing that the T101-PLL-DNA complexes were still entrapped within endocytotic vesicles. To facilitate a sufficient release of the corresponding polyplexes from the endosome, an adenovirus suspension was incorporated into the complexes before incubation. A sufficient transfection efficiency, determined by luciferase expression, was only achieved by the adenovirus-associated polyplexes; without the endosomolytic virus no transfection occurred.

To ensure the co-localization of the adenovirus with the polyplex in the endosome, Wagner et al. formed binary complexes by conjugating the virus to PLL using streptavidin-biotin binding or transglutaminase reaction, followed by the DNA complexation [97]. To achieve active targeting, ternary complexes were prepared by conjugating transferrin to PLL before addition to the binary complexes. The transfection efficiency was determined by measuring

the luciferase gene expression in different human and murine cell lines. Investigation of the endosomolytical activity revealed that the ternary complexes with the transglutaminase-conjugated adenovirus had a significantly better transfection efficiency than the complexes together with chloroquine or adenovirus. The specificity of transferrin targeting was confirmed on adenovirus-receptor lacking K562 cells, showing the highest transfection efficacy of the ternary complexes and possessing both the targeting agent for the transferrin receptor and the endosomolytical properties of the adenovirus.

Leamon et al. tagged folic acid to high molecular weight PLL using PEG spacers with different lengths and investigated the impact on transfection of different cell lines measuring the luciferase gene expression and  $\beta$ -galactosidase expression [87]. The application of PEG with a minimum molecular weight of 3400 has been shown to be most profitable, exhibiting a 10-fold to 74-fold enhancement of transfection efficiency in the different cell types compared to the polyplexes without the spacer. This finding correlates well with the “individual” folate receptor expression. Leamon et al. contributed the increased luciferase gene expression to the improved accessibility of the folate ligand for receptor binding.

Many research groups have taken advantage of the endosomolytic properties of PEI to design efficient non-viral vectors with enhanced transfection efficiency facilitated by the accelerated release of the polyplexes from the endosomal-lysosomal compartment. The use of endosomolytic agents, such as adenovirus, could be circumvented, reducing the competitive adenovirus-receptor targeting.

Lee et al. attached biotin-tagged PEGylated EGF non-covalently to the surface of streptavidin-coated PEI-DNA polyplexes, evaluating the effect of EGF-mono- and multi-PEGylation, biotin-streptavidin molar ratio and streptavidin-DNA molar ratio on polyplex stability, complex size and transfection efficiency [168]. Increasing amounts of streptavidin were bound to the PEI-DNA polyplexes by ionic interaction [streptavidin-PEI-DNA]. The mono-PEGylated EGF and multi-PEGylated EGF were non-covalently bound to polyplexes with a molar ratio of DNA-streptavidin of 1:100 by biotin-streptavidin interaction using increasing biotin-streptavidin ratios [EGF-PEG-biotin-streptavidin-PEI-DNA] (**Figure 8**). The mono-PEGylated EGF conjugated to the polyplex surface formed very stable polyplexes of a size up to 200nm, while complexes decorated with multi-PEGylated EGF exhibited abrupt aggregation. Transfection experiments were performed on the A431 cell line, which



over expresses EGF receptors, applying non-targeted PEI-DNA complexes, streptavidin-PEI-DNA polyplexes and mono- and multi-PEGylated EGF-coated EGF-PEG-biotin-streptavidin-PEI-DNA-complexes, determining the luciferase gene expression. Lee et al. revealed that the PEGylation reduces unspecific cell adhesion, while the conjugation of EGF enhanced receptor-mediated cell uptake, hence increasing transfection efficiency.

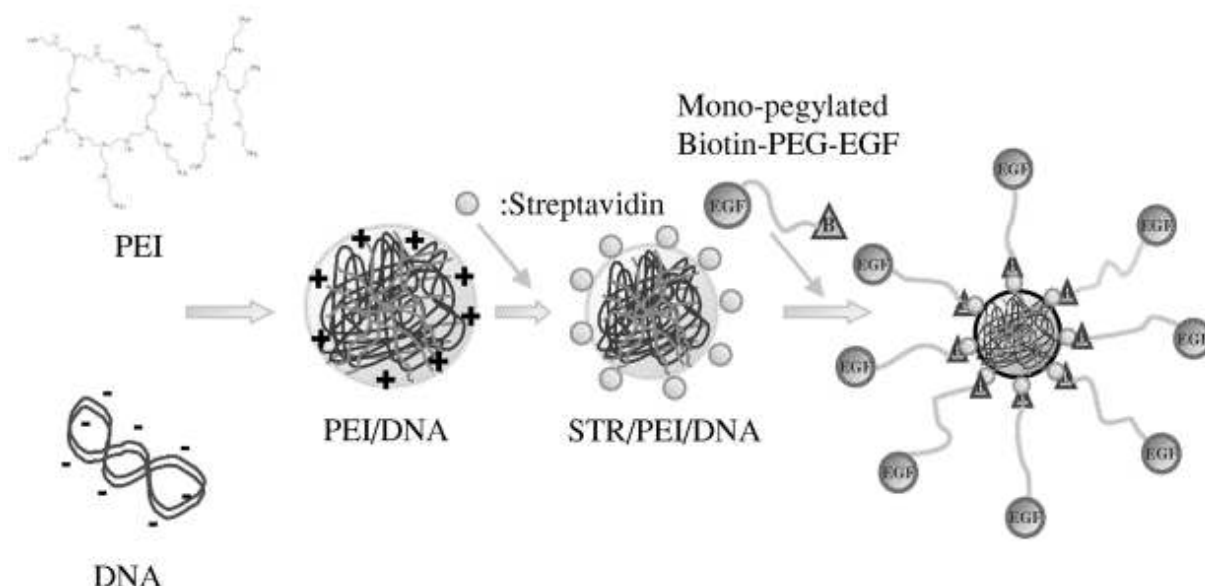


**Figure 8:** Schematic illustration of mono-PEGylated EGF-PEG-biotin-streptavidin-PEI-DNA complexes: DNA was condensed with an excess of PEI to form positively charged polyplexes, which, in a second step, have been coated with streptavidin by ionic interaction, yielding neutrally charged polyplexes. Finally biotin-PEG tagged EGF was conjugated to the complexes by non-covalent attachment to streptavidin, decorating the nanoparticle surface with a PEG-shield and the targeting agent. Reproduced from Lee et al. [168].

Kircheis et al. used the plasma protein transferrin to prevent unspecific interaction with plasma compounds and erythrocytes, demonstrating that transferrin exhibited a shielding effect on PEI 25000 even without prior PEGylation [167]. The in-vitro transfection experiment with K562 cells exhibited a significantly higher transfection efficiency of the transferrin-tagged polyplexes. Motivated by the successful application of the transferrin-tagged PEI-DNA polyplexes in the in-vitro experiments, Kircheis et al. investigated the transfection efficiency and organ distribution of transferrin-tagged and non-tagged PEI-DNA polyplexes in an *in vivo* subcutaneous tumor model. PEI with molecular weights of 800,000

and 25,000 were used for DNA complexation; the polyplexes were injected into mice and the transfection efficiency was assayed by the luciferase gene expression. These experiments showed that only the charge-shielded formulations of transferrin-incorporating PEI25000 and PEG-coated Transferrin-PEI800000-DNA polyplexes preferentially distributed in the distant tumor, confirming the protective properties of both agents against protein adsorption, enabling the design of long-circulating vectors for gene delivery.

## 9 Conclusions and future challenges

Biomimetic polymers are used in many different applications ranging from the targeting of single cell types for the delivery of drugs or DNA to modified biomaterials that interact with whole tissues, like implants or prostheses. This review displayed current strategies for biomimetic material design and hopefully gave further ideas for future developments. Selected examples demonstrated the importance of the polymer features to better achieve the intended goals for the biomaterial's main purpose.

The challenges in this field, however, are enormous and frequent, since the knowledge of the whole biological system or even the single cell, which is the main target in all these approaches, is still limited. We must gain a much deeper insight into the biological principles to understand all of the phenomena that are involved in small cellular events, like, for example, the transfer of genes by viruses or the attachment and differentiation of cells on biocompatible surfaces. However, the biomimetic materials introduced in this paper are also useful tools to investigate and elucidate all of these biological principles. Here especially, variable designs allow for the detailed exploration of different signaling molecules, leading to a much broader understanding of cellular communication.

Hopefully, some of the future developments will result in improvements of the therapy of various diseases, which cannot be treated today, and allow for the achievement of better healthcare.



# **Chapter 2**

## **Goal of the Thesis**

The number of patients in our society needing replacement of severed, missing or malfunctioning tissue due to diseases, traumata or age, is high and still growing. Burn wounds, bone diseases, diabetes or liver insufficiency are examples of such suffering. Conventional attempts of remedy like drug supplementation, mechanical devices or xenografts are often unsatisfactory and fall short of the goal of enabling normal life. An innovative therapy approach is Human Tissue Engineering, a discipline dedicated to the field of regenerative medicine. To fulfill the promises raised by first successes, significant research efforts have been designated on this area, focusing on various subjects, such as cells, scaffold materials, culture conditions, bioactive molecules, and others.

An important milestone on the route for Tissue Engineered products, was the use of “intelligent” materials, such as biomimetic polymers, which may themselves influence cell adhesion and direct cell development (**Chapter 1**). Biomimetic substances are designed to mimic a biological environment, insomuch eliciting cellular responses that help the material to better perform the intended task.

A polymer with favorable characteristics with regards to its use as scaffold material for Tissue Engineering applications is the poly(ethylene glycol)-block-poly(lactic acid) copolymer. The poly(ethylene glycol) block is responsible for suppression of unspecific protein adsorption, whereas the main advantages of the poly(lactic acid) block is its biodegradability. If the free group of the poly(ethylene glycol) block provides a reactive group, the polymer is easily processed into a biomimetic polymer, by covalent attachment of a bioactive molecule, such as bFGF. Diblock co-polymers with different molecular weight, namely MePEG<sub>2</sub>PLA<sub>20</sub>, MePEG<sub>2</sub>PLA<sub>40</sub>, and NH<sub>2</sub>PEG<sub>2</sub>PLA<sub>40</sub> were synthesized and characterized with the goal of obtaining substances processable to mechanically stable scaffolds for in vivo or in vitro experiments and first steps were undertaken towards the in vivo evaluation of these polymers (**Chapter 4**).

Although PEG chains largely suppress undesired protein adsorption, the shielding of the surface is not complete. As randomly adsorbed proteins are likely to interfere with the targeted tissue development, knowledge on the extent of shielding is crucial. We, therefore, investigated the amount of adsorbed protein to different polymers by processing them into thin films and investigating their interactions with proteins using quartz crystal microbalance techniques (**Chapter 5**).

Covalent linking of molecules to polymers has the advantage of constricting their operating range to the tethering site, thus diminishing undesired side-effects. Moreover, as diffusion of these molecules is inhibited, prolonged reaction times might be an additional benefit. Unfortunately, tethering might interfere with conformational changes of the molecules structure required for its interaction with the substrate or might even affect the active center of the molecule. Therefore, knowledge of the reaction site is crucial. Identification of the reaction sites was attempted using insulin as model protein. Therefore, polymers were linked to the proteins via small molecular weight tags. After removal of the polymer chains the succinic acid tags still marked the reaction sites and the modified proteins were characterized to identify the exact location of these tags (**Chapter 6**).

Chemical modification of proteins might alter the physico-chemical properties of the molecules. For example, tethering of hydrophilic polymers, like PEG, enhances the water solubility of the drug. But also modification of proteins by attachment of hydrophobic substances, such as fatty acids, might improve the characteristics of these proteins. Nature often uses fatty acids as membrane tethering moieties. Lipidized proteins are also candidates for alternative administration routes, like the oral route, being more stable and having enhanced adsorption properties. Unfortunately, modification of proteins might deteriorate their biological activity. Therefore, prior to use each synthesized conjugate must be tested in a suitable model system. Here, insulin was chosen as model protein. After attachment of fatty acids, its biological activity was tested in an insulin dependent chondrocyte cell culture system (**Chapter 7**).





# **Chapter 3**

## **Materials and Methods**

# 1 Materials

Bovine insulin and human insulin were generous donations from Aventis (Frankfurt/Main, Germany).

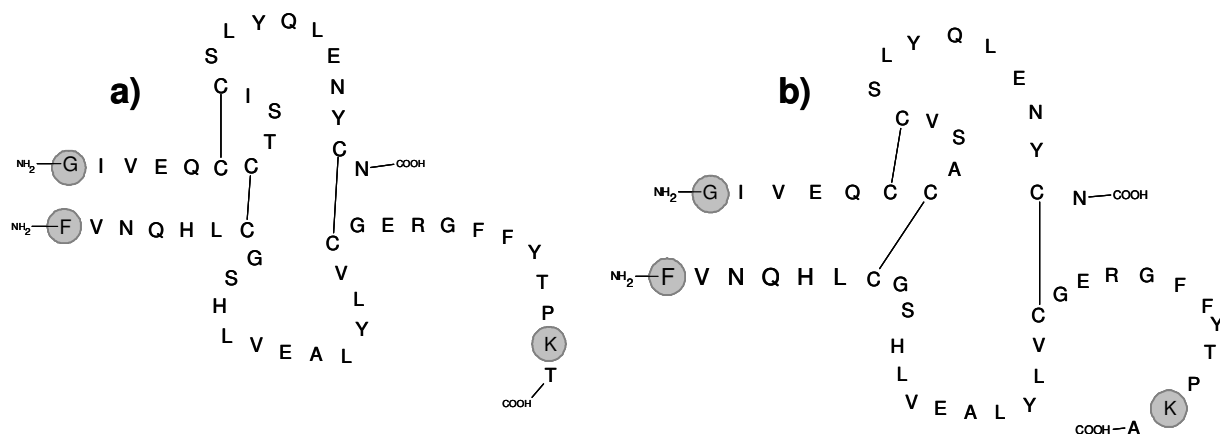


**Figure 1:** Chemical structure of human (a) and bovine (b) insulin. Amino acids carrying primary amine groups are marked with grey circles.

Basic fibroblast growth factor [bFGF] was purchased from Kaken Pharmaceutical (Tokyo, Japan). N-hydroxysuccinimide [NHS], N,N'-dicyclohexylcarbodiimide [DCC], ethylene oxide, potassium bis(trimethylsilyl)amide solution and sinapic acid [SA] were purchased from Fluka Chemie (Buchs, Switzerland) the latter in specially purified and prequalified for MALDI Mass Spectrometry use quality. Deuterated chloroform and deuterated acetonitrile were obtained from Deutero GmbH (Kastellaun, Germany). Ethanol and acetonitrile in ultra gradient HPLC grade were provided by Mallinckrodt Baker (Deventer, Holland). Trifluoroacetic acid was obtained from Riedel-de Haen (Seelze, Germany). Dichloromethane and chloroform HPLC grade and N-methyl-2-pyrrolidone [NMP], 1 N HCl and 0.1 N HCl were purchased from Carl Roth GmbH (Karlsruhe, Germany). Urea, bovine serum albumin, Sn(II) 2-ethylhexanoate, 3,6-dimethyl-1,4-dioxane-2,5-dione [D,L-dilactide] and Poly(ethylene glycol)methyl ether average MW 2000 [MePEG<sub>2</sub>] were obtained from Sigma-Aldrich (Steinheim, Germany). Tris(hydroxymethyl)-amino methane [Tris] was provided by Amersham Life Science (Buckinghamshire, UK). 5-aminoeosin [5-AE] and 5-((2-aminoethyl)amino)naphthalene-1-sulfonic acid, sodium salt [EDANS] were purchased

from Molecular Probes (Göttingen, Germany). Dithiothreitol [DTT] and iodoacetamide were obtained from Bio-Rad Laboratories GmbH (München, Germany).

Cell culture material was purchased from Corning Star (Bodenheim, Germany). Sterile substances for use in cell culture (like penicillin, non-essential amino acids, Dulbecco`s Modified Eagle`s Medium [DMEM], fetal bovine serum [FBS], N-(2-hydroxyethyl)piperazine-N´-(2-ethanesulfonic acid) [Hepes]) were purchased from Invitrogen (Karlsruhe, Germany).

Polished plano-plano AT-cut quartz crystals with a fundamental resonance frequency of five megahertz and a diameter of 14 mm were purchased from KVG (Neckarbischofsheim, Germany). Gold was obtained from Goodfellow (Bad Nauheim, Germany), and chrome was from Bal-Tec (Balzers, Liechtenstein). Octadecyltrichlorosilane 95% was purchased from Acros Organics (Geel, Belgium).

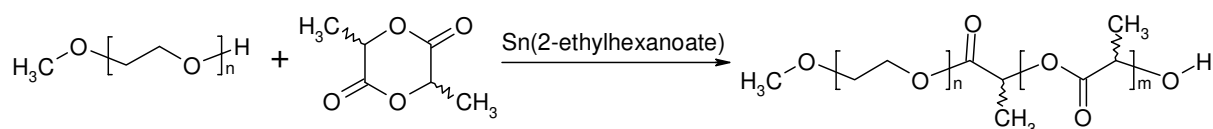
All other chemicals if not stated otherwise were purchased from Merck KGaA (Darmstadt, Germany) and used as received.

## 2 Methods

### 2.1 Synthesis and Characterization of PEG<sub>x</sub>PLA<sub>y</sub>

#### 2.1.1 Synthesis of MePEG<sub>x</sub>PLA<sub>y</sub>

For the polymerization of MePEG<sub>2</sub>PLA<sub>20</sub> a method from literature was adopted [132]. Indices in the names of the polymers always indicate the molecular weight of the respective block. The synthesis followed the procedure described as follows: To remove residual water, the educts (2 g of MePEG<sub>2</sub> and 20 g of D,L-dilactide) were dissolved each in 150 ml toluene. 20 ml of each solution were distilled off to remove traces of water through azeotropic distillation. Such pre-treated solutions were combined under a stream of dry nitrogen and 100 mg of 2-ethylhexanoate were added to the reaction batch. After the mixture was heated to reflux the nitrogen was turned off and the refluxing solution stirred for about eight hours. Subsequently the majority of the toluene was removed by means of a rotary evaporator. For further purification the residue was dissolved three times in dichloromethane and the solvent evaporated first under atmospheric pressure, then under reduced pressure. This procedure was repeated twice with acetone. The resulting film was dissolved in approximately 100 ml acetone and the polymer was precipitated in 3 l of water, cooled in an ice bath. The product was collected by filtration and dried at room temperature using a RV5 two stage vacuum pump from Edwards (Crawley, West Sussex, UK).



**Scheme 1:** Reaction scheme for the synthesis of MePEG<sub>x</sub>PLA<sub>y</sub>.

The above described synthesis protocol was modified in such, that a reduced total amount of solvent was used for the polymerization of MePEG<sub>2</sub>PLA<sub>20</sub> and MePEG<sub>2</sub>PLA<sub>40</sub>. Furthermore the quantity of a typical reaction batch was reduced. The new protocol is described as follows: 1 g MePEG<sub>2</sub> and 10 g of D,L-dilactide for MePEG<sub>2</sub>PLA<sub>20</sub> or 20 g of D,L-dilactide for MePEG<sub>2</sub>PLA<sub>40</sub> were dissolved separately in 40 ml toluene each and 5 ml of toluene were distilled off to remove traces of water. The dry solutions of MePEG and dilactide were combined under a stream of dry nitrogen and 50 mg 2-ethylhexanoate was added to the

reaction batch. After heating the solution to reflux, the flask was sealed. The refluxing reaction batch was stirred for nine hours with a magnetic stirrer, after which the polymer was collected and analyzed as described in the previous section.

For the synthesis in melt of the diblock co-polymer 0.5 g MePEG<sub>2</sub> were placed in a flask and heated at 110 °C to remove traces of water. After evacuation and filling the flask with argon, 5 g D,L-dilactide and 25 mg 2-ethylhexanoate were added. Temperature was increased at 140 °C, the flask sealed and the reaction batch stirred for 12 h hours. The product was dissolved in 50 ml acetone and precipitated in 2 l water cooled in an ice bath. The polymer was collected by filtration and dried at room temperature using a RV5 two stage vacuum pump from Edwards (Crawley, West Sussex, UK). Characterization of the polymer was performed by SEC as described in paragraph 2.1.5.

MePEG<sub>x</sub>PLA<sub>y</sub> and PLA for QCM investigations were synthesized as described above. The respective ratios of the different educts are shown in

**Table 1.**

**Table 1:** *Respective amounts of educts for the synthesis of different polymers.*

<b>Polymer</b>	<b>Educt 1</b>	<b>Educt 2</b>
PLA	25 µl Ethyl (S)-(-)-lactate	15.1 g D,L-dilactide
MePEG <sub>0,75</sub> PLA <sub>10</sub>	2.5 g MePEG <sub>0,75</sub>	33.3 g D,L-dilactide
MePEG <sub>0,75</sub> PLA <sub>95</sub>	0.15 g MePEG <sub>0,75</sub>	19.0 g D,L-dilactide
MePEG <sub>5</sub> PLA <sub>10</sub>	15 g MePEG <sub>5</sub>	30.0 g D,L-dilactide
MePEG <sub>5</sub> PLA <sub>95</sub>	1.5 g MePEG <sub>5</sub>	28.5 g D,L-dilactide
MePEG <sub>5</sub> PLLA <sub>10</sub>	15 g MePEG <sub>5</sub>	30.0 g L-dilactide

For some of the polymers the protocol had to be slightly adapted to meet the need of the specific polymer. MePEG<sub>5</sub>PLA<sub>10</sub> had to be precipitated in diethyl ether and MePEG<sub>5</sub>PLLA<sub>10</sub> was not dissolved in acetone, but in chloroform.

### **2.1.2 Investigation of the MePEG<sub>2</sub>PLA<sub>20</sub> Polymerization Reaction Kinetics**

For the investigation of the kinetics of the MePEG<sub>2</sub>PLA<sub>20</sub> synthesis, the polymerization reaction was started as described in the previous paragraph.

At different time points samples were drawn by first turning on the nitrogen stream and then removing 1 ml from the reaction batch using a dispensable syringe with needle. Subsequently, the solvent was evaporated first under gentle heating to 50 °C and then under reduced pressure. The residue was weighted and chloroform added to the samples to reach a final concentration of 20 mg substance per 2 ml CHCl<sub>3</sub>. Samples were filtered and SEC analyses were performed as described in paragraph **2.1.5**.

### **2.1.3 Purification of the Polymer**

Two different methods were used for purification of the reaction batch by separation into low molecular weight and high molecular weight fraction of the polymers. Thereby, advantage was taken of the ethanol solubility of short chain PLAs.

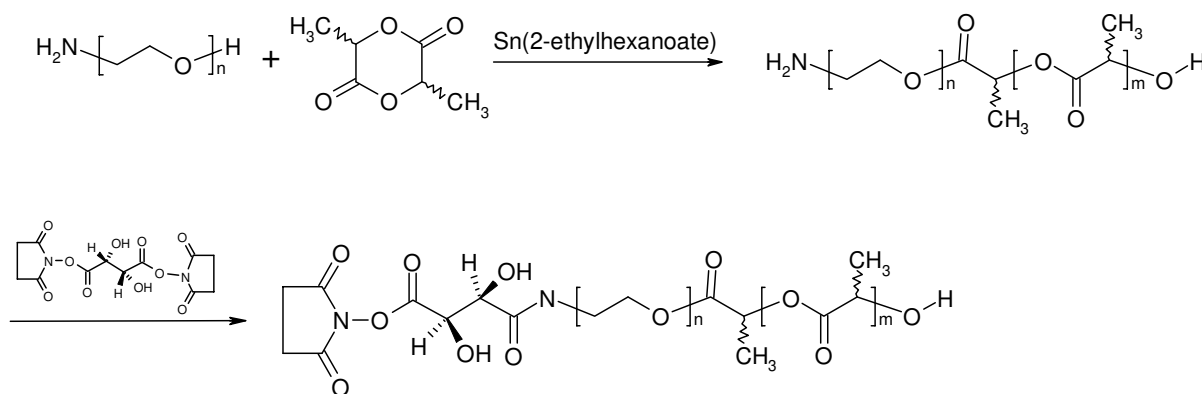
Firstly, the polymer was extracted at different temperatures with ethanol. Therefore, 40 ml of ethanol were added to 1 g of polymer and the system stirred with a magnetic stirrer. Temperature was slowly increased and 1 ml samples were drawn at T = 20 °C, 30 °C, 40 °C, 50 °C, 60 °C, 70 °C, 77 °C. The solvent was removed and the residue was dissolved in 1 ml chloroform. Samples were filtered and analyzed by SEC as described in the following paragraph (paragraph **2.1.5**).

For the second method used 0.75 g polymer were dissolved in 1.875 ml acetone and stirred with a magnetic stirrer at room temperature. Ethanol was added drop wise until the solution separated in two phases, henceforth called supernatant and residue. The two phases were collected separately and dried under reduced pressure. The substances were characterized using SEC, NMR and modulated differential scanning calorimetry [MDSC] techniques.

### 2.1.4 Synthesis and Activation of NH<sub>2</sub>PEG<sub>2</sub>PLA<sub>40</sub>

Besides the many favorable properties of MePEG<sub>2</sub>PLA<sub>40</sub> with regard to Tissue Engineering applications this polymer has the drawback of possessing no easy accessible functional group for the attachment of proteins. Therefore a new class of polymers was synthesized which featured an amine group instead of a methyl group at the free end of the PEG block and had a molecular weight of 2000 Da [NH<sub>2</sub>PEG<sub>2</sub>].

For the synthesis of NH<sub>2</sub>PEG<sub>2</sub> polymers a method described in literature was adopted [132]: 26 g of ethylene oxide were dissolved in 150 ml tetrahydrofurane [THF] cooled at -79 °C using a methanol/dry ice bath. 24 ml of a 0.5 M potassium bis(trimethylsilyl) amide solution in toluene were added and the reaction stirred for 36 h at room temperature. The solvent was removed from the reaction batch by means of a rotary evaporator. For purification the crude product was dissolved in 100 ml dichloromethane and centrifuged at 3000 rpm for 20 min. The supernatant was concentrated to a final volume of 50 ml and the product precipitated in four portions in 200 ml ice cooled diethyl ether. The product was immediately collected by filtration and dried at room temperature using a RV5 two stage vacuum pump from Edwards (Crawley, West Sussex, UK). The polymer was stored in a desiccator until further use. Characterization of the resulting polymer by <sup>1</sup>H-NMR and SEC was performed as described in detail elsewhere [132].



**Scheme 2:** Reaction scheme of the synthesis and activation of NH<sub>2</sub>PEG<sub>2</sub>PLA<sub>40</sub>.

For the synthesis of the NH<sub>2</sub>PEG<sub>2</sub>PLA<sub>40</sub> two different protocols were used.

Firstly, the modified method for the synthesis of MePEG<sub>2</sub>PLA<sub>40</sub> was followed. 1 g NH<sub>2</sub>PEG<sub>2</sub> and 20 g D,L-dilactide were dissolved separately in 50 ml toluene each and 15 ml of toluene were distilled off to remove traces of water. The pre-treated solutions of NH<sub>2</sub>PEG<sub>2</sub> and dilactide were combined under a stream of dry nitrogen. 500 µl of glacial acetic acid were added to the reaction batch, protonating the amino group of the PEG, thus preventing it to participate in the polymerization reaction. 50 mg of 2-ethylhexanoate were added as catalyst and the reaction batch was heated to reflux under stirring. After sealing the flask, the reaction was continued for about nine hours. To collect the product, the solvent was removed by means of a rotary evaporator. For further purification, the residue was twice dissolved in dichloromethane and the solvent removed under reduced pressure.

For the second method, a larger volume of solvent was used for the polymerization reaction. 1 g NH<sub>2</sub>PEG<sub>2</sub> and 20 g D,L-dilactide were dissolved separately in 150 ml toluene each and 25 ml of toluene were distilled off to remove traces of water. After combination of the solutions and the addition of 100 mg catalyst and 500 µl glacial acetic acid the flask was not sealed, but a constant stream of dry nitrogen was bubbled through the reaction batch being heated to reflux for nine hours. After cooling to room temperature, toluene was removed by evaporation and the polymer was purified and collected as described in the previous paragraph.

The activation of the polymer followed a procedure described in detail elsewhere [132]. In short, tartaric acid was activated using a combination of NHS/DCC in a mixture of dry 1,4-dioxane/ethyl acetate (4:1). Disuccinimidyl tartrate was collected by extraction with acetonitrile and removal of the solvent under reduced pressure. The reaction product was checked by <sup>1</sup>H-NMR.

The activated linker was covalently bound to the polymer by dissolving 6 g NH<sub>2</sub>PEG<sub>2</sub>PLA<sub>40</sub> and 0.12 g activated linker in 100 ml acetonitrile. 33 µl of triethyl amine were added and the reaction mixture heated to reflux for two hours. After 16 additional hours of stirring at room temperature, the solvent was removed by evaporation and the polymer extracted with 50 ml acetone. The polymer was collected by drop wise precipitating the acetone solution in 400 ml ice cooled water and immediate filtration, instantly followed by vacuum drying. Until further use, the polymer was stored in a desiccator. The product was characterized by SEC.



### **2.1.5 Characterization of Polymers by SEC**

To investigate the molecular weight distribution of synthesized polymers size exclusion chromatography was used. Analyses were performed on a 10AVP HPLC system from Shimadzu (Duisburg, Germany). For an optimal separation, a combination of a pre-column (Phenogel 5  $\mu\text{m}$ , 50 x 7.8mm) connected in a row to two identical analytical columns (Phenogel 1000 Å, 5  $\mu\text{m}$ , 300 x 7.8 mm, all from Phenomenex, Torrance, CA) was used as stationary phase. The columns were thermostated at 35 °C and chloroform was used as mobile phase with a flow rate of 0.9 ml/min. Chromatograms were collected using a RID 10A refractory index [RI] detector from Shimadzu (Duisburg, Germany).

For a typical analyses 20 mg polymer were dissolved in 2 ml chloroform and subsequently filtered through a chloroform resistant filter with a pore diameter of 0.2  $\mu\text{m}$  (Spartan 30/A from Schleicher & Schuell, Dassel, Germany). 50  $\mu\text{l}$  of the filtered polymer solution were injected and polymers formerly synthesized by Teßmar et al. [25] were used as references. Data was accumulated and analyzed using HPLC software Class VP 5.03 from Shimadzu.

### **2.1.6 Characterization of the Activated Polymer**

To confirm the reactivity of the activated polymer, a solution of an amine group containing dye was added to the polymer and the reaction product investigated by SEC.

5-aminoeosin was used as amine group containing dye. For sample preparation 20 mg polymer were dissolved in 200  $\mu\text{l}$  dye solution (0.836 mg dye in 500  $\mu\text{l}$  dimethylsulfoxide [DMSO]). Pure polymer and pure dye solution were prepared as references. Immediately after addition of the dye solution, samples were wrapped in aluminum foil and kept in the dark for three hours at room temperature. Subsequently, 1.5 ml chloroform were added to each sample and thereafter filtered through a chloroform resistant filter with a pore diameter of 0.2  $\mu\text{m}$  (Spartan 30/A from Schleicher & Schuell, Dassel, Germany). 50  $\mu\text{l}$  of the filtrate were injected and data was accumulated and analyzed using HPLC software Class VP 5.03 from Shimadzu.

Analyses were performed on a 10AVP HPLC system from Shimadzu (Duisburg, Germany). For an optimal separation, a combination of a pre-column (Phenogel 5  $\mu\text{m}$ , 50 x 7.8 mm) connected in a row to two identical analytical columns (Phenogel 1000 Å, 5  $\mu\text{m}$ , 300 x 7.8 mm, all from Phenomenex, Torrance, CA) was used as stationary phase. The columns

were tempered at 35 °C and chloroform was used as mobile phase with a flow rate of 0.9 ml/min. Chromatograms were collected using a RID 10A refractory index [RI] detector and a SPD 10AV<sup>VP</sup> UV detector at 523 nm, both from Shimadzu (Duisburg, Germany).

### 2.1.7 <sup>1</sup>H-NMR Analyses

For polymer analysis 20 mg of the analyte were dissolved in 1 ml deuterated chloroform and filtered in a NMR tube. For an analysis of the activated linker, 10 mg disuccinimidyl tartrate were dissolved in 1 ml deuterated acetonitrile and filtered in a NMR tube.

<sup>1</sup>H-NMR spectra were recorded on an Avance 600 spectrometer from Bruker (Rheinstetten, Germany) with TMS as internal standard.

### 2.1.8 MDSC Analysis of Polymers

Thermal properties of the polymers are relevant in consideration of processing these polymers further. Therefore glass transition temperatures [TG] of the substances were determined by modulated differential scanning calorimetry using a DSC 2920 equipped with a refrigerated cooling system and autosampler (TA Instruments, Alzenau, Germany).

Samples were prepared by precisely weighing about 2 mg of polymer in aluminum sample pans and sealing them using the TA Instruments sample encapsulation press. An empty sealed pan served as reference. For measurements the following protocol was followed: first, sample and reference were equilibrated at -40 °C for 15 min. For the amplification of the signal of the first glass transition temperature [TG1<sup>st</sup>] and the separation of relaxation phenomena, the pans were heated from -40 °C to 110 °C at a heating rate of 2 °C/min, using a sinusoidal temperature modulation with a period of 60 s and a temperature amplitude of 1 °C. After retaining the temperature at 110 °C for 5 min, the samples were cooled to -40 °C, equilibrated for 15 min and a second heating phase was started using the same protocol. As relaxation phenomena are less pronounced after the first heating and cooling cycle, glass transition temperatures were determined from the reversed heat flow of the second heating [10]. The thermograms were analyzed using the Thermal solution for NT software provided with the MDSC system.

### **2.1.9 Fabrication of Scaffolds for In-Vivo Testing of the Polymers**

Constructs for in-vivo applications were fabricated using a protocol adapted from Hacker et al. [24]. The devices were composed of a mixture of 70% activated NH<sub>2</sub>PEG<sub>2</sub>PLA<sub>40</sub> and 30% MePEG<sub>2</sub>PLA<sub>40</sub> or 100% of MePEG<sub>2</sub>PLA<sub>40</sub>. For scaffolds preparation the polymers were dissolved in a methyl ethyl ketone-tetrahydrofurane-mixture. As porogens, lipid microparticles in a size range from 100 µm to 300 µm made from a 1:1 mixture of Softisan® 154 and Witepsol® H42 (kindly provided by SASOL Germany (Witten, Germany)) were used, stored for 1 h at -20 °C prior to use. Porogen particles were transferred into the polymer solution and mixed for 5 min on ice. The resulting highly viscous dispersion was then injected into cubic Teflon® molds with a cylindrical cavity of 0.8 cm in diameter using a 10 ml polypropylene syringe. After a pre-extraction treatment step in n-hexane at 0 °C for 90 min, the filled molds were submerged in warm n-hexane to precipitate the polymer and extract the porogen particles concurrently in two steps: first the molds were incubated for 7.5 min at 45 °C and then for 22.5 min at 35 °C. Subsequently the molds were transferred into an n-hexane bath at 0 °C for 5 min. The resulting porous cylindrical polymeric constructs were vacuum-dried for 48 h, before being cut into 2 mm thick slices. They were stored in a desiccator until further use.

### **2.1.10 In-vivo Evaluation of Scaffolds**

For the in-vivo evaluation of scaffolds, bFGF was covalently attached to the constructs containing activated NH<sub>2</sub>PEG<sub>2</sub>PLA<sub>40</sub>. Scaffolds fabricated from MePEG<sub>2</sub>PLA<sub>40</sub> served as control.

All devices were incubated in 1.5 ml PBS buffer pH 8.0 containing 50 µg bFGF for 2 h at room temperature on a shaker. After washing the constructs in PBS pH 7.4, they were immersed in a 1% sodium dodecyl sulfate [SDS] solution in PBS pH 7.4 and placed on a shaker for 1 h at room temperature to remove adsorbed bFGF. The scaffolds were again washed with PBS and subsequently implanted into the back subcutis of mice. After three weeks three mice from each experimental group were sacrificed and the excised constructs were prepared for the evaluation of angiogenic effects and ingrowth of fibrovascular tissue.

Scaffolds were excised with the adjacent tissue, rinsed in PBS and fixed with 2.5% glutaraldehyde for 15 min. Subsequently, they were treated with 10% formaldehyde in PBS for storage. Fixed constructs were embedded in Tissue Tek and 10  $\mu$ m thick sections were cut on a cryotome and were stained with hematoxylin and eosin [H&E]. Images were taken with a camera coupled to an inverse light microscope.

## 2.2 Quartz Crystal Microbalance Methods

### 2.2.1 Preparation of the Gold Electrodes

To apply the gold electrodes on the surface of the quartz a vapor deposition apparatus (BAE 250 Coating Systems, from Blazers, Liechtenstein) was used. After applying high vacuum of  $10^{-8}$  to  $10^{-9}$  bar a 20 nm thick chrome layer was deposited as adhesive agent and then a 100 nm thick gold layer was deposited on top of the chrome. The back side of the quartz was treated the same way.

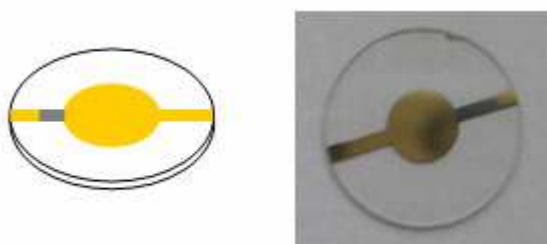


**Figure 2:** *Schematic drawing and picture of a quartz with deposited gold electrodes. The dimensions of the quartz were 14 mm in diameter and 0.33 mm in thickness. The gold electrode covered an area of  $0.3 \text{ cm}^2$ .*

The gold electrodes were thoroughly cleaned prior to use. Therefore the disks were immersed for three minutes in hot Piranha solution (a mixture of concentrated  $\text{H}_2\text{SO}_4$  and 30%  $\text{H}_2\text{O}_2$  solution in a volume ratio of 3:1 at approximately  $70 \text{ }^\circ\text{C}$ ), rinsed three times with double distilled water and dried under a stream of nitrogen. Afterwards the quartzes were cleaned for five minutes in argon plasma.

### 2.2.2 Spin Coating of Quartzes with Polymer Films

Polymers used for the preparation of films were synthesized as described in **Chapter 2.1**.

Polymer solutions for spin-coating were prepared in different manner depending on the material used. Most polymers were dissolved in a concentration of 10 mg substance per 1 ml acetone. Short chained PLAs (MePEG<sub>5</sub>PLA<sub>10</sub> and MePEG<sub>0,75</sub>PLA<sub>10</sub>) were dissolved at a concentration of 20 mg per 1 ml acetone, to give satisfying polymer films. As

MePEG<sub>5</sub>PLLA<sub>10</sub> is not soluble in acetone, a solution of 10 mg polymer in 1 ml chloroform was prepared.

The quartz was glued to the surface of a rotary device with the cleaned surface upwards using a double-side adhesive strip. In doing so measures were taken to protect the gold electrode from direct contact to the glue, as otherwise the gold would be removed from the quartz. 100 µl of polymer solution was placed in the center of the quartz and the disk accelerated to 1990 rotations per minute. After about 30 seconds of spinning the quartz was carefully detached from the spinning device and traces of glue removed by gently wiping the back of the disk with acetone, as well as removing the polymer from the outer end of the electrode contacts.

### **2.2.3 Modifications of Quartzes**

For rendering the surface of the quartz hydrophobic, octadecyltrichlorosilane was covalently attached to the free hydroxyl groups in the surface of the crystal. On gold, this substance is known to autopolymerize, covering the electrode with a hydrophobic film.

The reaction was performed under a nitrogen atmosphere. To remove excess water from toluene, azeotropic distillation was performed prior to use of the solvent. Cleaned quartzes were immersed under a stream of nitrogen in 50 ml of pre-treated toluene. To prevent mechanical abrasion of the gold layer, each quartz disk was placed in the solution individually suspended in a perforated Teflon pocket. 2.5 ml octadecyltrichlorosilane were added under nitrogen to the reaction batch and the solution was stirred under reflux for 24 hours. After cooling to room temperature, the disks were rinsed two times with toluene and one time with methanol and then immersed in methanol for two hours. If after drying the surface of the crystals seemed dull, the quartzes were immersed in 5 ml chloroform and placed in an ultrasonic bath for one minute. After twice rinsing with chloroform, the quartz was dried under a stream of nitrogen.

### **2.2.4 Cleaning of Modified Quartzes**

Modified quartzes could not be treated in the same manner as unmodified ones, as the hydrophobic layer would have been removed under the harsh conditions of the cleaning. Prior

to use and after each measurement modified quartzes had to undergo the following procedure: First they were placed in an aqueous solution of 1% SDS solution in ddH<sub>2</sub>O and sonicated for one minute. After thoroughly rinsing the crystal with double distilled water and drying under a stream of nitrogen, the quartz was then immersed in acetone and treated with ultrasound for one minute. After twice rinsing the crystal with fresh acetone, the quartz was finally dried under a stream of nitrogen.

### **2.2.5 Contact Angle Measurements**

To confirm the lipophilization reaction the wettability of quartzes was measured prior to and after modification. The sessile drop method was performed on an OCA15 apparatus (dataphysics, Filderstadt, Germany) and double distilled water drops with a volume of 1  $\mu$ l were used. Contact angles were measured on gold electrodes and pure quartz surface respectively on both sides of two different quartz disks.

### **2.2.6 QCM Measurements**

The QCM setup used is shown in **Figure 3**.

The experimental setup consisted of a solution reservoir placed in a water bath and heated at 37 °C. To ensure homogenous distribution of added protein solution, a magnetic stirrer was used. From this reservoir, which contained 2 ml solution, the solvent was pumped in a cycle using a peristaltic pump (Ismatec Reglo Digital, Ismatec Laboratoriumstechnik GmbH, Wertheim-Mondfeld, Germany) at a flow rate of 0.46 ml/min through the fluid chamber made of Teflon. In this fluid chamber designed in stagnation flow point geometry as show in **Figure 3** the quartz was placed exposing one side of the resonator to the aqueous solution. Spring contacts connected the gold electrodes of the quartz disk to the oscillatory circuit. The entire system was placed in a water-jacketed Faraday cage tempered at 37 °C. The oscillatory circuit was supplied with a voltage of 4 V by a DC power supply (HP E3630A, Hewlett-Packard, Palo Alto, CA, USA), and the frequency change of the resonator was recorded using a frequency counter (HP 53181A, Hewlett-Packard, Palo Alto, CA, USA), which was connected in turn via RS 232 to a personal computer.

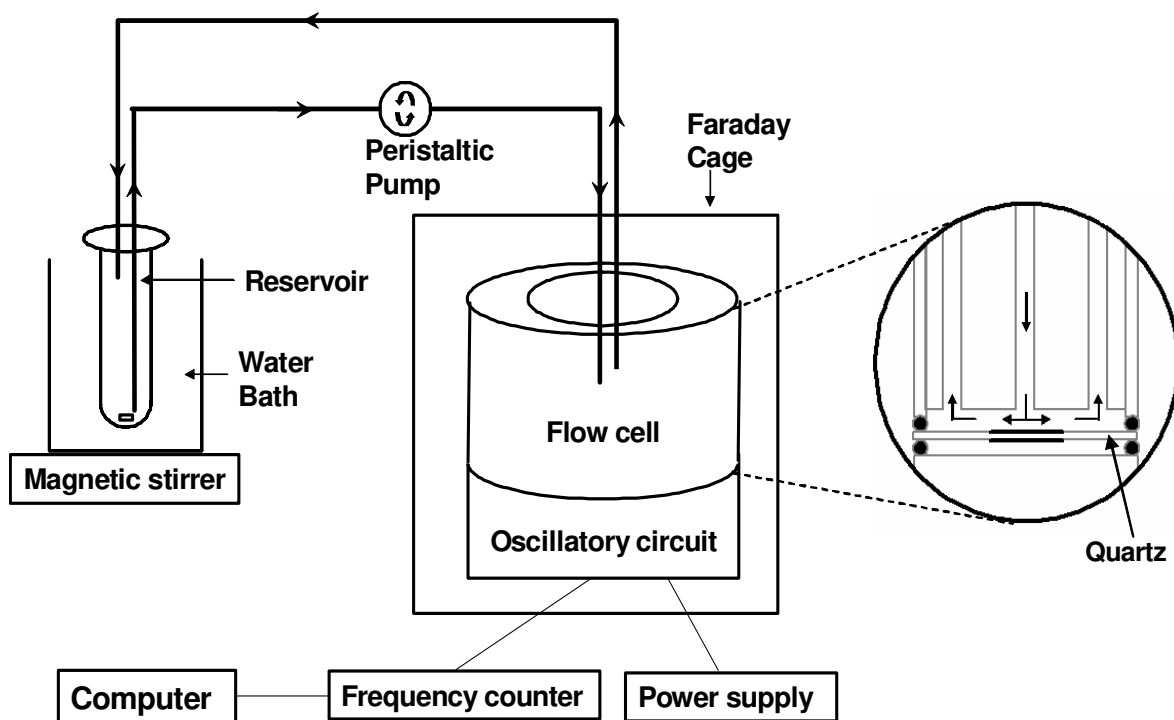


**Figure 3:** Experimental setup of the QCM used in adsorption measurements consisting of solution reservoir, peristaltic pump, flow cell (with quartz) and oscillatory circuit in a Faraday cage, power supply, frequency counter and personal computer. A lateral section of the flow cell displaying the flow duct and the quartz mounting is shown.

Until stated otherwise, for all experiments 0.1 M phosphate buffer adjusted to pH 8.0 and containing 3 mg urea per 40 ml solution was used, hereafter referred to as solution.

To ensure electricity conduct across the thickness of the quartz, silver glue was placed at the edge of the electrode contacts, and the glue was dried under a stream of nitrogen. After assembling the fluid chamber, the resonant frequency of the 5 MHz quartz was checked and the chamber was connected to the flow system, making sure, that no air bubbles were present anywhere in the flow system. After equilibrating the system for about one hour, 1 ml of the solvent was removed from the solution reservoir and 1 ml tempered protein solution (typically 1 mg bovine insulin per 1 ml solution) was added. Measurements were continued for another hour. After the end of experiment the fluid chamber was disassembled and thoroughly cleaned in an ultrasonic bath, first in 1% SDS solution and then in double distilled water.



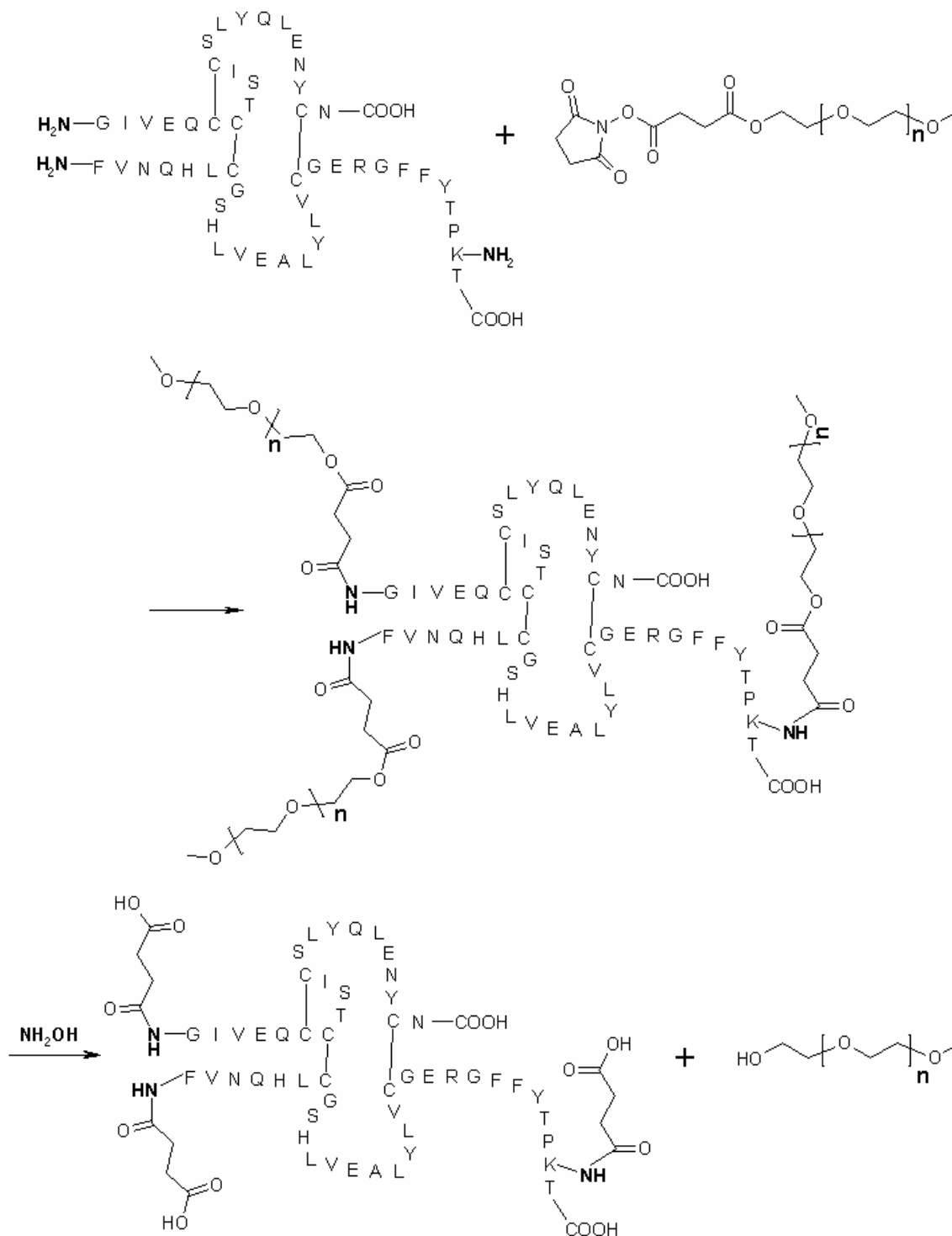
## 2.3 Identification of the Reaction Sites of Insulin

Modification of proteins with PEG to alter their physical or pharmacological characteristics is a frequently used technique [177]. Identification of the reaction sites is of vital importance to better characterize PEGylated proteins for the purpose of maximally retaining their biological activity. One approach to this goal is to mark the reaction sites by tags deriving from the activated polymer, as PEG chains often interfere with analytical methods. The route followed in this work is schematically displayed in **Scheme 3**.

### 2.3.1 Preparation of N-Succinimidyl Succinate of Poly(ethylene glycol)-monomethyl Ether [SS-PEG]

To match the needs of our experiments the applied polymer had to show two crucial features: an easily cleavable group in the backbone of the polymer as well as a terminal amine reactive group. We adopted a strategy described in literature consisting of two steps [178]. Starting from a commercially available monomethyl ether of poly(ethylene glycol), we firstly, synthesized a succinimidyl ester of MePEG<sub>2</sub>, the SPEG, which was subsequently converted to an amine reactive compound, the SSPEG, using standard DCC/NHS chemistry.

For the first step 10 g PEG were dissolved in 70 ml toluene and traces of water were removed by azeotropic distillation. 0.6 g of succinic acid anhydride were added and the reaction batch was stirred overnight at room temperature. The solvent was removed by means of a rotary evaporator. Twice the polymer was redissolved in dichloromethane and residual toluene was removed by azeotropic distillation. For further purification 2 g of the product were dissolved in 20 ml 0.1 M NaHCO<sub>3</sub>. The aqueous phase was extracted with 5 portions of 30 ml dichloromethane. After the combined lipophilic phases were dried with Na<sub>2</sub>SO<sub>4</sub>, the mixture was concentrated through evaporation of the solvent and the viscous solution dropped slowly into diethyl ether cooled in an ice bath. The precipitate was collected through filtration and dried under reduced pressure. The reaction was confirmed by <sup>1</sup>H-NMR spectroscopy.



**Scheme 3:** Schematic illustration of the PEGylation and De-PEGylation reaction of insulin.

For the second step, 1.0 g SPEG and 98 mg NHS were dissolved under gentle heating in 10 ml dried dioxane. After cooling to room temperature 155 mg DCC were added and the

mixture stirred overnight at room temperature. Insoluble dicyclohexylurea was removed by filtration and the filtrate was concentrated under reduced pressure. Twice the polymer was redissolved in 50 ml dichloromethane and residual dioxane was removed through azeotropic distillation. The highly viscous residue was diluted with dichloromethane and precipitated in 400 ml ice-cooled ether. Immediately the product was filtrated and dried under reduced pressure. The dried substance were analyzed by  $^1\text{H-NMR}$  and SEC.

For  $^1\text{H-NMR}$  analysis, 20 mg of the analyte were dissolved in 1 ml deuterated chloroform and filtered in a NMR tube.  $^1\text{H-NMR}$  spectra were recorded on an Avance 600 spectrometer from Bruker (Rheinstetten, Germany) with TMS as internal standard.

### **2.3.2 Synthesis of PEGylated Insulin**

After confirming the reactivity of SSPEG, the polymer protein conjugate was synthesized. As model protein for the PEGylation reaction human insulin was chosen, a molecule which possesses three primary amine groups (A1-Gly, B1-Phe, B29-Lys).

The reaction followed the protocol described as follows: in 1.1 ml of a 0.1 M  $\text{PO}_4^{3-}$  buffer adjusted at pH 8 and containing 7.5 mg urea per 100 ml, 7.0 mg of insulin were dissolved. A second solution was prepared by dissolving 90.6 mg activated PEG in 250  $\mu\text{l}$  double distilled  $\text{H}_2\text{O}$ . To 1000  $\mu\text{l}$  insulin solution immediately 200  $\mu\text{l}$  of PEG solution were added and left to react for 2 h at room temperature.

To monitor the reaction, at different time points 20  $\mu\text{l}$  samples were drawn from the reaction batch, and diluted by addition of 160  $\mu\text{l}$  dd $\text{H}_2\text{O}$ . Instantly 20  $\mu\text{l}$  1 N HCl was added to stop the reaction. The samples were analyzed by HPLC, GFC and MALDI-ToF as described in the following paragraphs.

For purification of the reaction batch, 1100  $\mu\text{l}$  of the solution were transferred into ultra centrifugation devices with a cut-off of 5000 Da (Vivaspin 2, from Sartorius, Göttingen, Germany), diluted with 900  $\mu\text{l}$  dd $\text{H}_2\text{O}$  and centrifuged for 30 min at 3000 rpm using a Megafuge 1.0 (Heraeus Sepatech, Osterode am Harz, Germany). The sample was washed by readjusting the volume at 2 ml using 0.1 M  $\text{NH}_4\text{HCO}_3$  buffer pH 8 and repeating the centrifugation procedure. Washing steps were performed four times giving 400  $\mu\text{l}$  of a concentrated sample solution.

### **2.3.3 De-PEGylation of Insulin**

The cleavage of the bondage between succinic acid and PEG was performed with hydroxylamine under slightly basic conditions, because in this environment  $\text{NH}_2\text{OH}$  will only cleave ester bondages but not amide bondages.

For the cleavage reaction 0.25  $\mu\text{mol}$  of PEGylated insulin were dissolved in 200  $\mu\text{l}$  0.1 M  $\text{NH}_4\text{HCO}_3$  buffer pH 8. 800  $\mu\text{l}$  of a freshly prepared 1.25 M  $\text{NH}_2\text{OH}$  solution adjusted to pH 10 were added and the solution incubated at 37 °C for 4 h.

To monitor the reaction, 50  $\mu\text{l}$  samples were drawn at different time points, diluted with 100  $\mu\text{l}$  ddH<sub>2</sub>O and the reaction was stopped by immediate addition of 50  $\mu\text{l}$  1 N HCl. Samples were analyzed by GFC and MALDI-ToF as described below.

After 4 h of incubation time, the reaction batch was transferred into ultra centrifugation devices with a cut-off of 5000 Da (Vivaspin 2, from Sartorius, Göttingen, Germany), diluted with 25 mM  $\text{NH}_4\text{HCO}_3$  buffer pH 8 and centrifuged for 30 min at 3000 rpm using a Megafuge 1.0 (Heraeus Sepatech, Osterode am Harz, Germany). For further purification the sample was washed twice by adjusting the sample to 2 ml with 25 mM  $\text{NH}_4\text{HCO}_3$  buffer pH 8 and centrifuged as recorded above. Finally the product was collected giving a total of 210  $\mu\text{l}$ .

### **2.3.4 Cleavage of Disulfide Bonds of Insulin and De-PEGylated Insulin**

For the permanent cleavage of disulfide bridges, DTT was used with subsequent treatment with iodoacetamide.

Therefore, 0.65 mg human insulin and 46 mg were dissolved in 600  $\mu\text{l}$  0.1 M Tris-buffer pH 7.5, or to 95  $\mu\text{l}$  purified de-PEGylated insulin solution, prepared as described above, 400  $\mu\text{l}$  0.125 M Tris-buffer pH 7.5 was added. To each solution, 20  $\mu\text{l}$  of DTT solution (1.66 mg DTT dissolved in 83  $\mu\text{l}$  0.1 M Tris-buffer pH 7.5) was added and the sample incubated at 40 °C for 2 h. After cooling to room temperature, 20  $\mu\text{l}$  iodoacetamide solution (3.9 mg iodoacetamide in 60  $\mu\text{l}$  0.1 M Tris buffer pH 7.5) were added to the reaction batch and the sample incubated in the dark for 1 h at room temperature.

For HPLC analysis as described below a 50  $\mu\text{l}$  sample of the insulin reaction batch was drawn, diluted with 100  $\mu\text{l}$  ddH<sub>2</sub>O and 50  $\mu\text{l}$  1 N HCl were added. The residual reaction batch was then transferred to a QuixSep Micro Dialyzer (Carl Roth GmbH, Karlsruhe Germany) equipped with a dialysis membrane with a cut-off of 1.0 (ZelluTrans/ Roth V Series from Carl Roth GmbH, Karlsruhe, Germany) and dialyzed against water for 20 hours. The obtained product was lyophilized.

The resulting dry powder was dissolved in 200  $\mu\text{l}$  0.1 M NH<sub>4</sub>HCO<sub>3</sub> buffer pH 7.5. 200  $\mu\text{l}$  0.1 N HCl were added and the sample analyzed by HPLC analysis.

### **2.3.5 Enzymatic Digestion of Insulin Chains**

The cleaved A and B chains of insulin, were separated and lyophilized after individual collection. Each substance was dissolved in 30  $\mu\text{l}$  25 mM NH<sub>4</sub>HCO<sub>3</sub> buffer pH 7.8. 50  $\mu\text{g}$  Endoproteinase GluC (Roche Applied Science, Penzberg, Germany) was reconstituted in 50  $\mu\text{l}$  ddH<sub>2</sub>O according to the manufacturer protocol. 0.5  $\mu\text{l}$  proteinase solution was added to each sample and incubated at 25 °C for 18 h. The samples were lyophilized and analyzed by MALDI-ToF.

### **2.3.6 Size Exclusion Chromatography [SEC] of Activated PEG**

Amine reactivity of the activated polymer was assessed by reaction of the polymer with a fluorescent dye (EDANS) and subsequent size exclusion chromatography analysis.

SEC experiments were conducted on a 10AVP HPLC system (Shimadzu, Duisburg, Germany), which was composed of binary pump, low pressure gradient unit, autosampler, column oven, UV detector and refractive index detector. Chloroform served as mobile phase and was degassed prior to use by purging with helium.

Samples were prepared by dissolving 10 mg SSPEG in 150  $\mu\text{l}$  dry DMSO which contained 3 mg EDANS. As control served polymer and EDANS dissolved in DMSO, respectively. All samples were incubated in the dark under gentle shaking for four hours. 1850  $\mu\text{l}$  chloroform were added to each sample and the mixtures were filtered using solvent resistant regenerated nitrocellulose membrane filters with a 0.2  $\mu\text{m}$  pore diameter (Spartan 30/A from Schleicher &

Schuell, Dassel, Germany). 50 µl of the filtrate were injected and separated at a flow rate of 0.9 ml/min on a Phenogel column (50 Å, 5 µm 300 x 7.8 mm) with precolumn (Phenogel 5 µm, 50 x 7.8 mm, all from Phenomenex, Torrance, CA) tempered to 35 °C. Spectra were recorded on a refractive index detector and an UV detector at 335 nm. Data was accumulated and analyzed using HPLC software Class VP 6.05 from Shimadzu.

### 2.3.7 HPLC Analysis

For HPLC analysis experiments were performed on a 10AVP HPLC system (Shimadzu, Duisburg, Germany), which was composed of degasser, binary pump, low pressure gradient unit, autosampler, column oven, UV detector and fluorescence detector.

**Table 2:** *Chromatographic conditions of HPLC experiments used for analysis of PEGylated insulin.*

Eluents	Solvent A: 900 ml ddH <sub>2</sub> O 100 ml acetonitrile 1 ml TFA	Solvent B: 100 ml ddH <sub>2</sub> O 900 ml acetonitrile 1 ml TFA
Gradient	0 min: 10% B in A; 13 min: 25% B in A; 18 min: 25% B in A; 22 min: 28% B in A;	32 min: 28% B in A; 37 min: 10% B in A; 42 min: Stop;
Flow rate	1 ml/min	
Column	Supelco Supelcosil™ LC-318 with pre-column	
UV-Detection	210 nm and 274 nm	
Fluorescence-Detection	$\lambda_{\text{ex}} = 274 \text{ nm}; \lambda_{\text{em}} = 308 \text{ nm}$	

For the analysis of PEGylated insulin, 50  $\mu$ l of the concentrated sample solution was separated on a RP 18 column tempered at 40 °C. Chromatograms were recorded on a Shimadzu SPD 10AV<sup>VP</sup> UV detector and a Shimadzu RF-355 fluorescence detector using the conditions shown in Table 2. Data was accumulated and analyzed using HPLC software Class VP 6.05 from Shimadzu.

For HPLC analysis of the cleaved insulin A chain and B chain 50  $\mu$ l of the solutions prepared as described in **Chapter 2.3.4** were separated on a RP 18 column. Chromatographic conditions used for these experiments are listed in **Table 3**:

**Table 3:** *Chromatographic conditions for HPLC analysis of separated insulin chains.*

Eluents	Solvent A: 25 mM NH <sub>4</sub> HCO <sub>3</sub> buffer pH 7.5 Solvent B: 35 mM NH <sub>4</sub> HCO <sub>3</sub> buffer pH 7.5 containing 65 % acetonitrile
Gradient	0 min: 0% B in A; 80 min: 0% B in A; 60 min: 100% B in A; 80 min: Stop; 61 min: 0% B in A;
Flow rate	1 ml/min
Column	Supelco Supelcosil <sup>TM</sup> LC-318 with pre-column
UV-Detection	210 nm and 274 nm
Fluorescence-Detection	$\lambda_{\text{ex}} = 274 \text{ nm}$ ; $\lambda_{\text{em}} = 308 \text{ nm}$

For a better resolution of the signals stemming from the B chain a new method (Method 2) was established:

**Table 4:** *Chromatographic conditions of HPLC analysis of separated de-PEGylated insulin chains.*

Eluents	Solvent A: 25 mM NH <sub>4</sub> HCO <sub>3</sub> buffer pH 7.5 Solvent B: 35 mM NH <sub>4</sub> HCO <sub>3</sub> buffer pH 7.5 containing 65 % acetonitrile
Gradient	0 min: 25% B in A; 50 min:100% B in A; 10 min: 25% B in A; 51 min:25% B in A; 11 min: 45% B in A; 60 min:25% B in A; 20 min: 45% B in A; 60 min: Stop; 40 min: 55% B in A;
Flow rate	1 ml/min
Column	Supelco Supelcosil™ LC-318 with pre-column
UV-Detection	210 nm and 274 nm
Fluorescence-Detection	$\lambda_{\text{ex}} = 274 \text{ nm}; \lambda_{\text{em}} = 308 \text{ nm}$

### 2.3.8 GFC Analysis of PEGylated and De-PEGylated Insulin

GFC analysis was performed using the same analytical set-up as for HPLC analysis. Measurements were again performed on a 10AVP HPLC system (Shimadzu, Duisburg, Germany). 50  $\mu\text{l}$  sample of PEGylated or de-PEGylated insulin solution prepared as described above were injected and analyzed using a Shodex OHpak SB-802.5HQ column with a Shodex OHpak-SB-G precolumn (Phenomenex, Aschaffenburg, Germany) tempered at 40 °C. Chromatograms were recorded on a Shimadzu SPD 10AV<sup>VP</sup> UV detector and a Shimadzu RF-355 fluorescence detector using the chromatographic conditions shown in **Table 5**. Data was accumulated and analyzed using HPLC software Class VP 6.05 from Shimadzu.



As mobile phase 0.05 M Tris buffer pH 8 containing various amounts of acetonitrile (20%, 10%, 0%) was used. Best results were obtained using pure Tris buffer.

**Table 5:** *Chromatographic conditions of GFC analysis of PEGylated insulin*

Eluents	0.05 M Tris buffer pH 8
Flow rate	0.8 ml/min
Column	Shodex OHpak SB-802.5HQ with pre-column
UV-Detection	210 nm and 274 nm
Fluorescence-Detection	$\lambda_{\text{ex}} = 274 \text{ nm}$ ; $\lambda_{\text{em}} = 308 \text{ nm}$

### 2.3.9 MALDI-ToF Analysis

For the low resolution method, analyses were performed on a HP G2030A System (GSG Mess- und Analysengeräte Vertriebsgesellschaft mbH, Karlsruhe, Germany) with the major components of a HP G2025A MALDI-ToF mass spectrometer coupled to a computer with printer. As matrix 10 mg sinapic acid were dissolved in 1 ml of a mixture of 70% acetonitrile and 30% ddH<sub>2</sub>O. Of a thoroughly blended 3:1 sample of analyte and matrix 1  $\mu\text{l}$  was placed on the mesa and the solvents evaporated under reduced pressure. Through addition of an average of 100 shots mass spectra were recorded in a range of 500 m/z to 15000 m/z.

For the analysis of the un-digested and digested insulin chains a high resolution method was used. Experiments were performed on a 4700 Proteomics Analyzer (ABI, Foster City, CA) with  $\alpha$ -cyano-4-hydroxy cinnamic acid as matrix.

## **2.4 Synthesis and Characterization of Lipophilized insulin**

### **2.4.1 Preparation of N-hydroxysuccinimide Ester of Palmitic Acid [Pal-NHS]**

The synthesis of Pal-NHS was performed following the method described in literature [179]. 0.05 mol of palmitic acid and 0.05 mol of N-hydroxysuccinimide were dissolved under gentle heating in 150 ml ethyl acetate. This solution was added to a solution of 1 mol DCC in 15 ml ethyl acetate and stirred for 15 hours at 4 °C. Insoluble dicyclohexylurea was removed by filtration and the filtrate was concentrated under reduced pressure. The crude product was redissolved in ethanol and left to crystallize at 4 °C for 3 h. The colorless precipitate was filtrated and dried under reduced pressure. The reaction was checked by <sup>1</sup>H-NMR.

### **2.4.2 <sup>1</sup>H-NMR Analysis**

<sup>1</sup>H-NMR spectra were recorded on an Avance 300 spectrometer from Bruker (Rheinstetten, Germany) with TMS as internal standard. For sample preparation, 20 mg of the amine reactive palmitic acid derivative were dissolved in 1 ml deuterated chloroform and filtered in a NMR tube. Unmodified palmitic acid measured in a second experiment served as control.

### **2.4.3 Preparation of Lipophilized Insulin**

For the syntheses of lipophilized insulin, 10 mmol bovine insulin were dissolved in a total volume of 35 ml N,N'-dimethylformamide [DMF], added in portions of 5 ml. To enhance the rather poor solubility of the protein, 25 µl of double distilled water containing 10 mmol NaHCO<sub>3</sub> was subjoined. A second solution of 5.35 mg Pal-NHS in 1 ml DMF was prepared. Combining the two solutions gave a reaction batch with a final molar ratio of insulin to palmitic acid of 2:3. The mixture was very gently shaken overnight at room temperature. To concentrate the reaction batch, DMF was evaporated under reduced pressure to a final volume of 8 ml. As lyophilization of this solution could not be performed, ultrafiltration was used instead. Therefore, 2 ml or 4 ml of the product were diluted by addition of 13 ml or 11 ml ddH<sub>2</sub>O respectively, and centrifuged at 3000 rpm for 30 min. Centriprep YM-3 Filter Devices from Millipore (Bedford, MA, USA) with a cut-off of

3000 Da were employed. Washing steps with ddH<sub>2</sub>O were repeated four times and the resulting turbid solutions were freeze-dried. The reaction was confirmed by high pressure liquid chromatography mass spectroscopy [HPLC-MS] and matrix assisted laser desorption ionization time of flight [MALDI-ToF].

#### 2.4.4 HPLC of Lipophilized Insulin

HPLC experiments were conducted on a 10AVP HPLC system (Shimadzu, Duisburg, Germany), which was composed of degasser, binary pump, low pressure gradient unit, autosampler, column oven, UV detector and fluorescence detector.

**Table 6:** *Chromatographic conditions of HPLC analysis of lipophilized insulin.*

Eluents	Solvent A: 900 ml ddH <sub>2</sub> O 100 ml acetonitrile 1 ml TFA	Solvent B: 100 ml ddH <sub>2</sub> O 900 ml acetonitrile 1 ml TFA
Gradient	0 min: 20% B in A; 30 min: 100% B in A; 40 min: 100% B in A;	49 min: 20% B in A; 60 min: Stop;
Flow rate	1 ml/min	
Column	Supelco Supelcosil <sup>TM</sup> LC-318 with pre-column	
UV-Detection	210 nm and 274 nm	
Fluorescence-Detection	$\lambda_{\text{ex}} = 274 \text{ nm}; \lambda_{\text{em}} = 308 \text{ nm}$	

For a typical experiment, 36  $\mu\text{l}$  of the concentrated solution was diluted with ddH<sub>2</sub>O to a final concentration of 0.2 mg insulin per milliliter sample. 50  $\mu\text{l}$  of this preparation was separated on a RP 18 column tempered at 40 °C. Chromatograms were recorded on a Shimadzu SPD 10AV<sup>VP</sup> UV detector and a Shimadzu RF-355 fluorescence detector using the conditions

shown in **Table 6**. Data was accumulated and analyzed using HPLC software Class VP 6.05 from Shimadzu.

#### **2.4.5 HPLC-MS**

For identification of the different insulin species separated by chromatography in-line HPLC - electrospray-mass spectroscopy was used. The analytical set-up consisted of a HPLC system including degasser, binary pump, autosampler, column oven and diode array detector (all from Hewlett-Packard, Waldbronn, Germany) coupled to an electrospray-mass spectrometer (ThermoQuest, San José, CA, USA). 20  $\mu$ l of the lipo-insulin solution were injected and run with a flow rate of 0.3 ml/min on a C18 column (Jupiter, Phenomenex, Torrance, CA). Chromatographic conditions regarding mobile phase and gradient were the same as those formerly described for HPLC experiments. Additionally to the diode array detector signals, total ion current chromatograms were recorded for substance identification and analysis. Mass measurements were performed in a range of 500 to 2200 masses per charge [m/z].

#### **2.4.6 MALDI-ToF of Lipophilized Insulin**

MALDI-ToF experiments were performed on a HP G2030A System (GSG Mess- und Analysengeräte Vertriebsgesellschaft mbH, Karlsruhe, Germany) with the major components of a HP G2025A MALDI-ToF mass spectrometer coupled to a computer with printer. As matrix 10 mg of sinapic acid were dissolved in 1 ml of a mixture of 70% acetonitrile and 30% ddH<sub>2</sub>O. Of a thoroughly blended 1:1 sample of analyte and matrix 1  $\mu$ l was placed on the mesa and the solvents evaporated under reduced pressure. Through addition of an average of 100 shots, mass spectra were recorded in a range of 500 m/z to 15000 m/z.

#### **2.4.7 Biological Activity of Lipo-Insulin**

Activity of the synthesized lipo-insulin was assessed in a cell culture proliferation system established by Kellner et al. [180]. Bovine chondrocytes, both primary and after the first passage, were used for this assay.

In short: primary chondrocytes were gained from the knee joints of six to twelve weeks old calves. Cells were used directly after isolation, or after 2-dimensional expansion, and were seeded at a concentration of 3300 cells/cm<sup>2</sup> in 12-well-plates. As cell culture medium DMEM supplemented with 50 U/ml penicillin, 50 µg/ml streptomycin, 10% FBS, 1% ascorbic acid, 1.15% proline, 1% HEPES buffer and 1% non-essential amino acids were used, with addition of insulin and lipophilized insulin in IGF buffer (100 mg bovine serum albumin were dissolved in 100 ml ddH<sub>2</sub>O with 60 µl acetic acid), corresponding to **Table 7**. Cell culture medium was exchanged every two days and new insulin or lipophilized insulin was supplemented. Harvesting of cells was performed after eight days of growth. Therefore, cells were washed with 1 ml PBS and trypsinized in 1 ml 0.25% trypsin solution. After transfer to 150 ml electrolyte solution counting occurred using a Coulter Multisizer II Coulter Counter (Beckman Coulter, Krefeld, Germany).

**Table 7:** *Experimental set-up of culture conditions of chondrocytes with supplements dissolved in IGF buffer.*

Group	CCM	IGF-Buffer	Supplement
Insulin 0.1	2 ml	100 µl	0.2 µg
Insulin 1	2 ml	100 µl	2.0 µg
Insulin 10	2 ml	100 µl	20.0 µg
Insulin 50	2 ml	100 µl	100.0 µg
Lipophilized Insulin 0.1	2 ml	100 µl	0.2 µg
Lipophilized Insulin 1	2 ml	100 µl	2.1 µg
Lipophilized Insulin 10	2 ml	100 µl	21.2 µg
Lipophilized Insulin 50	2 ml	100 µl	106.2 µg
Control (pure solvent)	2 ml	100 µl	0 µg

The experimental set-up consisted of nine groups with miscellaneous supplements comprising four different concentrations of insulin and lipophilized insulin, respectively (**Table 7**). For calculation of the required amount of lipophilized insulin, it was assumed that each insulin molecule was covalently bound to 1.5 palmitic acid chains increasing the molecular weight of lipophilized insulin to 6090 g/mol. The calculated amount of pure insulin was kept equal in each corresponding group of insulin and lipophilized insulin. Experiments were conducted in duplicate with  $n = 5$  for each group.

In a second experimental set-up, insulin was dissolved in IGF buffer and lipophilized insulin was dissolved in an organic solvent, N-methyl-2-pyrrolidone (**Table 8**).

Cells isolated like recorded above, were seeded in 12-well-plates at a density of 3300 cells per  $\text{cm}^2$ . The required amount of protein dissolved in 10  $\mu\text{l}$  NMP or 100  $\mu\text{l}$  IGF buffer respectively, was added to each group and aliquots of IGF-buffer or NMP were added in order that both solvents were present in each well. To investigate the effects of the solvents on cell proliferation two complementary groups were investigated: one were only the solvents were supplemented and an other were only CCM was used.

**Table 8:** *Experimental set-up of culture conditions of chondrocytes with lipophilized insulin dissolved in an organic solvent*

Group	CCM	NMP	IGF-Buffer	Supplement
Insulin 1	3 ml	10 $\mu\text{l}$	100 $\mu\text{l}$	0.2 $\mu\text{g}$
Insulin 10	3 ml	10 $\mu\text{l}$	100 $\mu\text{l}$	2.0 $\mu\text{g}$
Insulin 50	3 ml	10 $\mu\text{l}$	100 $\mu\text{l}$	20.0 $\mu\text{g}$
Lipophilized Insulin 1	3 ml	10 $\mu\text{l}$	100 $\mu\text{l}$	100.0 $\mu\text{g}$
Lipophilized Insulin 10	3 ml	10 $\mu\text{l}$	100 $\mu\text{l}$	0.2 $\mu\text{g}$
Lipophilized Insulin 50	3 ml	10 $\mu\text{l}$	100 $\mu\text{l}$	2.1 $\mu\text{g}$
Solvent	3 ml	10 $\mu\text{l}$	100 $\mu\text{l}$	21.2 $\mu\text{g}$
Control	3 ml	0 $\mu\text{l}$	0 $\mu\text{l}$	0 $\mu\text{g}$

Cell culture medium was exchanged every two days and new insulin or lipophilized insulin was supplemented. Harvesting of cells was performed after 14 days of growth. Therefore, cells were washed with 1 ml PBS and trypsinized in 1 ml 0.25% trypsin solution. After transfer to 150 ml electrolyte solution counting occurred using a Coulter Multisizer II Coulter Counter (Beckman Coulter, Krefeld, Germany).





# **Chapter 4**

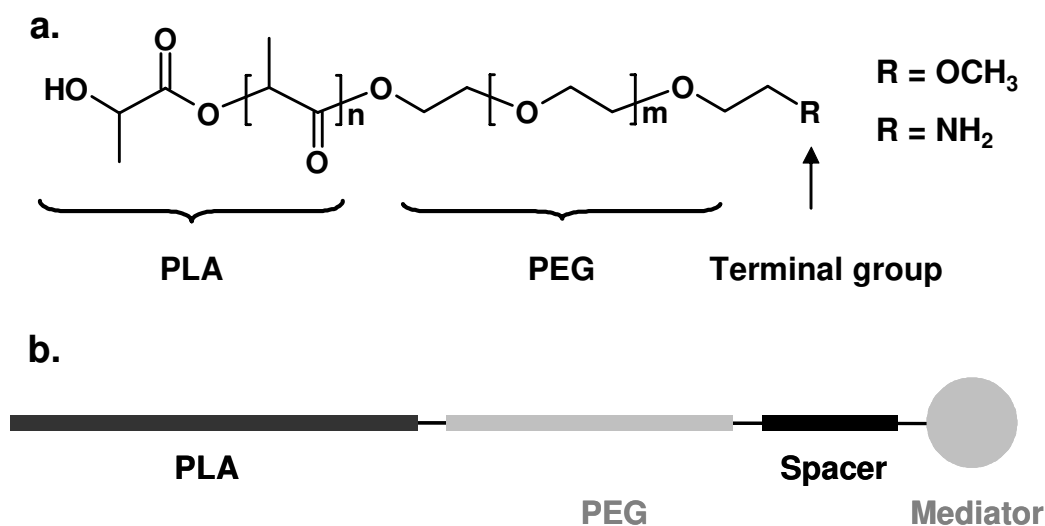
## **Synthesis and Characterization of Poly(ethylene glycol)co-poly(lactic acid)**

# 1 Introduction

Tissue Engineering is an emerging, interdisciplinary biotechnology area where medicine, cell and molecular biology, materials science and engineering intermingle, with the goal of generating constructs to replace or repair missing, severed or malfunctioning tissue. This discipline is based on three major pillars: cells, bioactive molecules and scaffold materials. The interplay of them or individual use might lead to the development of a construct with the designated qualities. Cells, preferentially autologous ones, are the material to create the desired tissue. Either already differentiated cells of the desired phenotype [181] or pluripotent stem cells [182] might be used. Limitation often lies in the difficult availability of the desired cells, being not at all or in scarce quantity obtainable. Secondly, among other factors bioactive molecules such as vitamins, drugs, growth factors or fragments thereof influence the further development of harvested cells. They can either initiate cell proliferation [183,184], leading to fast expansion of the original small collective, or they are able to trigger the internal signaling cascades which result in differentiation of progenitor cells to fully developed mature tissue [185,186]. Another fundamental feature is their ability to influence cell/material interactions to various effects, amongst others enhancing or oppressing adhesion of particular cells to a material [187]. Finally, biomaterials themselves can influence cell adhesion and development depending on their physical properties. A plethora of different biomaterials each with its own advantage to recommend them have been used, ranging from mechanically stable metal rods (such as titanium) [188], to hydrogel materials with favorable diffusion properties (such as alginates) [189], to biodegradable materials (such as poly(glycolic acid)) [190].

A frequently chosen polymer for Tissue Engineering applications is poly(lactic acid) [PLA]. Having been used for over 30 years as resorbable sutures and fixation devices, PLA has already been FDA approved for in vivo human use in several forms and formulations and profound knowledge on the properties of the material has been obtained [191]. In addition to the requested major feature of biocompatibility, the advantages of synthetic polymers: high purity, convenient processing and good mechanical properties, gained this polymer popularity for use as scaffold material [192]. A substantial prerequisite is its biodegradability, which occurs through hydrolysis, therefore showing little inter-individual variation, and its degradation product, lactic acid, already is present in natural metabolic pathways [193]. Many properties of the resulting polymer (e.g. degradation rate, crystallinity, and melting point)

depend on molecular weight and conformation of the monomers, giving the organic chemist a potent tool for tailor-made polymers. Also, due to its stability PLA is amenable to a wide variety of processing procedures (like melt spinning into fabrics [194], spin-casting of films [195], or production of bulk porous scaffolds [196]) resulting in devices, easily modeled in the desired shape, and which are good substrates for cell adhesion and proliferation. However, for in vivo use only selected proteins and therewith determined cells of a favored phenotype are wanted to adhere to these devices. Unfortunately the polymer shows no specificity at this vital point. To overcome this disadvantage, di-block copolymers composed of a poly(lactic acid) block with the advantages mentioned above, and a Methyl-poly(ethylene glycol) [PEG] block (**Scheme 1 a.**) were synthesized. Hydrophilic PEG chains attached to a surface are known to prevent or at least diminish protein adsorption [197].



**Scheme 1:** Structures of polymers synthesized by Teßmar et al.

a) Chemical structure of the polymer. b) Structure of the activated polymer with attached mediator molecule.

Replacing the terminal group at the free end of the PEG-block with a reactive amino group, new polymers were created which can be activated to react with bioactive molecules such as growth factors, vitamins or drugs, resulting in biomimetic polymers with ameliorated properties with regard to their application as Tissue Engineering scaffolds (**Scheme 1 b.**) [132]. Thus, not only adhesion, but moreover further development of the cells can be directed very pointedly, giving rise to the hope of creating superior scaffolds for Tissue Engineering purpose.

A method is described in literature to process these polymers into scaffolds for in vitro and in vivo cell experiments [24]. Therefore polymers of different compositions were needed (MePEG<sub>2</sub>PLA<sub>20</sub>, MePEG<sub>2</sub>PLA<sub>40</sub> and NH<sub>2</sub>PEG<sub>2</sub>PLA<sub>40</sub>). In the synthesis of diblock copolymers often the problem of nonuniform molecular weight distribution of the resulting polymers is encountered, which makes processing difficult. In this work it was tried to establish procedures to synthesize each of the aforementioned polymers in desired quality (regarding molecular weight distribution and processing properties) and new insights were gained on the reaction kinetics of the polymerization.

## 2 Results and Discussion

### 2.1 Reaction Kinetics of the MePEG<sub>2</sub>PLA<sub>20</sub> Synthesis

For the synthesis of the MePEGPLA polymer a method described in literature was adopted. Polymerization followed a catalytic ring-opening pathway with toluene as solvent, the free hydroxyl group of MePEG 2000 as initiator, D,L-lactic acid cyclic dimer as chain expander and stannous 2-ethyl-hexanoate as catalyst [141]. However, the result of the polymerization fell short of the goal, as the desired molecular weight could not be obtained by far and manufacture of mechanically stable scaffolds could not be achieved.

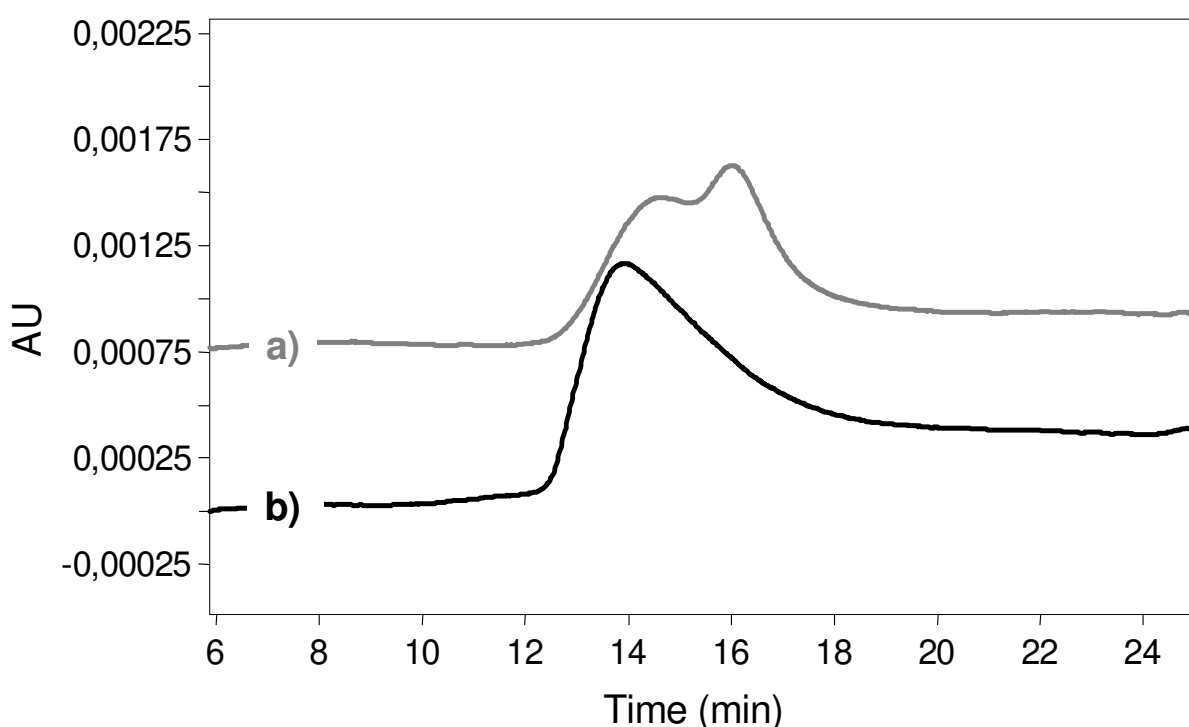


**Figure 1:** Refractive index detector chromatograms of SEC analysis of two different MePEG<sub>2</sub>PLA<sub>20</sub>. a) Newly synthesized polymer. b) Standard polymer with a nominal molecular weight of 22 kDa.

**Figure 1** clearly displays the differences between the newly synthesized polymer and a standard polymer obtained in a previous polymerization with a nominal molecular weight of 22 kDa. The newly synthesized polymer has a broader molecular weight distribution compared to the standard polymer, and the fraction of polymers with lower molecular weight, which are eluted at higher retention times, is much greater. This leads to the following

conclusions: either not the entire amount of the dilactide did react with the MePEG chains, so that resulting polymers were significantly shorter as expected or some co-initiator was present in the reaction batch, starting off new chains.

On our quest for gaining intelligence on the subject, we first checked the educts for integrity. <sup>1</sup>H-NMR analysis showed no changes in the structure of the substances and even buying new batches of material did not show the desired effect of prolonged polymer chains.

Hoping to gain knowledge on the kinetics of the polymerization reaction by monitoring the lengthening of the polymer chains over time, a reaction batch was synthesized and samples were drawn at various time points during the polymerization and analyzed by SEC (**Figure 2**).

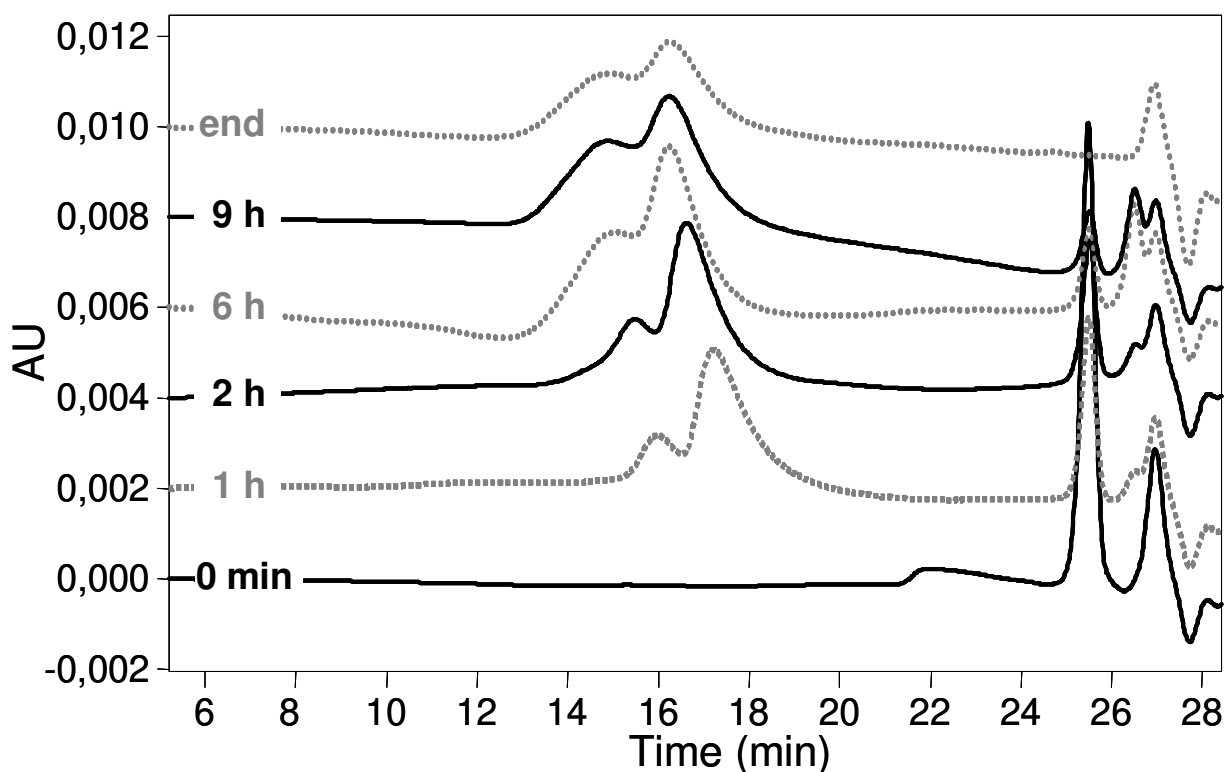


**Figure 2:** Kinetic of the polymerization of MePEG<sub>2</sub>PLA<sub>20</sub>. Chromatograms recorded by the refractive index detector. Samples taken from the crude reaction batch after various reaction time points, labeled accordingly, and after purification of the polymer (end).

Directly after the combination of the MePEG solution and the PLA solution (**Figure 2, 0 min**) the signal generated by MePEG can be observed at about 22 min and the higher and much sharper peak originating from eluted dilactide is detected at about 25 min. The

following signal pattern is attributed to the injection process, as it is present even if pure chloroform is analyzed. After one hour of polymerization (**Figure 2, 1 h**) a significant increase in molecular weight can be observed as the signal generated by the polymer is detected much earlier between 16 min and 18 min. Surprisingly, this signal shows a very clear bimodal distribution, which becomes less pronounced with increasing reaction time, finally merging to a very broad signal, with two culminations detectable. Besides, the formation of a new peak neighboring the injection pattern, at about 26 min could be observed. As this signal is not present in the chromatogram of the purified polymer, this substance could be either volatile or water soluble. One of these requirements, the water solubility, is met by the linear form of the lactic acid dimer, a very small molecule. Thus, the new peak might be assigned to this substance, which might be caused by traces of water still present in the reaction batch. Water or the open form of the lactic acid dimer might also act as initiators for new chains, which would then in consequence be 2 kDa shorter, than the MePEG originated ones. But the difference in molecular weight between the two peaks of the polymer signal is of more than this value. Besides, after one hour no new chains are generated, whereas the intensity of the signal attributed to the open form of the lactic acid, still increased. So, no satisfactory explanation for the bimodal distribution of the polymer signal could be found.

Examining the alteration over time of the detected polymer signal, the second peak seems to lose much of his prominence with increasing reaction times. Therefore, in another experiment the reaction time for the polymerization was increased to 24 h, hoping that with longer reaction times the overall molecular weight might be shifted to higher values.

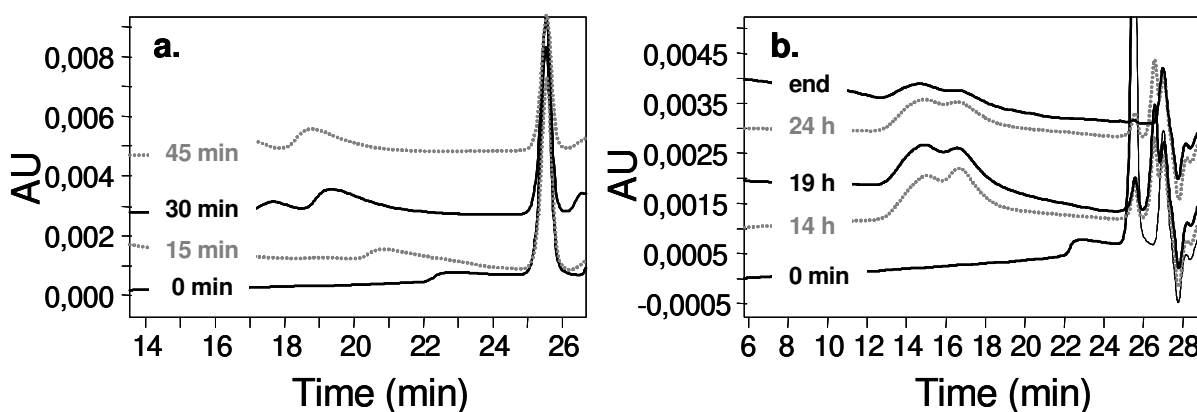


**Figure 3:** Investigation of the polymerization reaction of MePEG<sub>2</sub>PLA<sub>20</sub> in the first hour (**a.**) and up to 24 h (**b.**). Chromatograms were recorded by the refractive index detector. Samples were taken after various reaction time points, labeled accordingly and after purification of the polymer (*end*).

Investigation of the first hour of the polymerization revealed that bimodal distribution of the polymer signal can already be detected at 15 min and after 30 min the split of the signal is quite pronounced (**Figure 3, a.**). However, longer reaction times resulted in a considerable decrease of the low molecular weight fraction of the polymer (**Figure 3, b.**), causing the split almost to wear away. Extrapolating this observation led to the assumption that a still considerable longer polymerization time might result in a monomodal distribution of the molecular weight of the polymer.

## 2.2 Purification of the synthesized polymer with ethanol

To gain more information on the nature of the substances leading to the bimodal molecular weight distribution of the polymer and hopefully to establish a method for the separation of the low and high molecular weight fractions of the polymer another approach was tested. In contrast to high molecular weight PLA low molecular PLA is soluble in ethanol.

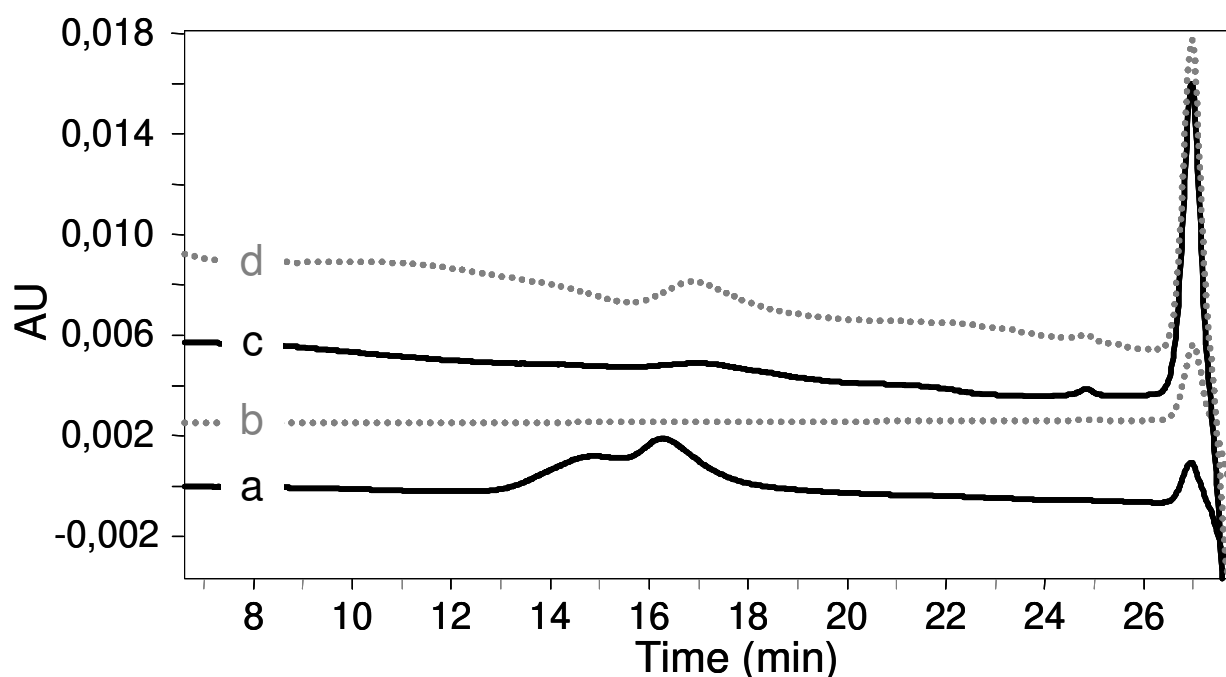


**Figure 4:** SEC chromatograms detected by the RI detector of samples collected during extraction of the polymer with ethanol.

**a:** Original polymer; **b:** Ethanol fraction collected at 20 °C; **c:** Ethanol fraction collected at 70 °C; **d:** Ethanol fraction collected at 77 °C



In a first attempt the polymer was extracted with ethanol at different temperatures, the supernatant was collected and volatiles were removed from the samples, which were subsequently analyzed by SEC (**Figure 4**).

Starting at 20 °C every 10 °C samples were collected. During the first steps of the experiment no polymer could be detected in the ethanol fraction. Between heating from 50 °C to 60 °C the solvent became turbid, but still no peak could be observed in the corresponding chromatogram. The analysis of the sample drawn at 70 °C hints at traces of a low molecular weight polymer being eluted at about 17 min and in the chromatogram of the sample last collected at 77 °C polymer is clearly detected at about 17 min, which correlates well with the low molecular weight fraction of the original polymer.

A method was found to remove some of the low molecular weight fraction of the polymer. However, this method is not quite satisfying. As the substance was applied as a solid some of the smaller chains might be enclosed in polymer particles thus escaping extraction.

Hence, in another experiment a solution of the polymer in acetone was prepared and ethanol added until the solution separated in two phases. The supernatant, which contained more solvent and less polymer, and the residue, which was highly viscous, were collected separately and analyzed by SEC (**Figure 5**).

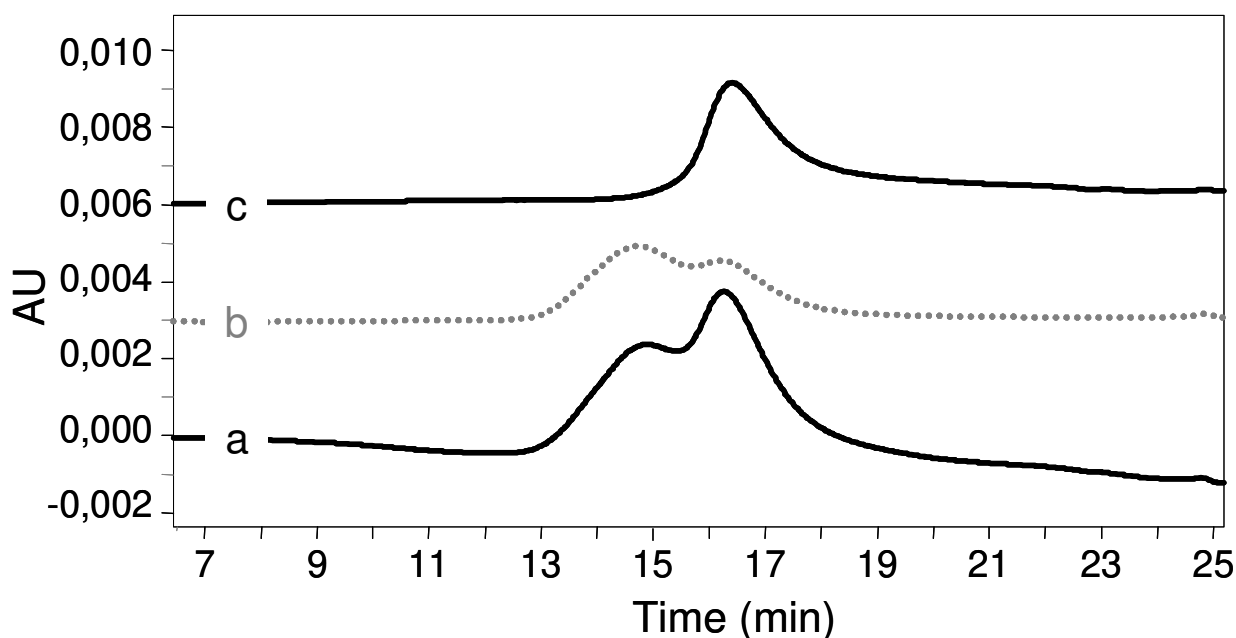


**Figure 5:** RI chromatograms of the substances collected in the phases generated by adding ethanol to an acetone solution of the polymer.

**a:** Original polymer; **b:** Residue; **c:** Supernatant

Chromatograms displayed in **Figure 5** clearly show that a separation of the substances leading to the bimodal distribution of the molecular weight of the polymer could be achieved in parts. The residue is enriched with long chain polymers compared to the mass distribution of the original polymer. In contrast, the supernatant contains mainly a portion of the small molecular weight fraction. To learn more about the composition of the different samples they were analyzed by <sup>1</sup>H-NMR techniques.

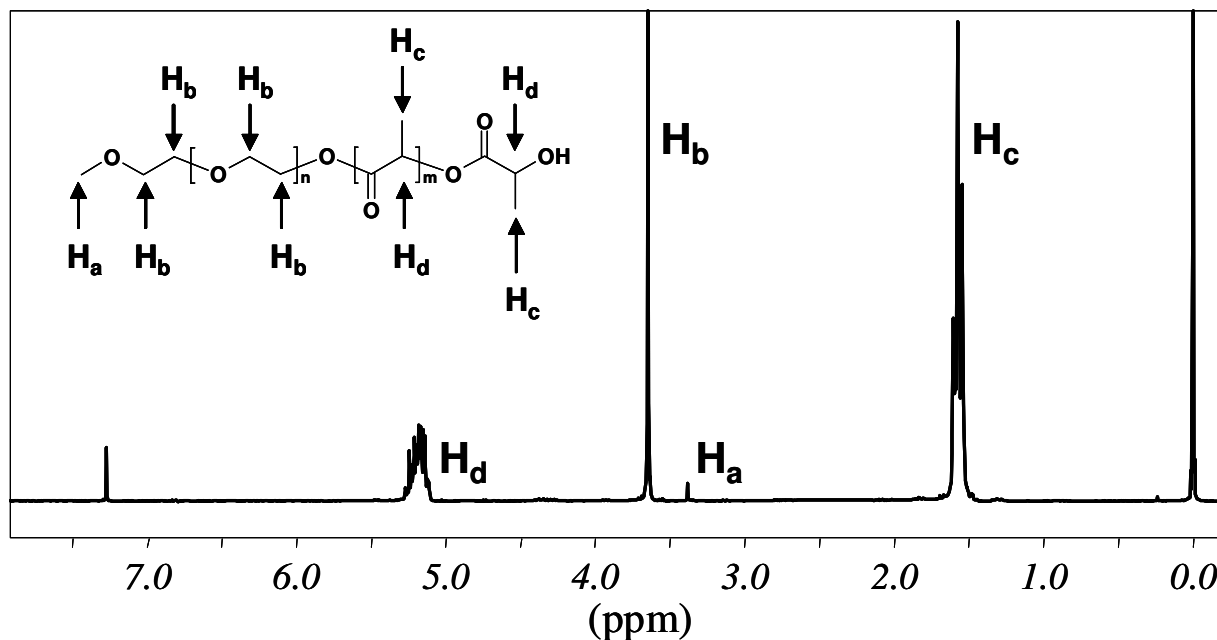


**Figure 6:** <sup>1</sup>H-NMR spectrum of MePEG<sub>2</sub>PLA<sub>20</sub> collected in CDCl<sub>3</sub> with TMS as internal standard.

<sup>1</sup>H-NMR spectra of the various polymer samples showed all a similar signal pattern (**Figure 6**), differing only in the intensity of the signals. The signal stemming from the methyl group of the MePEG (H<sub>a</sub>) could be detected at 3.38 ppm and the methylene repetitive unit of the MePEG (H<sub>b</sub>) caused a distinct signal at 3.64 ppm. The triplet observed at 1.56 ppm originated from the methyl group of the PLA (H<sub>c</sub>) and the multi-peaked signal at 5.17 ppm was attributed to the proton at the optically active center of the lactic acid monomer (H<sub>d</sub>).

**Table 1:** Integrals of the <sup>1</sup>H-NMR signals corresponding to the protons of MePEG<sub>2</sub>PLA<sub>20</sub>. The signal of the terminal methyl group of the MePEG was used as standard and set at 3.00.

Proton	Original Polymer	Residue	Supernatant
H <sub>a</sub>	3.00	3.00	3.00
H <sub>b</sub>	167.22	161.74	172.83
H <sub>c</sub>	758.59	957.32	533.43
H <sub>d</sub>	243.85	307.26	134.44

For comparison of the integrals calculated from the protons corresponding to the different polymers, the signals originating from H<sub>a</sub> were used as standard and the integrals set at 3.00 for each polymer (**Table 1**). As expected no remarkable differences in the ratios of H<sub>a</sub> to H<sub>b</sub>, the MePEG protons, could be seen for the different polymers (original polymer, residue, supernatant). Calculating the molecular weight of the MePEG chain by dividing the values of the H<sub>b</sub> proton signals by four, the number of protons of the monomer, and multiplying the resulting value by 44, the molecular weight of a monomer, values between 1.8 kDa and 1.9 kDa are obtained, which are in good agreement with the theoretical value of 2.0 kDa. In contrast, the signals stemming from H<sub>c</sub> and H<sub>d</sub>, which are protons attributed to the PLA chain, differ very distinctly in their ratio to the PEG protons. The molecular weights of the PLA chains can be calculated by multiplying the value of the H<sub>d</sub> signal by 72, the molecular weight of a PLA monomer, or by first dividing the value of the H<sub>c</sub> signal by three and subsequent multiplication by 72. This results in molecular weights of 18 kDa for the original polymer, 22 kDa to 23 kDa for the residue and 10 kDa to 13 kDa for the supernatant. So, the separation of the low and high molecular weight chains could be confirmed by a second method.

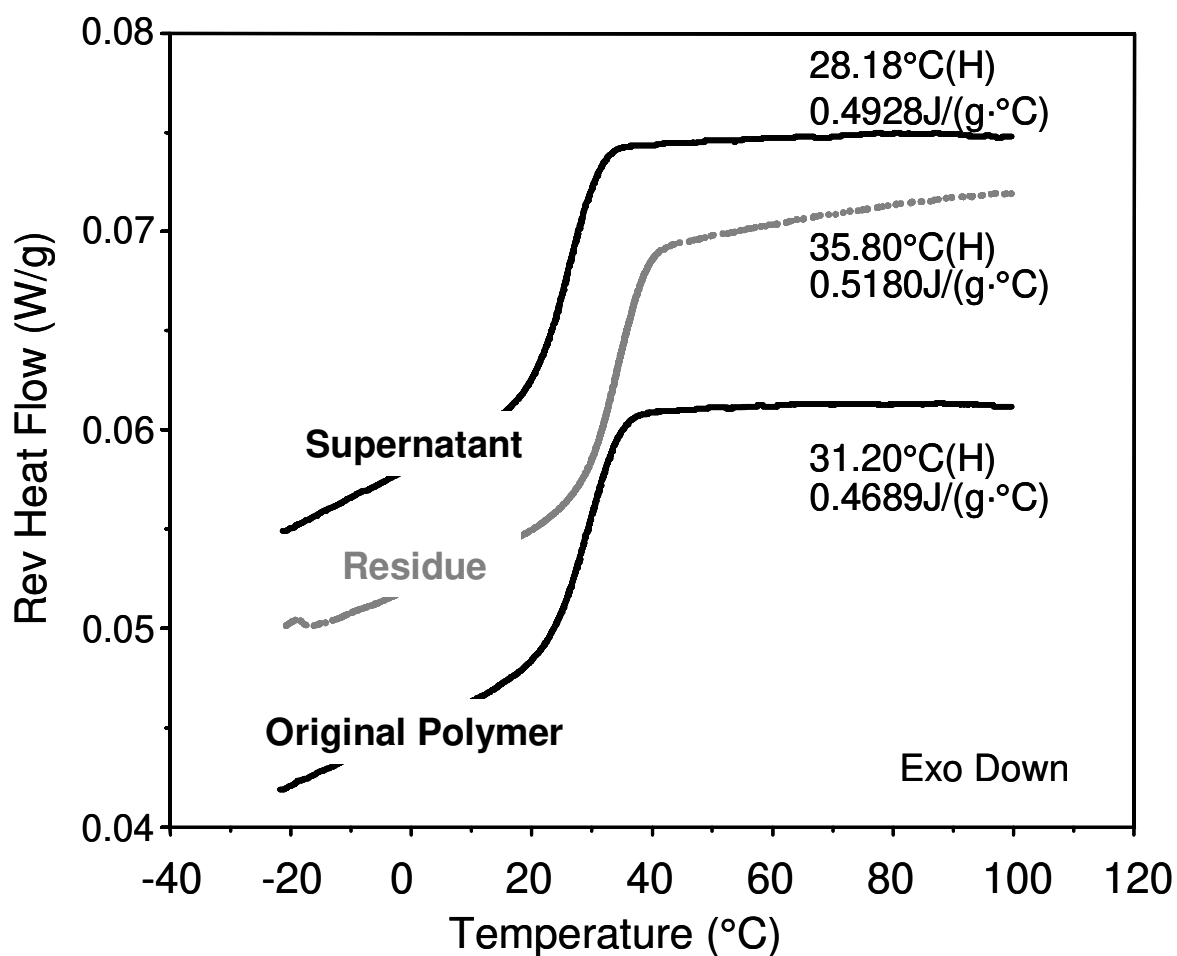


**Figure 7:** Thermograms of ethanol treated polymers (original polymer, supernatant residue) obtained by modulated DSC measurements for determination of the glass transition of the polymers.

To confirm NMR and SEC results the polymers were analyzed by MDSC (**Figure 7**). For calculation of the glass transition, the reversing heat flows of the second heating were used. Having a higher molecular weight, the residue shows a distinctly higher glass transition temperature compared to the low molecular weight polymers of the supernatant. Glass transition of the original polymer is settled between these two values, which correlate to the length of the polymer chains.

Considering the results of SEC, DSC and especially NMR analysis, the conclusion can be drawn that low and high molecular weight fractions differ only in the length of the PLA chain and not in their composition. Therefore, the assumption that the shorter fraction might be started by a different initiator can no longer be sustained.

### 2.3 Melt Synthesis of MePEG<sub>2</sub>PLA<sub>20</sub>

Although a method was found to separate the low and high molecular weight fraction of a synthesized polymer with bimodal molecular weight distribution, this is an additional time consuming and cumbersome step in the work-up of the polymer. Therefore it was tried to modify the parameters of the synthesis such as to directly result in a narrow molecular weight distribution of the polymer.

In literature the synthesis of PLA is not only described in solution but also in melt. Following this method some of the parameters which might influence the outcome of the polymerization can be circumvented. In the process, the effect of the solvent itself on the reaction, and also the influence of different concentrations of the reactants depending on the amount of solvent used, which might also play a role in the polymerization process, would be avoided.

Therefore, the synthesis of a MePEG<sub>2</sub>PLA<sub>20</sub> was performed in melt under an Argon atmosphere at 140 °C, and the resulting polymer was purified and analyzed by SEC (**Figure 8, b**).

### 2.4 Polymerization in Solvent with the Modified Methods of MePEG<sub>2</sub>PLA<sub>20</sub> and MePEG<sub>2</sub>PLA<sub>40</sub>

Although polymerization in melt yielded substances with the targeted molecular weight, the conditions used in this method are quite harsh (synthesis in vacuum at 140 °C). If the synthesis of MePEG<sub>2</sub>PLA<sub>20</sub> is performed in solution, not only the thermal load on the polymers is reduced, but also the handling of the reaction is much facilitated.

Knowing that longer reaction times at polymerization in solution, where the volume of the solvent usually decreases due to evaporation of part of the solvent, led to polymers with increased chain length, the influence of solvent volume on the product was investigated. Therefore a new reaction batch was synthesized using a substantially smaller amount of solvent volume. After eight hours of polymerization the crude product was purified, collected and analyzed by SEC (**Figure 8, a**).

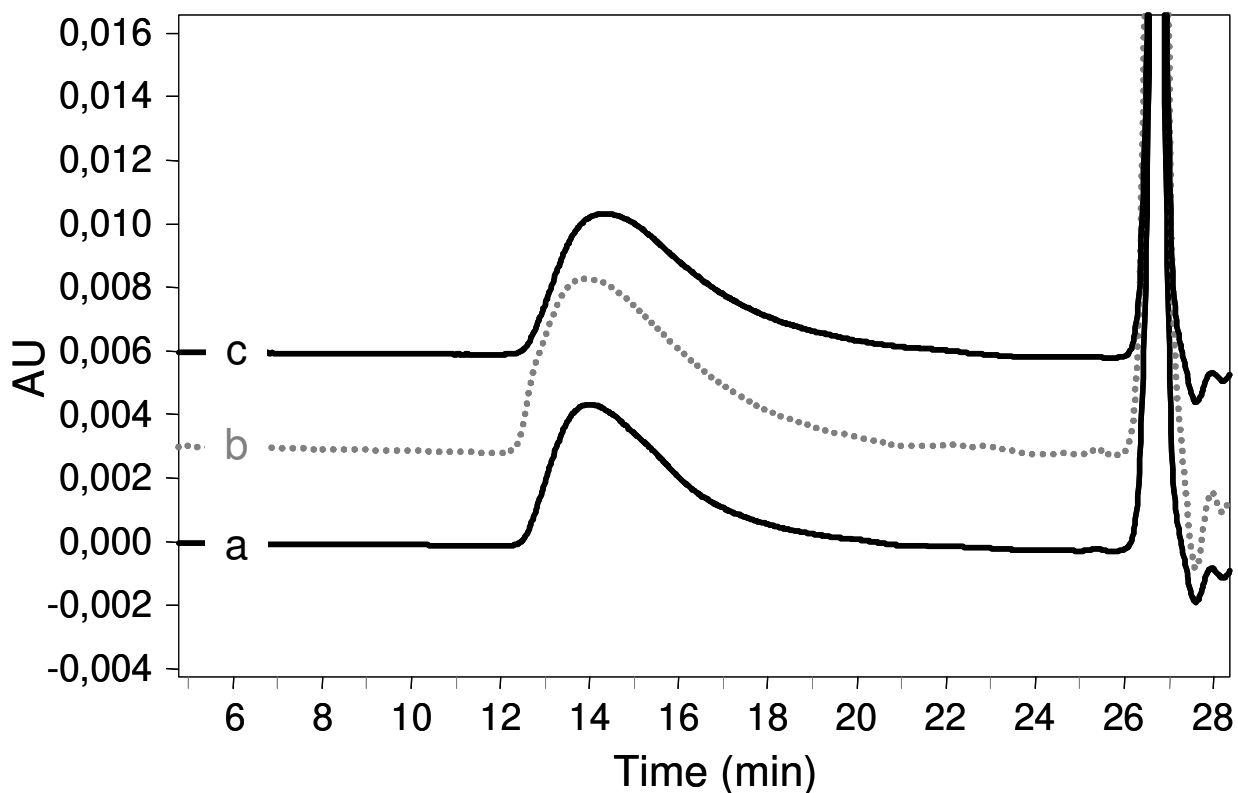


**Figure 8:** SEC chromatograms of differently synthesized MePEG<sub>2</sub>PLA<sub>20</sub> polymers collected using an RI detector.

**a:** Polymer synthesized using a small amount of solvent; **b:** Polymer synthesized in melt; **c:** Reference polymer

Comparing the chromatograms recorded while analyzing polymers synthesized with no or few solvent no difference can be detected with regard to final molecular weight of the products. Moreover, the mass of the resulting polymers do not differ substantially from those of the polymer used as reference. Therefore, the conclusion can be drawn that using the established method for the synthesis of MePEG<sub>2</sub>PLA<sub>20</sub> polymers with the aspired molecular weight are fabricated.

In another experiment the synthesis of MePEG<sub>2</sub>PLA<sub>40</sub> was performed. As this molecule with a molecular weight of 42 kDa results in more viscous solutions, the volume of the solvent had to be slightly increased. The product was purified collected and analyzed by SEC.

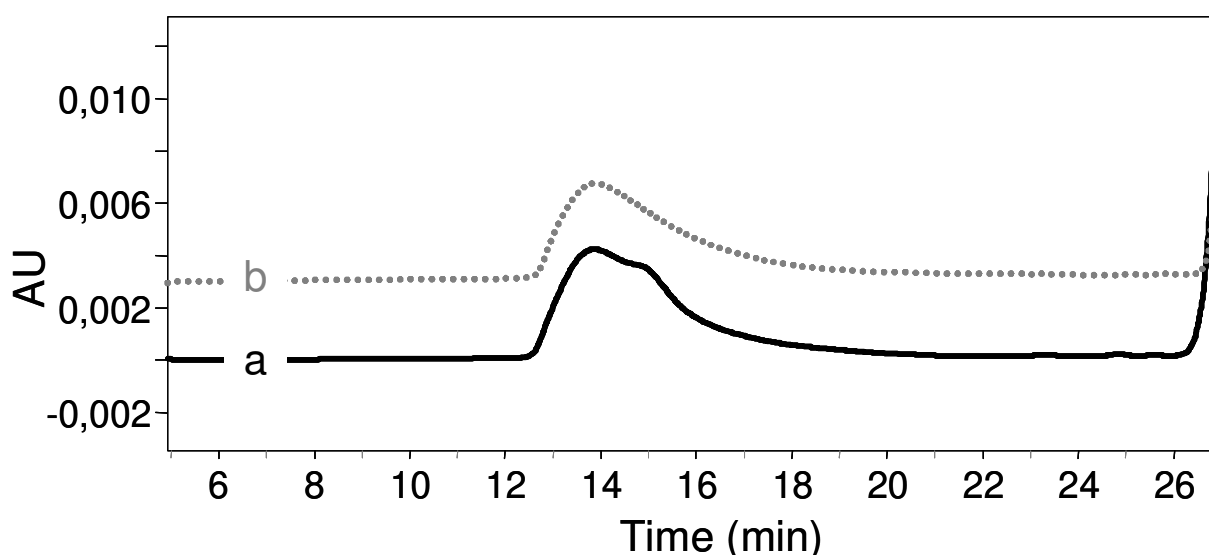


**Figure 9:** SEC chromatograms of MePEG<sub>2</sub>PLA<sub>40</sub> polymers collected using an RI detector. **a:** Polymer used as reference; **b:** Polymer synthesized with a small volume of solvent

In **Figure 9** it can clearly be seen, that the newly synthesized polymer had also a monomodal molecular weight distribution. Thus, it was confirmed, that the new method reliably yielded polymers with the desired molecular weight.

## 2.5 Synthesis of NH<sub>2</sub>PEG<sub>2</sub>PLA<sub>40</sub>

For the synthesis of biomimetic PEGPLAs it is imperative to use a bifunctional PEG chain as initiator, thus after polymerization the free end of the hydrophilic chain might react with a modulator molecule. Teßmar et al. used a PEG with a terminal hydroxyl group and an amine group at the other end of the polymer chain [132]. To prevent the reaction of the nucleophilic amine group with the dilactide, glacial acetic acid was added to the reaction batch protonating the amine.

The synthesis of a NH<sub>2</sub>PEG<sub>2</sub>PLA<sub>40</sub> was attempted following the newly established protocol. After eight hours of polymerization, the product was not a highly viscous solution, but a rather crystalline residue which smelled strongly of acetic acid. Analyzing the product by SEC revealed that the resulting polymer had a very low molecular weight of approximately 2000 to 5000 Da. Assuming that incomplete polymerization was due to the presence of acetic acid in the reaction batch, a new method was tried for the synthesis of NH<sub>2</sub>PEG<sub>2</sub>PLA<sub>40</sub>. Starting from a larger volume of solvent compared to the previous experiment, a constant

stream of nitrogen removed volatile components from the reaction batch, such as acetic acid and also toluene. After reaching the targeted amount of solvent, the nitrogen stream was stopped and the reaction continued. The resulting polymer was purified, collected and analyzed by SEC (**Figure 10**).

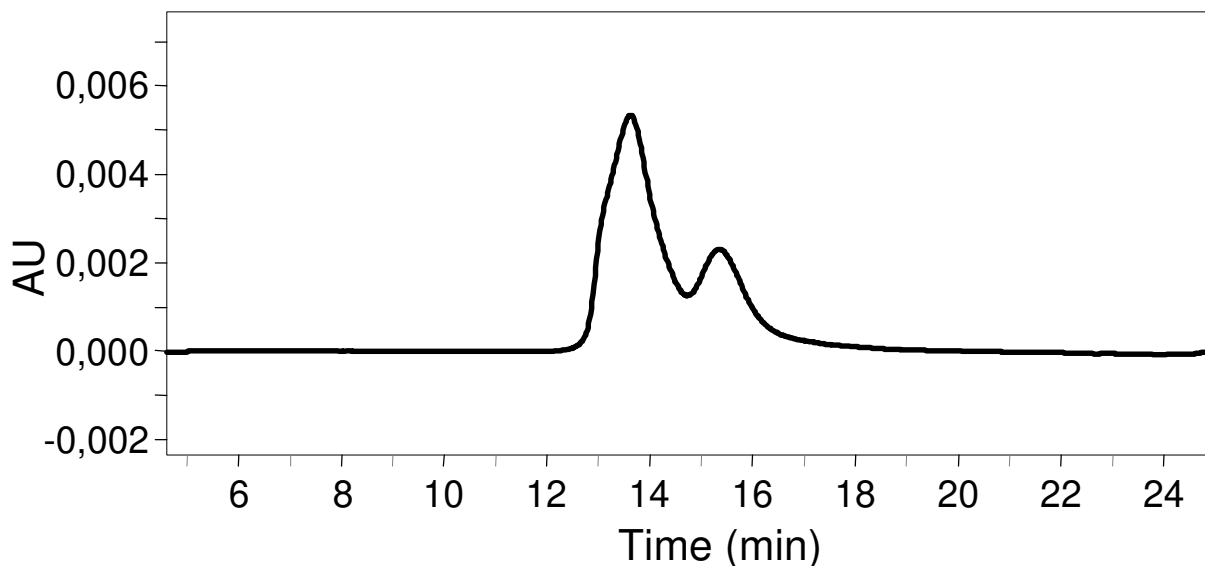


**Figure 10:** SEC chromatogram of  $\text{NH}_2\text{PEG}_2\text{PLA}_{40}$  collected using a RI detector.

The chromatogram of the synthesized  $\text{NH}_2\text{PEG}_2\text{PLA}_{40}$  shows a very clear bimodal molecular weight distribution, which might be the result of a too large solvent volume used. Yet even the starting material, a self synthesized  $\text{NH}_2\text{PEG}$ , shows a broader molecular weight distribution, compared to commercially available MePEG, a characteristic which will be passed on to the product.

However, scaffolds manufactured from this material showed a satisfying mechanical stability, enabling them for in vitro and in vivo cell experiments.

## 2.6 Activation of $\text{NH}_2\text{PEG}_2\text{PLA}_{40}$

To enable  $\text{NH}_2\text{PEG}_2\text{PLA}_{40}$  to react with proteins, first a linker, activated tartaric acid, was bound covalently to the terminal free amine group of the polymer. Prior to binding to the polymer the activation of the linker was checked by  $^1\text{H-NMR}$  (**Figure 11**).



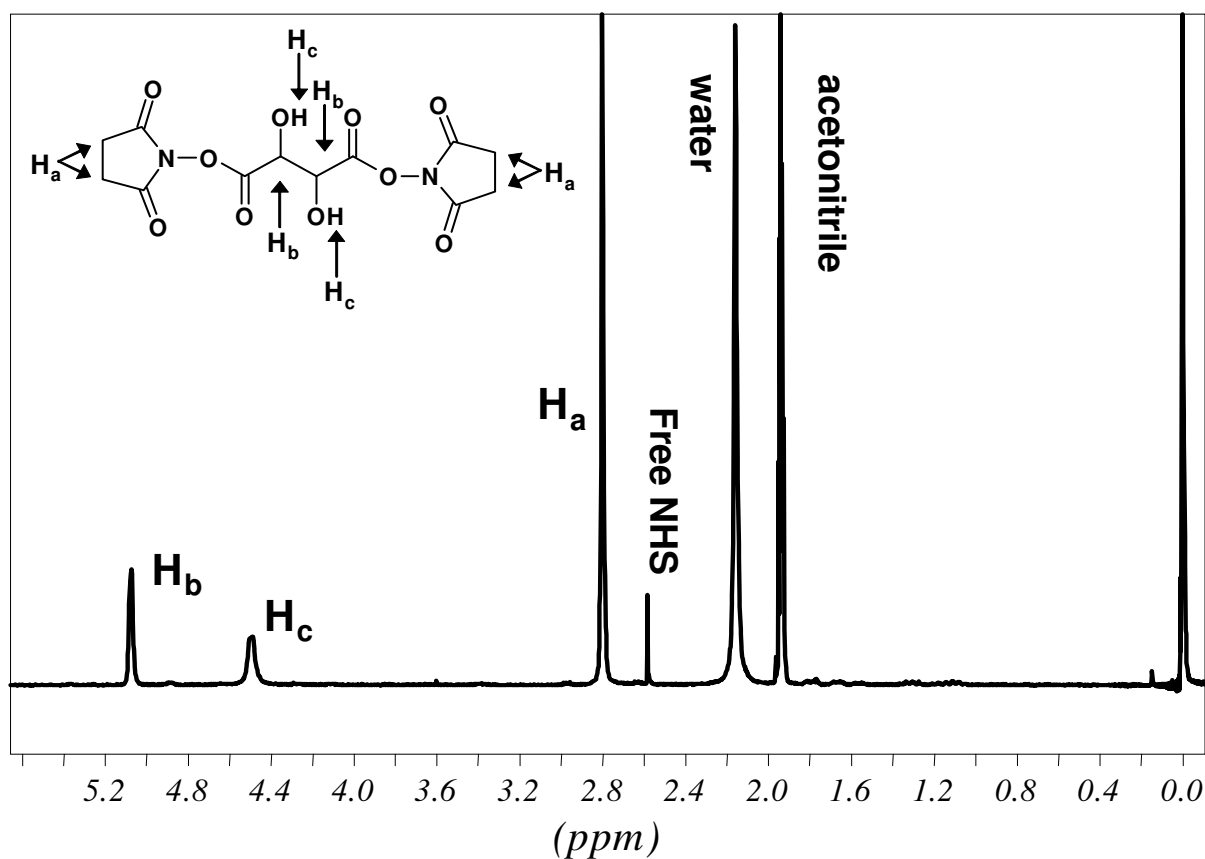


**Figure 11:**  $^1\text{H-NMR}$  spectrum of activated tartaric acid recorded in deuterated acetonitrile.

The signals of free and bound NHS can be detected in the resulting  $^1\text{H-NMR}$  at different ppm (free NHS: 2.58 ppm, bound NHS 2.80 ppm), confirming the activation of tartaric acid. Moreover, integrating the signals stemming from the protons of tartaric acid ( $\text{H}_b$  at 5.07 ppm and  $\text{H}_c$  at 4.49 ppm) and bound NHS ( $\text{H}_a$ ), ratios of  $\text{H}_a:\text{H}_b:\text{H}_c = 4:1:1$  were obtained, which correspond with the theoretical ratios.

To confirm the reactivity of the resulting activated polymer, a dye containing an amino group, 5-aminoeosin was bound to the polymer and the product subsequently analyzed by SEC (**Figure 12**).

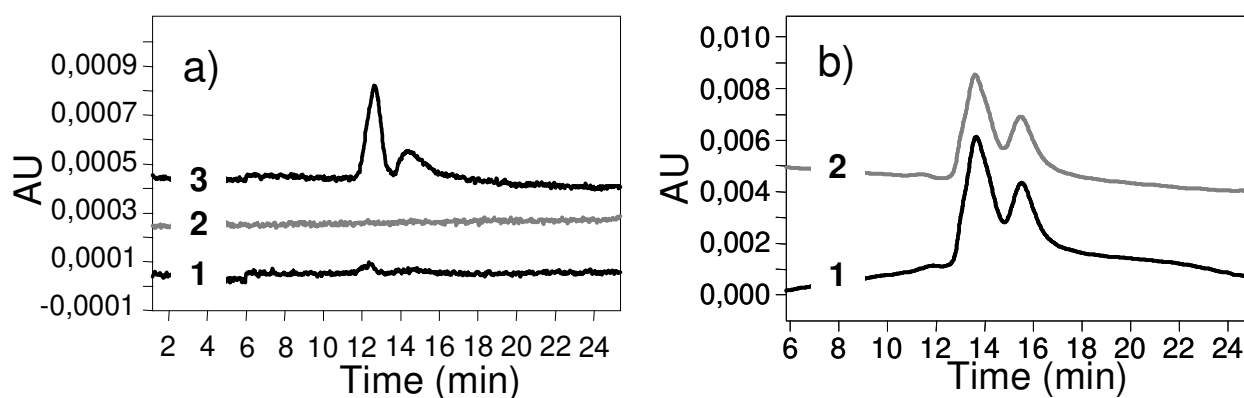


**Figure 12:** SEC chromatograms of the activated polymer after reaction with 5-aminoeosin.

**a)** UV-detector at 523nm. 1: Polymer; 2: Dye; 3: Polymer + Dye (reacted for 3h);

**b)** RI-detector. 1: Polymer; 2: Polymer + Dye (reacted for 3h)

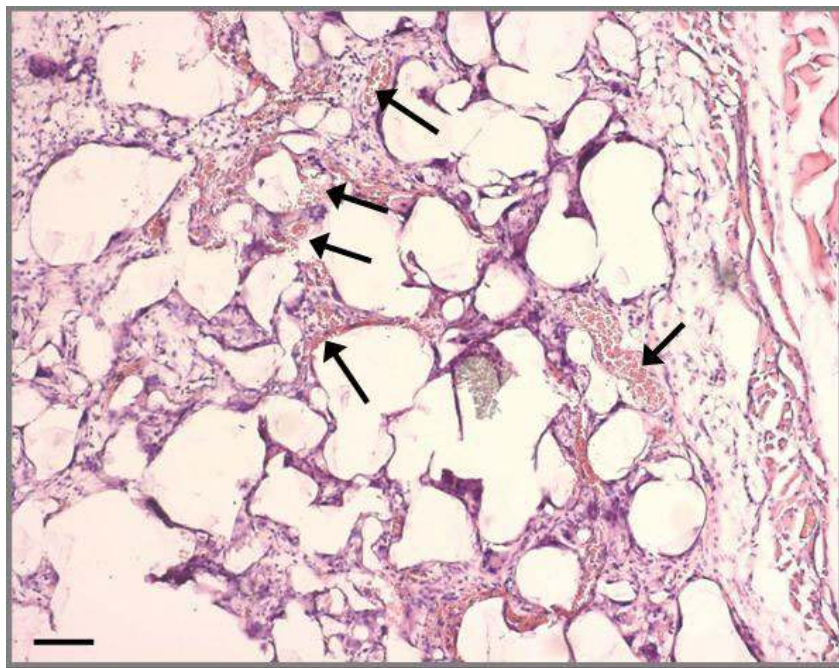
The intensities of the RI-detector signals were similar, proving that corresponding amounts of polymer were present in each sample. Regarding the UV-detector chromatograms, only the sample where dye and polymer were present showed adsorption, confirming the reactivity of the activated polymer

## 2.7 In Vivo Evaluation of PEG<sub>x</sub>PLA<sub>y</sub>

For evaluation of the synthesized polymers for in vivo Tissue Engineering applications, the polymers were processed into highly porous scaffolds using an anhydrous porogen leaching technique established by Hacker et al. [24]. bFGF was used as model protein, a growth factor frequently employed in cell culture, with well known angiogenesis inducing properties. As control group for the immobilized growth factor on the activated polymer served a group with only adsorbed protein. Scaffolds were implanted into the back subcutis of mice and excised after three weeks.

In **Figure 13** the effects of covalently bound bFGF are demonstrated. In the exemplarily shown section of the construct of activated polymers numerous capillaries can be seen. Besides the ingrowth of connective tissue is substantially pronounced, compared to the inactive polymer.

a)



b)

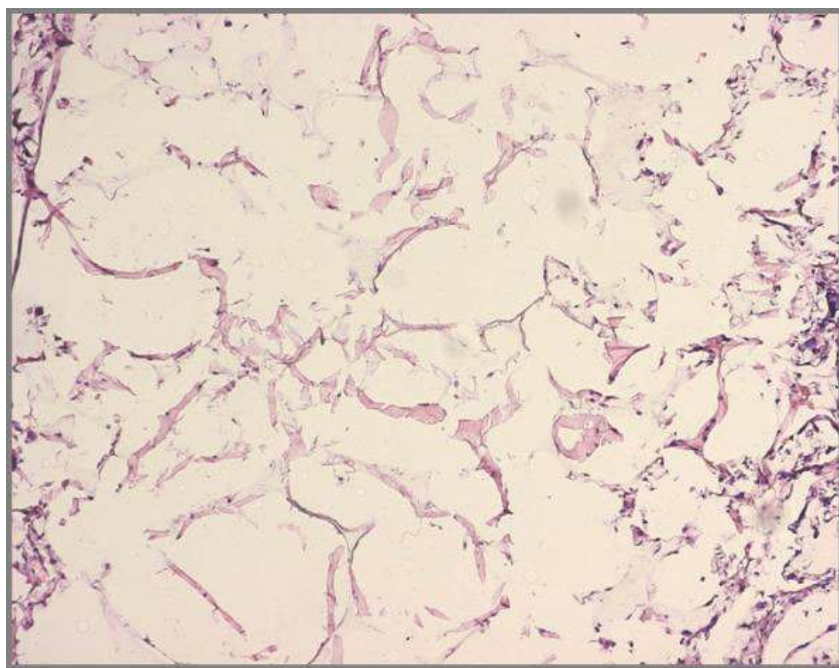


**Figure 13:** *H&E histology of scaffolds (magnification 100x) excised three weeks after implantation.*

**a)** *Scaffold of the activated polymer to which bFGF was covalently bound. b) Control scaffold of MePEG<sub>2</sub>PLA<sub>40</sub> with adsorbed bFGF. Black arrows mark capillaries within the construct. Scale bar: 100  $\mu$ m.*

### 3 Summary

Information was gained on the progress of the PEGPLA polymerization. Although not all of the mechanisms involved in this synthesis could be elucidated, a method was established for the synthesis of MePEG<sub>2</sub>PLA<sub>20</sub>, MePEG<sub>2</sub>PLA<sub>40</sub> and also for the synthesis of NH<sub>2</sub>PEG<sub>2</sub>PLA<sub>40</sub>. The polymers were processed into scaffolds and evaluated in an in vivo experiment and proved their superiority compared to standard used material.

Thus, the manufacture of this very promising candidate for Tissue Engineering applications was significantly optimized.

# **Chapter 5**

## **Investigation of Protein Adsorption on MePEG<sub>x</sub>PLA<sub>y</sub>**

## 1 Introduction

The interaction of proteins with solid surfaces is a fundamental phenomenon with implications for nanotechnology, biomaterials and biotechnological processes. In nanotechnology, protein-surface interactions are pivotal for the assembly of interfacial constructs [198]. In the biomaterials field, protein adsorption is the first step towards the integration of the implanted device or material with tissue [199], as cells depend on specific proteins for anchorage and extracellular instructions [200]. Even though cell attachment and spreading may occur without serum proteins, this is a nonphysiological interface [199], which can impair cell activity and contribute to cell death [201]. As protein-surface interactions are highly dependent on the individual properties of the analyzed system, they must be assessed separately for each individual setup. A great variety of methods has been established on the route to elucidating adsorption behaviour of proteins. They range from optical methods, which involve fluorescence or chemiluminescence labelling of proteins, to radiolabelling of the proteins, both purely quantitative methods. Solid-state NMR [202] and attenuated total reflection FTIR [ATR-FTIR] spectroscopy [203] may be used to detect changes in the protein structure, whereas atomic force microscope [AFM] based methodology provides information on the magnitude and nature of protein adhesion forces [204]. However most of these methods are expensive, use hazardous materials and require laborious preparations and long analysis times. The quartz crystal microbalance [QCM] is a simple, cost effective, high-resolution mass sensing technique, [205] which provides real-time analysis while being a non-invasive analytical method.

Here the impact of the PEG content on the surface properties of PEG<sub>x</sub>PLA<sub>y</sub> films was investigated with regard to its influence on protein adsorption. This is of significance as PEG chains are used to shield PLA derived devices (microparticles, scaffolds for Tissue Engineering applications) from unspecific protein adsorption.

The basis of the QCM is the converse piezoelectric effect, which occurs in crystals without a centre of symmetry: application of a voltage across these crystals causes a corresponding mechanical strain [206]. Sandwiching these crystals, such as quartz, between two electrodes connected to alternating current results in a mechanical oscillation of a standing shear wave across the crystal disk [205]. The direction of oscillation depends on the angle of cut of the crystal with respect to its crystallographic axes [207]. The mode most sensitive to mass

change is the thickness shear mode [TSM] which is characteristic for AT- or BT-cut crystals (**Figure 1**). AT-cut crystals, cut at  $+35^{\circ} 10'$  angle from the z-axis, show stable resonant frequencies over a wide range of temperatures and therefore are used for the majority of piezoelectric work in analytical chemistry [208]. These crystals can either be part of an oscillatory circuit, or alternating voltages at various frequencies are applied across the crystal by an external instrument, the latter method being to date fewer used [209]. There are two general classes of piezoelectric devices: bulk acoustic wave [BAW], also known as QCM or TMS, and surface acoustic wave [SAW], where both electrodes are placed on the same side of the crystal [210]. Although SAW devices are more mass sensitive than BAW devices, in practice they exhibit various problems like attenuation of the acoustic waves [211] and therefore BAW devices are more frequently used, due to their robust nature, availability and affordable electronics.

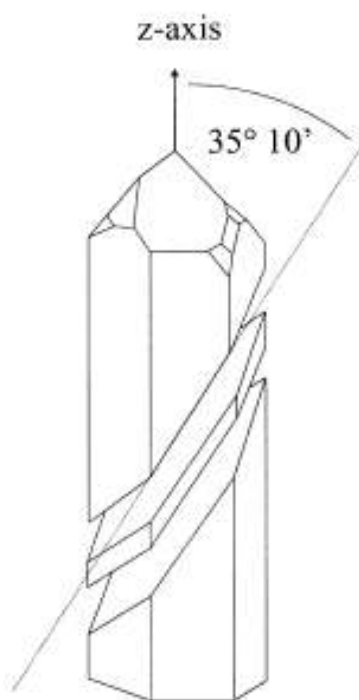


**Figure 1:** AT-cut of a quartz crystal. A quartz plate is cut with an angle of  $35^{\circ} 10'$  with respect to the optical z-axis from the mother quartz. Reproduced from [207].

The vibration of the quartz is described by the amplitude of the oscillation, corresponding to the energy initially imported, and the resonant frequency, determined by physical characteristics of the crystal. Fractional changes in thickness of the quartz in consequence of

mass adsorption result in fractional changes in frequency. This dependency can be described by the empirically developed equation of Sauerbrey [212]:

$$\Delta F = \frac{-2f_0^2 \Delta m}{A\sqrt{\mu_q \rho_q}} = -C\Delta m$$

where  $\Delta F$  = measured frequency shift in Hz,  $f_0$  is the fundamental resonant frequency in Hz,  $\Delta m$  = mass change in g,  $A$  = piezoelectrically active area in  $\text{cm}^2$ ,  $\mu_q$  = shear modulus of quartz and  $\rho_q$  = density of quartz. Most of this parameters can be summarized to  $C$  = mass sensitivity constant, characteristic for a certain quartz. The piezoelectrically active area of QCM is the area between the electrodes, where sensitivity is highest in the centre and decreases monotonically in a Gaussian-like manner towards the periphery [206]. The Sauerbrey equation can only be applied for the deposition of uniformly distributed, rigid masses in gas phase deposition. Although many attempts were made to find an equation applicable to solution phase sensing (e.g. Kanazawa and Gordon [213,214], or Bruckstein and Shay [215]), no overall answer was found. To date it is agreed that changes in frequency of a quartz with only one electrode in contact with the liquid can be the result of one or a combination of following reasons [205]: 1) a pure elastic mass adsorption to the quartz, or b) a pure liquid viscosity-density change in the solution adjacent to the electrode, or c) a dissipation of energy due to binding of an inelastic mass. For evaluation of the viscoelastic character of adsorbed masses quartz crystal microbalance-dissipation [QCM-D] measurements might be used [216]. If no great change in viscosity or density of the liquid phase is expected and the bound mass is elastic, after calibration the QCM might be used as a very sensitive and precise analytical tool. By coating the surface of the electrodes with various materials, the properties of these applied substances might be investigated. Some methods of thin film formation are: vapour deposition (metals), self assembled monolayers fabrication (SH-terminated substances) or spin-casting of films (polymers). After functionalization with materials that interact selectively with a target substance, biosensors are engineered that might elucidate kinetics and extend of binding between two substances.

So, besides being a fundamental tool in analytical electrochemistry, the future of the QCM lies in applications in the area of chemical sensors or biosensors and drug discovery.



In this work an attempt was made to elucidate the binding extent between proteins and poly(lactic acid)-co-poly(ethylene glycol) polymers, with varying molecular weight and molar composition of each block.

## 2 Results and Discussion

### 2.1 Preparation of Quartzes

For the analysis of materials using the QCM it is necessary to coat the quartz disk with a thin layer of this substance. Many methods are known for thin film formation, but for polymers the method of choice is the spin-coating procedure, as it reproducibly allows for the formation of very thin, homogenous films without time consuming preparations.

The films thus obtained were thinner than 1  $\mu\text{m}$  (measured with a micrometer screw) and appeared to have a smooth surface apart from a narrow ring in the periphery of the quartz, but since it is distinctly remote from the gold electrode, this is negligible.

Immersing spin-coated quartzes in phosphate buffer revealed the hydrophobicity of the polymer coated surface, and after about five minutes the films started to detach from the surface of the quartz, starting in the rim regions. For materials not firmly attached to the quartz it is impossible to be investigated by QCM as the oscillation of the crystal is not transferred to the analyte. The necessity was concluded to render the surface of the quartz hydrophobic and so to achieve increased adhesive forces between crystal and polymer film.

Before and after transformation of the quartzes their contact angle towards water was measured (**Figure 2**).

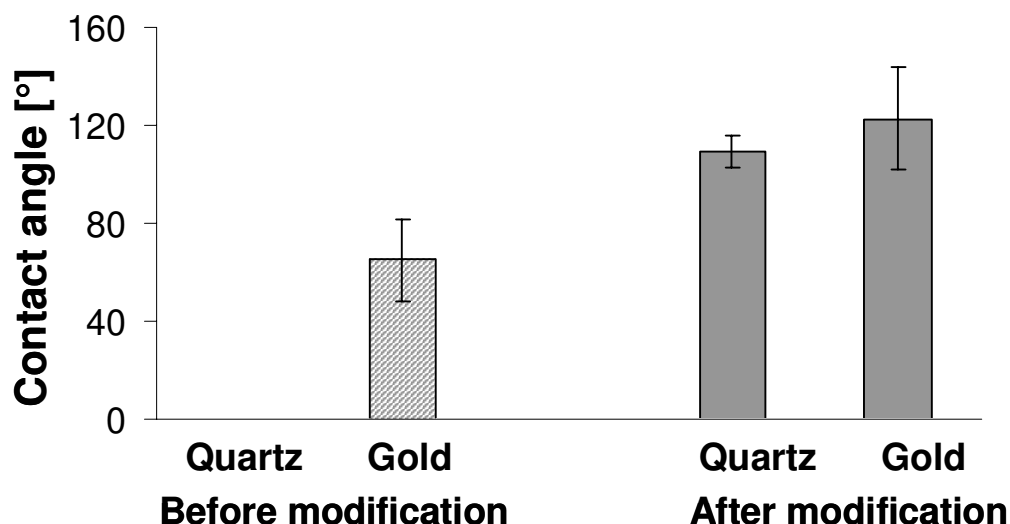


**Figure 2:** Contact angle of water measured on quartz and gold electrode before and after lipophilization with octadecyltrichlorosilane. Investigation of two different quartzes with  $n = 4$ .

It can clearly be seen, that the physical properties of the quartz changed from hydrophilic before treatment (no contact angle towards water detectable) to quite hydrophobic (contact angle towards water of about 100 °).

When modified quartzes were coated with a polymer film and immersed in water, no detachment of the film could be observed after 24 h of incubation.

## 2.2 QCM experiments

To investigate the adsorption properties of the modified gold electrode towards bovine insulin, in a first experiment 200  $\mu\text{g}$  of insulin were added to the solution reservoir and the frequency shift upon time of the oscillatory system was recorded. After the frequency had reached a constant value, the protein concentration in the system was increased by adding a new amount of insulin.

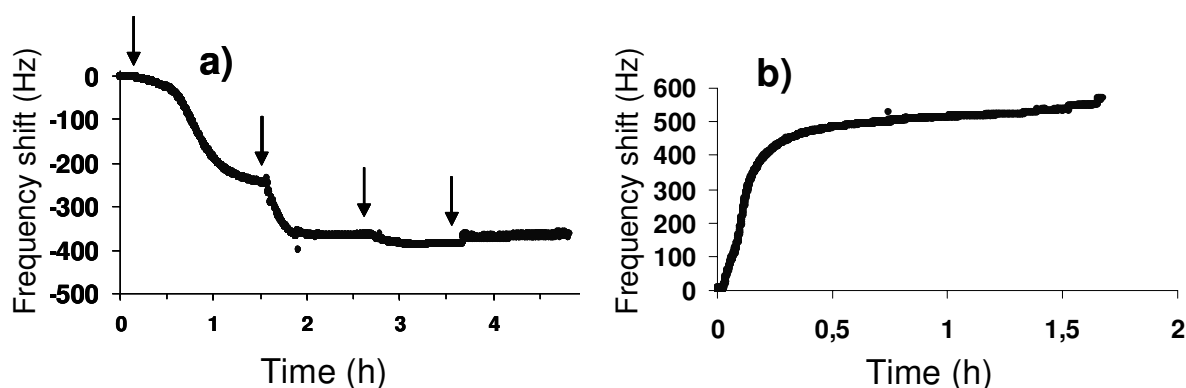


**Figure 3:** *a)* Time resolved resonant frequency shift of a modified 5 MHz quartz disk upon addition of bovine insulin. 200  $\mu$ l of a solution of 1 mg bovine insulin in 1ml solvent were added at different time points marked by arrows ( $t_1 = 0.162$  h,  $t_2 = 1.584$  h,  $t_3 = 2.662$  h,  $t_4 = 3.623$  h). Prior to addition 200  $\mu$ l solvent were removed from the solution reservoir. Measurements were performed in 0.1 M  $PO_4^{3-}$ , 1.25 M urea, pH 8. *b)* Resonant frequency shift upon washing of the system with 1% SDS solution.

In **Figure 3, a** it can clearly be seen, that upon the addition of the first portion of insulin, which led to a final concentration of 100  $\mu$ g insulin per ml solvent, the frequency of the oscillatory system decreased slowly but steadily. The addition of the second amount of protein (190  $\mu$ g/ml final concentration) also led to distinctly lower frequency values, although a constant value was much faster reached. Third addition of insulin led to a slight decrease in frequency whereas fourth addition of protein had no further effect. This led to the conclusion that higher amounts of insulin might result in faster reaching frequency constancy and the surfaces of the electrodes can only bind a certain amount of insulin as increasing the concentration of the protein did not cause a further drop in frequency. For further experiments a final concentration of 500  $\mu$ g insulin per millilitre solvent was used.

To confirm that adsorption of the protein to the surface of the quartz was due only to adhesive forces, a washing step was performed after the end of the adhesion experiment. Therefore 1% SDS solution was pumped for about 1.5 h through the system, while monitoring the resonant frequency shift of the quartz disk. **Figure 3, b** shows an initially pronounced increase of the resonant frequency which might be due to the detachment of adsorbed insulin from the electrodes. The frequency value finally reached after washing, differs slightly from the

starting frequency, and might be attributed to the different compositions of the solvents used for adsorption and washing experiment.

### 2.3 Insulin on Gold and PLA

Having established the experimental setup, the adsorption of 1 mg insulin on modified gold electrodes was monitored over time (**Figure 4**).

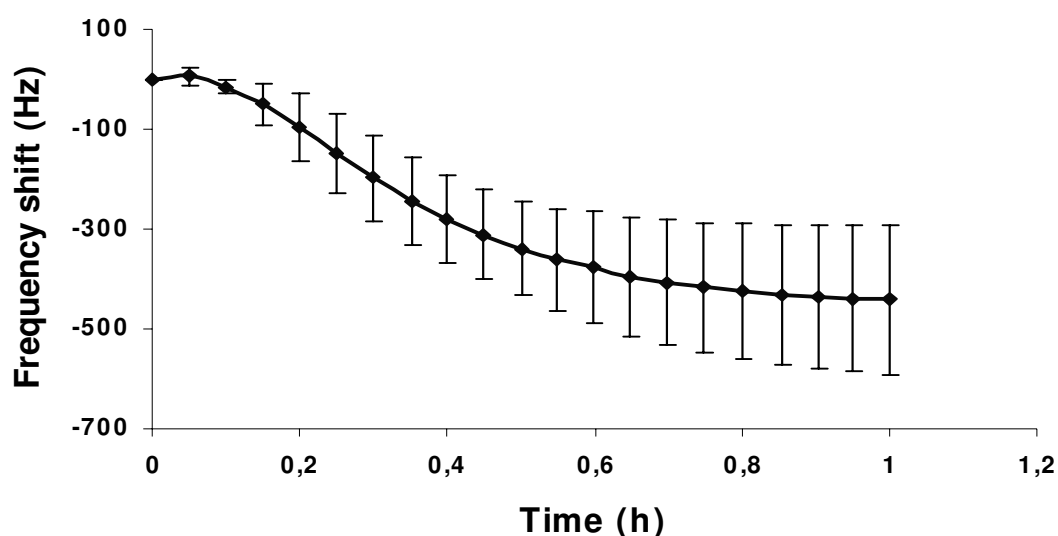


**Figure 4:** Time resolved resonant frequency shift of a modified 5 MHz quartz disk upon addition of bovine insulin ( $c = 500 \mu\text{g/ml}$ ). Measurements were performed in  $0.1 \text{ M PO}_4^{3-}$ ,  $1.25 \text{ M urea}$ ,  $\text{pH } 8$  with  $n = 3$ .

After addition of protein to the system, resonant frequency of the quartz decreases steadily until reaching a final value of about 440 Hz. However the adsorption of insulin started very slowly, the slope of graph first being shallow, but increasing upon time, indicating that adsorbed insulin facilitates the adhesion of new proteins.

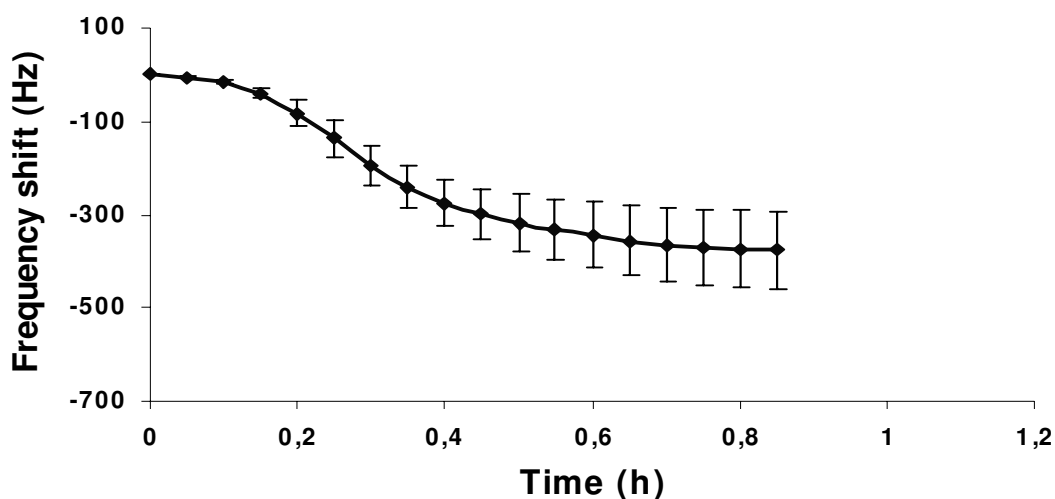


**Figure 5:** Time resolved resonant frequency shift of a modified 5 MHz quartz disk coated with a thin film of PLA upon addition of bovine insulin ( $c = 500 \mu\text{g/ml}$ ). Measurements were performed in  $0.1 \text{ M PO}_4^{3-}$ ,  $1.25 \text{ M urea}$ ,  $\text{pH } 8$  with  $n = 3$ .

Compared to the graph of insulin adsorption on gold the adhesion of protein on poly(lactic acid) films follows roughly the same pattern though some differences can be spotted (**Figure 5**). After a short lag time a decrease in frequency shift can be observed. Although the decrease is steeper compared to adsorption on gold the values finally reached are slightly higher ( $-380 \text{ Hz}$  for PLA compared to  $-440 \text{ Hz}$  for gold) and the minimal value is faster reached. Also standard deviation from the mean values are slightly lower indicating a more uniformly composed surface compared to the pure gold electrode, giving proof of the high quality of the prepared films.

## 2.4 Insulin on MePEG<sub>x</sub>PLA<sub>y</sub>

If films of MePEG<sub>x</sub>PLA<sub>y</sub> polymers are prepared, the different blocks will align themselves in such manner, that the hydrophilic PEG chains will protrude outwards shielding the hydrophobic surface [195]. In consequence films containing PEG should show lower protein adsorption and a lesser drop in frequency.

For adsorption studies MePEG<sub>x</sub>PLA<sub>y</sub> in different compositions were used: MePEG<sub>0,75</sub>PLA<sub>95</sub>, MePEG<sub>0,75</sub>PLA<sub>10</sub>, MePEG<sub>5</sub>PLA<sub>95</sub>, MePEG<sub>5</sub>PLA<sub>10</sub>.

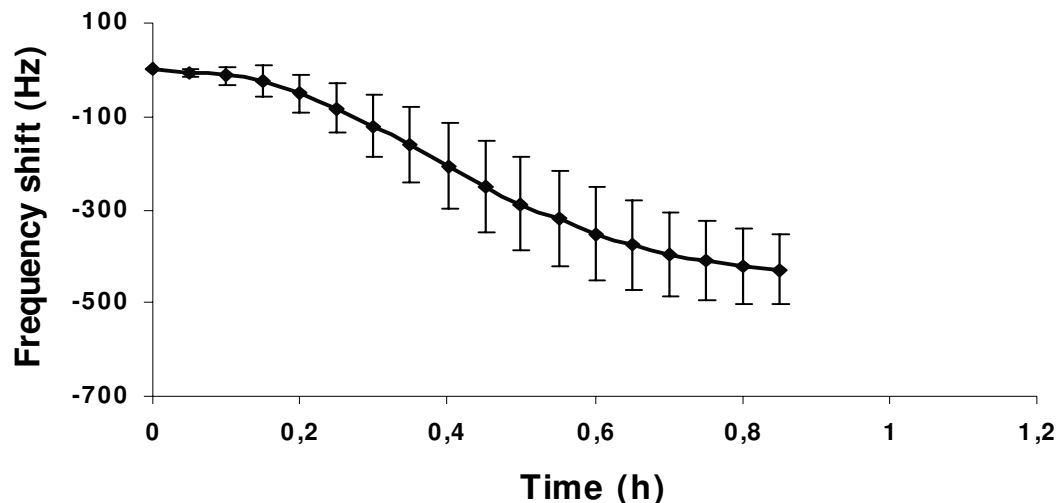


**Figure 6:** Time resolved resonant frequency shift of a modified 5 MHz quartz disk coated with a thin film of MePEG<sub>0.75</sub>PLA<sub>95</sub> upon addition of bovine insulin ( $c = 500 \mu\text{g/ml}$ ). Measurements were performed in  $0.1 \text{ M PO}_4^{3-}$ ,  $1.25 \text{ M urea}$ , pH 8 with  $n = 3$ .

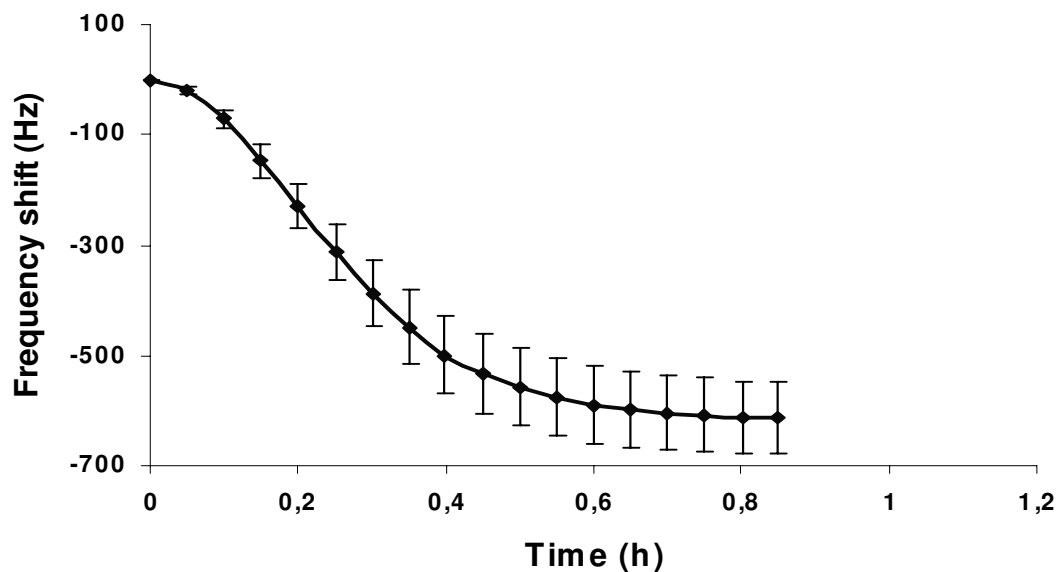


**Figure 7:** Time resolved resonant frequency shift of a modified 5 MHz quartz disk coated with a thin film of MePEG<sub>0.75</sub>PLA<sub>10</sub> upon addition of bovine insulin ( $c = 500 \mu\text{g/ml}$ ). Measurements were performed in  $0.1 \text{ M PO}_4^{3-}$ ,  $1.25 \text{ M urea}$ , pH 8 with  $n = 3$ .

In contrary to our expectations, films containing short chain PEGs of 750 Da molecular weight (**Figure 6, Figure 7**) show a greater drop in frequency than PLA films (430 Hz and 610 Hz compared to 380 Hz), indicating a more pronounced protein adsorption. An explanation for this untypical behaviour might be that short PEG chains favor the wetting of the otherwise water-repellent surface enabling an amplified contact of hydrophobic protein and PLA chains [195], without being able to act as a protein adsorption shield, due to their short operating range. Another explanation might be that PEG chains on the surface prevent a firm binding of the protein molecules to the surface, due to sterical hindrance and the inelastic bound mass causes a pronounced decrease in frequency [205]. These theories are both consistent with the finding that higher fractions of PEG cause a more distinct drop in frequency.

Long chain PEGs of 5000 Da molecular weights show a completely different adsorption pattern (**Figure 8, Figure 9**).

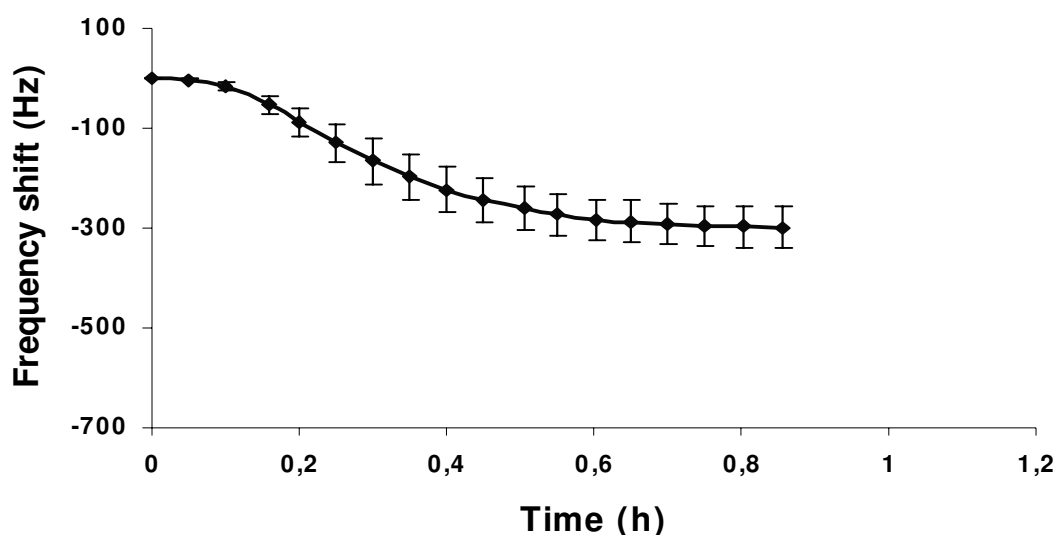


**Figure 8:** Time resolved resonant frequency shift of a modified 5 MHz quartz disk coated with a thin film of MePEG<sub>5</sub>PLA<sub>95</sub> upon addition of bovine insulin ( $c = 500 \mu\text{g/ml}$ ). Measurements were performed in  $0.1 \text{ M PO}_4^{3-}$ ,  $1.25 \text{ M urea}$ ,  $\text{pH } 8$  with  $n = 3$ .

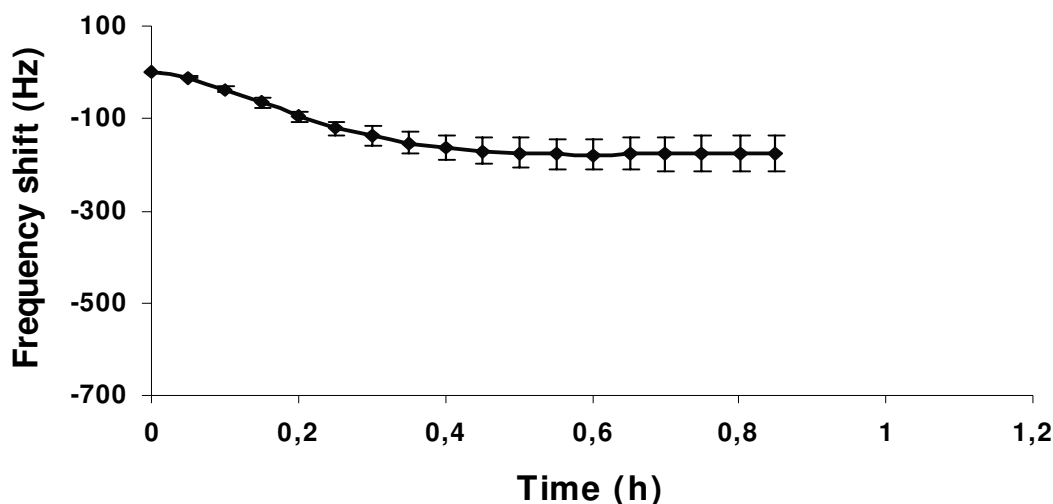


**Figure 9:** Time resolved resonant frequency shift of a modified 5 MHz quartz disk coated with a thin film of MePEG<sub>5</sub>PLA<sub>10</sub> upon addition of bovine insulin ( $c = 500 \mu\text{g/ml}$ ). Measurements were performed in  $0.1 \text{ M PO}_4^{3-}$ ,  $1.25 \text{ M urea}$ ,  $\text{pH } 8$  with  $n = 3$ .

It can clearly be seen, that the final reached value of oscillation frequency after adsorption of insulin to these films is distinctly higher compared to the value reached on PLA, indicating a shielding of the surface against protein adsorption. On MePEG<sub>5</sub>PLA<sub>95</sub> a minimal value of -300 Hz is reached, which is slightly higher than the value reached on PLA (-380 Hz). On MePEG<sub>5</sub>PLA<sub>10</sub> a final value of -180 Hz is reached after insulin adsorption, due to increased PEG content and therewith better shielding efficiency. However favorable the high PEG content is with regard to oppressed protein adsorption, another characteristic influenced by the PEG amount is its low glass transition temperature, which influences the mechanical stability of a resulting film. If a quartz disk coated with this polymer is vigorously shaken in water at 37 °C, the film will dissolve from the surface. However, as the resonant frequencies determined after adsorption measurements on these films were constant in three different analyzes, the final values reached were not equal to those on gold and the film on the electrodes looked macroscopically intact after measurements, the conclusion was drawn, that the film remained intact during analysis and adsorption was indeed performed on the polymer and not the electrode.



In another experiment a polymer synthesized out of the optically active L-lactic acid was used, the MePEG<sub>5</sub>PLLA<sub>10</sub>. Many characteristics of this polymer, like crystallinity or solubility, differ from those of the optically inactive derivative MePEG<sub>5</sub>PLA<sub>10</sub>.

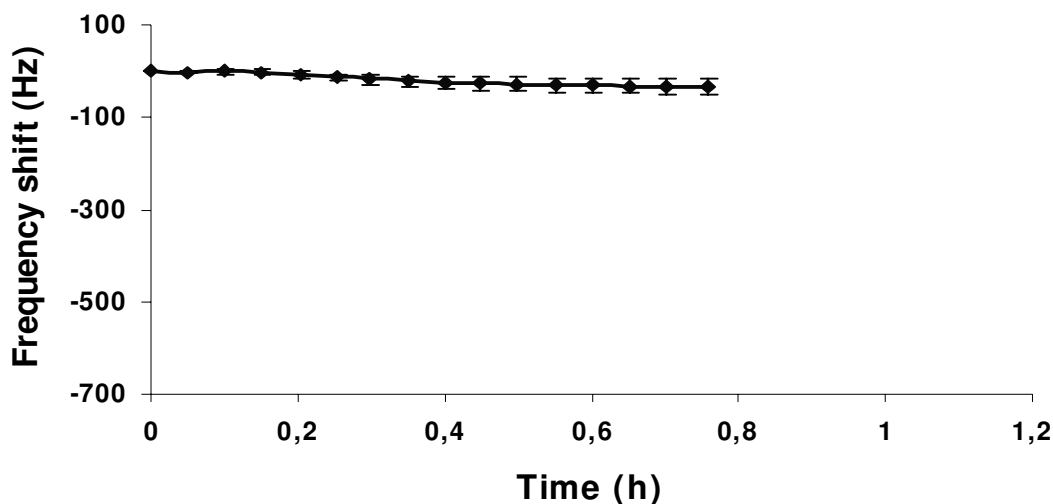


**Figure 10:** Time resolved resonant frequency shift of a modified 5 MHz quartz disk coated with a thin film of MePEG<sub>5</sub>PLLA<sub>10</sub> upon addition of bovine insulin ( $c = 500 \mu\text{g/ml}$ ). Measurements were performed in  $0.1 \text{ M PO}_4^{3-}$ ,  $1.25 \text{ M urea}$ ,  $\text{pH } 8$  with  $n = 3$ .

**Figure 10** displays the adsorption behavior of insulin towards this polymer. Comparing the resulting graph to one obtained investigating protein adsorption to MePEG<sub>5</sub>PLA<sub>10</sub>, no definite drop in frequency can be detected and therefore it can be assumed that no insulin at all or to a much lesser extent binds to the surface of this polymer. As MePEG<sub>5</sub>PLLA<sub>10</sub> shows a higher degree in crystallinity compared to the optically inactive form, water-uptake and swelling occur much retarded [217]. In the glassy state the interactions between polymer and protein are less pronounced than in the swollen state, resulting in reduced adsorption of protein to non-swollen polymers.

All former experiments were performed in  $0.1 \text{ M PO}_4^{3-}$ ,  $1.25 \text{ M urea}$ , at a pH of eight. Under these basic conditions insulin has rather lipophilic properties, one effect being its reluctance to dissolve in aqueous media. To investigate the behavior of insulin in its protonated therefore hydrophilic form, in a control experiment  $0.1 \text{ N HCl}$  was used as solvent (**Figure 11**).

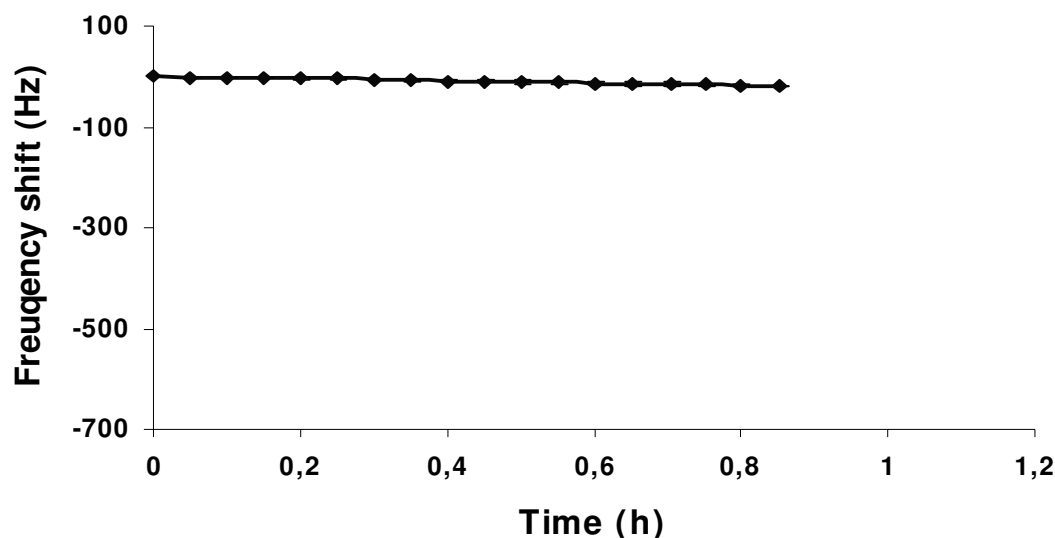


**Figure 11:** Time resolved resonant frequency shift of a modified 5 MHz quartz disk coated with a thin film of PLA upon addition of bovine insulin ( $c = 500 \mu\text{g/ml}$ ). Measurements were performed in 0.1 N HCl with  $n = 3$ .

In measurements performed in 0.1 N HCl amino functions of insulin would be protonated resulting in a charged molecule, which would be reluctant to adhere to a lipophilic surface, as for example the PLA film, but might rather remain dissolved in the hydrophilic solvent. This assumption is confirmed by the graph shown in **Figure 11**, where no drop in frequency can be detected.

The resonant frequency shifts detected over time in the aforementioned adsorption experiments differ very drastically in their magnitude compared with values found in literature of about 100 Hz. To clarify which component of the system (polymer, protein or measurement parameters) are the cause for the detected changes in frequencies, as a control a new protein, bovine serum albumin, was analyzed for its adsorption behavior on PLA in the solvent used for former experiments and in phosphate buffer saline, pH 7.4, a solvent frequently used for QCM measurements (**Figure 12**).

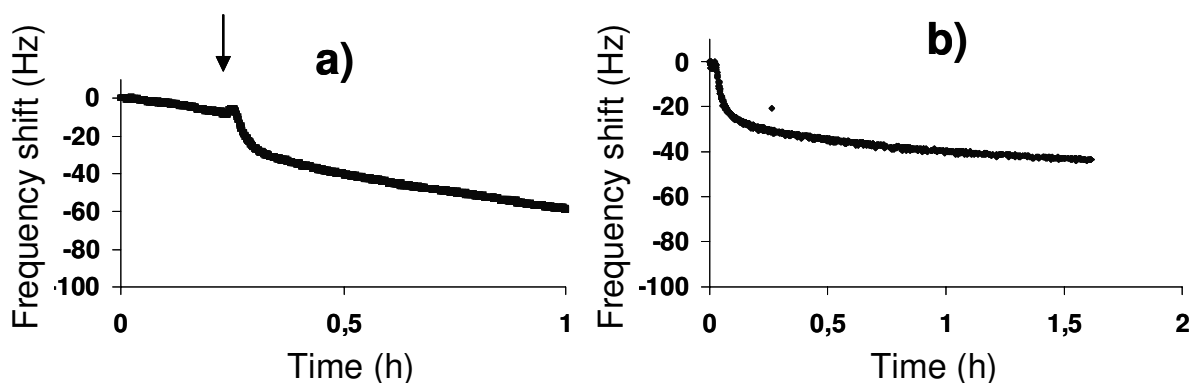


**Figure 12:** Exemplarily shown time resolved resonant frequency shift of a modified 5 MHz quartz disk coated with a thin film of PLA upon addition of bovine serum albumin ( $c = 500 \mu\text{g/ml}$ ). In **a)** measurements were performed in  $0.1 \text{ M PO}_4^{3-}$ ,  $1.25 \text{ M urea}$ ,  $\text{pH } 8$ . The arrow indicates addition of protein. In **b)** measurements were performed in  $\text{PBS}$ ,  $\text{pH } 7.4$ .

The drop in frequencies in both experiments ranges in the magnitude of 30 Hz, proving that the pronounced shift in resonant frequency in former measurements can be attributed to insulin.

Insulin itself is a rather small protein with a molecular weight of about 5.8 kDa. Bovine serum albumin has a molecular weight of about 66 kDa, but being a rather polar molecule it might attach to a minor extent to the lipophilic surface. But even fibrinogen, which is known as a rather “sticky” molecule and has a molecular weight of 340 kDa does not show such a pronounced frequency shift, albeit measured on other surfaces.

Two possible explanations for the untypical behavior of insulin might be offered: either insulin might form aggregates consisting of several molecules, or the drop in frequency might not be due only to mass deposition, but also depend on other factors.

During some analyzes, a slight turbidity of the reservoir solution could be detected, supposedly caused by insulin aggregates. Under the used conditions (shear stress, basic environment) insulin is known to form aggregates. However, through gentle mixing the solution with a pipette, the detected turbidity disappeared, and whether or not turbidity was present during analyzes, the final reached oscillatory frequencies were in the same range.

The uptake of water in films can also lead to very substantial frequency changes, but swelling of films can be excluded as reason for resulting adsorption patterns, because frequency

decrease could always be linked to the addition of insulin, irrespective of the time needed for stabilization of the resonant frequency, which ranged between one hour and half an hour.

Therefore the conclusion can be drawn, that the frequency decrease can not only be attributed to mass deposition, but other factors, like for example viscosity-density changes at the film-liquid interface, have addition effects.

### 3 Summary

A procedure was established to investigate the adsorption of insulin to MePEG<sub>x</sub>PLA<sub>y</sub> derivatives consisting of blocks of PEG and PLA with varying molecular weights. The surface of the quartzes had to be modified in order to provide adequate adhesion of the polymer film. Short PEG chains seem to facilitate the adsorption of the protein by enhancing the wettability of the polymer surface, whereas longer PEG chains show the expected protein repellent effect.

Further analyses have to elucidate the influence of different parameters, like temperature, shear stress and concentration, on the extent of insulin adsorption.



# **Chapter 6**

## **Determination of Reaction Sites of Insulin**

# 1 Introduction

As described in the previous chapter PEG, as a hydrophilic and uncharged polymer, is known to resist unspecific protein adsorption [218], making surfaces to which it is attached equally inert to protein adsorption. This favorable characteristic is mainly based on its physicochemical properties, most prominent among them the effects of the unique balance of hydrophobicity/hydrophilicity and the readiness to occupy a large volume in an aqueous environment [177]. The well-documented relative physiological inertness and acceptable toxicological profile are two more features to recommend PEG for in vivo applications [219].

Since in the 1970s, PEG was attached to various molecules for enhancing the therapeutic and biotechnological potential of peptides, proteins and drugs [220]. The goal was to modify many of the substances features whilst maintaining the main biological functions of the original molecule. PEGylation of proteins and peptides modifies the solubility of the original substance both in organic and aqueous media by conveying the physical properties of the polymer to the conjugate [177,221]. A second benefit enjoyed by modified proteins is the prolonged serum half-lives, which is due to molecular mass increase and consequential reduced renal ultrafiltration [222], reduction of the degradation rate by proteolytic enzymes [221] and prevention of the approach of antibodies and antigen possessing cells, leading also to reduced immunogenicity of the original substance [223]. Linear PEG chains have been observed to stabilize the unfolded state of proteins by intermingling with the polypeptide chains [224]. In a few cases, passive tumor targeting of the protein-polymer conjugates could be detected, a phenomenon known as enhanced permeation and retention [226].

Numerous strategies targeting various moieties have been devised leading to PEG-protein conjugates. Most frequently used is amino group coupling. Either  $\alpha$ -amines found at the N-terminus of proteins or  $\epsilon$ -amines from lysine side chains are alkylated or acylated with activated PEG polymers [177]. Arginine [226], carboxyl group [177] or hydroxyl group [227] modification is rarely used due to harsh reaction conditions or lacking selectivity, whereas cysteine residue coupling is highly selective, but few proteins possess thiols suitable for the covalent linking of PEG [228].

To retain the biological activity of a protein, its active site must be protected from PEGylation. Targeting the polysaccharides of glycoproteins is an elegant method to



circumvent this problem [229]. Other approaches involve the use of specific enzymes [230] or active-site protecting agents during the coupling reaction [177].

Characterization of protein-polymer conjugates is of vital importance, as the synthesis leads to a population of products which may have different biological properties. MALDI-ToF and GPC, although made cumbersome by the polydispersity of the polymer [228], still give an idea of the number of PEG chains attached, but identification of the PEGylation sites often proves more difficult. While Edman degradation will easily identify the exact location of the PEG chains linked to small peptides, this approach is difficult if not impossible to follow with larger conjugates. Enzymatic digestion of these molecules and subsequent analysis of the smaller fragments is often hampered by sterical hindrance of the bound polymer [177]. Therefore new PEG derivatives were engineered with improved properties regarding reaction site identification, such as PEG–biotin which avails the well-characterized biotin-avidin interaction [231], or PEGs linked to unnatural peptides through an easy cleavable group, which upon removal of the PEG chain leave the peptide tags on the protein backbone [232].

In this work, succinic acid was used as tag, linked to the PEG chain by means of an ester function, which is easily cleavable under mild basic conditions. After removal of the PEG chains, the resulting product was investigated for reactive sites, now marked by attached succinic acid.

## 2 Results and Discussion

### 2.1 Synthesis of amine reactive polymer

To commercially available MePEG<sub>2</sub> succinic acid was covalently linked through an easily cleavable ester group, followed by activation of the free end of the succinic acid. The first step of the reaction was checked by <sup>1</sup>H-NMR (**Figure 1**).

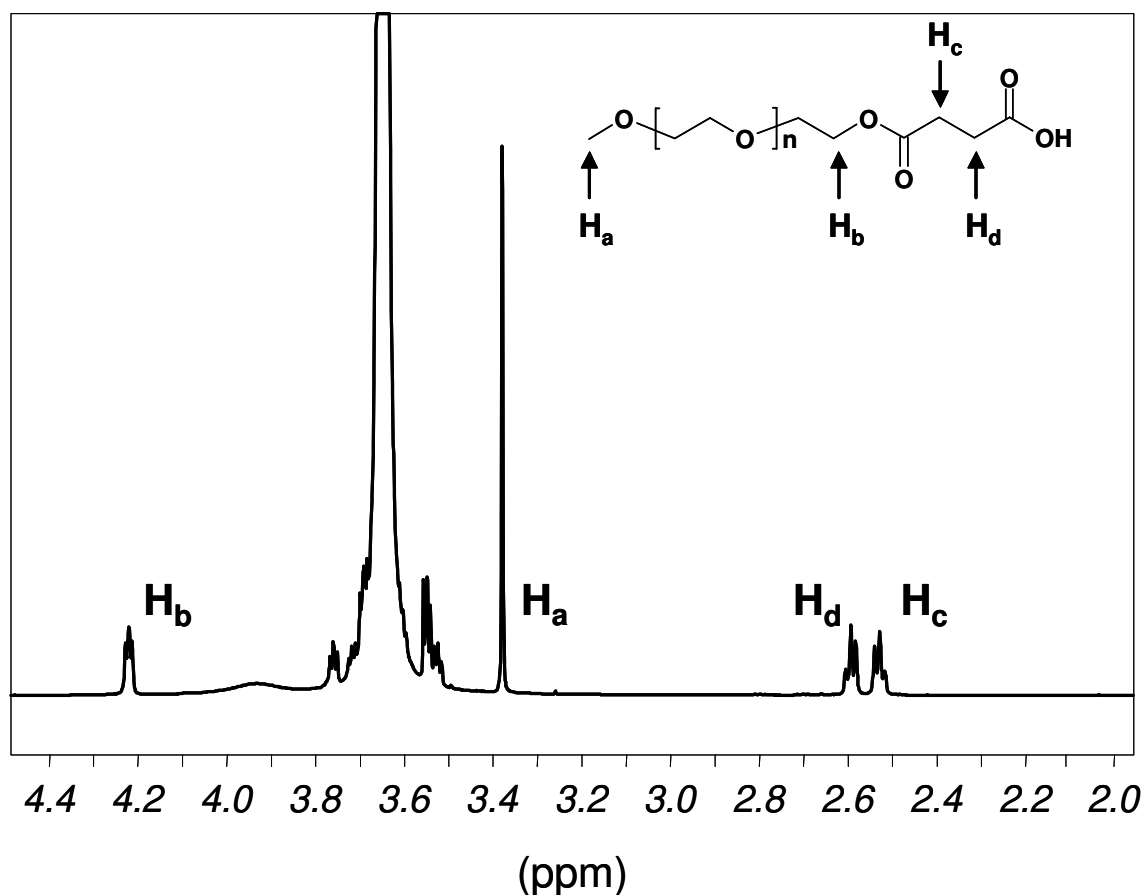


**Figure 1:** <sup>1</sup>H-NMR spectrum of MePEG<sub>2</sub> processed with succinic acid anhydride. Protons relevant for identification are marked with arrows. Spectra were taken in CDCl<sub>3</sub> with TMS as internal standard.

In addition to the signal at 3.37 ppm which originates from the terminal methoxy group of the PEG and the very pronounced signal at 3.65 ppm which can be attributed to the ethylene groups of the PEG chain, new signals can be detected. The triplet at 4.22 ppm can be assigned to the methylene group adjacent to the newly formed ester group. The two signals at 2.52 ppm and 2.60 ppm stem from covalently bound succinic acid, free succinic acid and succinic

anhydride causing signals at other ppm values (2.50 ppm and 3.01 ppm, respectively). Integrating the signals relevant for substance identification and setting the value of the integral of the methoxy group at 3.00 (the number of protons), a value of 1.98 for the integral of  $H_b$  is obtained. This result is in good agreement with the theoretical value, confirming the reaction of MePEG and succinic anhydride.

Trying to confirm the next step of the reaction, the activation of the free end of the succinic acid also by  $^1H$ -NMR proved difficult, as the protons of bound NHS caused the appearance of a new signal between the signals of succinic acid, making integration of the respective signals difficult.

Therefore the reactivity of the polymer was rather confirmed using SEC. For sample preparation, an amine containing fluorescent dye, EDANS, was bound to the polymer and the product subsequently analyzed by SEC. As control served pure polymer and pure dye incubated under the same conditions as the reaction batch.

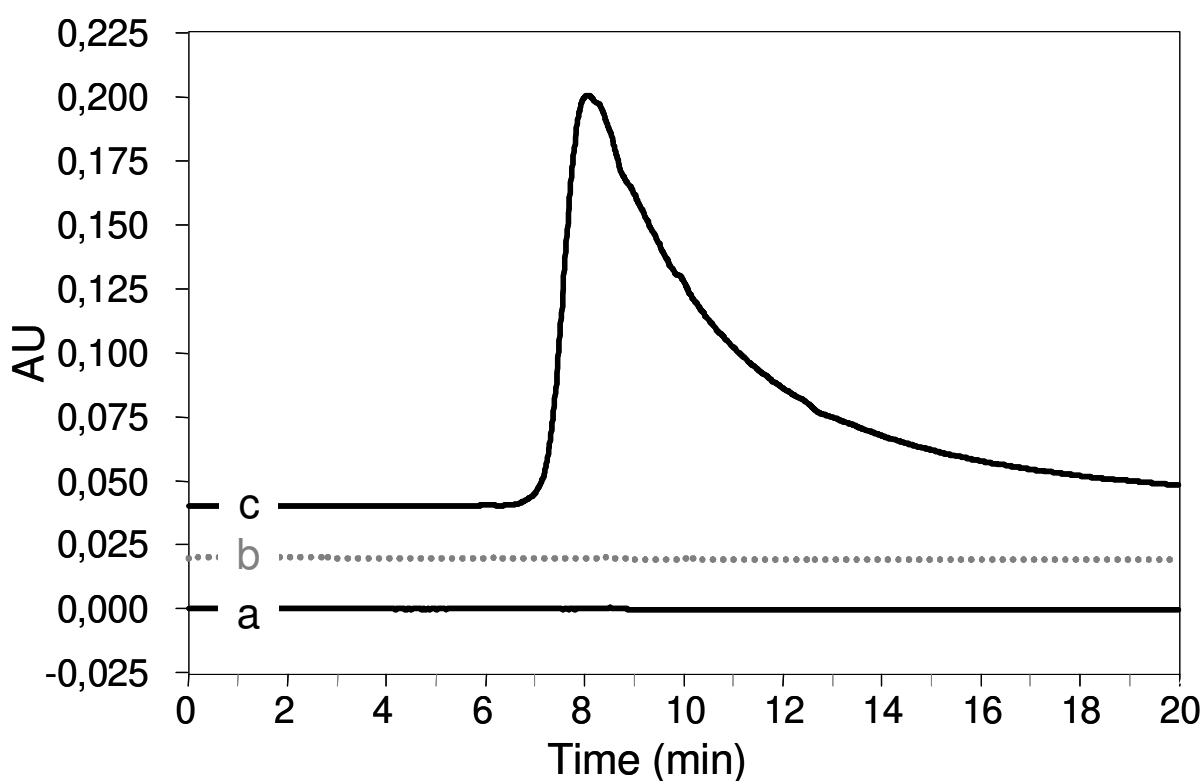


**Figure 2:** SEC chromatograms of the activated polymer after incubation with an amine containing dye, EDANS. Data collected at 335 nm with an UV-detector.

**a:** polymer; **b:** EDANS; **c:** polymer + EDANS

In **Figure 2** it can clearly be seen, that only the sample containing both activated polymer and dye shows a significant adsorption at about 9 min of elution time. As expected the pure polymer and the pure dye samples show no adsorption, the latter being due to the fact, that EDANS is a polar molecule, which does not dissolve in chloroform, used as mobile phase.

## 2.2 Binding of Activated PEG to Insulin

Having confirmed the reactivity of the polymer, PEG-protein conjugates were synthesized, choosing human insulin as model compound. Human insulin possesses three amino groups, which all can participate in the reaction, the two  $\alpha$ -amino groups at the N-terminus of the A-chain (A1-Gly) and B-chain (B1-Phe) and the  $\epsilon$ -amino group of lysine (B29-Lys). PEG was used in a 15-fold molar excess compared to insulin. The reaction was monitored by HPLC, GFC and MALDI-ToF.

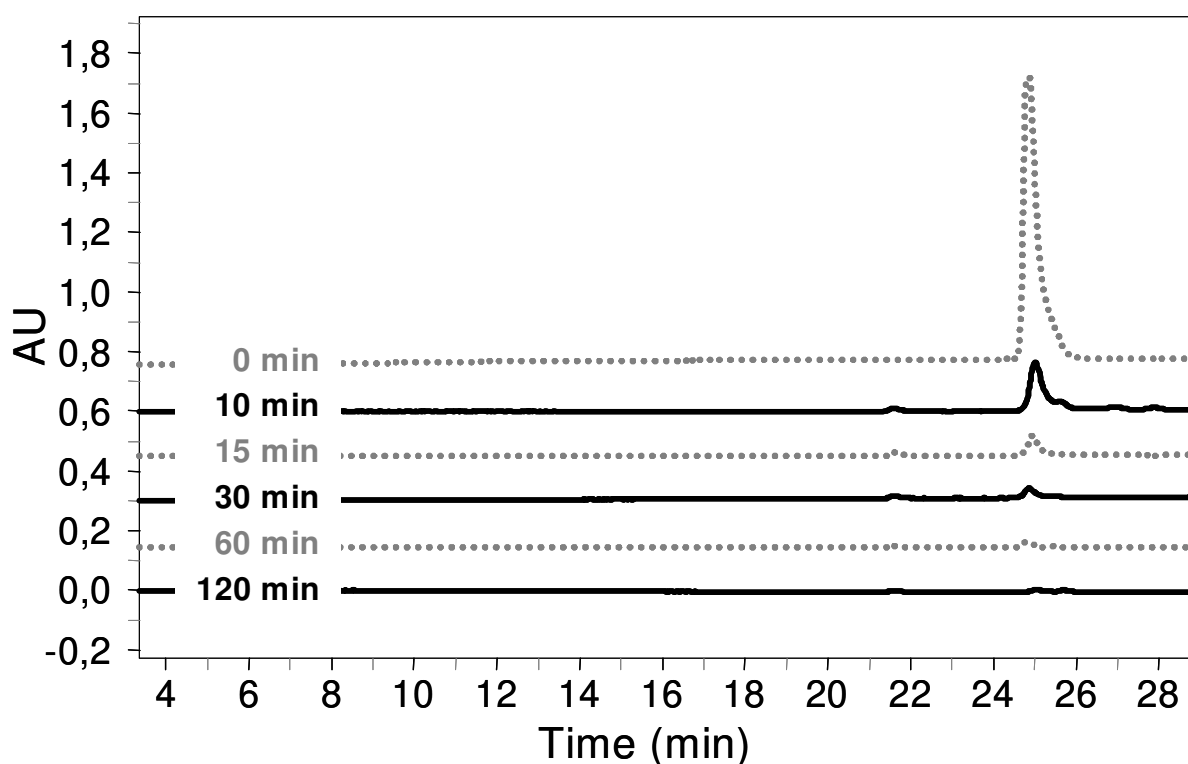


**Figure 3:** Investigation of the kinetic of the coupling reaction of activated PEG and insulin. Samples were drawn at different time points, labeled accordingly, and investigated by RP-HPLC. Chromatograms were recorded using a fluorescence detector at  $\lambda_{ex}=274$  nm and  $\lambda_{em}=308$  nm.

The HPLC chromatograms reveal that insulin causes initially a very strong signal at about 25 min (**Figure 3**). This signal clearly decreases after 10 min due to the coupling of insulin to PEG. The signal diminishes further with proceeding reaction until it disappears completely after 2 h. Thus, the conclusion can be drawn, that after 2 h of reaction time, no native insulin is still present in the reaction batch.

To confirm this conclusion, the product was analyzed by aqueous GFC (**Figure 4**).

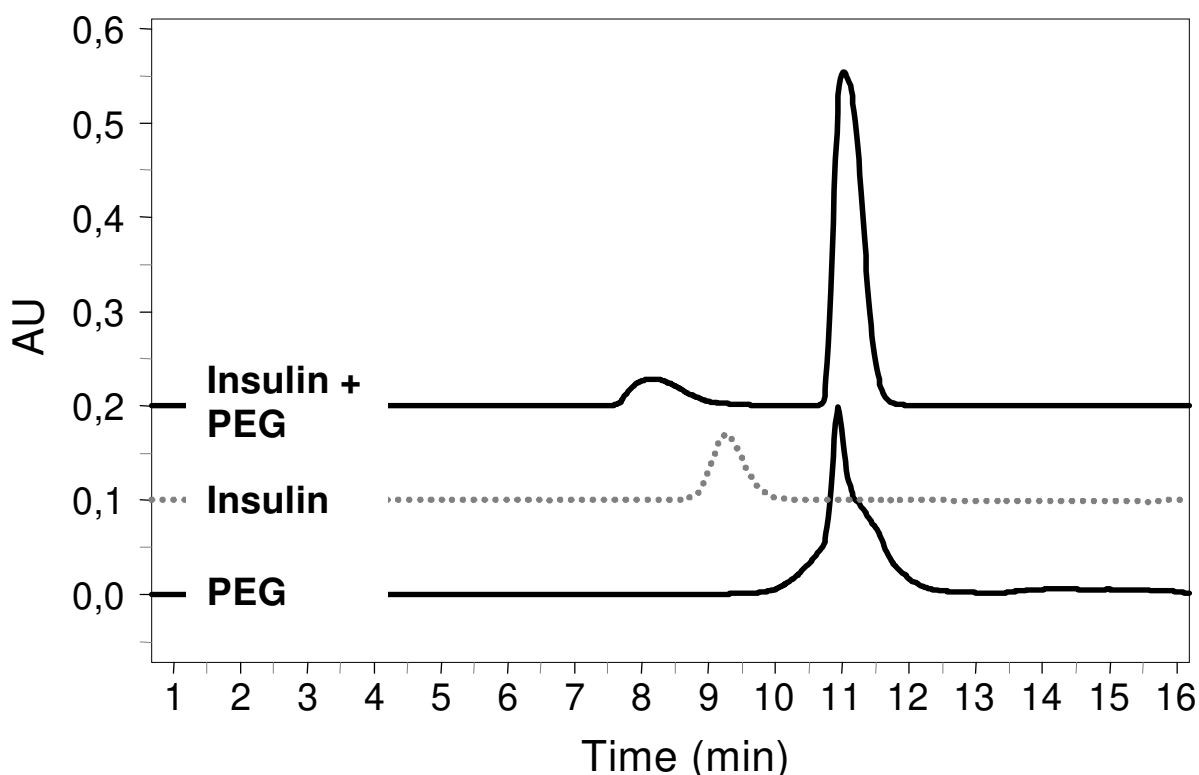


**Figure 4:** GFC chromatograms of the educts and the product of the PEGylation reaction. Data was recorded at 274 nm using an UV-detector. 0.05 M Tris-buffer, pH 8 with 20% acetonitrile was used as mobile phase.

Analyzing the educts of the coupling reaction and the product obtained after 2 h of processing by GFC, it can clearly be seen, that insulin has been modified in the course of the reaction. Native insulin is detected at about 9.5 min, whereas in the product sample this signal shifts to lower retention time, which signifies an increase in the molecular weight of the substance. The signal detected later on in the product sample at 11.5 min ought to be attributed to unreacted PEG.

Using these analysis conditions, the differences in retention times between native insulin and PEGylated insulin are rather insignificant, making a clear differentiation between the two protein species difficult. Therefore, the influence of the acetonitrile content in the mobile phase was investigated for its effect on protein elution, to develop a method with a more pronounced difference in the retention time of insulin and PEGylated insulin.

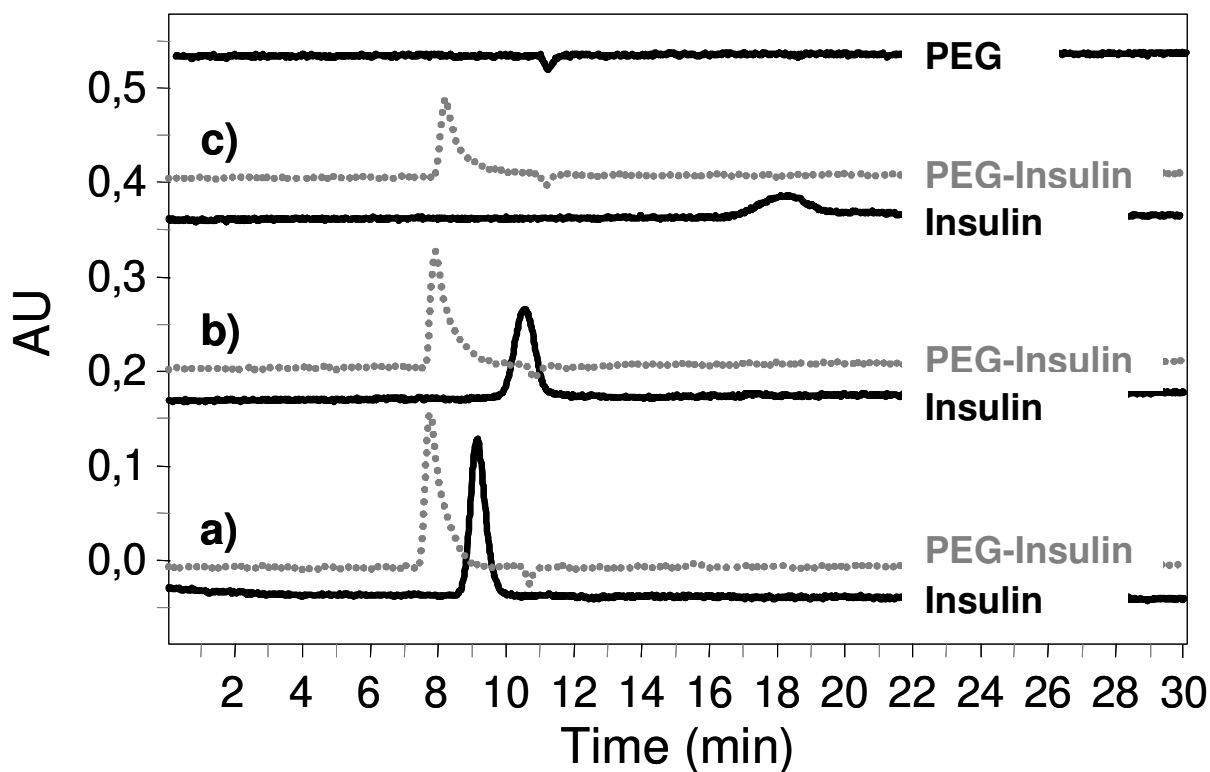


**Figure 5:** Influence of acetonitrile on the retention time of insulin and PEGylated insulin. GFC chromatograms recorded with a fluorescence detector. Mobile phase consisted of 0.05 M Tris-buffer, pH 8 and varying amounts of acetonitrile: **a)** 20%, **b)** 10%, **c)** 0%.

With 20% acetonitrile as mobile phase the signals of insulin and PEGylated insulin are both very distinct and sharp, but retention times for the two samples are very similar (**Figure 5**). Decreasing the acetonitrile content up to 10%, the retention time of insulin slightly increases and the signal broadens. At 0% acetonitrile the difference in retention times between the two samples is very pronounced, but the shape of the insulin signals is rather diffuse. This might be due to adsorption effects of the protein to the column material. PEGylated insulin, protected by the PEG chains shows no such diffuse signals.

Resulting in a good separation of insulin and PEGylated insulin, for all following analyzes the method with no acetonitrile in the mobile phase was used for GFC.

The coupling of PEG to insulin was investigated by a third method, MALDI-ToF (**Figure 6**).

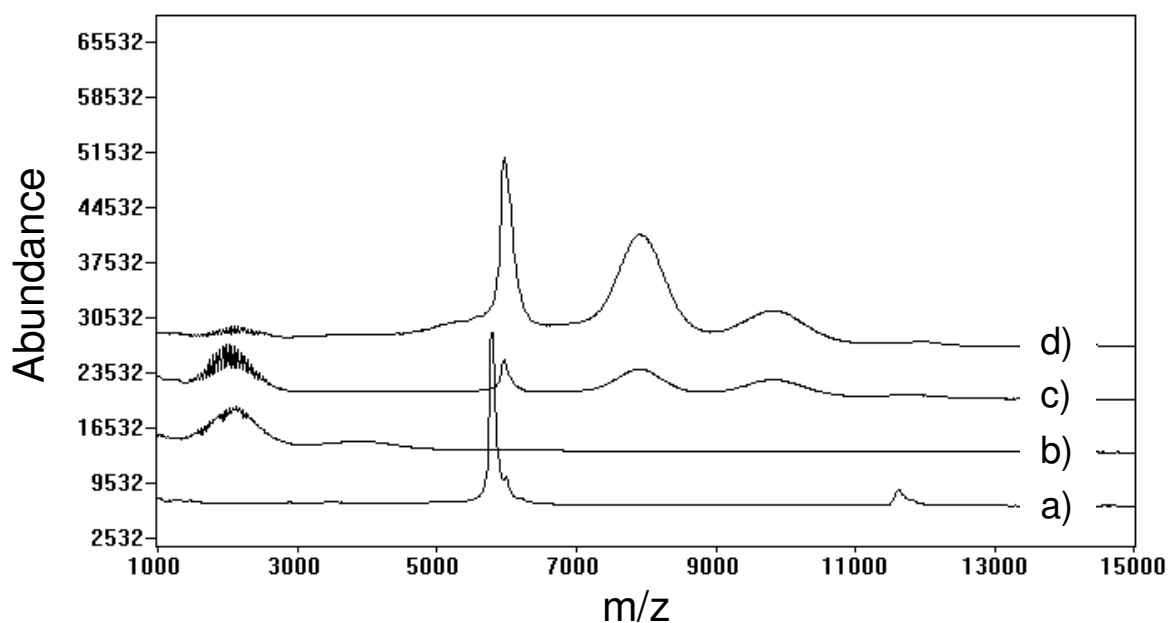


**Figure 6:** MALDI-ToF spectra of insulin (**a**), activated PEG (**b**), and PEGylated insulin prior to (**c**) and after purification (**d**).

Investigating the sample containing native insulin, beside the expected signal at 5.8 kDa a second signal can be detected at about 12 kDa, which may be assigned to the insulin dimers [233]. Activated PEG samples result in a multi-spiked signal at about 2 kDa in consequence of polymer polydispersity, and less pronounced signals at about 4 kDa, due to conjugation of two polymer chains. Analyzing the product of the coupling reaction, the intensity of the protein and protein polymer conjugates is low compared to the unreacted polymer signal and MALDI measurements are difficult. Purifying the product by ultrafiltration definitely facilitates subsequent measurements and signal intensity shifts in favor of protein and protein conjugates detection. Insulin with one or two PEG chains attached can now clearly be identified, the signals of the protein conjugates made broad, as the polydispersity of PEG is reflected into the molecular weight distribution of the product.

The influence of purification on the quality of analysis measurements can also be detected in GFC chromatograms (**Figure 7**). In chromatograms recorded with an UV detector both insulin and PEG cause very pronounced signals. Prior to purification, the signal stemming from the polymer dwarfs the protein derived signal, making detection difficult. After

purification, the intensities of the two signals are in the same range. Chromatograms recorded with the fluorescence detector are not affected by the presence of PEG.

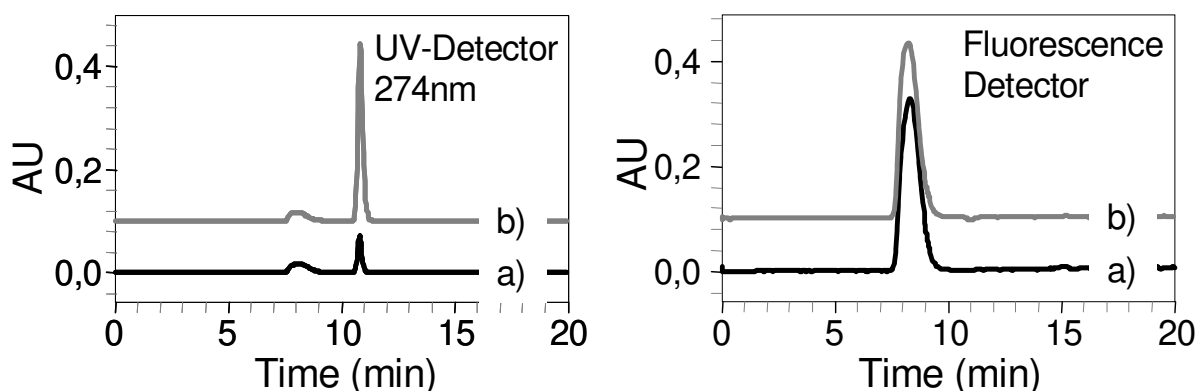


**Figure 7:** SEC chromatograms of PEGylated insulin prior to (b)) and after (a)) purification.

Oxy- and thioester are susceptible to cleavage by basic or neutral hydroxylamine solutions, whereas amide linkages are stable under these conditions. Therefore it should be possible to cleave the linkage between PEG and succinic acid (an ester), whereas the bond between succinic acid and the protein remains untouched (an amine). After removal of the PEG chains, succinic acid will still mark the reactive site, and subsequent analysis is much facilitated, as a consequence of the absence of the bulky PEG.

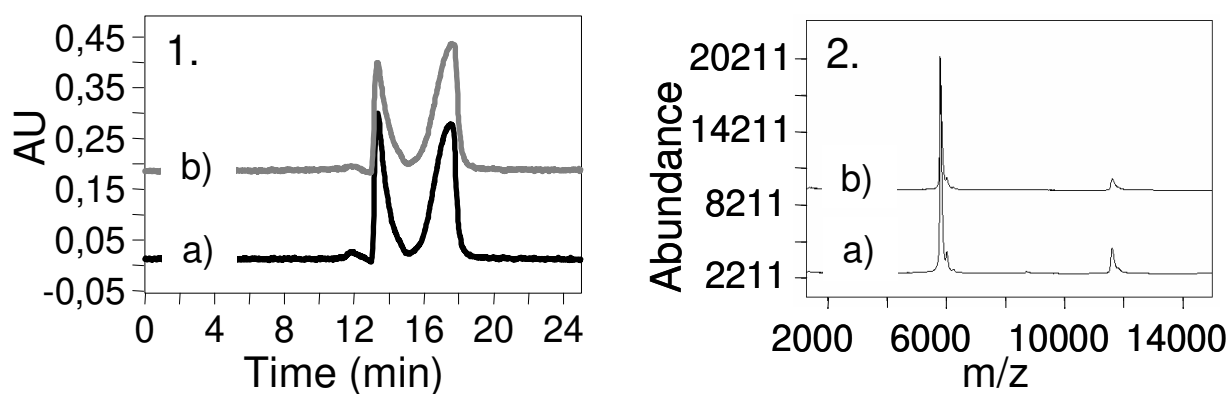


**Figure 8:** GFC (1.) and MALDI-ToF (2.) analyses of human insulin treated at 37 °C for 0 min (a) or 4 h (b) respectively in 1 M  $\text{NH}_2\text{OH}$  solution. No influence of the processing on insulin can be detected.

To determine the cleavage conditions where the protein is stressed minimally while the removal of PEG is performed, parameters such as incubation temperature (25 °C and 37 °C),



incubation time (1 h to 24 h) and pH of the solution (pH 8 and pH 10) were investigated. Having found the optimal conditions, pure insulin was treated according to these conditions and subsequently analyzed by GFC and MALDI.

After incubating insulin for 4 h with 1 M  $\text{NH}_2\text{OH}$  solution pH 8 and subsequent analysis of the protein, no modification of the protein can be detected, compared with the result of the analysis of the sample drawn at 0 min of reaction time. The second signal detected in the GFC chromatograms derives from insulin dimers, which are known to form under basic conditions. MALDI spectra show no alteration of the molecular weight of insulin.

In consequence, PEGylated insulin was treated with the newly established method. Samples were drawn at different time points and subsequently analyzed by SEC.

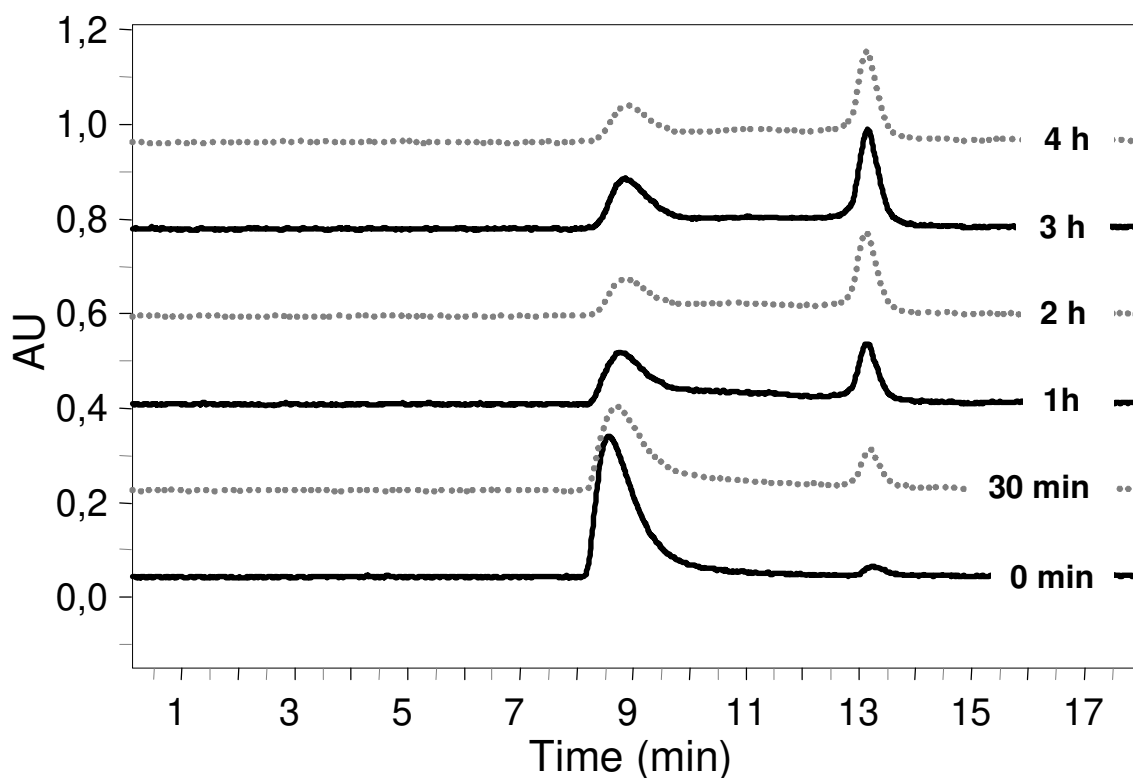


**Figure 9:** GFC analysis of PEGylated insulin treated with 1 M hydroxylamine solution. Chromatograms were recorded with a fluorescence detector. Samples were drawn after different time points labeled accordingly and analyzed using 0.05 M Tris buffer pH 8 as mobile phase.

GFC analysis reveals that treatment of PEGylated insulin with hydroxylamine favors the appearance of a new signal. The corresponding substance is eluted at 13.5 min retention time, indicating a lower molecular weight compared to the protein conjugate. The signal of the original substance diminishes over time, but it does not disappear completely, albeit a slight shift in retention time can be detected at later time points. This leads to the conclusion that at over time a different substance is detected, which has a retention time very similar to that of PEGylated insulin. The cleavage of PEGylated insulin with hydroxylamine should result in insulin with different numbers of succinic acid attached. Succinic acid has a molecular weight of 100 Da, a mass deviation which would not account for the pronounced difference in retention time of the two detected signals. But considering differences in conformation and adsorption behavior caused by binding of the linker, the new signal might still be attributed to insulin modified with succinic acid.

To support this assumption, MALDI-ToF analyses of these samples were performed (**Figure 10**).

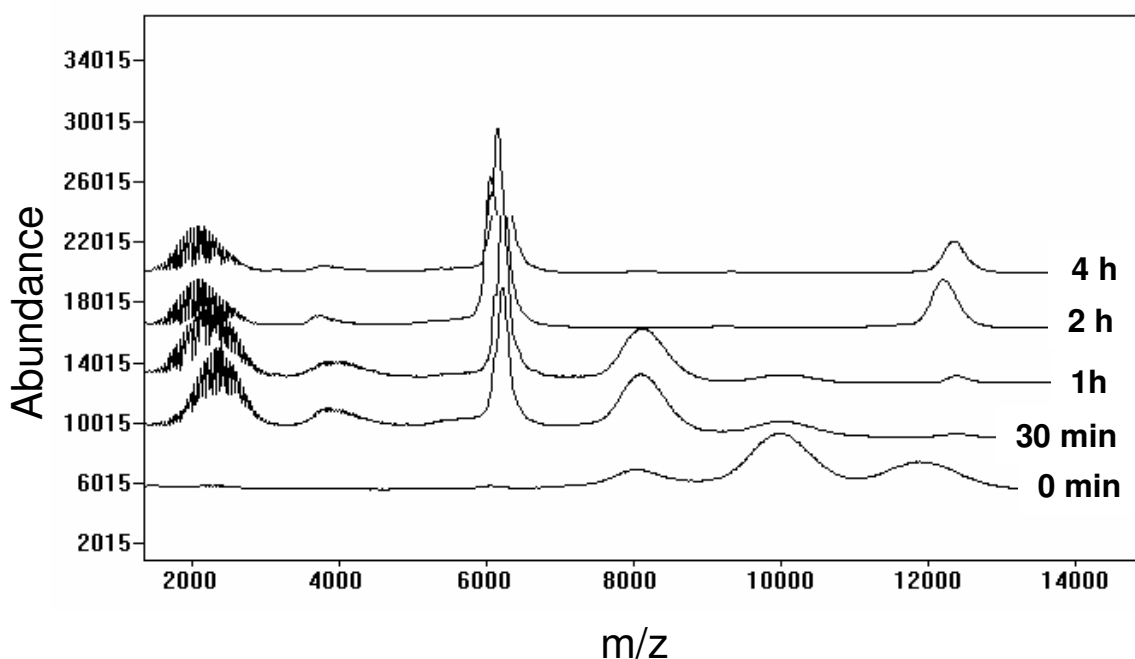


**Figure 10:** MALDI-ToF analysis of PEGylated insulin treated with 1 M hydroxylamine solution. Samples were drawn at different time points labeled accordingly.

At 0 min incubation time of PEGylated insulin with hydroxylamine substances with masses corresponding to those of insulin with one, two or three PEG chains attached, respectively,

can be detected. In samples drawn after 30 min, the PEG signal at about 2 kDa is very pronounced and a new signal at about 6 kDa, which might be attributed to insulin succinic acid compounds, is detected, whereas the signals of triple and double PEGylated insulin are substantially diminished. After 2 h of incubation time PEG protein conjugates can no longer be detected in the corresponding sample. Thus the cleavage of PEG from insulin was verified.

After subsequent purification of the protein, the two chains of insulin were separated by cleavage of the disulfide bridges of the molecule and the result investigated by HPLC. As removal of PEG should result in protein chains comprising succinic acids and therewith free acidic groups, this would hopefully lead to better resolution of single and double modified protein chains in a basic environment.

Firstly, pure human insulin was separated in A chain and B chain and the product analyzed by HPLC (**Figure 11**).

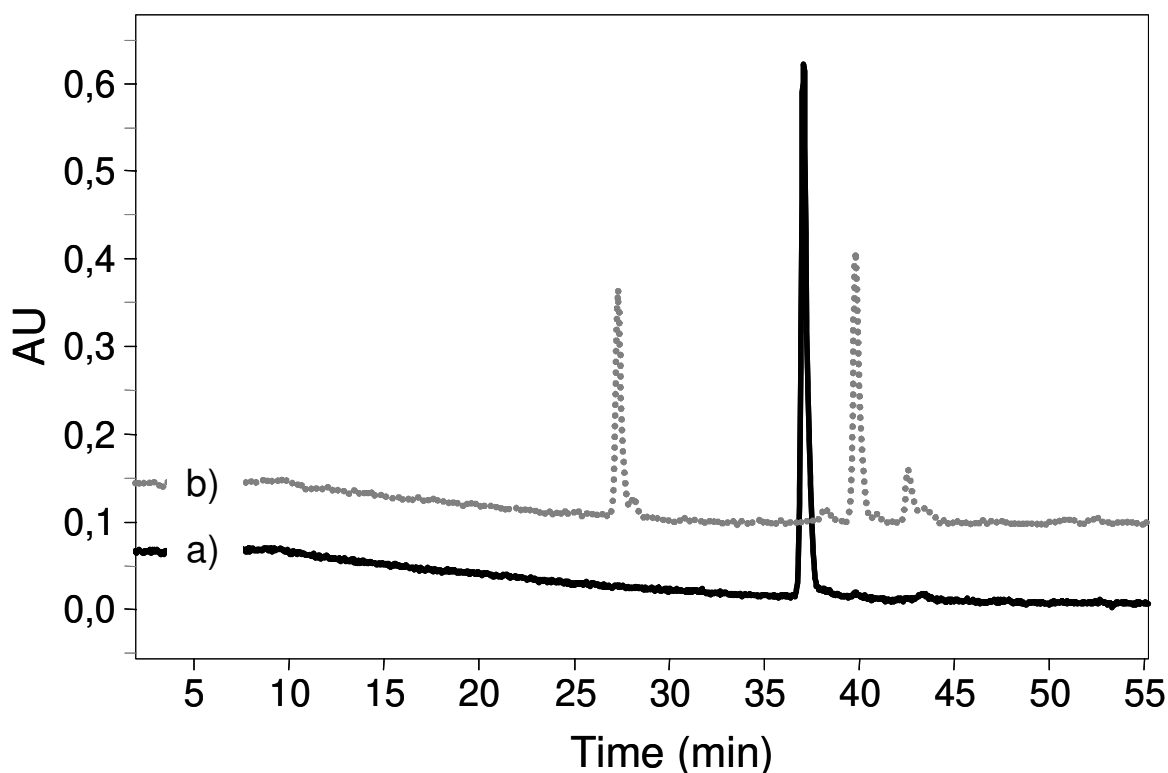


**Figure 11:** HPLC chromatograms of insulin prior to (a)) and after (b)) cleavage of the disulfide bonds. Chromatograms were recorded with a fluorescence detector and  $\text{NH}_4\text{HCO}_3$  buffer-acetonitrile was used as mobile phase.

Analyses revealed that the cleavage of disulfide bonds was successfully completed and good separation of A and B chain could be achieved. With HPLC-MS the first signal at 27 min was identified as deriving from the A chain, whereas the later signals at 40 min could be attributed to the B chain.

As the cleavage of disulfide bonds was successfully accomplished with native insulin, in the next step de-PEGylated insulin was treated accordingly. HPLC analysis revealed the cleavage of disulfide bonds, but separation of the different protein species was unsatisfactory (**Figure 12**). Therefore a new method was established (Method 2) for better separation of differently substituted chains (**Figure 13**).

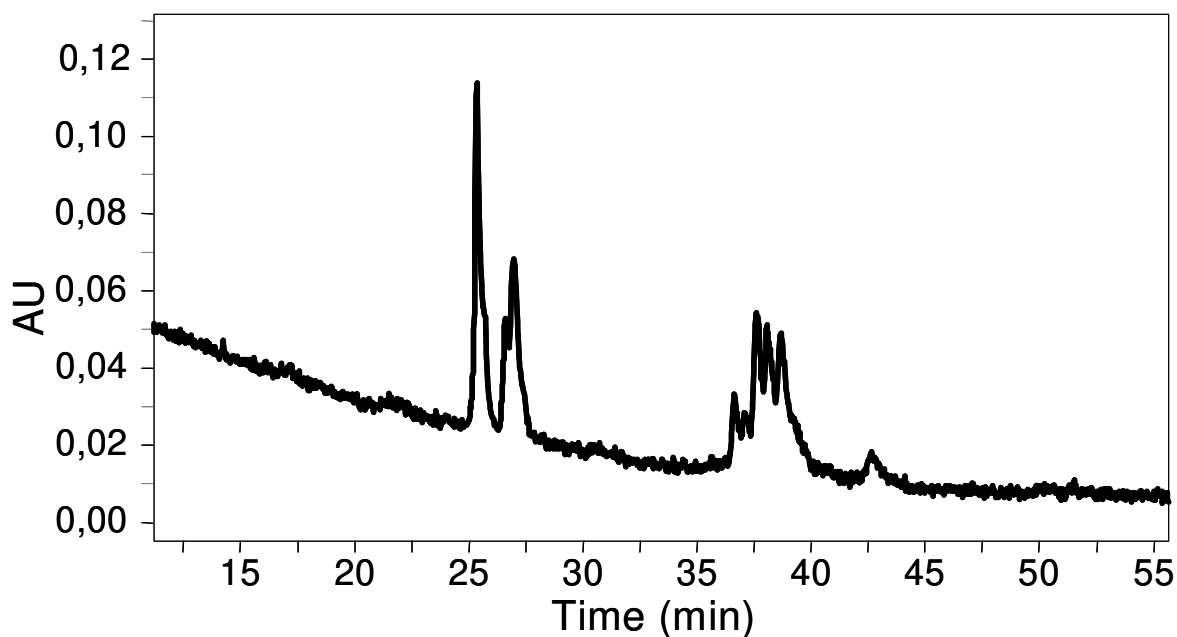


**Figure 12:** HPLC chromatograms of PEGylated insulin after cleavage of the disulfide bonds. Chromatograms were recorded with a fluorescence detector and  $\text{NH}_4\text{HCO}_3$  buffer-acetonitrile was used as mobile phase.

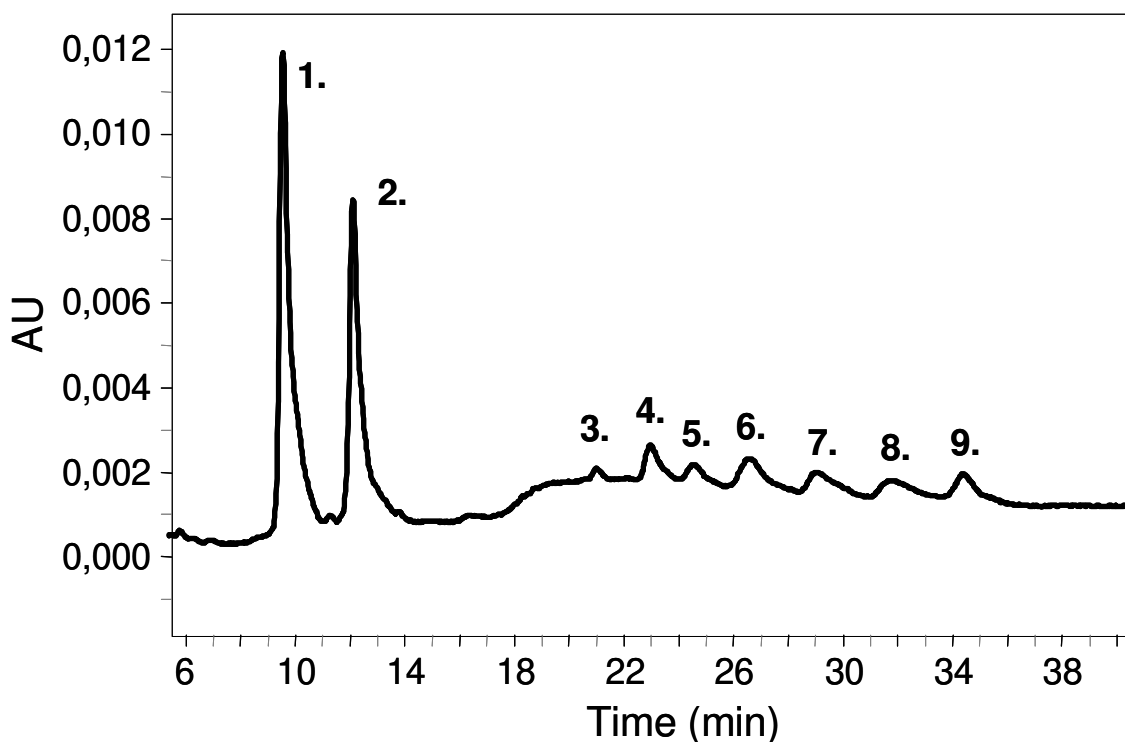


**Figure 13:** HPLC chromatograms of PEGylated insulin after cleavage of the disulfide bonds analyzed according to Method 2 as described in **Chapter 3**. Chromatograms were recorded with an UV detector at 274 nm and  $\text{NH}_4\text{HCO}_3$  buffer-acetonitrile was used as mobile phase.

The separated signals were collected individually and analyzed by MALDI-ToF. As differently charged ions could be detected in the resulting spectra ( $+\text{H}^+$ ,  $+\text{Na}^+$ ,  $+\text{K}^+$ ,  $+\text{NH}_4^+$ ), the signal with the highest intensity was used as basis for calculation. Results are displayed in **Table 1**.

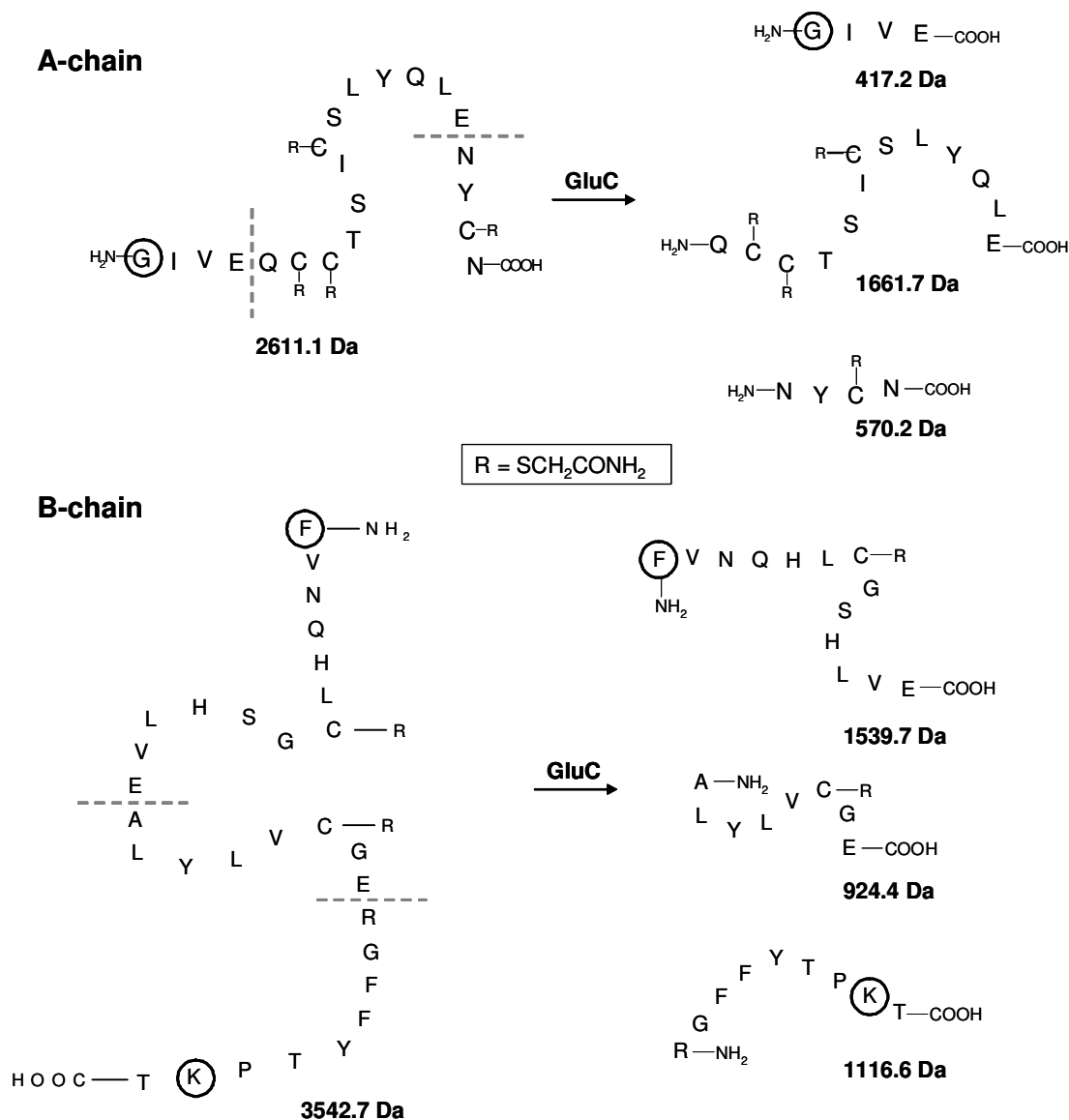
**Table 1:** Elution time and molecular weight as determined by MALDI-ToF analysis of substances obtained after cleavage of the disulfide bonds of de-PEGylated insulin.

Number	Elution time (min)	Mass (Da)	Substance
1.	9.6	2733	A chain + succinic acid + Na <sup>+</sup>
2.	12.1	2611	A chain + K <sup>+</sup>
3.	21.0	3743	B chain + (2 x succinic acid) + H <sup>+</sup>
4.	23.0	3758	B chain + (2 x succinic acid) + NH <sub>4</sub> <sup>+</sup>
5.	24.6	3725	B chain + (2 x succinic acid) – H <sub>2</sub> O
6.	26.5	3643	B chain + succinic acid + H <sup>+</sup>
7.	29.0	3658	B chain + succinic acid + NH <sub>4</sub> <sup>+</sup>
8.	31.8	3658	B chain + succinic acid + NH <sub>4</sub> <sup>+</sup>
9.	34.4	3542	B chain + H <sup>+</sup>

According to literature cleavage of insulin disulfide bonds and subsequent treatment with iodoacetamide results in an A chain with a mass of 2611.09 Da and a B chain with 3542.73 Da, respectively. These values were used as basis for identification of the analyzed molecules.

To get more knowledge on the ratio between single, double and unmodified proteins, the signals detected in HPLC chromatograms were integrated. Comparing the relative areas calculated for A chain derived signals, a ratio of 56.7% modified A chain compared to 43.3% native A chain was obtained. Integrating B chain derived signals, only 17.7% of unmodified B chain could be detected compared to 59.6% B chain with one succinic acid attached (6.: 18.9%; 7.: 14.8; 8.: 15.9%) and 32.7% double modified B chain (3.: 3.5%; 4.: 19.2%; 5.: 10%). These results clearly show that the reactivity of the primary amino groups present on the B chain towards activated PEG is notably higher (only 17.7% unmodified B chain)

compared to that of the primary amino group present on the A chain (43.3% unmodified A chain). However, still the question remains, which of the B chains amino groups is more reactive.



**Scheme 1:** Schematic illustration of the enzymatic digestion of the A and B chain of human insulin using GluC. Dashed lines indicate cleavage sites. Cysteine residues are modified using iodoacetamide. Amino acids possibly bearing succinic acid residues are marked with circles.

To investigate the respective reactivity of the individually amino groups more closely, enzymatic digestion of the collected protein fractions was performed. As enzyme

Endoproteinase Gluc-C was used, a serine protease which cleaves peptide bonds terminally at glutamic acid (**Scheme 1**).

Enzymatic cleavage of the A chain should result in three peptide fragments: fragment one ranging from A1 to A4 with 417.2 Da of molecular weight, fragment two ranging from A5 to A17 with 1661.7 Da and fragment three ranging from A18 to A21 with 570 Da of molecular weight. Furthermore, the first fragment may additionally carry a succinic acid tag. Analyzing the samples containing the enzymatic digest of fraction 1. and 2., collected as stated in **Table 1**, only the fragment with 1661.7 Da molecular weight could be detected (**Figure 14**).

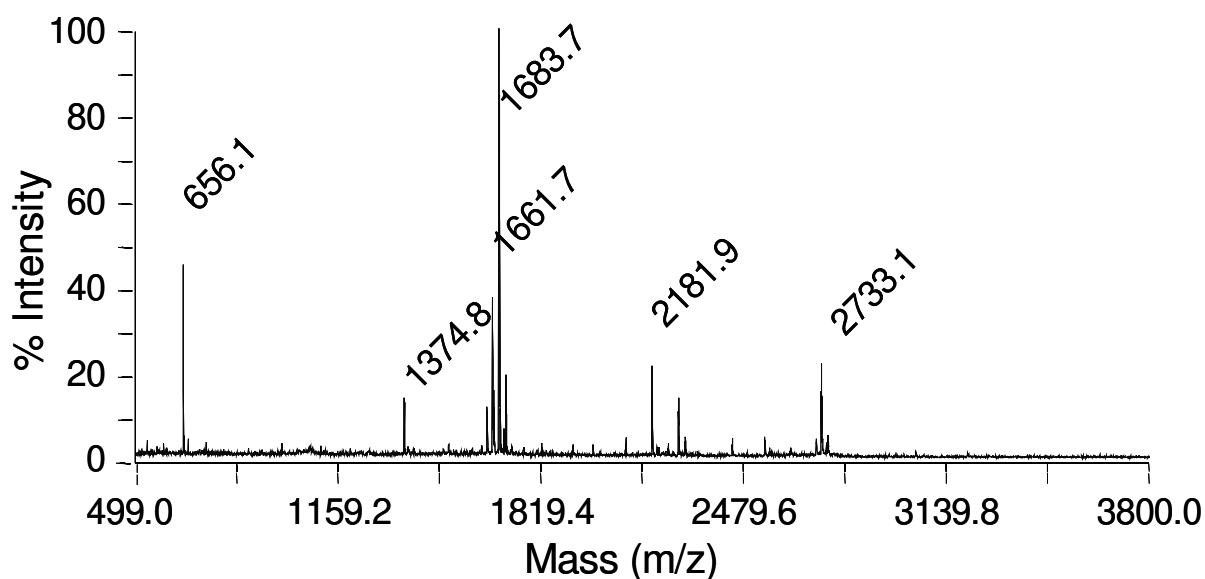


**Figure 14:** MALDI-ToF spectrum of the enzymatic digestion of fraction 1.. The sodium salt of undigested A chain modified with succinic acid (2733.1 Da) and fragment 2 of the A chain (1661.7 Da) can be detected.

Modified or unmodified fragment one which might carry the succinic acid tag could not be detected in either fraction. The low molecular weight of the molecule of 417.2 Da or 517.2 Da, respectively might thwart detection.

Enzymatic cleavage of the B chain should also result in three peptide fragments: fragment one ranging from B1 to B13 with 1537.7 Da, fragment two ranging from B14 to B21 with 924.4 Da and fragment three ranging from B22 to B30 with 1116.6 Da of molecular weight. Fragment 1 and 3 from the B chain may carry succinic acid tags.



Fractions 3., 4., and 5. collected using HPLC analysis, which contained double modified B chains of insulin, were also enzymatically digested. Subsequent MALDI-ToF measurements detected signals with masses corresponding to those of fragment 1 with succinic acid attached (1639.7 Da) and fragment 3 with succinic acid tag (1216.6 Da). Besides a signal corresponding to 2122 Da was detected, which may be attributed to a peptide fragment ranging from B14 to B30 with a succinic acid tag and an eliminated water molecule. The signal attributed to fragment 2 was either of very low intensity, or not detectable at all. Traces of fragment 3 without succinic acid tag could also be detected (**Figure 15**).

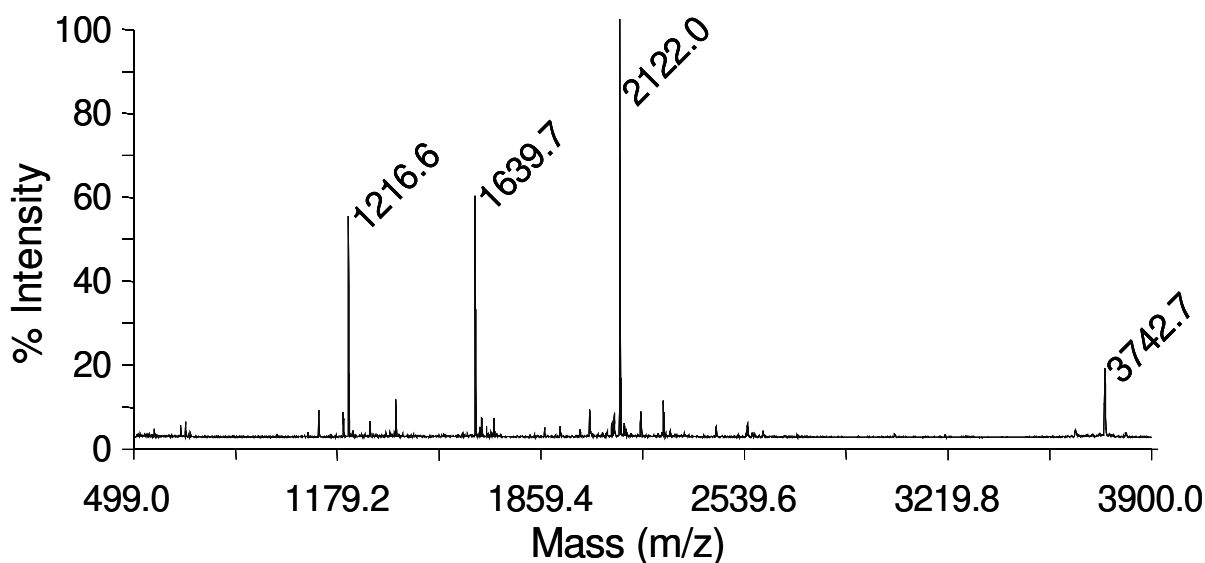


**Figure 15:** MALDI-ToF spectrum of the enzymatic digestion of fraction 3.. Undigested B chain modified with two succinic acids (3742.7 Da), fragment 1 modified with succinic acid (1639.7 Da), fragment 3 modified with succinic acid (1216.6 Da) and a peptide sequence composed of fragment 2 and fragment 3 with succinic acid attached and eliminated water (2122.0 Da) can be detected.

In fraction 6., 7., and 8., preliminary MALDI-ToF analysis revealed single modified B chains. After enzymatic digestion, modified fragment 1 could be detected in all of these samples, albeit in fraction 8 traces of unmodified fragment 1 were present. Fragment 3 was detected with and without succinic acid attached and non-cleaved fragment 2 and 3 (again with and without succinic acid tag) were also present in the samples (**Figure 16**).

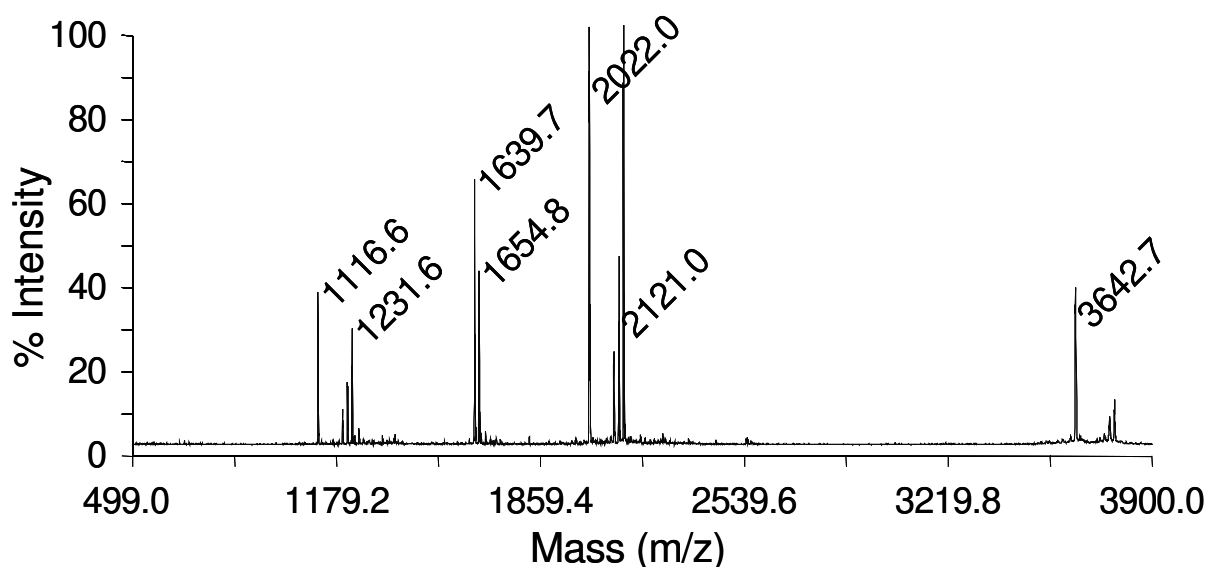


**Figure 16:** MALDI-ToF spectrum of the enzymatic digestion of fraction 6.. Undigested B chain modified with one succinic acid (3642.7 Da) , fragment 1 modified with succinic acid (1639.7 Da), the ammonium salt of fragment 3 modified with succinic acid (1231.6 Da) or the pure fragment 3 (1116.6 Da) and a peptide sequence composed of fragment 2 and fragment 3 with or without succinic acid attached and eliminated water (2122.0 Da or 2022.0 Da, respectively) can be detected.

In fraction 9., unmodified fragment 1 and 3 of the B chain of insulin and non-cleaved fragment two and three could be detected after enzymatic digestion (**Figure 17**).

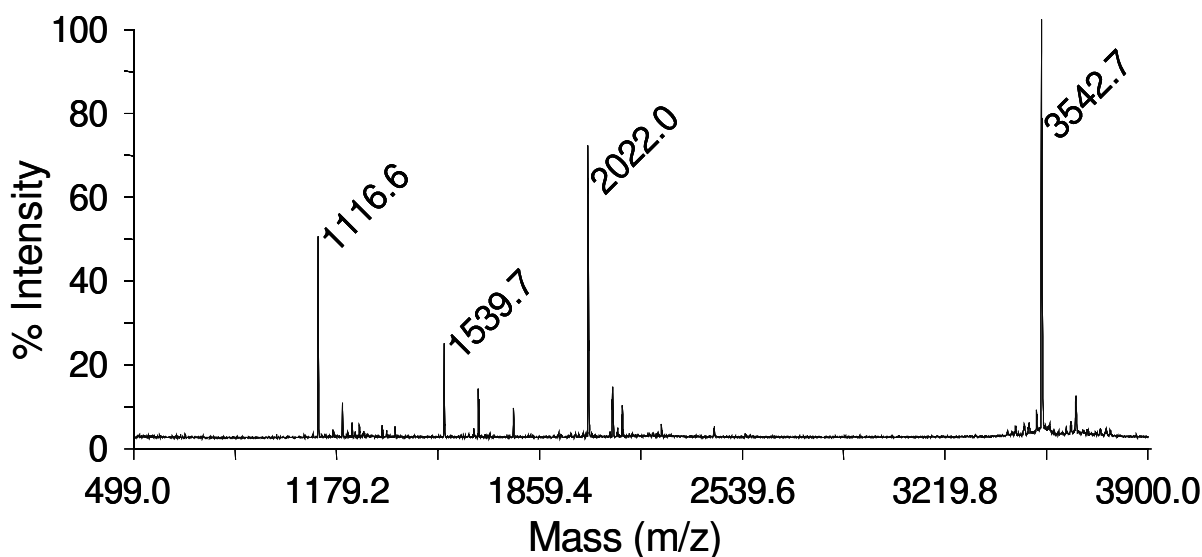


**Figure 17:** MALDI-ToF spectrum of the enzymatic digestion of fraction 9.. Undigested B chain (3542.7 Da) , fragment 1 (1539.7 Da), fragment 3 (1111.6 Da) and a peptide sequence composed of fragment 2 and fragment 3 (2022.0 Da) can be detected.

With these results it is not possible to calculate exact ratios of modified to unmodified fragment one or fragment three of the B chain, respectively, as in the enzymatic digest of each fraction 6., 7., and 8. both fragments, one and three, carrying succinic acid tags can be detected together. However, of unmodified fragment 1, only traces could be detected and the intensity of the signal attributed to modified fragment 3 is distinctly lower compared to the signal of fragment three carrying no succinic acid tag. Therefore, the conclusion can be drawn, that the terminal amino group of the B chain shows a greater reactivity towards activated PEG than the  $\epsilon$ -amino group of B29.

### **3 Summary**

A method was developed to identify the reaction sites of insulin by attaching PEG chains to the protein and subsequently removing them under mild conditions, while leaving tags attached to the reaction sites. By cleavage of the A and B chain, subsequent HPLC analysis and MALDI-ToF identification it was possible to calculate the amount of single, double or unmodified chains, respectively. Although no separation between the conformational isomers of single modified B chains could be achieved, this method still describes a mild and easy way for identification of reaction sites of proteins.

# **Chapter 7**

## **Synthesis and Characterization of Lipophilized Insulin**

## 1 Introduction

Since its discovery and introduction into clinical practice in the 1920s, the insulin molecule was subject to vast and exhaustive research work. Being the substance to treat Insulin Dependent Diabetes Mellitus [IDDM], a disease with growing incidence in the population due to hereditary and environmental factors, not only production and purification, but also pharmaceutical formulations and methods of delivery of this protein were of paramount concern. Two different strategies can be followed to battle IDDM. Cell-based insulin replacement would be the most favorable route as transplantation of pancreatic islet might allow for a better regulation of insulin delivery to diabetic patients. Unfortunately, although some important breakthroughs have been achieved in this field [234] this method is still far from going public. The second strategy implies exogenous administration to patients of the dire needed lacking hormone. Genetically engineered insulin analogs with modified time-action profile, such as short-acting insulin analogs, e.g. Insulin Asp(B10) or Insulin Lispro, or long-acting insulin analogs, e.g. NovoSol Basal or HOE901, present a powerful tool to achieve improved glucose control [235], but they still leave the formidable task of delivering these remedies to patients. Being a protein, the conventional route to insulin administration is via subcutaneous injection. The main drawback of this cumbersome method is the need of multiple daily injections leading to pain and inflammatory risk. So a plethora of controlled drug delivery systems has been developed, ranging from simple infusion pumps, to feed back signal regulated controlled release devices [236,237,238]. Moreover, alternative routes of insulin administration such as nasal [239], pulmonal [240], buccal [241], peroral [239,242] rectal [243,244], have been thoroughly investigated. The most familiar, easy and patient friendly of all routes of application would be the oral route. The major challenges encountered on this way are protection of insulin during its passage through the denaturing environment of the stomach and enhancement of absorption from the small intestine. Protection can easily be provided by coating with a pH responsive polymer. But for a rather polar, large molecule like insulin with an isoelectric point at pH 5.5, it is quite difficult to cross the relative impermeable mucosal membrane. To facilitate absorption following oral administration bioadhesive polymers, which might increase the time of drug retention in the target area, or penetration enhancers, which might fluidize lipid membranes, have been used [242]. Another straightforward approach would be to lipophilize the protein by covalently attaching long chain fatty acids to the molecule. Thus, membrane crossing of the resulting

product is substantially facilitated. A second benefit is the increased stability of the protein. Linkage of palmitic acid, a C16 fatty acid, to insulin might be a step towards an oral application form of this protein [245].

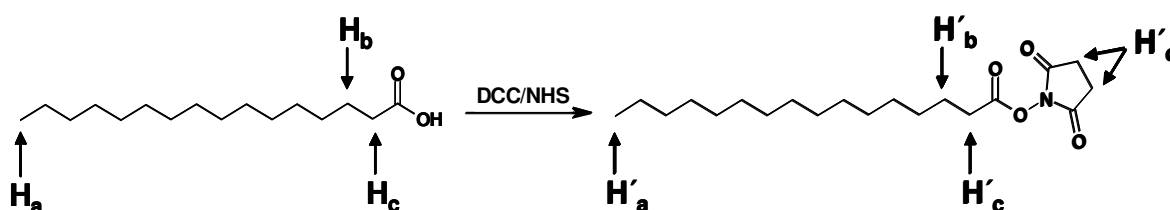
Modification of proteins by attachment of saturated fatty acids is not unheard of in nature. Myristoylation or palmitoylation can often be found related to membrane associated proteins, pointing at their role as membrane tethering moieties [246]. Myristyl is usually attached via a stable amide linkage to the protein in question [247], whereas palmitoylation, which occurs posttranslational, gives oxy- or thioester functions [248]

In this work the modification of insulin with palmitic acid is described using standard DCC/NHS chemistry and its subsequent characterization by HPLC and MALDI-ToF. First steps were undertaken to investigate the bioactivity of the product in a cell based proliferation assay.

## 2 Results and Discussion

### 2.1 Preparation of N-hydroxysuccinimide Ester of Palmitic Acid [Pal-NHS]

The first step towards lipophilized insulin implies the activation of palmitic acid. Possessing only a terminal carboxylic group, fatty acids are not able to react with amines without catalyst. A mild and specific activation of the acid can be performed with DCC and NHS, resulting in the succinimidyl ester, a highly amine reactive substance, which can also be isolated and stored until further use (**Scheme 1**).



**Scheme 1:** Reaction scheme of the activation of palmitic acid. Carbon atoms bearing the protons relevant for NMR identification are marked with arrows.

The conversion of palmitic acid to its activated, amino reactive form was checked by  $^1\text{H-NMR}$  spectroscopy. Typical signals for unreacted palmitic acid are the triplet at 0.88 ppm generated by the terminal methyl group ( $\text{H}_a$  in **Scheme 1**), the five peaked signal at 1.62 ppm originating from the methylene group in  $\beta$  position ( $\text{H}_b$ ) and the triplet at 2.35 ppm stemming from the methylene group adjacent to the carboxylic function ( $\text{H}_c$ ). If the NHS ester of the fatty acid is engineered, the quintet at 1.62 ppm shifts to 1.75 ppm ( $\text{H}'_b$ ) and the triplet at 2.35 ppm to 2.60 ppm ( $\text{H}'_c$ ). Additionally, a new signal at 2.84 ppm can be detected resulting from the protons of the succinimide group ( $\text{H}'_d$ ). **Figure 1** shows  $^1\text{H-NMR}$  spectra of palmitic acid, the educt, and the product obtained after re-crystallization from ethanol. All postulated signals can be identified and the shift of signals between native and activated form can clearly be seen, proving that the activation was successful.



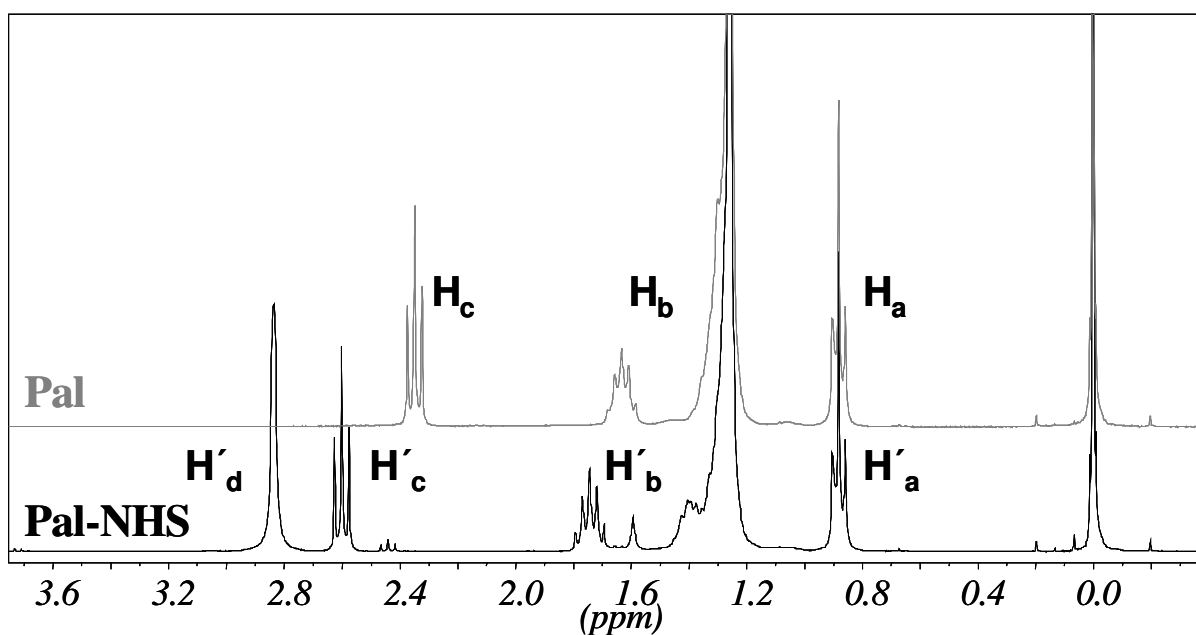


**Figure 1:**  $^1\text{H-NMR}$  spectra of palmitic acid (upper graph) and the NHS-ester of palmitic acid (lower graph) recorded in  $\text{CDCl}_3$  with TMS as internal standard.

Furthermore, knowledge on the purity of the reaction product was gained by calculating the integrals of the signals pointed out above. In **Table 1** the theoretical and calculated values are listed. Comparison between corresponding integrals shows that the product could be synthesized in good purity.

**Table 1:** Comparison between theoretical and experimentally acquired values of the integrated  $^1\text{H-NMR}$  signals typical for Pal-NHS. The integral of the signal generated by the  $\text{H}'_c$  protons was used as reference and set at 2.000.

Signal	$\text{H}'_d$	$\text{H}'_c$	$\text{H}'_b$	$\text{H}'_a$
Theoretical values	4.000	2.000	2.000	3.000
NMR integrals	4.000	2.000	2.014	3.027

## 2.2 Synthesis and Characterization of Lipophilized Insulin

Three major limitations are encountered on the way to lipidized proteins: the incompatibility in reaction media of the two compounds [249], the insolubility of the product in water [250]

and the often reduced biological activity of the protein-lipid complex [251]. Nonetheless, high transport across biological membranes [252], high stability [253] and long plasma half-lives [254] are the advantages, which justify the effort exerted in this research field. Numerous examples may be cited to support these assumptions. Insulin chemically modified with palmitic acid showed enhanced adsorption from the large intestine [245], whereas lipidized salmon calcitonin exhibited not only enhanced oral bioavailability, but also improved pharmacokinetic and pharmacodynamic [254] behaviors.

For the synthesis of lipophilized insulin different ratios of the amine reactive acid in relation to the protein amount were used, to engineer insulin with various amounts of lipid attached. Bovine insulin possesses three primary amine groups (A1-Gly, B1-Phe and B29-Lys) all accessible for reactions with the activated palmitic acid. In the first attempt, we settled for equimolar amounts between the amine groups of protein and the fatty acids, i.e. a molar ratio of one mol of insulin to three mol of palmitic acid.

Analyzing the resulting product with RP-HPLC, only one dominant peak could be detected. Further investigations with HPLC-MS revealed that this peak was generated by a substance having a mass of 1613.7 Th or 2150.9 Th respectively (**Figure 2**). Assuming that the first species is the fourfold charged ion and the latter the threefold charged ion, a total molecular weight of 6450.8 Da or 6449.7 Da respectively can be calculated. This molecular weight is in good agreement with the numeral molecular weight of triple palmitoylated insulin of 6448 Da. Thus, we identified the main signal of our reaction batch as corresponding to insulin to which three palmitic acid chains were covalently attached.

Minor peaks were eluted at about 30 min and were identified as originating from insulin with two palmitic acid chains attached. Different retention times might be attributed to variable structures of the conformational isomers, depending on which two of the possible three amine groups participated in the reaction.

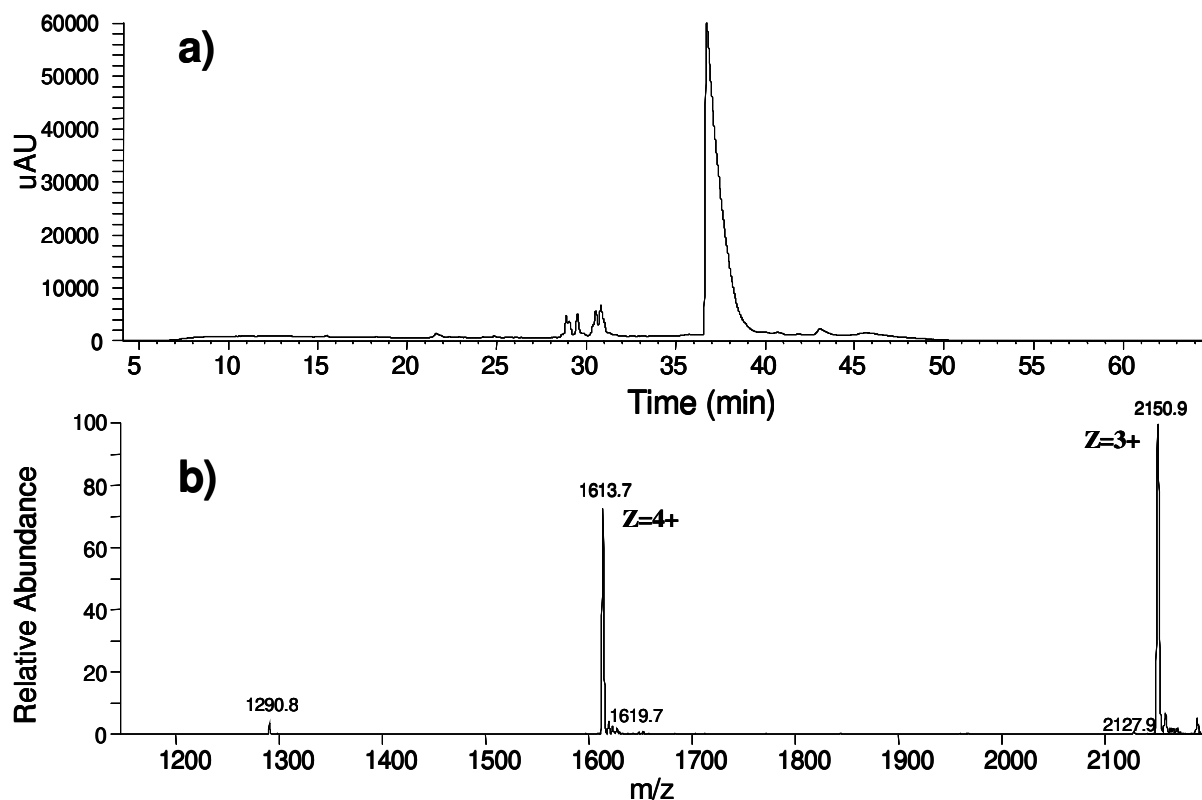


**Figure 2:** HPLC-MS spectra of lipophilized insulin synthesized with a ratio of one mol insulin to three mol palmitic acid. **a)** UV spectra recorded at 274 nm. **b)** Mass spectrum of the substances eluted at retention times between 35.9 min and 39.7 min.

HPLC-MS results could be confirmed by MALDI-ToF spectra, where once again the main peak showed a mass corresponding to triple palmitoylated insulin (**Figure 3**).

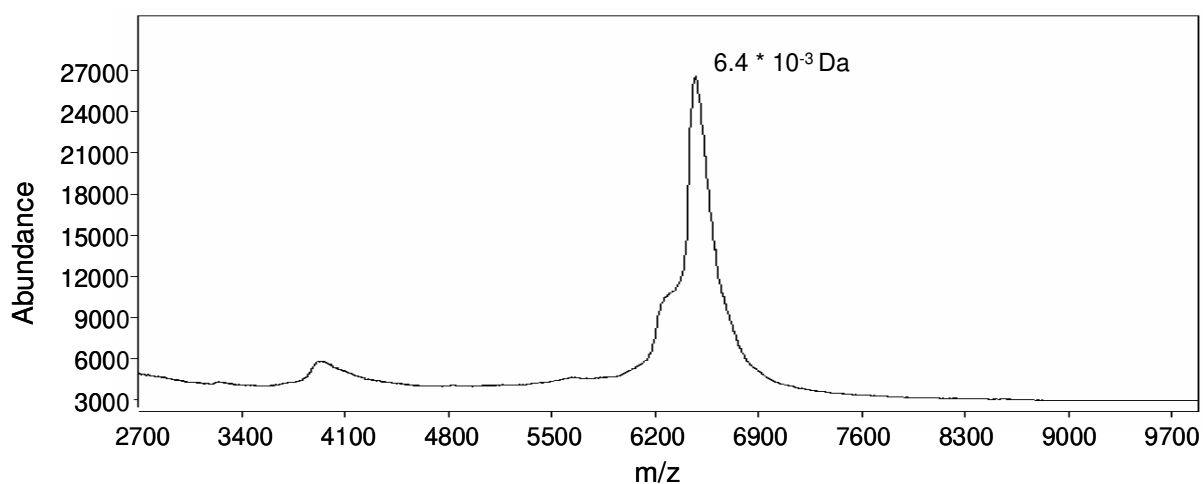


**Figure 3:** MALDI-ToF spectrum of lipophilized insulin synthesized with a ratio of one mol insulin to three mol palmitic acid. The main peak is generated by triple palmitoylated insulin.

Triple palmitoylated insulin is a substance with very poor solubility in aqueous media. Unfortunately, for most applications solubility in water is a very treasured feature. Thus, we decided to reduce the amount of palmitic acid in the reaction batch in order to synthesize the whole range of possible derivatives (simple, double, and triple palmitoylated insulin). Using a ratio of 1 mol insulin to 1.5 mol palmitic acid we met this goal and a mixture of various derivatives of insulin could be synthesized. The reaction batch was once again separated by HPLC (**Figure 4**) and the derivatives identified by HPLC-MS.

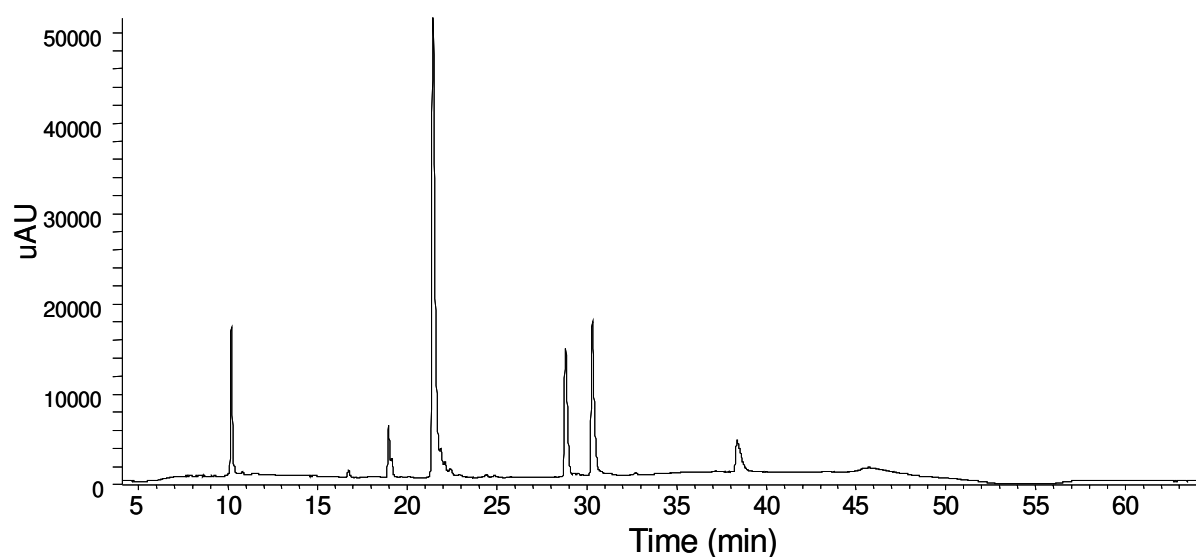


**Figure 4:** HPLC chromatogram of lipophilized insulin synthesized with a ratio of 1.0 mol insulin to 1.5 mol palmitic acid. UV-spectrum recorded at 274 nm.

For calculation of the theoretical molecular weight of the products we used a value of approximately 5733 Da for bovine insulin found in literature. Mass spectra showed fourfold and threefold charged ions, from which we used the latter for mass calculation of the detected molecules (**Table 2**). As theoretical and nominal values are in good correspondence, we identified the substance eluting at approximately 10 min as being native insulin, the two signals detected between 18 min and 22 min with similar masses, as originating from insulin with one palmitic chain attached, the peaks eluting at 28 min and 30 min as corresponding to double palmitoylated insulin, and the signal eluted last at approximately 38 min was attributed to triple palmitoylated insulin. Differences in elution times of substances with the same molecular weight were once again attributed to conformational differences of these molecules, depending on which amine group reacted with the palmitic acid.

**Table 2:** Retention time and mass per charge of different insulin - palmitic acid- derivatives separated by HPLC-MS. Molecular weights were calculated from triple charged ions. For theoretical MW calculations the mass of bovine insulin was assumed as being 5733 Da.

Retentiontime (s)	m/z	MW <sub>nominal</sub> (Da)	MW <sub>theoretical</sub> (Da)	Substance
9.95-10.06	1912.8	5735	5733	Insulin
18.50-18.96	1991.9	5973	5971	Insulin + 1Fatty acid
20.98-21.35	1992.2	5974	5971	Insulin + 1Fatty acid
28.35-28.91	2071.9	6213	6210	Insulin + 2Fatty acids
29.90-30.22	2071.4	6211	6210	Insulin + 2Fatty acids
37.90-38.53	2151.2	6451	6448	Insulin + 3Fatty acids

MALDI-ToF analysis confirmed the presence of all four insulin derivatives in the reaction batch (**Figure 5**).

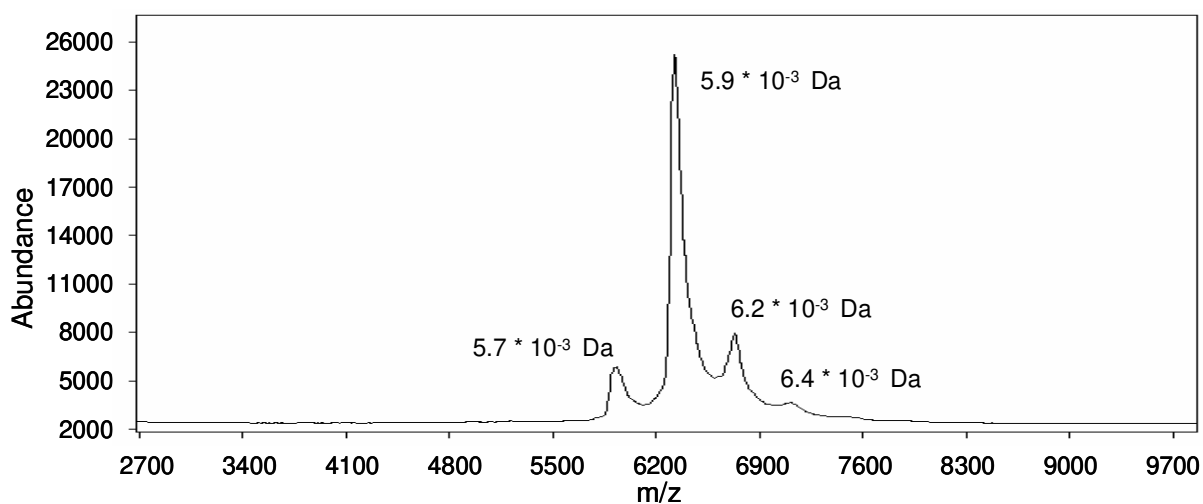


**Figure 5:** MALDI-ToF spectrum of lipophilized insulin synthesized with a ratio of 1.0 mol insulin to 1.5 mol palmitic acid. Native insulin and insulin with one, two or three palmitic acid chains attached covalently could be detected.

### 2.3 Processing of Lipophilized Insulin

A frequently encountered restriction in the lipidization of proteins is the need of finding a reaction media, where both, the polypeptide and the lipid are soluble. In the majority of cases the two components are incompatible in aqueous media, necessitating the use of solubility enhancers or the design of complex systems, such as reversed micelles [249]. In another approach, organic solvents like DMF or DMSO might be chosen. Although good solvents for most proteins and lipids, these organic solvents are hampered by relatively high boiling points, making removal from the reaction batch difficult, and by their toxicity (LD50 oral, rat is 2800 mg/kg for DMF).

The reaction between insulin and palmitic acid was carried out in DMF, which had to be removed completely prior to further use of the protein. One approach to the solution of this problem is to use preparative HPLC with the additional benefit of being able to separate and to collect different insulin species for further study. The HPLC method described above gives good resolution of the different substances, but the proteins elute over a long period of time, making the method time consuming and non-economic. Therefore, we varied some of the chromatographic parameters employed for analysis, on our search for a method as compact as possible, giving in the same time good resolution of insulin derivatives. Increasing the initial amount of acetonitrile as far as 40% did not result in a significant shorter retention time for triple palmitoylated insulin (**Figure 6**). However native insulin was eluted very fast and detected together with the injection peak. By shortening the first step of the gradient, the time until the percentage of mobile phase B was increased to 100 per cent, from 30 min to 10 min, we were able to significantly decrease the run time to a total value of 20 min, at the same time distinctly separating all significant peaks (**Figure 6**).

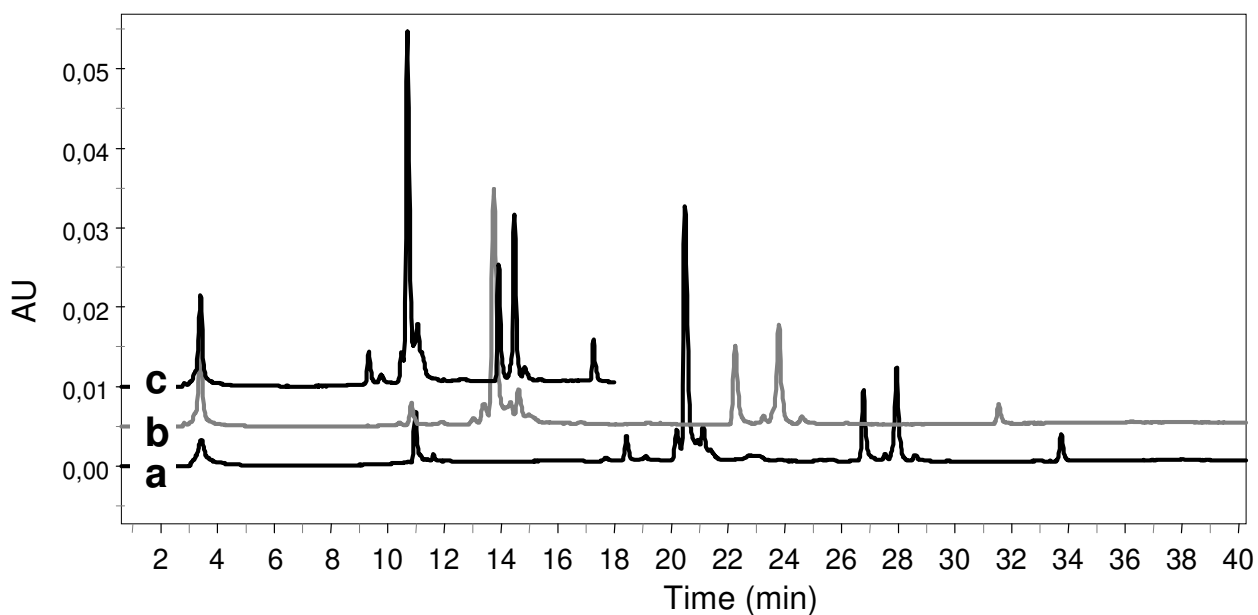


**Figure 6:** Influence of acetonitrile on HPLC chromatograms of lipophilized insulin synthesized with a ratio of 1.0 mol insulin to 1.5 mol palmitic acid. **a)** 20% initial amount of acetonitrile. **b)** 40% initial amount of acetonitrile. **c)** 40% initial amount of acetonitrile and first step of the gradient reduced to 10min.

Deciding to use the substance mixture and not the individual substances in the bioactivity assay, the goal was to remove the organic solvent from the reaction batch. As freeze-drying of the product did not succeed, the method of choice was ultrafiltration, a fast and easy method to separate substances with different molecular weights. To monitor the separation, the filtrate was checked by HPLC for residual insulin. The supernatant was freeze-dried to obtain a substance with improved shelf life and the product analyzed by HPLC. The investigation of the filtrate by MALDI-ToF or HPLC revealed that no insulin was lost during the filtration process, as it could not be detected in this phase by either method. In both chromatograms in **Figure 7**, taken pre and post filtration and freeze-drying, the same signal pattern can be observed, clearly indicating that filtration and subsequent freeze drying have no significant effect on the original composition of our product.

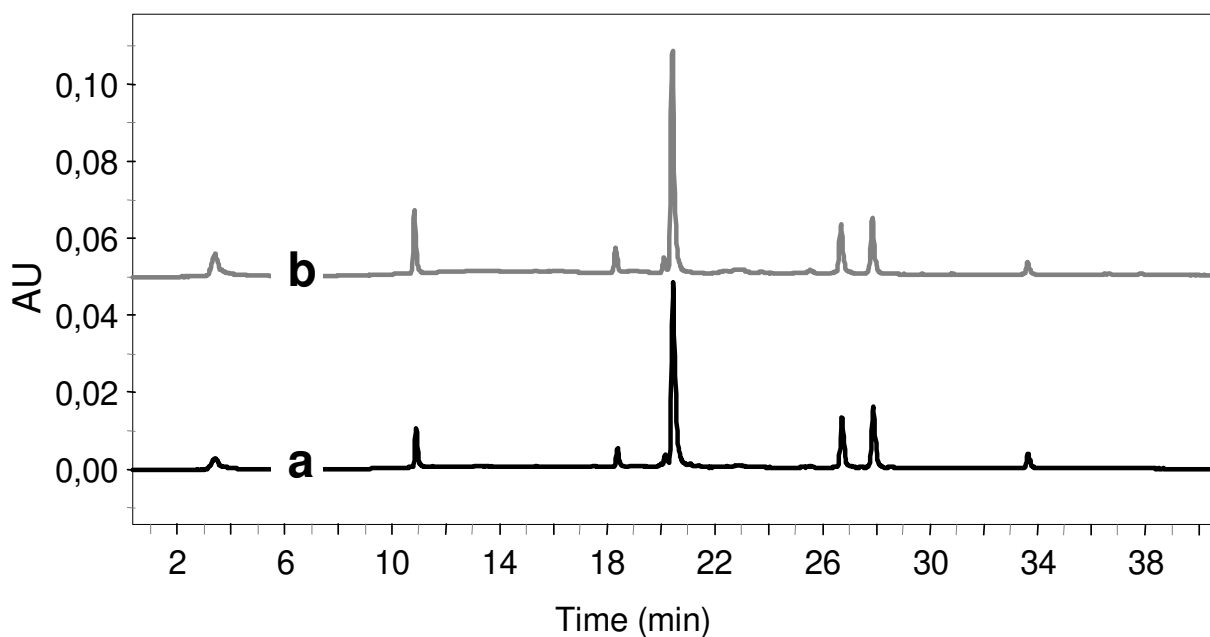


**Figure 7:** HPLC chromatogram of lipophilized insulin synthesized with a ratio of 1.0 mol insulin to 1.5 mol palmitic acid. **a)** Chromatogram of the reaction batch taken after reduction of DMF. **b)** Chromatogram of the purified and freeze-dried product.

For further experiments, freeze dried insulin was used synthesized with a molar ratio of 1 mol insulin to 1.5 mol palmitic acid [lipo-insulin 1.5].

## 2.4 Bioassay of Lipophilized Insulin

Insulin is a protein frequently used in cell culture due to its well known ability to enhance cell proliferation and differentiation. To prove the biological activity of modified insulin we investigated the influence of insulin and lipo-insulin 1.5 on the proliferation of bovine chondrocytes.

Hence, four different concentrations of each protein were added to the cell culture, while molar amounts of insulin and lipophilized insulin were kept equal in corresponding groups. Proteins were supplied as solutions in IGF-buffer. While native insulin dissolved in a short period of time, lipo-insulin 1.5 gave a turbid solution. As control, only IGF-buffer was supplied to one cell group. After cultivation for eight days and subsequent harvest, cells were counted and the obtained numbers served as proliferation markers. Resulting cell numbers are shown in **Figure 8**.



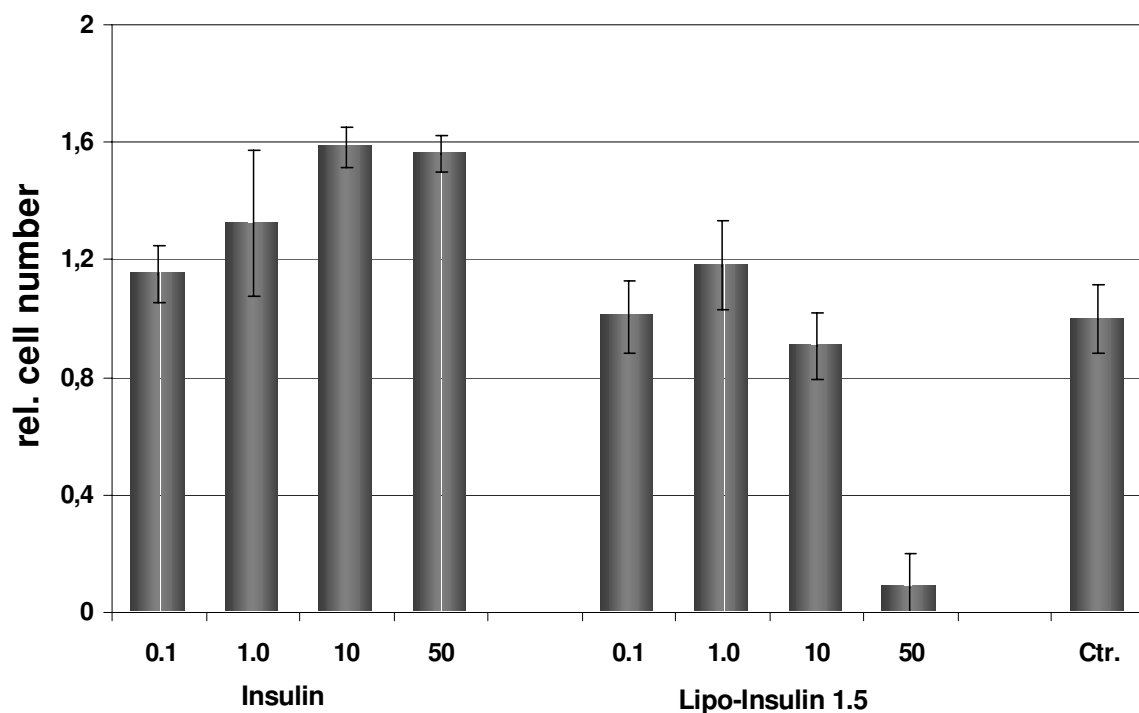


**Figure 8:** *Effects of insulin and lipo-insulin 1.5 on cell numbers after eight days of cultivation. Four different protein concentrations of each protein were evaluated. In the insulin group figures represent ng/ml of the protein. Molar amounts of supplemented insulin and lipophilized insulin were equal in corresponding groups.  $n = 5$  with error bars representing the standard deviations from the mean.*

As expected, insulin shows a concentration dependent positive effect on the proliferation of bovine chondrocytes. Especially in groups with higher amounts of insulin (10 ng/ml and 50 ng/ml) a distinct increase in cell number compared to the control group can be observed. In contrast, lipophilized insulin shows a somewhat incoherent tendency. Lower lipo-insulin 1.5 concentrations (Lipo-Insulin 1.0) hint at enhancement of proliferation. But higher lipophilized insulin concentrations show a definite decrease in cell number. This effect might be due to the presence of undissolved substance in cell culture wells. Directly after addition of the protein we could observe with 100-fold magnification small fragments of lipophilized insulin, which were still present after two days of cultivation. Endocytosis of such particles might lead to over-stimulation and death of the cells, as it has already been shown, that at high concentrations insulin shows not an antiapoptotic, but a toxic effect on cells [255]. Higher amounts of lipophilized insulin were also associated with a higher decrease in cell numbers.

Thus, the necessity was concluded to completely dissolve the lipophilized insulin before application to cells.

In a first approach solubility enhancers were tested for their ability to promote protein solubility: Pluronic F68, Tween 80, PEG 400. But even in concentrations as high as 10% (m/V), which are far from typically employed values, these surface-active agents fell short of the goal. Hence a decision was made in favor of biocompatible organic solvents. We settled for N-methyl-2-pyrrolidone a solvent applied in other cell culture models in concentrations as high as 10% [256].

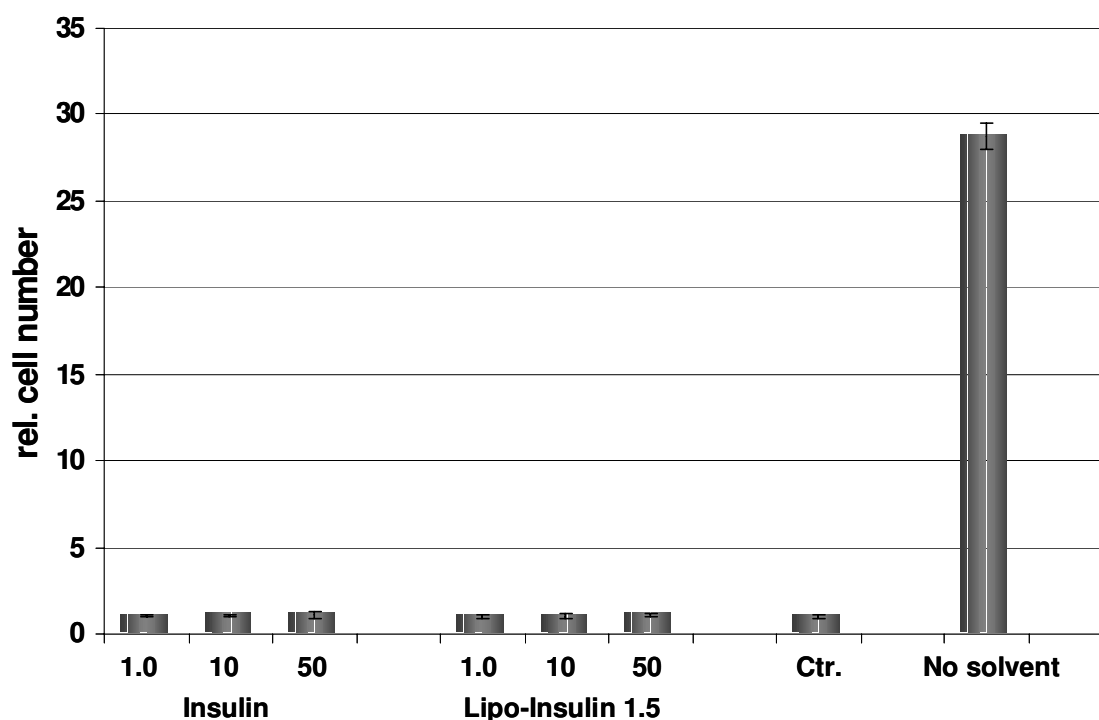


**Figure 9:** Effects of insulin and lipo-insulin 1.5 on cell numbers after fourteen days of cultivation in the presence of the proteins. Three different protein concentrations were evaluated. In the insulin group figures represent ng/ml of the protein and molar amounts of insulin and lipophilized insulin were equal in corresponding groups. As control served groups supplemented with both solvents [Ctr.] or with no additional supplements [No solvent].  $n = 6$  with error bars representing the standard deviations from the mean.

In the following experiment insulin was dissolved in IGF-buffer, whereas lipophilized insulin was dissolved in the organic solvent. Nonetheless, each group was supplemented with both solvents and three different concentrations of the proteins were investigated. As control

served groups supplemented with both solvents or without solvents. Cells were cultured for eight or fourteen days and counted after harvest. Exemplarily, relative cell numbers counted after fourteen days of cultivation and serving as marker for cell growth are shown in **Figure 9**.

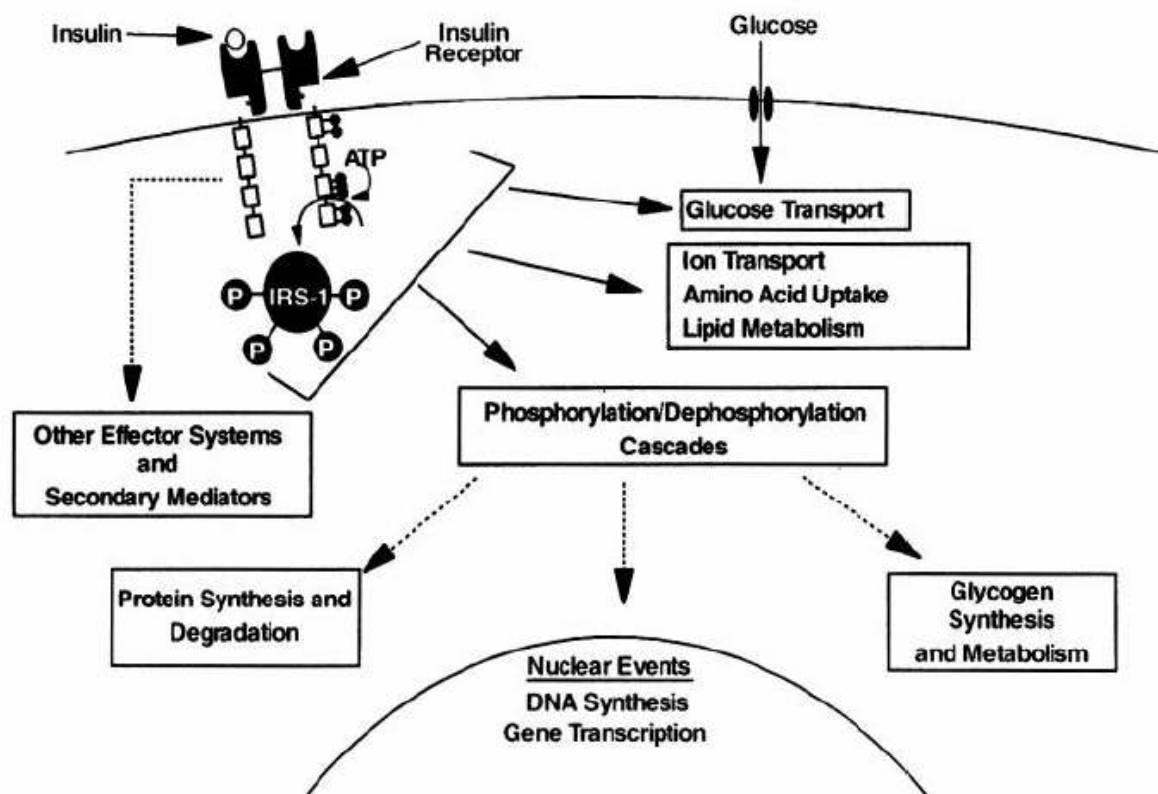
This graph shows very clearly that N-methyl-2-pyrrolidon interferes with cell proliferation. Even though, absolute cell numbers slightly increased in each well compared to initially seeded cell numbers, neither insulin nor lipophilized insulin showed under these conditions a positive effect on cell proliferation.

Having identified the organic solvent as the reason for diminished cell growth, measures were undertaken to reduce the total amount of solvent used, hoping that lower concentrations would be tolerated better. 2 mg of lipophilized insulin could be dissolved in as little as 10  $\mu$ l of N-methyl-2-pyrrolidon. Unfortunately, the substance precipitated upon insertion into the cell culture medium leading to the problems mentioned above.

The problem of reduced solubility, encountered here on the way to bioactivity testing, often occurs with lipophilized proteins. Not only solubility in water might be a problem of protein-fatty acid complexes, but also their bioactivity can be diminished compared to the original protein. The question of reduced bioavailability must be assessed separately for each processed protein, as it is often caused by deteriorated receptor binding ability, either through sterical hindrance or removal of essentially needed functional groups, which depend on the modification site. Moreover, fundamental features like hydrophilicity or conformation might be changed.

Insulin binds to the insulin receptor [IR] and to a much lesser extent to the insulin-like growth factor [IGF] receptor. The insulin receptor is a member of the Type II tyrosine kinase receptor family consisting of two extracellular  $\alpha$ -subunits and two transmembrane  $\beta$ -subunits with intrinsic tyrosine kinase activity. In contrast to most growth factor receptors, IR is dimeric even if not activated. Upon binding of insulin, the tyrosine kinase activity is increased and a high affinity pocket for e.g. SH2 domains containing proteins is formed. Among other adaptor proteins, IR substrate 1 or 2 are needed for activation of downstream cascades. The regulatory effects thereof affected fall into two categories: metabolic effects of short or long duration on

the uptake, transport, intermediary metabolism and storage of small food molecules, and mitogenic effects realized at gene level (**Scheme 2**).



**Scheme 2:** *The insulin-signaling system affects numerous intracellular processes. The small circles attached to the intracellular portion of the insulin receptor and the insulin receptor substrate 1 [IRS-1] represent some site of phosphorylation. Reproduced from [255].*

Although some of the mechanisms of insulin action are elucidated, e.g. the ras-raf cascade activation, or the phosphatidylinositol-3-kinase activation, some key points still elude clarification, also due to the complex interactions of the different cascades. So, much research work is done in this field.

It has been postulated that the major determinant for mitogenic activity after insulin receptor activation is the retarded rate of dissociation of the ligand from the receptor, be it the IR or the IGF receptor. If chemically modified insulin by attachment of palmitic acid might or might not show such a delayed dissociation has to be revealed by further studies.

### 3 Summary

Following the instructions by Lapidot et al. the synthesis of various derivatives of insulin covalently attached to fatty acids succeeded. The product was characterized by HPLC and HPLC-MS, and a method for using MALDI-ToF techniques was established. A method for the purification of the reaction batch was developed. Moreover, first steps towards the investigation of biological activity of the proteins in a cell culture model were undertaken, handicapped by the poor solubility in water of the substance.

Further research work will be needed to establish a working model, either by isolating the different compounds and assessing them separately, or by finding an over-all solvent for lipophilized insulin, which does not interfere with the test system.

Then much needed knowledge can be gained.



# **Chapter 8**

## **Summary and Conclusion**

The field of Tissue Engineering has been subject to substantial research work in recent years. Although many important breakthroughs have been achieved, the goal of producing constructs to repair missing, severed or malfunctioning tissues in the needed quantities is still far from being reached. Therefore the struggle continues in various areas, such as synthesis and characterization of scaffold materials for enhanced cell growth, or investigation of the impact of modified bioactive molecules on the development of cells.

In this work (**Chapter 4**) the synthesis of MePEG<sub>2</sub>PLA<sub>20</sub> and MePEG<sub>2</sub>PLA<sub>40</sub> was investigated more closely. These polymers are often used in Tissue Engineering applications, as they are biocompatible, biodegradable and easily modeled into scaffolds. It could be shown, that the use of a large volume of solvent for the polymerization reaction, results in the formation of two fractions of polymers, which differ only in the length of the PLA chain, but make further processing of the polymers difficult. If the volume of solvent for the synthesis is reduced, the resulting polymers show a monomodal molecular weight distribution with the targeted average molecular weight. These polymers can be processed into mechanically stable devices for in-vivo and in-vitro experiments. As the aforementioned polymers possess no functional group, making a conversion into a biomimetic material difficult, a second class of polymers was investigated. The amine group on NH<sub>2</sub>PEG<sub>2</sub>PLA<sub>40</sub> can easily be activated to react with bioactive molecules, resulting in biomimetic polymers. For the synthesis of NH<sub>2</sub>PEG<sub>2</sub>PLA<sub>40</sub> initially a large volume of solvent has to be used, which is removed over time through a stream of nitrogen, concomitantly removing acetic acid. After activation, these polymers were blended with MePEG<sub>2</sub>PLA<sub>40</sub> and could be processed into mechanically stable scaffolds, to which bFGF was bound as model protein. In the following in-vivo experiments, biomimetic scaffolds proved their superiority compared to the control, as increased tissue ingrowth and vascularization of the constructs could be detected.

In another study the impact of the PEG content on the surface properties of MePEG<sub>x</sub>PLA<sub>y</sub> films was investigated (**Chapter 5**) using the quartz crystal microbalance. The surface of the quartz disks had to be modified using octadecyltrichlorosilane to provide adequate adhesion of the polymer films. To investigate protein adsorption behavior, insulin was chosen as model protein. On films containing PEG<sub>5</sub> chains, lower protein adsorption could be detected compared to pure PLA chains, confirming the shielding of the surface. If the diblock-copolymer consisted of short PLA chains (10 Da) the effect was more pronounced compared to longer PLA chains (95 Da). Films containing short chain PEGs (0.75 Da) showed a higher degree of protein adsorption compared to PLA films. This paradox effect might result from



enhanced wetting of the films due to the hydrophilic PEG chains, whereas the protective characteristics no longer have any effects, given the shortness of the chains. A second reason might be the inelastic binding of proteins because of sterical hindrance on account of PEG chains present on the surface, which may cause a decrease in resonant frequency.

By covalently linking PEG chains to proteins, the favorable characteristics of the polymer may be transferred to the resulting conjugate. Going one step further, covalent linking of proteins to scaffolds would provide the advantage of limited operating range and prolonged reaction times compared to proteins administered in solution, as these proteins might not leave their tethering site. To get more information on the resulting conjugate, knowledge of the reaction sites is of utter importance (**Chapter 6**). Binding of PEG chains to succinic acid resulted in an easily cleavable ester group. After activation of the free end of the succinic acid the polymer was bound to insulin, chosen as model protein, via a more stable amid linkage. Removal of the polymer under mild basic conditions with hydroxylamine, resulted in polymers with succinic acid tags still marking the reaction sites. After cleavage of disulfide bonds and HPLC separation coupled to MALDI-ToF analysis, it could be shown, that the amino group of the A chain is less reactive, compared to those of the B chain. Subsequent enzymatic digestion and MALDI-ToF analysis of the fractions obtained by HPLC analysis confirmed the presence of tags, although no information could be obtained on the individual reactivity of each of the two amino groups on the B chain. Still, the developed method provides a mild and easy way for the identification of the reaction sites of proteins.

A different attempt on the modification of proteins was to bind fatty acids to the protein backbone, a reaction which often occurs *in vivo*. Besides possibly increasing their biological activity, proteins thus modified might be successfully chosen for alternative administration routes, e.g. the oral route. As described in **Chapter 7**, a method was found to synthesize and purify lipidized bovine insulin and the product characterized by HPLC and MALDI-ToF. The biological activity of the modified protein was assessed in an insulin dependent cell culture model. Due to its poor solubility in water, the necessary concentrations of protein could not be reached in aqueous media, and application of a suspension to the culture medium resulted in cell death. The use of N-methylpyrrolidone as solvent also had a negative effect on cell growth. Further research work will be needed to find a solvent for lipidized insulin, which does not interfere with the test system.

Some important results could be achieved: 1. development of a method for the synthesis of biomimetic polymers of the general structure of PEG<sub>x</sub>PLA<sub>y</sub> with superior characteristics with regard to Tissue Engineering applications; 2. the general practicability of QCM techniques for the investigation of protein adsorption to these polymers could be shown; 3. determination of reaction sites of a model protein, insulin, towards activated PEG could be performed; 4. first attempts were undertaken to investigate the biological activity of lipophilized insulin in an insulin dependent cell culture model. But still substantial research work has to be done to elucidate all mechanisms implied in these analysis and to transfer established procedures to other systems.

# References

- [1]. H. Hoecker, Polymeric materials as biomaterials under particular consideration of biodegradable polymers, *Macromol. Symp.* 130 (1998) 161--168.
- [2]. R. Langer, L.G. Cima, J.A. Tamada, E. Wintermantel, Future directions in biomaterials, *Biomaterials* 11 (1990) 738--745.
- [3]. S. Zhou, X. Liao, X. Li, X. Deng, H. Li, Poly-d,l-lactide-co-poly(ethylene glycol) microspheres as potential vaccine delivery systems, *J. Controlled Release* 86 (2003) 195--205.
- [4]. L. J. Bonassar, C.A. Vacanti, Tissue engineering: the first decade and beyond, *J. Cell Biochem.* 30-31 (1998) 297--303.
- [5]. J. A. Hubbell, Biomaterials in tissue engineering, *Bio/Technology* 13 (1995) 565--576.
- [6]. K. James, J. Kohn, New Biomaterials for Tissue Engineering, *MRS Bull.* (1996) 22--26.
- [7]. D. W. Hutmacher, J.C. Goh, S.H. Teoh, An introduction to biodegradable materials for tissue engineering applications, *Ann. Acad. Med. Singapore* 30 (2001) 183--191.
- [8]. R. Langer, Biomaterials and Biomedical Engineering, *Chem. Eng. Sci.* 50 (1995) 4109--4121.
- [9]. D. Klee, H. Hoecker, Polymers for biomedical applications: improvement of the interface compatibility, *Adv. Polym. Sci.* 149 (1999) 1--57.
- [10]. A. Lucke, J. Tessmar, E. Schnell, G. Schmeer, A. Gopferich, Biodegradable poly(D,L-lactic acid)-poly(ethylene glycol)-monomethyl ether diblock copolymers: structures and surface properties relevant to their use as biomaterials, *Biomaterials* 21 (2000) 2361--2370.
- [11]. B. D. Ratner, The engineering of biomaterials exhibiting recognition and specificity, *J. Mol. Recognit.* 9 (2002) 617--625.
- [12]. B. D. Ratner, Molecular design strategies for biomaterials that heal, *Macromol. Symp.* 130 (1998) 327--335.
- [13]. B. K. Mann, R.H. Schmedlen, J.L. West, Tethered-TGF-[beta] increases extracellular matrix production of vascular smooth muscle cells, *Biomaterials* 22 (2001) 439--444.
- [14]. P. R. Kuhl, L.G. Griffith-Cima, Tethered epidermal growth factor as a paradigm for growth factor-induced stimulation from the solid phase, *Nat. Med.* 2 (1996) 1022--1027.
- [15]. M. Kantlehner, P. Schaffner, D. Finsinger, J. Meyer, A. Jonczyk, B. Diefenbach, B. Nies, G. Holzemann, S.L. Goodman, H. Kessler, Surface coating with cyclic RGD peptides stimulates osteoblast adhesion and proliferation as well as bone formation, *ChemBiochem.* 1 (2000) 107--114.
- [16]. H. Shin, K. Zygourakis, M.C. Farach-Carson, M.J. Yaszemski, A.G. Mikos, Attachment, proliferation, and migration of marrow stromal osteoblasts cultured on

- biomimetic hydrogels modified with an osteopontin-derived peptide, *Biomaterials* 25 (2004) 895--906.
- [17]. K. Bhadriraju, L.K. Hansen, Hepatocyte adhesion, growth and differentiated function on RGD-containing proteins, *Biomaterials* 21 (2000) 267--272.
- [18]. B. K. Mann, A.T. Tsai, T. Scott-Burden, J.L. West, Modification of surfaces with cell adhesion peptides alters extracellular matrix deposition, *Biomaterials* 20 (1999) 2281--2286.
- [19]. C. W. Cho, Y.S. Cho, H.K. Lee, Y. Yeom, I, S.N. Park, D.Y. Yoon, Improvement of receptor-mediated gene delivery to HepG2 cells using an amphiphilic gelling agent, *Biotechnol. Appl. Biochem.* 32 ( Pt 1) (2000) 21--26.
- [20]. P. S. Stayton, A.S. Hoffman, N. Murthy, C. Lackey, C. Cheung, P. Tan, L.A. Klumb, A. Chilkoti, F.S. Wilbur, a. Press et, Molecular engineering of proteins and polymers for targeting and intracellular delivery of therapeutics, *J. Controlled Release* 65 (2000) 203--220.
- [21]. L. G. Cima, Polymer substrates for controlled biological interactions, *J. Cell Biochem.* 56 (1994) 155--161.
- [22]. T. Blunk, A. Gopferich, J. Tessmar, Special issue Biomimetic Polymers, *Biomaterials* 24 (2003) 4335--4335.
- [23]. H. Shin, S. Jo, A.G. Mikos, Biomimetic materials for tissue engineering, *Biomaterials* 24 (2003) 4353--4364.
- [24]. M. Hacker, J. Tessmar, M. Neubauer, A. Blaimer, T. Blunk, A. Gopferich, M.B. Schulz, Towards biomimetic scaffolds: Anhydrous scaffold fabrication from biodegradable amine-reactive diblock copolymers, *Biomaterials* 24 (2003) 4459--4473.
- [25]. J. Tessmar, A. Mikos, A. Gopferich, The use of poly(ethylene glycol)-block-poly(lactic acid) derived copolymers for the rapid creation of biomimetic surfaces, *Biomaterials* 24 (2003) 4475--4486.
- [26]. E. Ruoslahti, M.D. Pierschbacher, New perspectives in cell adhesion: RGD and integrins, *Science* 238 (1987) 491--497.
- [27]. U. Hersel, C. Dahmen, H. Kessler, RGD modified polymers: biomaterials for stimulated cell adhesion and beyond, *Biomaterials* 24 (2003) 4385--4415.
- [28]. R. G. LeBaron, K.A. Athanasiou, Extracellular matrix cell adhesion peptides: functional applications in orthopedic materials, *Tissue Eng.* 6 (2000) 85--103.
- [29]. K. Shakesheff, S. Cannizzaro, R. Langer, Creating biomimetic micro-environments with synthetic polymer-peptide hybrid molecules, *J. Biomater. Sci. Polym. Ed.* 9 (1998) 507--518.
- [30]. W. L. Murphy, D.J. Mooney, Molecular-scale biomimicry, *Nat. Biotechnol.* 20 (2002) 30--31.

## References

---

- [31]. C. Miller, H. Shanks, A. Witt, G. Rutkowski, S. Mallapragada, Oriented Schwann cell growth on micropatterned biodegradable polymer substrates, *Biomaterials* 22 (2001) 1263--1269.
- [32]. J. H. Ward, R. Bashir, N.A. Peppas, Micropatterning of biomedical polymer surfaces by novel UV polymerization techniques, *J. Biomed. Mater. Res.* 56 (2001) 351--360.
- [33]. Y. Hu, S.R. Winn, I. Krajchich, J.O. Hollinger, Porous polymer scaffolds surface-modified with arginine-glycine-aspartic acid enhance bone cell attachment and differentiation in vitro, *J. Biomed. Mater. Res.* 64A (2003) 583--590.
- [34]. D. M. Ferris, G.D. Moodie, P.M. Dimond, C.W. Gioranni, M.G. Ehrlich, R.F. Valentini, RGD-coated titanium implants stimulate increased bone formation in vivo, *Biomaterials* 20 (1999) 2323--2331.
- [35]. F. A. van der, A. Sonnenberg, Function and interactions of integrins, *Cell Tissue Res.* 305 (2001) 285--298.
- [36]. M. D. Pierschbacher, E. Ruoslahti, Cell attachment activity of fibronectin can be duplicated by small synthetic fragments of the molecule, *Nature (London, United Kingdom)* 309 (1984) 30--33.
- [37]. R. O. Hynes, Integrins: versatility, modulation, and signaling in cell adhesion, *Cell* 69 (1992) 11--25.
- [38]. S. P. Massia, J.A. Hubbell, An RGD spacing of 440 nm is sufficient for integrin alpha V beta 3- mediated fibroblast spreading and 140 nm for focal contact and stress fiber formation, *J. Cell Biol.* 114 (1991) 1089--1100.
- [39]. N. J. Boudreau, P.L. Jones, Extracellular matrix and integrin signalling: the shape of things to come, *Biochem. J.* 339 (1999) 481--488.
- [40]. A. Woods, J.R. Couchman, Syndecans: synergistic activators of cell adhesion, *Trends Cell Biol.* 8 (1998) 189--192.
- [41]. A. D. Cardin, H.J. Weintraub, Molecular modeling of protein-glycosaminoglycan interactions, *Arterioscler. , Thromb. , Vasc. Biol.* 9 (1989) 21--32.
- [42]. M. E. Hasenbein, T.T. Andersen, R. Bizios, Micropatterned surfaces modified with select peptides promote exclusive interactions with osteoblasts, *Biomaterials* 23 (2002) 3937--3942.
- [43]. B. Alberts, D. Bray, J. Lewis, M. Raff, K. Roberts, J.D. Watson, *Molecular Biology of the Cell*, Garland Publishing, Inc., New York & London, (1994) 502--502.
- [44]. R. Gref, P. Couvreur, G. Barratt, E. Mysiakine, Surface-engineered nanoparticles for multiple ligand coupling, *Biomaterials* 24 (2003) 4529--4537.
- [45]. N. Ferrara, T. Davis-Smyth, *The Biology of Vascular Endothelial Growth Factor*, *Endocr. Rev.* 18 (1997) 4--25.
- [46]. C. J. Powers, S.W. McLeskey, A. Wellstein, Fibroblast growth factors, their receptors and signaling, *Endocr. Relat. Cancer* 7 (2000) 165--197.

## References

---

- [47]. J. Folkman, Y. Shing, *Angiogenesis*, *J. Biol. Chem.* 267 (1992) 10931--10934.
- [48]. S. B. Trippel, Growth factor actions on articular cartilage, *J. Rheumatol.*, Suppl. 43 (1995) 129--132.
- [49]. P. Chen, K. Gupta, A. Wells, Cell movement elicited by epidermal growth factor receptor requires kinase and autophosphorylation but is separable from mitogenesis, *J. Cell Biol.* 124 (1994) 547--555.
- [50]. G. Schultz, D.S. Rotatori, W. Clark, EGF and TGF- $\alpha$  in wound healing and repair, *J. Cell Biochem.* 45 (1991) 346--352.
- [51]. T. Blunk, A.L. Sieminski, K.J. Gooch, D.L. Courter, A.P. Hollander, A.M. Nahir, R. Langer, G. Vunjak-Novakovic, L.E. Freed, Differential effects of growth factors on tissue-engineered cartilage, *Tissue Eng.* 8 (2002) 73--84.
- [52]. C. A. Stuart, R.W. Furlanetto, H.E. Lebovitz, The insulin receptor of embryonic chicken cartilage, *Endocrinology* 105 (1979) 1293--1302.
- [53]. J. Massague, TGF- $\beta$  signal transduction, *Annu. Rev. Biochem.* 67 (1998) 753--791.
- [54]. B. Alberts, D. Bray, J. Lewis, M. Raff, K. Roberts, J.D. Watson, *Molecular Biology of the Cell*, Garland Publishing, Inc., New York & London, (1994) 769--769.
- [55]. R. A. Ignatz, J. Massague, Transforming growth factor- $\beta$  stimulates the expression of fibronectin and collagen and their incorporation into the extracellular matrix, *J. Biol. Chem.* 261 (1986) 4337--4345.
- [56]. P. G. Robey, M.F. Young, K.C. Flanders, N.S. Roche, P. Kondaiah, A.H. Reddi, J.D. Termine, M.B. Sporn, A.B. Roberts, Osteoblasts synthesize and respond to transforming growth factor-type  $\beta$  (TGF- $\beta$ ) in vitro, *J. Cell Biol.* 105 (1987) 457--463.
- [57]. C. Lilli, L. Marinucci, G. Stabellini, S. Belcastro, E. Becchetti, C. Balducci, N. Staffolani, P. Locci, Biomembranes enriched with TGF- $\beta$ .1 favor bone matrix protein expression by human osteoblasts in vitro, *J. Biomed. Mater. Res.* 63 (2002) 577--582.
- [58]. F. Lecanda, L.V. Avioli, S.L. Cheng, Regulation of bone matrix protein expression and induction of differentiation of human osteoblasts and human bone marrow stromal cells by bone morphogenetic protein-2, *J. Cell Biochem.* 67 (1997) 386--396.
- [59]. D. J. Rickard, T.A. Sullivan, B.J. Shenker, P.S. Leboy, I. Kazhdan, Induction of rapid osteoblast differentiation in rat bone marrow stromal cell cultures by dexamethasone and BMP-2, *Dev. Biol.* 161 (1994) 218--228.
- [60]. I. Mellman, Endocytosis and molecular sorting, *Annu. Rev. Cell Dev. Biol.* 12 (1996) 575--625.
- [61]. B. Alberts, D. Bray, J. Lewis, M. Raff, K. Roberts, J.D. Watson, *Molecular Biology of the Cell*, Garland Publishing, Inc., New York & London, (1994) 618--626.
- [62]. R. J. Stockert, The asialoglycoprotein receptor: relationships between structure, function, and expression, *Physiol. Rev.* 75 (1995) 591--609.

## References

---

- [63]. Z. M. Qian, H. Li, H. Sun, K. Ho, Targeted drug delivery via the transferrin receptor-mediated endocytosis pathway, *Pharmacol. Rev.* 54 (2002) 561--587.
- [64]. C. Mineo, R.G.W. Anderson, Potocytosis, *Histochem. Cell Biol.* 116 (2002) 109--118.
- [65]. T. H. Hermanson, *Bioconjugate Techniques*, Academic Press, San Diego, California, USA, (1996) 169--180.
- [66]. M. A. Gilles, A.Q. Hudson, C.L. Borders, Jr., Stability of water-soluble carbodiimides in aqueous solution, *Anal. Biochem.* 184 (1990) 244--248.
- [67]. G. Barany, R.B. Merrifield, *Solid-Phase Peptide Synthesis*, in: E. Gross, J. Meienhofer (Eds.), *The Peptides*, Academic Press, New York; USA, (1980) 1--284.
- [68]. T. H. Hermanson, *Bioconjugate Techniques*, Academic Press, San Diego, California, USA, (1996) 177--180.
- [69]. J. M. Steward, J.D. Young, *Solide Phase Peptide Synthesis*, Pierce Chemical Company, Rockford, Illinois, USA, (1984) 31--31.
- [70]. T. H. Hermanson, *Bioconjugate Techniques*, Academic Press, San Diego, California, USA, (1996) 139--140.
- [71]. J. R. Merwin, E.P. Carmichael, G.S. Noell, M.E. DeRome, W.L. Thomas, N. Robert, G. Spitalny, H.C. Chiou, CD5-mediated specific delivery of DNA to T lymphocytes: compartmentalization augmented by adenovirus, *J. Immunol. Methods* 186 (1995) 257--266.
- [72]. B. Stella, S. Arpicco, M.T. Peracchia, D. Desmaele, J. Hoebeker, M. Renoir, J. D'Angelo, L. Cattel, P. Couvreur, Design of folic acid-conjugated nanoparticles for drug targeting, *J. Pharm. Sci.* 89 (2000) 1452--1464.
- [73]. E. S. Lee, K. Na, Y.H. Bae, Polymeric micelle for tumor pH and folate-mediated targeting, *J. Controlled Release* 91 (2003) 103--113.
- [74]. J. M. Bobbitt, Periodate oxidation of carbohydrates, *Adv. Carbohydr. Chem.* 11 (1956) 1--41.
- [75]. T. H. Hermanson, *Bioconjugate Techniques*, Academic Press, San Diego, California, USA, (2004) 114--116.
- [76]. T. H. Hermanson, *Bioconjugate Techniques*, Academic Press, San Diego, California, USA, (2004) 185--185.
- [77]. L. Peng, G.J. Calton, J.W. Burnett, Effect of borohydride reduction on antibodies, *Appl. Biochem. Biotechnol.* 14 (1987) 91--99.
- [78]. M. A. Zanta, O. Boussif, A. Adib, J.P. Behr, In Vitro Gene Delivery to Hepatocytes with Galactosylated Polyethylenimine, *Bioconjug. Chem.* 8 (1997) 839--844.
- [79]. E. Wagner, M. Cotten, K. Mechtler, H. Kirlappos, M.L. Birnstiel, DNA-binding transferrin conjugates as functional gene-delivery agents: synthesis by linkage of



## References

---

- polylysine or ethidium homodimer to the transferrin carbohydrate moiety, *Bioconjug. Chem.* 2 (1991) 226--231.
- [80]. T. H. Hermanson, *Bioconjugate Techniques*, Academic Press, San Diego, California, USA, (1996) 138--138.
- [81]. P. Erbacher, A.C. Roche, M. Monsigny, P. Midoux, Glycosylated polylysine/DNA complexes: gene transfer efficiency in relation with the size and the sugar substitution level of glycosylated polylysines and with the plasmid size, *Bioconjug. Chem.* 6 (1995) 401--410.
- [82]. T. H. Hermanson, *Bioconjugate Techniques*, Academic Press, San Diego, California, USA, (1996) 148--148.
- [83]. M. D. Partis, D.G. Griffiths, G.C. Roberts, R.B. Beechey, Crosslinking of protein by  $\omega$ -maleimido alkanoyl N-hydroxysuccinimido esters, *J. Protein Chem.* 2 (1983) 263--277.
- [84]. J. R. Heitz, C.D. Anderson, B.M. Anderson, Inactivation of yeast alcohol dehydrogenase by N-alkylmaleimides, *Arch. Biochem. Biophys.* 127 (1968) 627--636.
- [85]. C. F. Brewer, J.P. Riehm, Evidence for possible nonspecific reactions between N-ethylmaleimide and proteins, *Anal. Biochem.* 18 (1967) 248--255.
- [86]. J. C. Olivier, R. Huertas, H.J. Lee, F. Calon, W.M. Pardridge, Synthesis of Pegylated Immunonanoparticles, *Pharm. Res.* 19 (2002) 1137--1143.
- [87]. C. P. Leamon, D. Weigl, R.W. Hendren, Folate copolymer-mediated transfection of cultured cells, *Bioconjug. Chem.* 10 (1999) 947--957.
- [88]. T. H. Hermanson, *Bioconjugate Techniques*, Academic Press, San Diego, California, USA, (1996) 228--232.
- [89]. T. H. Hermanson, *Bioconjugate Techniques*, Academic Press, San Diego, California, USA, (2004) 64--66.
- [90]. J. Carlsson, H. Drevin, R. Axen, Protein thiolation and reversible protein-protein conjugation. N-Succinimidyl 3-(2-pyridyldithio)propionate, a new heterobifunctional reagent, *Biochem. J.* 173 (1978) 723--737.
- [91]. T. H. Hermanson, *Bioconjugate Techniques*, Academic Press, San Diego, California, USA, (1996) 77--83.
- [92]. P. Erbacher, J.S. Remy, J.P. Behr, Gene transfer with synthetic virus-like particles via the integrin-mediated endocytosis pathway, *Gene Ther.* 6 (1999) 138--145.
- [93]. E. Wagner, M. Zenke, M. Cotten, H. Beug, M.L. Birnstiel, Transferrin-polycation conjugates as carriers for DNA uptake into cells, *Proc. Natl. Acad. Sci. U. S. A.* 87 (1990) 3410--3414.
- [94]. T. H. Hermanson, *Bioconjugate Techniques*, Academic Press, San Diego, California, USA, (1996) 570--571.

## References

---

- [95]. N. M. Green, L. Konieczny, E.J. Toms, R.C. Valentine, Use of bifunctional biotinyl compounds to determine the arrangement of subunits in avidin, *Biochem. J.* 125 (1971) 781--791.
- [96]. T. H. Hermanson, *Bioconjugate Techniques*, Academic Press, San Diego, California, USA, (1996) 375--384.
- [97]. E. Wagner, K. Zatloukal, M. Cotten, H. Kirlappos, K. Mechtler, D.T. Curiel, M.L. Birnstiel, Coupling of adenovirus to transferrin-polylysine/DNA complexes greatly enhances receptor-mediated gene delivery and expression of transfected genes, *Proc. Natl. Acad. Sci. U. S. A.* 89 (1992) 6099--6103.
- [98]. B. Xu, S. Wiehle, J.A. Roth, R.J. Cristiano, The contribution of poly-L-lysine, epidermal growth factor and streptavidin to EGF/PLL/DNA polyplex formation, *Gene Ther.* 5 (1998) 1235--1243.
- [99]. R. Langer, N.A. Peppas, *Advances in biomaterials, drug delivery, and bionanotechnology*, *AIChE J.* 49 (2003) 2990--3006.
- [100]. K. Y. Lee, D.J. Mooney, Hydrogels for tissue engineering, *Chem. Rev.* 101 (2001) 1869--1879.
- [101]. J. L. Drury, D.J. Mooney, Hydrogels for tissue engineering: scaffold design variables and applications, *Biomaterials* 24 (2003) 4337--4351.
- [102]. P. Eiselt, Y. Lee Kuen, D.J. Mooney, Rigidity of two-component hydrogels prepared from alginate and poly(ethylene glycol)-diamines, *Macromolecules* 32 (1999) 5561--5566.
- [103]. Y. Lee Kuen, A. Rowley Jon, P. Eiselt, E.M. Moy, H. Bouhadir Kamal, D.J. Mooney, Controlling mechanical and swelling properties of alginate hydrogels independently by cross-linker type and cross-linking density, *Macromolecules* 33 (2000) 4291--4294.
- [104]. J. A. Rowley, G. Madlambayan, D.J. Mooney, Alginate hydrogels as synthetic extracellular matrix materials, *Biomaterials* 20 (1999) 45--53.
- [105]. A. Loeb sack, K. Greene, S. Wyatt, C. Culberson, C. Austin, R. Beiler, W. Roland, P. Eiselt, J. Rowley, a. Burg et, In vivo characterization of a porous hydrogel material for use as a tissue bulking agent, *J. Biomed. Mater. Res.* 57 (2001) 575--581.
- [106]. J. A. Rowley, D.J. Mooney, Alginate type and RGD density control myoblast phenotype, *J. Biomed. Mater. Res.* 60 (2002) 217--223.
- [107]. Y. Suzuki, M. Tanihara, K. Suzuki, A. Saitou, W. Sufan, Y. Nishimura, Alginate hydrogel linked with synthetic oligopeptide derived from BMP-2 allows ectopic osteoinduction in vivo, *J. Biomed. Mater. Res.* 50 (2000) 405--409.
- [108]. J.-K. Francis Suh, H.W.T. Matthew, Application of chitosan-based polysaccharide biomaterials in cartilage tissue engineering: a review, *Biomaterials* 21 (2000) 2589--2598.

- [109]. Y. C. Wang, S.H. Kao, H.J. Hsieh, A Chemical Surface Modification of Chitosan by Glycoconjugates To Enhance the Cell-Biomaterial Interaction, *Biomacromolecules* 4 (2003) 224--231.
- [110]. A. H. Zisch, U. Schenk, J.C. Schense, S.E. Sakiyama-Elbert, J.A. Hubbell, Covalently conjugated VEGF--fibrin matrices for endothelialization, *J. Controlled Release* 72 (2001) 101--113.
- [111]. J. C. Schense, J.A. Hubbell, Cross-linking exogenous bifunctional peptides into fibrin gels with factor XIIIa, *Bionconjug. Chem.* 10 (1999) 75--81.
- [112]. G. M. Cruise, D.S. Scharp, J.A. Hubbell, Characterization of permeability and network structure of interfacially photopolymerized poly(ethylene glycol) diacrylate hydrogels, *Biomaterials* 19 (1998) 1287--1294.
- [113]. P. D. Drumheller, J.A. Hubbell, Polymer networks with grafted cell adhesion peptides for highly biospecific cell adhesive substrates, *Anal. Biochem.* 222 (1994) 380--388.
- [114]. J. A. Burdick, K.S. Anseth, Photoencapsulation of osteoblasts in injectable RGD-modified PEG hydrogels for bone tissue engineering, *Biomaterials* 23 (2002) 4315--4323.
- [115]. D. L. Hern, J.A. Hubbell, Incorporation of adhesion peptides into nonadhesive hydrogels useful for tissue resurfacing, *J. Biomed. Mater. Res* 39 (1998) 266--276.
- [116]. S. Jo, P.S. Engel, A.G. Mikos, Synthesis of poly(ethylene glycol)-tethered poly(propylene fumarate) and its modification with GRGD peptide, *Polymer* 41 (2000) 7595--7604.
- [117]. S. Jo, H. Shin, A.G. Mikos, Modification of Oligo(poly(ethylene glycol) fumarate) Macromer with a GRGD Peptide for the Preparation of Functionalized Polymer Networks, *Biomacromolecules* 2 (2001) 255--261.
- [118]. H. Shin, S. Jo, A.G. Mikos, Modulation of marrow stromal osteoblast adhesion on biomimetic oligo[poly(ethylene glycol) fumarate] hydrogels modified with Arg-Gly-Asp peptides and a poly(ethyleneglycol) spacer, *J. Biomed. Mater. Res* 61 (2002) 169--179.
- [119]. R. A. Stile, K.E. Healy, Thermo-responsive peptide-modified hydrogels for tissue regeneration, *Biomacromolecules* 2 (2001) 185--194.
- [120]. G. W. Plant, S. Woerly, A.R. Harvey, Hydrogels containing peptide or aminosugar sequences implanted into the rat brain: influence on cellular migration and axonal growth, *Exp. Neurol.* 143 (1997) 287--299.
- [121]. Y. W. Tong, M.S. Shoichet, Peptide surface modification of poly(tetrafluoroethylene-co-hexafluoropropylene) enhances its interaction with central nervous system neurons, *J. Biomed. Mater. Res* 42 (1998) 85--95.
- [122]. Y. W. Tong, M.S. Shoichet, Enhancing the neuronal interaction on fluoropolymer surfaces with mixed peptides or spacer group linkers, *Biomaterials* 22 (2001) 1029--1034.

## References

---

- [123]. H. B. Lin, C. Garcia-Echeverria, S. Asakura, W. Sun, D.F. Mosher, S.L. Cooper, Endothelial cell adhesion on polyurethanes containing covalently attached RGD-peptides, *Biomaterials* 13 (1992) 905--914.
- [124]. Y. S. Lin, S.S. Wang, T.W. Chung, Y.H. Wang, S.H. Chiou, J.J. Hsu, N.K. Chou, K.H. Hsieh, S.H. Chu, Growth of endothelial cells on different concentrations of Gly-Arg-Gly-Asp photochemically grafted in polyethylene glycol modified polyurethane, *Artif. Organs* 25 (2001) 617--621.
- [125]. K. H. Park, Arg-Gly-Asp (RGD) sequence conjugated in a synthetic copolymer bearing a sugar moiety for improved culture of parenchymal cells (hepatocytes), *Biotechnol. Lett.* 24 (2002) 1401--1406.
- [126]. Y. Ito, Tissue engineering by immobilized growth factors, *Mater. Sci. Eng., C* 6 (1998) 267--274.
- [127]. Y. Ito, J. Zheng, Y. Imanishi, K. Yonezawa, M. Kasuga, Protein-free cell culture on an artificial substrate with covalently immobilized insulin, *Proc. Natl. Acad. Sci. U. S. A.* 93 (1996) 3598--3601.
- [128]. P. Schaffner, J. Meyer, M. Dard, R. Wenz, B. Nies, S. Verrier, H. Kessler, M. Kantelechner, Induced tissue integration of bone implants by coating with bone selective RGD-peptides in vitro and in vivo studies, *J. Mater. Sci.: Mater. Med.* 10 (1999) 837--839.
- [129]. J. J. Yoon, Y.S. Nam, J.H. Kim, T.G. Park, Surface immobilization of galactose onto aliphatic biodegradable polymers for hepatocyte culture, *Biotechnol. Bioeng.* 78 (2002) 1--10.
- [130]. R. A. Quirk, W.C. Chan, M.C. Davies, S.J.B. Tendler, K.M. Shakesheff, Poly(L-lysine)-GRGDS as a biomimetic surface modifier for poly(lactic acid), *Biomaterials* 22 (2001) 865--872.
- [131]. A. D. Cook, J.S. Hrkach, N.N. Gao, I.M. Johnson, U.B. Pajvani, S.M. Cannizzaro, R. Langer, Characterization and development of RGD-peptide-modified poly(lactic acid-co-lysine) as an interactive, resorbable biomaterial, *J. Biomed. Mater. Res.* 35 (1997) 513--523.
- [132]. J. K. Tessmar, A.G. Mikos, A. Gopferich, Amine-reactive biodegradable diblock copolymers, *Biomacromolecules* 3 (2002) 194--200.
- [133]. C. Fischbach, J. Tessmar, A. Lucke, E. Schnell, G. Schmeer, T. Blunk, A. Gopferich, Does UV irradiation affect polymer properties relevant to tissue engineering?, *Surf. Sci.* 491 (2001) 333--345.
- [134]. E. Allemann, R. Gurny, E. Doelker, Drug-loaded nanoparticles. Preparation methods and drug targeting issues, *Eur. J. Pharm. Biopharm.* 39 (1993) 173--191.
- [135]. M. Ogris, S. Brunner, S. Schuller, R. Kircheis, E. Wagner, PEGylated DNA/transferrin-PEI complexes: reduced interaction with blood components, extended circulation in blood and potential for systemic gene delivery, *Gene Ther.* 6 (1999) 595--605.

- [136]. J. E. O'Mullane, K. Petrak, L.E.F. Hutchinson, E. Tomlinson, The effect of adsorbed coats of poloxamers 237 and 338 on the in vitro aggregation and in vivo distribution of polystyrene latex (PSL) particles, *Int. J. Pharm.* 63 (1990) 177--180.
- [137]. D. V. Bazile, C. Ropert, P. Huve, T. Verrecchia, M. Marland, A. Frydman, M. Veillard, G. Spenlehauer, Body distribution of fully biodegradable [<sup>14</sup>C]-poly(lactic acid) nanoparticles coated with albumin after parenteral administration to rats, *Biomaterials* 13 (1992) 1093--1102.
- [138]. S. Mitra, U. Gaur, P.C. Ghosh, A.N. Maitra, Tumour targeted delivery of encapsulated dextran-doxorubicin conjugate using chitosan nanoparticles as carrier, *J. Controlled Release* 74 (2001) 317--323.
- [139]. G. Storm, S.O. Belliot, T. Daemen, D.D. Lasic, Surface modification of nanoparticles to oppose uptake by the mononuclear phagocyte system, *Adv. Drug Delivery Rev.* 17 (1995) 31--48.
- [140]. R. Kircheis, L. Wightman, A. Schreiber, B. Robitza, V. Rossler, M. Kursa, E. Wagner, Polyethylenimine/DNA complexes shielded by transferrin target gene expression to tumors after systemic application, *Gene Ther.* 8 (2001) 28--40.
- [141]. D. Bazile, C. Prud'homme, M.T. Bassoulet, M. Marland, G. Spenlehauer, M. Veillard, Stealth Me.PEG-PLA Nanoparticles Avoid Uptake by the Mononuclear Phagocytes System, *J. Pharm. Sci.* 84 (1995) 493--498.
- [142]. S. Stolnik, L. Illum, S.S. Davis, Long circulating microparticulate drug carriers, *Adv. Drug Delivery Rev.* 16 (1995) 195--214.
- [143]. K. Na, T. Bum Lee, K.H. Park, E.K. Shin, Y.B. Lee, H.K. Choi, Self-assembled nanoparticles of hydrophobically-modified polysaccharide bearing vitamin H as a targeted anti-cancer drug delivery system, *Eur. J. Pharm. Sci.* 18 (2003) 165--173.
- [144]. E. Wagner, D. Curiel, M. Cotten, Delivery of drugs, proteins and genes into cells using transferrin as a ligand for receptor-mediated endocytosis, *Adv. Drug Delivery Rev.* 14 (1994) 113--135.
- [145]. E. A. Putnam, N. Yen, G.E. Gallick, P.A. Steck, K. Fang, B. Akpakip, A.F. Gazdar, J.A. Roth, Autocrine growth stimulation by transforming growth factor-alpha in human non-small cell lung cancer, *Surg. Oncol.* 1 (1992) 49--60.
- [146]. Y. Li, M. Ogris, E. Wagner, J. Pelisek, M. Ruffer, Nanoparticles bearing polyethyleneglycol-coupled transferrin as gene carriers: preparation and in vitro evaluation, *Int. J. Pharm.* 259 (2003) 93--101.
- [147]. D. Pan, J.L. Turner, K.L. Wooley, Folic acid-conjugated nanostructured materials designed for cancer cell targeting, *Chem. Commun.* 19 (2003) 2400--2401.
- [148]. A. Patchornik, A. Berger, E. Katchalski, Poly-L-histidine, *J. Am. Chem. Soc.* 79 (1957) 5227--5230.
- [149]. C. Y. Wang, L. Huang, Polyhistidine mediates an acid-dependent fusion of negatively charged liposomes, *Biochemistry* 23 (1984) 4409--4416.

## References

---

- [150]. E. Wagner, M. Cotten, R. Foisner, M.L. Birnstiel, Transferrin-polycation-DNA complexes: the effect of polycations on the structure of the complex and DNA delivery to cells, *Proc. Natl. Acad. Sci. U. S. A.* 88 (1991) 4255--4259.
- [151]. W. T. Godbey, K.K. Wu, A.G. Mikos, Size matters: molecular weight affects the efficiency of poly(ethylenimine) as a gene delivery vehicle, *J. Biomed. Mater. Res* 45 (1999) 268--275.
- [152]. T. Bieber, W. Meissner, S. Kostin, A. Niemann, H.P. Elsasser, Intracellular route and transcriptional competence of polyethylenimine-DNA complexes, *J. Controlled Release* 82 (2002) 441--454.
- [153]. A. von Harpe, H. Petersen, Y. Li, T. Kissel, Characterization of commercially available and synthesized polyethylenimines for gene delivery, *J. Controlled Release* 69 (2000) 309--322.
- [154]. P. Erbacher, T. Bettinger, P. Belguise-Valladier, S. Zou, J.L. Coll, J.P. Behr, J.S. Remy, Transfection and physical properties of various saccharide, poly(ethylene glycol), and antibody-derivatized polyethylenimines (PEI), *J. Gene Med.* 1 (1999) 210--222.
- [155]. J. H. van Steenis, E.M. van Maarseveen, F.J. Verbaan, R. Verrijck, D.J.A. Crommelin, G. Storm, W.E. Hennink, Preparation and characterization of folate-targeted pEG-coated pDMAEMA-based polyplexes, *J. Controlled Release* 87 (2003) 167--176.
- [156]. A. V. Kabanov, V.A. Kabanov, DNA Complexes with Polycations for the Delivery of Genetic Material into Cells, *Bioconjug. Chem.* 6 (1995) 7--20.
- [157]. K. A. Mislick, J.D. Baldeschwieler, J.F. Kayyem, T.J. Meade, Transfection of folate-polylysine DNA complexes: evidence for lysosomal delivery, *Bioconjug. Chem.* 6 (1995) 512--515.
- [158]. D. T. Curiel, S. Agarwal, E. Wagner, M. Cotten, Adenovirus enhancement of transferrin-polylysine-mediated gene delivery, *Proc. Natl. Acad. Sci. U. S. A.* 88 (1991) 8850--8854.
- [159]. R. Blumenthal, P. Seth, M.C. Willingham, I. Pastan, pH-dependent lysis of liposomes by adenovirus, *Biochemistry* 25 (1986) 2231--2237.
- [160]. M. Cotten, F. Langle-Rouault, H. Kirlappos, E. Wagner, K. Mechtler, M. Zenke, H. Beug, M.L. Birnstiel, Transferrin-polycation-mediated introduction of DNA into human leukemic cells: stimulation by agents that affect the survival of transfected DNA or modulate transferrin receptor levels, *Proc. Natl. Acad. Sci. U. S. A.* 87 (1990) 4033--4037.
- [161]. C. Plank, B. Oberhauser, K. Mechtler, C. Koch, E. Wagner, The influence of endosome-disruptive peptides on gene transfer using synthetic virus-like gene transfer systems, *J. Biol. Chem.* 269 (1994) 12918--12924.
- [162]. L. C. Smith, J. Duguid, M.S. Wadhwa, M.J. Logan, C.H. Tung, V. Edwards, J.T. Sparrow, Synthetic peptide-based DNA complexes for nonviral gene delivery, *Adv. Drug Delivery Rev.* 30 (1998) 115--131.

## References

---

- [163]. J. Chen, S. Gamou, A. Takayanagi, N. Shimizu, A novel gene delivery system using EGF receptor-mediated endocytosis, *FEBS Lett.* 338 (1994) 167--169.
- [164]. C. Plank, K. Zatloukal, M. Cotten, K. Mechtler, E. Wagner, Gene transfer into hepatocytes using asialoglycoprotein receptor mediated endocytosis of DNA complexed with an artificial tetra-antennary galactose ligand, *Bioconjug. Chem.* 3 (1992) 533--539.
- [165]. W. T. Godbey, K.K. Wu, A.G. Mikos, Tracking the intracellular path of poly(ethylenimine)/DNA complexes for gene delivery, *Proc. Natl. Acad. Sci. U. S. A.* 96 (1999) 5177--5181.
- [166]. T. Bettinger, J.S. Remy, P. Erbacher, Size Reduction of Galactosylated PEI/DNA Complexes Improves Lectin-Mediated Gene Transfer into Hepatocytes, *Bioconjug. Chem.* 10 (1999) 558--561.
- [167]. R. Kircheis, T. Blessing, S. Brunner, L. Wightman, E. Wagner, Tumor targeting with surface-shielded ligand-polycation DNA complexes, *J. Controlled Release* 72 (2001) 165--170.
- [168]. H. Lee, T.H. Kim, T.G. Park, A receptor-mediated gene delivery system using streptavidin and biotin-derivatized, pegylated epidermal growth factor, *J. Controlled Release* 83 (2002) 109--119.
- [169]. K. Kataoka, A. Harada, Y. Nagasaki, Block copolymer micelles for drug delivery: design, characterization and biological significance, *Adv. Drug Delivery Rev.* 47 (2001) 113--131.
- [170]. H. Harma, T. Soukka, S. Lonnberg, J. Paukkunen, P. Tarkkinen, T. Lovgren, Zeptomole detection sensitivity of prostate-specific antigen in a rapid microtitre plate assay using time-resolved fluorescence, *Luminescence* 15 (2000) 351--355.
- [171]. D. Wang, D.R. Robinson, G.S. Kwon, J. Samuel, Encapsulation of plasmid DNA in biodegradable poly(-lactic-co-glycolic acid) microspheres as a novel approach for immunogene delivery, *J. Controlled Release* 57 (1999) 9--18.
- [172]. M. Nishikawa, L. Huang, Nonviral vectors in the new millennium: delivery barriers in gene transfer, *Hum. Gene Ther.* 12 (2001) 861--870.
- [173]. R. E. Donahue, S.W. Kessler, D. Bodine, K. McDonagh, C. Dunbar, S. Goodman, B. Agricola, E. Byrne, M. Raffeld, R. Moen, +, Helper virus induced T cell lymphoma in nonhuman primates after retroviral mediated gene transfer, *J. Exp. Med.* 176 (1992) 1125--1135.
- [174]. S. Parthasarathi, A. Varela-Echavarria, Y. Ron, B.D. Preston, J.P. Dougherty, Genetic rearrangements occurring during a single cycle of murine leukemia virus vector replication: characterization and implications, *J. Virol.* 69 (1995) 7991--8000.
- [175]. D. F. Purcell, C.M. Broscius, E.F. Vanin, C.E. Buckler, A.W. Nienhuis, M.A. Martin, An array of murine leukemia virus-related elements is transmitted and expressed in a primate recipient of retroviral gene transfer, *J. Virol.* 70 (1996) 887--897.
- [176]. R. J. Cristiano, L.C. Smith, M.A. Kay, B.R. Brinkley, S.L.C. Woo, Hepatic gene therapy: efficient gene delivery and expression in primary hepatocytes utilizing a

## References

---

- conjugated adenovirus-DNA complex, *Proc. Natl. Acad. Sci. U. S. A.* 90 (1993) 11548--11552.
- [177]. F. M. Veronese, Peptide and protein PEGylation: a review of problems and solutions, *Biomaterials* 22 (2001) 405--417.
- [178]. J. Tessmar, K. Kellner, M.B. Schulz, T. Blunk, A. Goepferich, Toward the Development of Biomimetic Polymers by Protein Immobilization: PEGylation of Insulin as a Model Reaction, *Tissue Eng.* 10 (2004) 441--453.
- [179]. Y. Lapidot, S. Rappoport, Y. Wolman, Use of esters of N-hydroxysuccinimide in the synthesis of N-acylamino acids, *J. Lipid Res.* 8 (1967) 142--145.
- [180]. K. Kellner, J. Tessmar, S. Milz, P. Angele, M. Nerlich, M.B. Schulz, T. Blunk, A. Goepferich, PEGylation does not impair insulin efficacy in three-dimensional cartilage culture: An investigation toward biomimetic polymers, *Tissue Eng.* 10 (2004) 429--440.
- [181]. U. R. Goessler, K. Hormann, F. Riedel, Tissue engineering with chondrocytes and function of the extracellular matrix (review), *Int. J. Mol. Med.* 13 (2004) 505--513.
- [182]. R. Cortesini, Stem cells, tissue engineering and organogenesis in transplantation, *Transplant Immunol.* 15 (2005) 81--89.
- [183]. F. Sarac, S. Yildiz, F. Saygili, G. Ozgen, C. Yilmaz, T. Kabalak, M. Tuzun, Insulin alters the proliferation of subcutaneous and visceral adipose cells, *Biotechnol. Biotechnol. Equip.* 19 (2005) 128--132.
- [184]. G. Ulrich-Merzenich, C. Metzner, B. Schiermeyer, H. Vetter, Vitamin C and vitamin E antagonistically modulate human vascular endothelial and smooth muscle cell DNA synthesis and proliferation, *Eur. J. Nutr.* 41 (2002) 27--34.
- [185]. C. Morszeck, C. Moehl, W. Goetz, A. Heredia, T.E. Schaeffer, N. Eckstein, C. Sippel, K.H. Hoffmann, In vitro differentiation of human dental follicle cells with dexamethasone and insulin, *Cell Biol. Int.* 29 (2005) 567--575.
- [186]. A. Martin, F.J. Unda, C. Begue-Kirn, J.V. Ruch, J. Arechaga, Effects of aFGF, bFGF, TGF $\beta$ 1 and IGF-I on odontoblast differentiation in vitro, *Eur. J. Oral Sci.* 106 (1998) 117--121.
- [187]. B. T. Houseman, M. Mrksich, The microenvironment of immobilized Arg-Gly-Asp peptides is an important determinant of cell adhesion, *Biomaterials* 22 (2001) 943--955.
- [188]. H. L. Holtorf, J.A. Jansen, A.G. Mikos, Ectopic bone formation in rat marrow stromal cell/titanium fiber mesh scaffold constructs: Effect of initial cell phenotype, *Biomaterials* 26 (2005) 6208--6216.
- [189]. X. L. Xu, J. Lou, T. Tang, K.W. Ng, J. Zhang, C. Yu, K. Dai, Evaluation of different scaffolds for BMP-2 genetic orthopedic tissue engineering, *J. Biomed. Mater. Res. Part B* 75B (2005) 289--303.
- [190]. L. Wu, J. Ding, Effects of porosity and pore size on in vitro degradation of three-dimensional porous poly(D,L-lactide-co-glycolide) scaffolds for tissue engineering, *J. Biomed. Mater. Res. Part A* 75A (2005) 767--777.



## References

---

- [191]. W. H. Wong, D.J. Mooney, Synthesis and properties of biodegradable polymers used as synthetic materials for tissue engineering, (1997) 51--82.
- [192]. H. Matthew, Polymers for Tissue Engineering Scaffolds, in :S. Dumitriu (Ed.), Polymeric Biomaterials, Marcel Dekker, Inc, New York & Basel, (2002) 167--186.
- [193]. L. Li, S. Ding, C. Zhou, Preparation and degradation of PLA/chitosan composite materials, *J. Appl. Polym. Sci.* 91 (2004) 274--277.
- [194]. A. G. Mikos, Y. Bao, L.G. Cima, D.E. Ingber, J.P. Vacanti, R. Langer, Preparation of poly(glycolic acid) bonded fiber structures for cell attachment and transplantation, *J. Biomed. Mater. Res.* 27 (1993) 183--189.
- [195]. E. Kiss, I. Bertoti, E.I. Vargha-Butler, XPS and Wettability Characterization of Modified Poly(lactic acid) and Poly(lactic/glycolic acid) Films, *J. Colloid Interface Sci.* 245 (2002) 91--98.
- [196]. W. L. Murphy, D.H. Kohn, D.J. Mooney, Growth of continuous bone-like mineral within porous poly(lactide-co-glycolide) scaffolds in vitro, *J. Biomed. Mater. Res.* 50 (2000) 50--58.
- [197]. W. R. Gombotz, G. Wang, T.A. Horbett, A.S. Hoffman, Protein adsorption to poly(ethylene oxide) surfaces, *J. Biomed. Mater. Res.* 25 (1991) 1547--1562.
- [198]. J. Texter, M. Tirrell, Chemical Processing by Self-Assembly, *AIChE J.* 47 (2001) 1706--1710.
- [199]. F. Grinnell, Cellular adhesiveness and extracellular substrata, *Int. Rev. Cytol.* 53 (1978) 65--144.
- [200]. C. J. Wilson, R.E. Clegg, D.I. Leavesley, M.J. Percy, Mediation of Biomaterial-Cell Interactions by Adsorbed Proteins: A Review, *Tissue Eng.* 11 (2005) 1--18.
- [201]. D. Hanein, H. Sabanay, L. Addadi, B. Geiger, Selective interactions of cells with crystal structures; implications for the mechanism of cell adhesion, *J. Cell. Sci.* 104 (1993) 275--288.
- [202]. J. R. Long, W.J. Shaw, P.S. Stayton, G.P. Drobny, Structure and Dynamics of Hydrated Statherin on Hydroxyapatite As Determined by Solid-State NMR, *Biochemistry* 40 (2001) 15451--15455.
- [203]. J. S. Sharp, J.A. Forrest, R.A.L. Jones, Surface denaturation and amyloid fibril formation of insulin at model lipid-water interfaces, *Biochemistry* 41 (2002) 15810--15819.
- [204]. M. S. Wang, L.B. Palmer, J.D. Schwartz, A. Razatos, Evaluating Protein Attraction and Adhesion to Biomaterials with the Atomic Force Microscope, *Langmuir* 20 (2004) 7753--7759.
- [205]. K. A. Marx, Quartz crystal microbalance: a useful tool for studying thin polymer films and complex biomolecular systems at the solution-surface interface, *Biomacromolecules* 4 (2003) 1099--1120.

## References

---

- [206]. D. A. Buttry, M.D. Ward, Measurement of interfacial processes at electrode surfaces with the electrochemical quartz crystal microbalance, *Chem. Rev. (Washington, D. C. )* 92 (1992) 1355--1379.
- [207]. A. Janshoff, C. Steinem, Quartz crystal microbalance for bioanalytical applications, *Sensors Update* 9 (2001) 313--354.
- [208]. J. F. Alder, J.J. McCallum, Piezoelectric crystals for mass and chemical measurements. A review, *Analyst (Cambridge, U. K. )* 108 (1983) 1169--1189.
- [209]. M. D. Ward, D.A. Buttry, In situ interfacial mass detection with piezoelectric transducers, *Science (Washington, D. C. )* 249 (1990) 1000--1007.
- [210]. R. L. Bunde, E.J. Jarvi, J.J. Rosentreter, Piezoelectric quartz crystal biosensors, *Talanta* 46 (1998) 1223--1236.
- [211]. D. S. Ballantine, Jr., H. Wohltjen, Surface acoustic wave devices for chemical analysis, *Anal. Chem.* 61 (1989) 704A--715A.
- [212]. G. Sauerbrey, The use of quartz oscillators for weighing thin layers and for microweighing, *Z. Phys.* 155 (1959) 206--222.
- [213]. K. K. Kanazawa, J.G. Gordon, II, The oscillation frequency of a quartz resonator in contact with a liquid, *Anal. Chim. Acta* 175 (1985) 99--105.
- [214]. K. K. Kanazawa, J.G. Gordon, II, Frequency of a quartz microbalance in contact with liquid, *Anal. Chem.* 57 (1985) 1770--1771.
- [215]. S. Bruckenstein, M. Shay, Experimental aspects of use of the quartz crystal microbalance in solution, *Electrochim. Acta* 30 (1985) 1295--1300.
- [216]. C. Modin, A.L. Stranne, M. Foss, M. Duch, J. Justesen, J. Chevallier, L.K. Andersen, A.G. Hemmersam, F.S. Pedersen, F. Besenbacher, QCM-D studies of attachment and differential spreading of pre-osteoblastic cells on Ta and Cr surfaces, *Biomaterials* 27 (2006) 1346--1354.
- [217]. J. Blomqvist, B. Mannfors, L.-O. Pietila, Amorphous cell studies of polyglycolic, poly(-lactic), poly(,-lactic) and poly(glycolic/-lactic) acids, *Polymer* 43 (2002) 4571--4583.
- [218]. O. Kinstler, G. Molineux, M. Treuheit, D. Ladd, C. Gegg, Mono-N-terminal poly(ethylene glycol)-protein conjugates, *Adv. Drug Delivery Rev.* 54 (2002) 477--485.
- [219]. J. M. Harris, *Poly(ethylene glycol) Chemistry*, Plenum Press, New York,(1992).
- [220]. A. Abuchowski, T. van Es, N.C. Palczuk, F.F. Davis, Alteration of immunological properties of bovine serum albumin by covalent attachment of polyethylene glycol, *J. Biol. Chem.* 252 (1977) 3578--3581.
- [221]. S. Herman, G. Hooftman, E. Schacht, Poly(ethylene glycol) with reactive endgroups: I. Modification of proteins, *J. Bioact. Compat. Polym.* 10 (1995) 145--187.

- [222]. P. Caliceti, F.M. Veronese, Pharmacokinetic and biodistribution properties of poly(ethylene glycol)-protein conjugates, *Adv. Drug Delivery Rev.* 55 (2003) 1261--1277.
- [223]. P. Caliceti, O. Schiavon, F.M. Veronese, Immunological properties of uricase conjugated to neutral soluble polymers, *Bioconjug. Chem.* 12 (1 A.D.) 515--522.
- [224]. E. V. Amirgoulova, J. Groll, C.D. Heyes, T. Ameringer, C. Roecker, M. Moeller, G.U. Nienhaus, Biofunctionalized polymer surfaces exhibiting minimal interaction towards immobilized proteins, *ChemPhysChem* 5 (2004) 552--555.
- [225]. L. W. Seymour, Y. Miyamoto, H. Maeda, M. Brereton, J. Strohalm, K. Ulbrich, R. Duncan, Influence of molecular weight on passive tumour accumulation of a soluble macromolecular drug carrier, *Eur. J. Cancer* 31 (1995) 766--770.
- [226]. J. A. J. Yankeelov, [52] Modification of arginine by diketones, Volume 25 (1972) 566--579.
- [227]. R. B. Greenwald, A. Pendri, D. Bolikal, Highly Water Soluble Taxol Derivatives: 7-Polyethylene Glycol Carbamates and Carbonates, *J. Org. Chem.* 60 (1995) 331--336.
- [228]. F. M. Veronese, G. Pasut, PEGylation, successful approach to drug delivery, *Drug Discov. Today* 10 (2005) 1451--1458.
- [229]. M. Wilchek, E.A. Bayer, Labeling glycoconjugates with hydrazide reagents, in: *Methods in Enzymology*, Academic Press, (1987) 429--442.
- [230]. H. Sato, Enzymatic procedure for site-specific pegylation of proteins, *Adv. Drug Delivery Rev.* 54 (2002) 487--504.
- [231]. H. Lee, T.G. Park, A novel method for identifying PEGylation sites of protein using biotinylated PEG derivatives, *J. Pharm. Sci.* 92 (2003) 97--103.
- [232]. F. M. Veronese, B. Sacca, P.P. de Laureto, M. Sergi, P. Caliceti, O. Schiavon, P. Orsolini, New PEGs for peptide and protein modification, suitable for identification of the PEGylation site, *Bioconjug. Chem.* 12 (2001) 62--70.
- [233]. H. B. Olsen, N.C. Kaarsholm, Structural effects of protein lipidation as revealed by LysB29-myristoyl, des(B30) insulin, *Biochemistry* 39 (2000) 11893--11900.
- [234]. C. B. Newgard, While tinkering with the b-cell... Metabolic regulatory mechanisms and new therapeutic strategies, *Diabetes* 51 (2002) 3141--3150.
- [235]. Z. Vajo, W.C. Duckworth, Genetically engineered insulin analogs: diabetes in the new millennium, *Pharmacol. Rev.* 52 (2000) 1--9.
- [236]. A. S. Cunha, J.L. Grossiord, F. Puisieux, M. Seiller, Insulin in w/o/w multiple emulsions: preparation, characterization and determination of stability towards proteases in vitro, *J. Microencapsul.* 14 (1997) 311--319.
- [237]. S. B. Leichter, M.E. Schreiner, L.R. Reynolds, T. Bolick, Long-term follow-up of diabetic patients using insulin infusion pumps. Considerations for future clinical application, *Arch. Intern. Med.* 145 (1985) 1409--1412.

## References

---

- [238]. S. Y. Jeong, S.W. Kim, D.L. Homberg, J.C. McRea, Insulin Delivery Systems, in: J.M. Anderson, S.W. Kim, *Advances in Drug Delivery Systems*, Elsevier, Amsterdam, (1986) 143--152.
- [239]. N. Tsuneji, N. Yuji, N. Naoki, S. Yoshiki, S. Kunio, Powder dosage form of insulin for nasal administration, *J. Controlled Release* 1 (1984) 15--22.
- [240]. D. R. Owens, B. Zinman, G. Bolli, Alternative routes of insulin delivery, *Diabet. Med.* 20 (2003) 886--898.
- [241]. T. Nagai, R. Konishi, Buccal/gingival drug delivery systems, *J. Controlled Release* 6 (1987) 353--360.
- [242]. R. Narayani, Oral Delivery of Insulin - Making Needles Needless, *Trends Biomaterials Artificial Organs* 15 (1 A.D.) 12--16.
- [243]. T. Nishihata, J.H. Rytting, A. Kamada, T. Higuchi, M. Routh, L. Caldwell, Enhancement of rectal absorption of insulin using salicylates in dogs, *J. Pharm. Pharmacol.* 35 (1983) 148--151.
- [244]. T. Yagi, N. Hakui, Y. Yamasaki, R. Kawamori, M. Shichiri, H. Abe, S. Kim, M. Miyake, K. Kamikawa, T. Nishihata, A. Kamada, Insulin suppository: enhanced rectal absorption of insulin using an enamine derivative as a new promoter, *J. Pharm. Pharmacol.* 35 (1983) 177--178.
- [245]. M. Hashizume, T. Douen, M. Murakami, A. Yamamoto, K. Takada, S. Muranishi, Improvement of large intestinal absorption of insulin by chemical modification with palmitic acid in rats, *J. Pharm. Pharmacol.* 44 (1992) 555--559.
- [246]. R. A. J. McIlhinney, The fats of life: the importance and function of protein acylation, *Trends Biochem. Sci.* 15 (1990) 387--391.
- [247]. L. A. Paige, M.J. Nadler, M.L. Harrison, J.M. Cassady, R.L. Geahlen, Reversible palmitoylation of the protein-tyrosine kinase p56lck, *J. Biol. Chem.* 268 (1993) 8669--8674.
- [248]. E. N. Olson, D.A. Towler, L. Glaser, Specificity of fatty acid acylation of cellular proteins, *J. Biol. Chem.* 260 (1985) 3784--3790.
- [249]. S. Robert, D. Domurado, D. Thomas, J. Chopineau, Fatty Acid Acylation of RNase A Using Reversed Micelles as Microreactors, *Biochem. Biophys. Res. Commun.* 196 (1993) 447--454.
- [250]. M. Hashimoto, K. Takada, Y. Kiso, S. Muranishi, Synthesis of palmitoyl derivatives of insulin and their biological activities, *Pharm. Res.* 6 (1989) 171--176.
- [251]. F. Al Obeidi, V.J. Hruby, N. Yaghoubi, M.M. Marwan, M.E. Hadley, Synthesis and biological activities of fatty acid conjugates of a cyclic lactam  $\alpha$ -melanotropin, *J. Med. Chem.* 35 (1992) 118--123.
- [252]. E. Yodoya, K. Uemura, T. Tenma, T. Fujita, M. Murakami, A. Yamamoto, S. Muranishi, Enhanced permeability of tetragastrin across the rat intestinal membrane and

## References

---

- its reduced degradation by acylation with various fatty acids, *J. Pharmacol. Exp. Ther.* 271 (1994) 1509--1513.
- [253]. H. Bundgaard, J. Moess, Prodrugs of peptides. 6. Bioreversible derivatives of thyrotropin-releasing hormone (TRH) with increased lipophilicity and resistance to cleavage by the TRH-specific serum enzyme, *Pharm. Res.* 7 (1990) 885--892.
- [254]. J. Wang, D. Chow, H. Heiati, W.C. Shen, Reversible lipidization for the oral delivery of salmon calcitonin, *J. Controlled Release* 88 (2003) 369--380.
- [255]. M. M. Y. Chi, A.L. Schlein, K.H. Moley, High insulin-like growth factor 1 (IGF-1) and insulin concentrations trigger apoptosis in the mouse blastocyst via down-regulation of the IGF-1 receptor, *Endocrinology* 141 (2000) 4784--4792.
- [256]. F. M. Ingels, P.F. Augustijns, Biological, pharmaceutical, and analytical considerations with respect to the transport media used in the absorption screening system, caco-2, *J. Pharm. Sci.* 92 (2003) 1545--1558.



# Appendices

# 1 Abbreviations

$^1\text{H-NMR}$	proton nuclear magnetic resonance spectroscopy
5-AE	5-aminoeosin
ADR	adriamycin
AFM	atomic force microscopy
ASGPr	asialoglycoprotein receptor
ATR-FTIR	attenuated total reflection Fourier spectroscopy
BAW	bulk acoustic waves
BMP	bone morphogenic protein
CCM	cell culture medium
$\text{CDCl}_3$	deuterated chloroform
CHO	Chinese hamster ovary
DCC	dicyclohexyl carbodiimide
ddH <sub>2</sub> O	double distilled water
D,L-dilactide	3,6-dimethyl-1,4-dioxane-2,5-dione
DMAP	4-dimethylaminopyridine
DMEM	Dulbecco`s Modified Eagle`s Medium
DMF	N,N`-dimethylformamide
DMSO	dimethylsulfoxide
DTT	dithiothreitol
EDANS	5-((2-aminoethyl)amino)naphthalene-1-sulfonic acid, Na-salt
EDC	1-ethyl-3-(3-dimethylaminopropyl)-carbodiimide hydrochloride
ECM	extra cellular matrix
EGF	epidermal growth factor
FBS	fetal bovine serum
FBP	folate binding protein



---

(b)FGF	( <i>basic</i> ) fibroblast growth factor
GFC	gel permeation chromatography
H&E	hematoxylin and eosin
Hepes	N-(2-hydroxyethyl)piperazine-N'-(2-ethanesulfonic acid)
HPLC	high pressure liquid chromatography
HPLC-MS	high pressure liquid chromatography mass spectroscopy
HPMA	N-(2-hydroxypropyl)methacrylamide)
IDDM	insulin dependent diabetes mellitus
IGF-I	insulin like growth factor I
IR	infra red
Lipo-insulin 1.5	lipophilized insulin synthesized in a molar ratio of insulin to fatty acid of 1 to 1.5
MAb	monoclonal antibodies
MALDI-ToF	matrix assisted laser desorption ionization time of flight
MePEG <sub>2</sub>	poly(ethylene glycol)-monomethyl ether with 2 kDa MW
MePEG <sub>x</sub> PLA <sub>y</sub>	poly(ethylene glycol)-monomethyl ether poly(D,L lactic acid) <b>or:</b> $\alpha$ -Hydro- $\omega$ -methoxy-poly(oxy-1-oxopropane-2,1-diyl-block-oxyethylene)
MCF-7	human breast adenocarcinoma cell line
(r)MSC	( <i>rat</i> ) marrow stromal cells
MDSC	modulated differential scanning calorimetry
NCA	N-carboxy anhydride
NH <sub>2</sub> PEG	poly(ethylene glycol)-monoamine
NHS	N-hydroxysuccinimide
NHS-LC-biotin	N-succinimidyl-6-(biotinamido)hexanoate
NHS-PEG-maleimide	N-(hydroxysuccinimidyl-poly(ethylene glycol)-maleimide
NMP	N-methyl pyrrolidone
OPF	oligo(poly(ethylene glycol) fumarate)
PAA	poly(acrylic acid)

---

PAA-b-PI	copolymer poly(acrylic acid)-b-polyisoprene
PAL-NHS	N-hydroxysuccinimide Ester of Palmitic Acid
PBS	phosphate buffered saline
PEG	poly(ethylene glycol)
PEG-PCL	poly(ethylene glycol)-co-poly(caprolactone)
PEG-PEI	poly(ethylene glycol)-co-poly(ethyleneimine)
PEG-PPF	poly(ethylene glycol)-co-poly(propylene fumarate)
PEI	poly(ethyleneimine)
PMMA	poly(methylmethacrylate)
PLGA	poly(lactic-co-glycolic acid)
PLA	poly(lactic acid)
PLL	poly(L-lysine)
Poly(H <sub>2</sub> NPEGCA-co-HDCA)	poly[aminopoly(ethylene glycol)cyanoacrylate-co-hexadecyl cyanoacrylate]
Poly-His	poly(L-histidine)
Poly(His)-PEG	poly(L-histidine)-co-poly(ethylene glycol)
PS	polystyrene
PVA	poly(vinyl alcohol)
QCM	quartz crystal microbalance
RES	reticuloendothelial system
RGD	peptide sequence Arg-Gly-Asp
RI	refractive index
SA	succinic acid
SAW	surface acoustic waves
SDS	sodium dodecyl sulfate
SEC	size exclusion chromatography
SPDP	N-succinimidyl 3-(2-pyridyldithio)propionate

---

SPEG	succinic acid monoester of poly(ethylene glycol)-monomethyl ether
SSPEG	N-succinimidyl succinate of poly(ethylene glycol)-monomethyl ether
Streptavidin-PEI-DNA	streptavidin covalently linked to PEI-DNA polyplexes
Sulfo-NHS	N-hydroxysulfosuccinimide
TGF- $\alpha$	transforming growth factor- $\alpha$
TG1 <sup>st</sup>	glass transition temperature at first heating cycle
THF	tetrahydrofurane
TMS	tetramethylsilane
Tris	Tris(hydroxymethyl)-amino methane
TSM	thickness shear mode
UV	ultra violet
VEGF	vascular endothelial growth factor
WGA	wheat germ agglutinin

## 2 Acknowledgements

Many thanks go to all the people, giving me a helpful hand on the way to prepare this thesis.

Firstly I thank Professor Göpferich, who gave me the opportunity to prepare this work at his department. I am grateful for his support and encouragement on the sometimes stony road towards the finish line.

I also like to thank Dr. Torsten Blunk for the productive discussions during the meetings and Dr. Jörg Teßmar for his patience during my introduction to polymer synthesis and analysis and his assistance throughout my work.

I am very grateful towards Dr. Michael Hacker and Dr. Markus Neubauer for performing polymer processing and in vivo testing.

I appreciate very much the help Robert Knerr gave me during my work with the QCM.

I am much in the dept of Angelika Beriè for performing MALDI-ToF and QCM analysis.

I am also very grateful towards Christine Niel and Manuele Avola for their assistance during polymer synthesis and the good time we had as lab mates.

I also like to thank Josef Kiermaier for performing HPLC-MS experiments, Dr. Burgemeister for the analysis of the NMR samples and Dr Hochmuth for high resolution MALDI-ToF analysis, and I appreciate very much the readiness they always should for discussing the results of the experiments.

I also like to thank all the present and former technical assistants of the department: Andrea Blaimer, Stefan Kolb, Renate Liebl, Christine Niel, Edith Schindler, Albert Weingart for their support during work and their cheerfulness on all occasions.

I appreciate very the help of the secretaries of the department Lydia Frommer and Liane Öttl.

I also like to thank very much the former and present colleagues who created an atmosphere of friendship and made life enjoyable during PhD work. I specially like to thank:

- Bernhard Appel for his friendship and his readiness for sport or cooking activities
- Christian Guse, Florian Sommer, Axel Ehmer for their support not only during decathlon training
- Uta Lungwitz for the eventful collaboration during our time as lab mates

- Daniela Eyrich and Stephanie Könnings for their honest friendship an especially for introducing Beaker

I also like to thank Christian Guse, Martina Hubensack and Erich Schneider for our irregular but nice Schafkopf-evenings.

I would also like to thank my family for the encouragement they provided and Albert Grundsteiner for his endless patience and support.

To all: Thank you very much!

### 3 Curriculum vitae

Name: Sigrid Drotleff  
Date of birth: January 12, 1975  
Place of birth: AgnetheIn, Romania  
Nationality: German  
Marital status: single

#### **Education:**

09/81 – 08/85      elementary School, Kirchberg/Romania  
09/85 – 07/89      Comprehensive School, Kirchberg/Romania  
09/89 – 07/95      Grammar School, Apian Gymnasium, Ingolstadt

#### **Professional Training**

11/95 – 04/00      Study of Pharmacy at the University of Regensburg, Regensburg  
05/00 – 04/01      Traineeship at the Ostentor Apotheke, Regensburg  
07/2001              Acquisition of the license to practise as pharmacist  
08/01 – present      PhD program at the Department of Pharmaceutical Technology,  
University of Regensburg, Regensburg, Prof. Achim Göpferich

#### **Publications and Conference Abstracts**

S. Drotleff, J. Tessmar, K. Kellner, M. Hacker, M. Neubauer, M. Schulz, T. Blunk, A. Goepferich: Biomimetic Polymers for Tissue Engineering - Characterisation of Polymers and of Proteins for their Surface Modification. 5. Jahres-Meeting der Gesellschaft für Zell- und Gewebezüchtung, Regensburg (2002).

M. Hacker, T. Vogel, M. Neubauer, S. Drotleff, J. Teßmar, T. Blunk, A. Göpferich, M.B. Schulz: Solid lipid templating: anhydrous scaffold fabrication for tissue engineering. DPhG Jahrestagung, Würzburg, Germany (2003).

S. Drotleff, U. Lungwitz, M. Breunig, A. Dennis, T. Blunk, J. Tessmar, A. Goepferich: Biomimetic polymers in pharmaceutical and biomedical sciences. *Eur J Pharm Biopharm* **58** (2), 385-407 (2004).

U. Lungwitz, M. Breunig, S. Drotleff, R. Knerr, A. Goepferich: Low Molecular Weight Linear Polyethylenimines for Non-Viral Transfection. Controlled Release Society German Chapter Annual Meeting, Heidelberg, Germany (2005).

R. Knerr, B. Weiser, S. Drotleff, C. Steinem, A. Göpferich: Protein adsorption and cell adhesion on RGD modified PEG monolayers. Life Science Interface Summer School, University of Nottingham, Nottingham, UK (2005).

R. Knerr, S. Drotleff, C. Steinem, A. Göpferich: Self-assembling PEG Derivatives for Protein-repellant Biomimetic Model Surfaces on Gold. *Biomaterialien* **7** (1), 12-20 (2006).